



Technical Guidelines for

**Seismic Retrofit of Existing Reinforced
Concrete Buildings in Bangladesh for Extended
Application of PWD Seismic Retrofit Manual**

March 2022

Prepared by

SATREPS-TSUIB Project

A Japan-Bangladesh Joint Research Project

The University of Tokyo
&
Housing and Building Research Institute

Foreword

Natural hazards like earthquake focused in this technical report are inevitable, and disaster mitigation is a global issue that we should tackle. These problems and proposed strategies to reach their solutions for making society more disaster-resilient are not local to one country and should, therefore, be shared among related countries and regions.

Bangladesh is located in an earthquake-prone region and has been under the rapid growth of economy and urbanization, causing densely constructed and populated cities. Although the Bangladesh National Building Code (BNBC) including seismic provisions was first published in 1993 and the revised code BNBC 2020 was enforced very recently, older buildings and even some newer buildings have not been constructed with proper seismic design concept and/or supervisions, leaving a huge number of existing vulnerable buildings in urban centers to future earthquake events. Seismic evaluation and retrofitting of such vulnerable buildings are therefore of great urgency for a safer and more resilient society to future damaging earthquakes, which is also a key for a continued and sustainable development of the society.

Motivated by the imminent threat exposed to the society of Bangladesh, a research project collaborating with the Government of Bangladesh was proposed and launched in 2015 entitled “The Project for Technical Development to Upgrade Structural Integrity of Buildings in Densely Populated Urban Areas and Its Strategic Implementation towards Resilient Cities in Bangladesh (TSUIB)” under JICA(Japan International Cooperation Agency) and JST(Japan Science and Technology Agency) joint program for “Science and Technology Research Partnership for Sustainable Development (SATREPS)”. The major tasks and expected outputs from the SATREPS-TSUIB project include the development of seismic evaluation and retrofit procedures that are suitable for reinforced concrete buildings in Bangladesh with scientific evidence and data, and this report offers evidence-based and practical guidelines and recommendations derived after the 6-year research project. Although Japan has repeatedly learned bitter lessons from damaging earthquakes and accordingly implemented seismic upgrading of existing vulnerable buildings, we do not have a cure-all medicine and the best solution in one area may not always be so in another area. It may often need to be customized to fit the needs and availability of each societal environment since the societal and design/construction practice background were different from those in Japan, and this is one of the most essential policies that we have emphasized and shared with research group members throughout the project. The implemented policy can be found in various parts of the guidelines.

Another feature that should be addressed is that the guidelines are designed to be cross-referred with closely related technical manuals for seismic evaluation and retrofit design, which were both developed in the preceded JICA CNCRP project (2011-2015) followed by the JICA BSPP project (2016-2021). These manuals provide the fundamental concept and methods of seismic evaluation and retrofitting of reinforced concrete buildings in Bangladesh while the guidelines cover extended data and/or information in detail for their practical application to those with low strength concrete, high axial loads, URM infills, flat-plate system, etc., which are often found in reinforced concrete buildings in Bangladesh and accordingly focused in the SATREPS-TSUIB project.

Our road to the goal was not flat and smooth; we faced significantly restricted activities due to a safety reason after a terror attack in Dhaka that occurred just at the beginning of the project and COVID-19 that caused the pandemic in the final corner of the project. Also, during the project, we lost the most valuable person, Dr. Jamir Reza Choudhury, the Vice Chancellor of University of Asia Pacific and the Chairperson of the Joint Coordination Committee of the project, who had always provided us with clear and brilliant directions with compassionate suggestions. Nevertheless, both Bangladeshi and Japanese colleagues have been collaborating to successfully achieve the goal through finding a way out of such difficulties and crises, and we would like to express our sincere gratitude for their greatest efforts and contributions to the project. Their efforts have been definitely the source of our success and we are very proud of them. We do hope and believe that all the achievements including knowledge, skills, experiences, and confidence obtained and developed during the project can serve as a basis for making a more earthquake-resilient society of Bangladesh.

This project has been long supported by the Government of Bangladesh, JICA Headquarter, JICA Bangladesh Office, and JST, which fully understand the impact of the research outputs on the society of Bangladesh. Dr. Kaoru Takara, Professor of Kyoto University and Research Supervisor of SATREPS-TSUIB project, visited Dhaka and encouraged us for a fruitful and best achievement to the goal. Mr. Koichiro Miyara and Ms. Atsuko Himeno, Project Coordinators; have spared no effort to accommodate local arrangements for smooth implementation of on-site research activities in Bangladesh. Finally, we would like to take this opportunity to thank all of them for their valuable supports.

Yoshiaki Nakano
SATREPS-TSUIB project Japan side Leader
Professor,
Institute of Industrial Science,
The University of Tokyo

Md. Ashraful Alam
SATREPS-TSUIB project Bangladesh side Leader
Director General,
Housing and Building Research Institute,
Ministry of Housing and Public Works

Preface

Recent earthquakes in and around Bangladesh have highlighted the importance of preparedness for future catastrophic earthquakes to make the society seismically resilient. Seismic evaluation of existing RC buildings and strengthening are urgent for future preparedness. Government of Bangladesh has initiated several research projects to develop seismic evaluation and strengthening methods. In this regard, a “Manual for Seismic Retrofit Design of Existing Reinforced Concrete Buildings” has been prepared by Public Works Department (PWD) under CNCRP project, a PWD-JICA technical cooperation project (2011-2015). The PWD manual is mainly developed based on the Japanese seismic retrofit guidelines (JBDPA guidelines) incorporating the seismic design standard in Bangladesh national building code (BNBC). Since the buildings’ structural system and characteristics are different from Japan, still there are several issues being addressed and the development of the PWD manual is going on. The PWD seismic retrofit manual is being revised by PWD-JICA another technical cooperation project called BSPP project (2016-2021). The first revision of the PWD manual will be published soon. However, there is several issues that exists in RC building in Bangladesh, are addressed in the first version of PWD manual which is not incorporated in the BSPP manual. These issues are low strength concrete, inadequate beam-column joints and consideration of lateral strength of unreinforced masonry infill. In addition, the PWD manual does not consider the retrofit procedure of flat plate structures which is also commonly found in Bangladesh. This current seismic retrofit guideline is developed to address the aforementioned issues and discusses the evaluation procedure considering these unsolved issues.

This seismic retrofit guideline is developed for extended application of PWD seismic retrofit manual that is developed thorough BSPP project. This guideline consists of six distinct chapters including the introduction chapter. Chapter 2 shows the design flow of seismic retrofit. Chapter 3 discusses about retrofitting techniques about exterior beam-column joint, flat plate-column joint, masonry infill wall and column jacketing using CFRP. Chapter 4 verifies the performance evaluation of post installed bonded anchor in low strength concrete. Chapter 5 illustrates alternative retrofit construction techniques. Finally, chapter 6 shows examples of seismic retrofit of moment-resisting frame structure and flat plate structure.

This current guideline and PWD manual should be used together. That is why there are several cross-referencing for each chapter. However, seismic retrofit of flat plate structure is a new part and aspect for retrofit of existing RC buildings in Bangladesh.

This guideline was developed based on several research work in different direction within the duration of the project. The Working Group 3 team are highly grateful to all Junior Consultants for their great effort to conduct the experiment, building investigation and also compilation of the SATREPS-TSUIB guideline during the project tenure. This guideline was also developed based on discussion between Bangladesh and Japanese

counterpart. The Working Group 3 team are highly acknowledging to JICA for arranging such types of discussion meetings.

Finally, this guideline will be very helpful for future preparedness of earthquake disaster in Bangladesh.

Yasushi Sanada
SATREPS-TSUIB project WG3 Japan side leader
Professor
Department of Architectural Engineering
Osaka University

AFM Saiful Amin
SATREPS-TSUIB project WG3 Bangladesh side leader
Professor
Department of Civil Engineering
Bangladesh University of Engineering and Technology

Joint Coordination Committee

Chairperson

Jamilur Reza Choudhury

University of Asia Pacific (- April 2020)

Md. Jahangir Alam

University of Science and Technology Chittagong (December 2021-)

Working Groups of SATREPS-TSUIB project

Working Group 1 (WG1): Data collection on building stock in Dhaka

Co-Leader Yoshiaki Nakano The University of Tokyo

Co-Leader Md Ashraful Alam Housing and Building Research Institute

Working Group 2 (WG2): Development of seismic performance evaluation methodologies

Co-Leader Masaki Maeda Tohoku University

Co-Leader MD Rafiqul Islam Public Works Department

Working Group 3 (WG3): Development of seismic retrofit schemes

Co-Leader Yasushi Sanada Osaka University

Co-Leader AFM Saiful Amin Bangladesh University of Engineering and Technology

Working Group 4 (WG4): Development of efficient and effective urban planning strategies

Co-Leader Michio Ubaura Tohoku University

Co-Leader Md. Akter Mahmud Jahangirnagar University

Working Group 3 (WG3)

Co-Leader	Yasushi Sanada	Osaka University
Co-Leader	AFM Saiful Amin	Bangladesh University of Engineering and Technology
	Susumu Takahashi	Daido University
	Masaki Maeda	Tohoku University
	Matsutaro Seki	Building Research Institute
	Joji Sakuta	Horie Engineering and Architectural Research Institute Co., Ltd
	Yoshiaki Nakano	The University of Tokyo
	Kazuto Matsukawa	The University of Tokyo
	Yuji Haga	The University of Tokyo
	Iftekhhar Anam	University of Asia Pacific
	Md. Ashraful Alam	University of Asia Pacific
	Syed Jamal Uddin Ahmed	University of Asia Pacific
	Md. Mizanur Rahman	Bangladesh University of Engineering and Technology
	Fatema-Tuz-Zahura	Ahsanullah University of Engineering and Technology
	Md. Ashraful Alam	Housing and Building Research Institute
	Shakhawat Hossain	Housing and Building Research Institute
	Md. Arifujjaman	Housing and Building Research Institute
	Md. Shafiul Islam	Housing and Building Research Institute
	MD Rafiqul Islam	Public Works Department
	Debasish Sen	Ahsanullah University of Engineering and Technology
	Md. Abdul Malek Sikder	Senior Research Consultant, SATREPS-TSUIB project
	Md. Abdur Rahman Bhuiyan	Senior Research Consultant, SATREPS-TSUIB project
	Anik Das	Junior Research Consultant, SATREPS-TSUIB project
	S. M. Muhaiminul Islam	Junior Research Consultant, SATREPS-TSUIB project
	Md. Ibnul Warah	Housing and Building Research Institute
	Zasiah Tafheem	Ahsanullah University of Engineering and Technology
	Nandita Saha	University of Asia Pacific

Authors

Yasushi Sanada	Osaka University
AFM Saiful Amin	Bangladesh University of Engineering and Technology
Masaki Maeda	Tohoku University
Yoshiaki Nakano	The University of Tokyo
Matsutaro Seki	Building Research Institute
Kazuto Matsukawa	The University of Tokyo
Susumu Takahashi	Daido University
Md Shafiul Islam	Housing and Building Research Institute
Debasish Sen	Ahsanullah University of Engineering and Technology
Nandita Saha	University of Asia Pacific
HM Golam Samdani	Osaka University
Murshalin Ahmed	Osaka University

List of Authors by each chapter

Chapter 1 General (Sanada, Nakano)

Chapter 2 Design Flow of the Seismic Retrofit to Improve Structural Integrity (Sanada)

Chapter 3 Target Structural Components to be Seismically Retrofitted

3.1 (Sanada) / 3.2 (Takahashi) / 3.3 (Sen, Islam, Maeda, Seki) / 3.4 (Matsukawa, Amin)

Chapter 4 Post Installed Bonded Anchor (Saha, Sanada)

Chapter 5 Instruction of Retrofit Construction

5.1 (Takahashi, Samdani) / 5.2 (Sen)

Chapter 6 Examples of Seismic Retrofit

6.1 (Ahmed, Yoon) / 6.2 (Samdani, Takahashi)

Appendix Pilot Project for Ferrocement Retrofit Construction in Bangladesh (Sen, Seki)

Table of Contents

Foreword	i
Preface	iii
Joint Coordination Committee.....	v
Working Groups of SATREPS-TSUIB project	v
Working Group 1 (WG1): Data collection on building stock in Dhaka	v
Working Group 2 (WG2): Development of seismic performance evaluation methodologies.....	v
Working Group 3 (WG3): Development of seismic retrofit schemes	v
Working Group 4 (WG4): Development of efficient and effective urban planning strategies.....	v
Working Group 3 (WG3).....	vi
Authors	vii
List of Tables.....	xi
List of Figures	xii
Chapter 1 General.....	1
1.1 General principle	1
1.2 Scope of application	5
1.3 Definitions	7
1.4 Notations	7
Chapter 2 Design Flow of the Seismic Retrofit to Improve Structural Integrity	9
2.1 General	9
2.2 Design flow considering the structural integrity	10
Chapter 3 Target Structural Components to be Seismically Retrofitted	13
3.1 Exterior beam-column joint.....	13
3.1.1 General.....	13
3.1.2 Scope	13
3.1.3 Design criteria.....	15
3.1.4 Failure mechanism identification after wing wall installation.....	15
3.1.5 Strength index C and Ductility index F of exterior columns with wing wall(s).....	15

3.2 Flat plate-column joint	19
3.2.1 General.....	19
3.2.2 Application of wing wall	21
3.2.3 Application of drop panel	27
3.3 Masonry infill wall	31
3.3.1 General.....	31
3.3.2 Introduction to ferrocement	33
3.3.3 General flow of structural design of ferrocement strengthening	35
3.3.4 Judgement of applicability of ferrocement retrofit.....	37
3.3.5 Selection of target failure mechanism	39
3.3.6 Selection of ferrocement configuration	40
3.3.7 Strength index C	41
3.3.8 Ductility index F	52
3.3.9 Application Example	55
3.4 Column Jacketing using Carbon Fiber Reinforced Plastics	65
3.4.1 General.....	65
3.4.2 Shear strength (Q_{su})	66
3.4.3 Flexural strength (M_u).....	66
3.4.4 Construction.....	66
3.4.5 Example of application: An RC column of a five-story office building in Dhaka constructed in 1985	69
Chapter 4 Post Installed Bonded Anchor.....	71
4.1 General	71
4.2 Scope	72
4.3 Design guidelines for post installed single bonded anchor in low strength concrete	74
4.3.1 Tensile capacity	74
4.3.2 Shear Test	83
4.4 Limitations	85
Chapter 5 Instruction on Retrofit Construction.....	87
5.1 Drop panel installation	87
5.2 Ferrocement application to masonry infill walls	91

Chapter 6 Examples of Seismic Retrofit.....	95
6.1 Moment-resisting frame structure	95
6.1.1 General.....	95
6.1.2 Scope	95
6.1.3 Outline of the structure	95
6.1.4 Seismic evaluation of the building	97
6.1.5 Seismic retrofit of the building.....	98
6.2 Example calculation of flat plate structure	104
6.2.1 General.....	104
6.2.2 Seismic retrofit using drop panel.....	105
6.2.3 Seismic retrofit using wing walls	110
Appendix Pilot Project for Ferrocement Retrofit Construction in Bangladesh	A-1
Background of this pilot project	A-2
Formation of pilot project for ferrocement retrofit	A-2
A.1 Retrofit Design	A-3
A.2 Construction Work	A-18

List of Tables

Table 3.3.1 Material specification	33
Table C.3.3.1 Failure mechanisms of masonry infilled RC frame strengthened with ferrocement	39
Table C.3.3.2 Summary of the experimental and calculated lateral strengths (Sen 2020)	51
Table 3.3.2 Suggested F-index for different failure mechanisms.....	52
Table C.3.3.3 Idealized C-F relationship of FC laminated Masonry infilled RC frame.....	54
Table 3.3.3 Column dimension	55
Table 3.3.4 Masonry infill-wall properties	55
Table C.4.1 Summary of the calculation of design tensile capacity of a sample specimen	77
Table 6.1.1 Summary	95
Table 6.1.2 Column Layout.....	97
Table 6.1.3 Material property	97
Table 6.1.7 Summary of strengthened member performance.....	102
Table 6.1.8 Seismic performance of 1 st floor in the X-Direction	103
Table 6.2.1 Summary of materials.....	105
Table 6.2.2 Summary of the seismic evaluation.....	107
Table 6.2.3 Ductility index F and strength index C	109
Table 6.2.4 Summary of the seismic evaluation using drop panel	110
Table 6.2.5 Ductility index F and strength index C	116
Table 6.2.6 Summary of the seismic evaluation using wing walls.....	117

List of Figures

Figure C.1.1 CNCRP Manuals 2015a and 2015b for Seismic Retrofit of RC Buildings in Bangladesh	2
Figure C.1.2 Cross-referred CNCRP/BSPP Manuals and SATREPS/TSUIB Guidelines for Seismic Evaluation and Retrofit of Existing RC Buildings in Bangladesh	3
Figure C.1.3 Special issues addressed in the CNCRP Manual (CNCRP Seismic Evaluation Manual)	5
Figure C.1.4 Damage to beam-column joints, losing a building's integrity (2005 Kashmir earthquake)	6
Figure 2.1 General design flow diagram of the seismic retrofit for existing RC buildings in Bangladesh considering the specific problems on the structural integrity	10
Figure C.3.1.1 Close-up of the first judgement in the general design flow diagram	14
Figure 3.1.1 Wing wall length determination	15
Figure C.3.1.2 Specimens and loading scheme	17
Figure C.3.1.3 Experimental results	18
Figure 3.2.1.1 Flowchart for seismic retrofit of existing RC structures with flat plate-column joints	19
Figure 3.2.1.2 An example of flat plate structure to which this section is applied	20
Figure 3.2.2.1 Flowchart of seismic retrofit of existing RC flat plate-column joint by wing wall(s)	21
Figure 3.2.2.2 Moment diagram of flat plate retrofitted by wing wall(s)	22
Figure 3.2.2.3 Column with wing walls	22
Figure 3.2.2.4 The nodal moment at the flexural yielding of slab	23
Figure 3.2.2.5 Critical section of punching shear failure	24
Figure 3.2.2.6 Specimens	24
Figure 3.2.2.7 Outline of experiment	25
Figure 3.2.2.8 Experimental result (Specimen FP-W1)	25
Figure 3.2.2.9 Experimental result (Specimen FP-W2)	25
Figure 3.2.2.10 Assumed moment diagram	27
Figure 3.2.3.1 Flowchart of seismic retrofit of existing RC flat plate-column joint by drop panel	28
Figure 3.2.3.2 Moment diagram of flat plate retrofitted by drop panel	28
Figure 3.2.3.3 Critical section of punching shear failure	29
Figure 3.2.3.4 Experimental result (Specimen FP-D1)	30
Figure 3.3.1: Different types of wire mesh (Naaman, 2000)	34
Figure 3.3.2 Schematic diagram of ferrocement strengthened masonry infill	34
Figure C.3.3.1 Wire mesh attachment process suggested in field of practice in Pakistan (Shahzada, 2007)	35
Figure 3.3.3 General design flow of ferrocement strengthening	36
Figure 3.3.4 Failure mechanisms after ferrocement strengthening of masonry infilled RC frame	37
Figure 3.3.5 Schematic diagram of impact of ferrocement strengthening of un-strengthened masonry infilled RC frame having less contact length ($a_c/h \leq 0.2$)	38
Figure 3.3.6 Schematic diagram of the impact of ferrocement strengthening on un-strengthened masonry infilled RC frame having larger contact length ($a_c/h > 0.2$) [Schematic diagram]	38
Figure 3.3.7 Conceptual diagram of target failure mechanism selection procedure	40

Figure C.3.3.2: (a) Idealized load transfer mechanism of diagonal compression (Type I) (Sen 2020) and (b) concept of idealized diagonal strut width.....	43
Figure C.3.3.3 Surrounding RC column (a) un-deformed shape, (b) deformed shape and (c) curvature distribution.....	45
Figure C.3.3.4 Idealized load transfer mechanism of diagonal cracking and sliding (Type II) (Sen 2020)	45
Figure C.3.3.5 a) masonry infill, and b) ferrocement layer at diagonal cracking	46
Figure C.3.3.6 a) State of stress on diagonal wallet and b) Corresponding Mohr's circle representation	47
Figure C.3.3.7 Relationship between diagonal shear strength and masonry prism strength (Sen 2020).....	47
Figure C.3.3.8 Idealized load transfer mechanism of overall flexural failure (Type III) (Sen 2020).....	48
Figure C.3.3.9 Idealized load transfer mechanism of column punching and joint sliding (Type IV) (Sen 2020)	49
Figure C.3.3.10 Typical shear-slip relationship of construction joint	50
Figure C.3.3.11 Typical shear-slip relationship of construction joint (Paulay et al. 1974).....	51
Figure C.3.3.12 Calculated and experimental capacities of all investigated specimens (Sen 2020).....	52
Figure C.3.3.13 F-indices for test specimen.....	53
Figure 3.3.8 Architectural plan (dimensions are in mm).....	55
Figure 3.3.9 Seismic index (I_s) of the investigated building	56
Figure 3.3.10 Showing masonry infill used for FC lamination	57
Figure 3.3.11 Different failure modes	60
Figure 3.3.12 Showing location of ferrocement strengthening.....	61
Figure 3.4.1 Drawings of CFRP retrofitted specimens.....	67
Figure 3.4.2 Ratio of tested Q_{su} to calculated Q_{su} of CFRP retrofitted specimens.....	68
Figure C.4.1 Bonded anchor (JBDPA, 2001)	71
Figure C.4.2 Application of post installed bonded anchor in retrofitting	72
Figure 4.1(a) Basic failure modes of post-installed bonded single anchors and (b) Effective projected failure area of bonded anchor (R.Tanaka, K.Oba).....	75
Figure C.4.3 Calculated diameter of concrete cone failure surface	77
Figure C.4.4 Temporary wooden supports of anchor and rebar (from left).....	78
Figure C.4.5 Test set up of pullout test to determine tensile capacity of (a) anchor in RC slab and (b) rebar in pure low strength concrete	79
Figure C.4.6 Experimental failure area vs calculated failure area of pullout test of post installed bonded rebar in pure 12.2 N/mm ² concrete block (N. Saha et al.,2020).....	80
Figure C.4.7 (a) Bond failure of steel/adhesive interface and adhesive/concrete interface (from left) (N. Saha et al., 2020) and (b) Anchor specimen with tensile fracture	80
Figure C.4.8 Experimental tensile capacity of anchors compared to the design calculations (N. Saha, 2018)	81
Figure C.4.9 Effects of concrete strength, rebar diameter and embedment length on tensile capacity of post installed single bonded anchors (N. Saha et al.,2020).....	82
Figure C.4.10 Experimental results versus design data by this guideline (N. Saha et al., 2020).....	82
Figure C.4.11 Experimental shear test loading set up on concrete block (a) side view, (b) front view and (c) concrete bearing failure of shear test (N. Saha et al. ,2020)	85

Figure 5.1.1 Retrofit of flat plate structures by drop panel	87
Figure 5.1.2 Drop panel installation	88
Figure 5.1.3 Construction flow chart for drop panel installation	88
Figure 5.1.4 Mark a drill.....	89
Figure 5.1.5 Drill a hole.....	89
Figure 5.1.6 Insert glue.....	89
Figure 5.1.7 Install an anchor	89
Figure 5.1.8 Arrangement of reinforcement.....	90
Figure 5.1.9 Formwork of the drop panel.....	90
Figure 5.2.1 Construction procedure for FC lamination.....	91
Figure 5.2.2 Removal of existing mortar (plaster) from infill masonry	92
Figure 5.2.3 Application of initial mortar layer.....	92
Figure 5.2.4 Attachment of nail after drilling.....	93
Figure 5.2.5 Attachment of wire mesh	93
Figure 5.2.6 Application of second layer of mortar.....	94
Figure 6.1.1 Typical floor plan	96
Figure 6.1.2 Column schedule.....	96
Figure 6.1.3 Column layout.....	97
Figure 6.1.6 Structural performance curve.....	98
Figure 6.1.7 Strengthening proposal 1 st floor	99
Figure 6.2.1 Typical plan of the existing building	104
Figure 6.2.2 Flow Diagram of Seismic Retrofit using drop panel.....	105
Figure 6.2.3 Assumed critical section of the column with drop panel	106
Figure 6.2.4 Nodal moment of slab (Grid Y2)	107
Figure 6.2.5 Relationship between strength index C and ductility index F	109
Figure 6.2.6 Comparison between seismic demand and capacity	110
Figure 6.2.7 Flow Diagram of Seismic Retrofit using wing wall.....	111
Figure 6.2.8 Layout of the wing wall after installation	111
Figure 6.2.9 Plan of Column with wing walls.....	112
Figure 6.2.10 Assumed diagram after retrofitting by wing walls (X2 Grid).....	113
Figure 6.2.11 Relationship between strength index C and ductility index F	116
Figure 6.2.12 Comparison between seismic demand and capacity	117

This Page is Intentionally Left Blank

This Page is Intentionally Left Blank

Chapter 1 General

1.1 General principle

- (1) The Technical Guidelines shall apply to seismic retrofitting of existing reinforced concrete buildings in Bangladesh.
- (2) The Guidelines shall apply to obtain technically appropriate procedures, schemes and data for extended application of “Manual for Seismic Retrofit Design of Existing Reinforced Concrete Buildings (PWD 2021a)” and “Manual for Retrofit Construction and Supervision of Reinforced Concrete Buildings (PWD 2021b).”

C.1.1 [Commentary]

Seismic retrofit needs to be performed when an existing building do not satisfy the seismic demand as a result of the seismic evaluation; thus, the seismic evaluation and retrofit are a couple of actions under common social and academic backgrounds. Therefore, the following descriptions are also in common with those in an accompanied publication of *Technical Guidelines for Seismic Evaluation of Existing Reinforced Concrete Buildings in Bangladesh for Extended Application of BSPP Seismic Evaluation Manual*.

(1) Bangladesh is located in an earthquake-prone region and has been under the rapid growth of economy and urbanization, causing densely constructed and populated cities. Although the Bangladesh National Building Code (BNBC) including seismic provisions was first published in 1993 and the revised code BNBC 2020 was enforced very recently, older buildings and even some newer buildings have not been constructed with proper seismic design concept and/or supervisions, leaving a huge number of existing vulnerable buildings in urban centers to future earthquake events. Seismic evaluation and retrofit of such vulnerable buildings are therefore of great urgency for a safer and more resilient society to future damaging earthquakes.

In light of such an imminent threat to expanding cities in Bangladesh, a technical cooperation project for Capacity Development on Natural Disaster Resistant Techniques of Construction and Retrofitting for Public Buildings (CNCRP) started in 2011 focusing on seismic evaluation and retrofit of existing vulnerable reinforced concrete (RC) buildings in Bangladesh. It was a multi-fold project, emphasizing its major outputs of the development of seismic retrofit design/construction manuals for existing RC buildings (PWD 2015a and 2015b, **Fig. C.1.1**) along with a seismic evaluation manual (PWD 2015c). This project was followed by the Project on Promoting Building Safety for Disaster Risk Reduction (BSPP) and the above manuals were revised and published in 2021 (PWD 2021a and PWD 2021b for the seismic retrofit manuals). These manuals were developed referring to the *Standard for Seismic Evaluation of Existing Reinforced Concrete Buildings*, *Guidelines for Seismic Retrofit of Existing Reinforced Concrete Buildings*, and *Technical Manual for Seismic Evaluation and Seismic Retrofit of Existing Reinforced Concrete Buildings* (JBDPA 2004) that were exclusively developed for buildings in Japan; therefore, further studies were highly expected to enrich the

manuals for more rational contents suitable for buildings in Bangladesh since the societal and design/construction practice background were different from those in Japan.

Motivated by these findings and experiences during the CNCRP project, a research project collaborating with the Government of Bangladesh was proposed and launched in 2015 titled “*Technical Development to Upgrade Structural Integrity of Buildings in Densely Populated Urban Areas and Its Strategic Implementation towards Resilient Cities in Bangladesh (TSUIB)*” under Japan International Cooperation Agency (JICA) and Japan Science and Technology Agency (JST) joint program for “*Science and Technology Research Partnership for Sustainable Development (SATREPS)*.” The major tasks and expected outputs from the SATREPS-TSUIB project include the development of seismic evaluation and retrofit procedures that are suitable for buildings in Bangladesh with scientific evidence and data which did not appear in the CNCRP Manuals. As can be found subsequently in Section 1.2 and Chapters 2 through 6, the present Guidelines provide procedures, schemes and data to retrofit existing RC buildings typically found in Bangladesh, which are essential to appropriately upgrade the seismic capacity index of a structure, I_s , but are not illustrated in the CNCRP/BSPP Manuals.



Figure C.1.1 CNCRP Manuals 2015a and 2015b for Seismic Retrofit of RC Buildings in Bangladesh

(2) As can be found in **Fig. C.1.2**, the fundamental concept and calculation procedure (or basic flow) for seismic retrofit design, construction, and supervision are found in the CNCRP/BSPP Manuals, and the present Guidelines, therefore, provide essential and imperative procedures, schemes and data to appropriately retrofit existing RC buildings with specific characteristics in Bangladesh. The SATREPS-TSUIB Guidelines and CNCRP/BSPP Manuals are expected to be cross-referred because the Guidelines are designed to provide missing information and/or data in the CNCRP/BSPP Manuals while the manuals contain the fundamental concept and methods of the seismic retrofit. For example, structural engineers can follow the basic procedure to perform the seismic retrofit design and/or construction of a building which appears in the CNCRP/BSPP

Manuals, and they can refer to the SATREPS-TSUIB Guidelines to assure the structural integrity for substandard beam-column joints, flat plate-column connections, or unreinforced masonry (URM) walls which are not specified in the CNCRP/BSPP Manuals if the target building concerned contains such structural components, as is often found in Bangladesh.

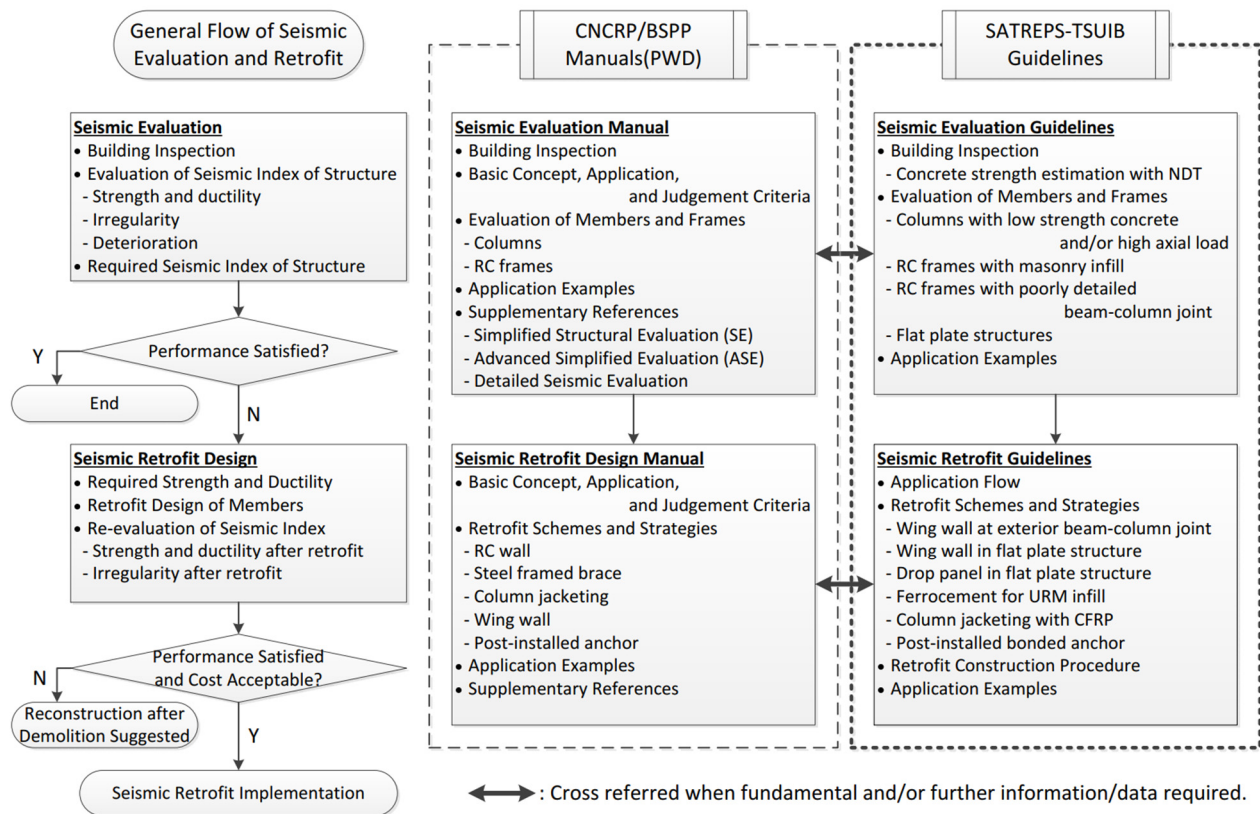


Figure C.1.2 Cross-referred CNCRP/BSPP Manuals and SATREPS/TSUIB Guidelines for Seismic Evaluation and Retrofit of Existing RC Buildings in Bangladesh

References

- [1] Public Works Department (PWD) (2021a): Manual for Seismic Retrofit Design of Existing Reinforced Concrete Buildings (TBD), under the Project on Promoting Building Safety for Disaster Risk Reduction (BSPP), A Technical Cooperation Project between PWD and JICA.
- [2] Public Works Department (PWD) (2021b): Manual for Retrofit Construction and Supervision of Reinforced Concrete Buildings (TBD), under the Project on Promoting Building Safety for Disaster Risk Reduction (BSPP), A Technical Cooperation Project between PWD and JICA.
- [3] Public Works Department (PWD) (2015a): Manual for Seismic Retrofit Design of Existing Reinforced Concrete Buildings, under the Project for Capacity Development on Natural Disaster Resistant Techniques

of Construction and Retrofitting for Public Buildings (CNCRP), A Technical Cooperation Project between PWD and JICA.

- [4] Public Works Department (PWD) (2015b): Manual for Retrofit Construction and Supervision of Reinforced Concrete Buildings, under the Project for Capacity Development on Natural Disaster Resistant Techniques of Construction and Retrofitting for Public Buildings (CNCRP), A Technical Cooperation Project between PWD and JICA.
- [5] Public Works Department (PWD) (2015c): Manual for Seismic Evaluation of Existing Reinforced Concrete Buildings, under the Project for Capacity Development on Natural Disaster Resistant Techniques of Construction and Retrofitting for Public Buildings (CNCRP), A Technical Cooperation Project between PWD and JICA.
- [6] Japan Building Disaster Prevention Association (JBDPA) (2004): Standard for Seismic Evaluation of Existing Reinforced Concrete Buildings, 2001, Guidelines for Seismic Retrofit of Existing Reinforced Concrete Buildings, 2001 and Technical Manual for Seismic Evaluation and Seismic Retrofit of Existing Reinforced Concrete Buildings, 2001.

1.2 Scope of application

The Guidelines shall apply to retrofit the following RC structural components which affect the loss of the structural integrity of a building concerned.

- (1) Beam-column joint insufficiently anchored beam longitudinal rebar.
- (2) Flat plate-column joint.
- (3) URM wall.
- (4) Column made with low-strength concrete.

C.1.2 [Commentary]

Fig. C.1.3 illustrates the typical problems in existing RC buildings in Bangladesh identified through the CNCRP project; thus, further studies were recommended by the project. Some of the problems may cause loss of the structural integrity of a building resulting in serious damage and/or collapse under earthquakes: beam-column joint with short straight anchorage of beam longitudinal rebar, usage of URM wall, and low-strength column under high axial compression. The SATREPS-TSUIB project, therefore, focused on these urgent problems affecting the structural integrity which must be appropriately considered in the seismic retrofit design/construction of existing RC buildings in Bangladesh. In addition to the above structural components, considering a wide application of flat plate system in Bangladesh, the flat plate-column joint was also included for one of the primary targets to be examined and retrofitted if necessary.

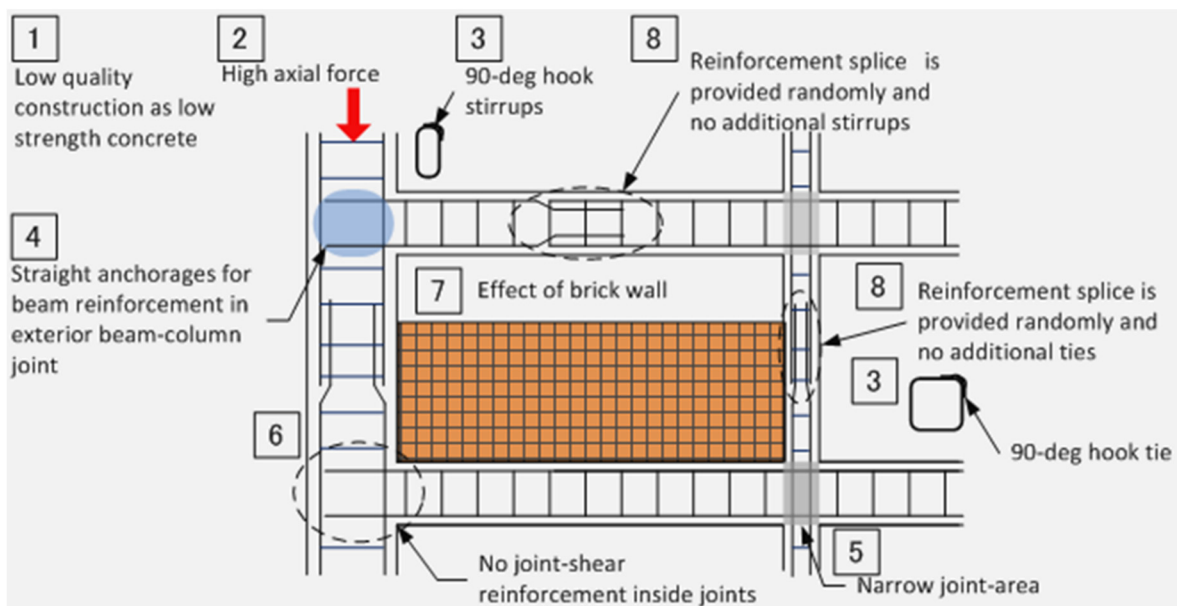


Figure C.1.3 Special issues addressed in the CNCRP Manual (CNCRP Seismic Evaluation Manual)

(1) Improperly designed or supervised RC buildings often have poorly detailed beam-column joints with insufficient embedment length and/or anchorage details of beam reinforcing bars into the joint, which leads to pullout failure of reinforcing bars and eventually hampers a structure to reach its potential seismic performance expected in the design, as shown in **Fig. C.1.4**. To improve such structural weakness is fundamental and essential to seek strategies to upgrade the seismic capacity of buildings with structural integrity as well as to properly predict the seismic performance of retrofitted buildings expected during earthquake events.

(2) Flat plate structures are one of design and construction trends generally found in urban centers of Bangladesh because they can offer design-flexible interior space without beam sections and fashionable facade. Flat plate structures, however, should be more carefully designed and constructed so that the connections with columns and slabs, generally much thinner than beams, should behave in a ductile manner under lateral loads, which often needs more engineering knowledge and experiences than ordinary buildings. Bangladeshi engineers often point out, however, that even newer flat plate buildings are questionable in their seismic performance, and they are also targeted buildings to be urgently evaluated and retrofitted if needed.

(3) Frames with URM walls are common in RC buildings in Bangladesh. As has been well accepted in the earthquake engineering community, the URM greatly (both positively and negatively) contributes to the seismic performance of buildings, particularly in the in-plane direction, although it has been generally neglected in the seismic design. The quantitatively verified data on the strength, ductility, failure modes, and their governing parameters of URM infilled RC frames obtained by the SATREPS-TSUIB project play an important role in the seismic retrofit design as well as seismic evaluation. However, the out-of-plane resistance should be considered to effectively apply URM walls to the seismic retrofit.

(4) Low strength concrete and/or high axial loads acting on RC columns significantly affect their strength and ductility. In particular, a high concrete axial load ratio ($= N/(A_g F_c)$ where N : axial load, A_g : sectional area of column, and F_c : compressive strength of concrete) with the low-strength concrete under a high axial load may lead their premature failure. Increasing the column axial resistance ($= A_g F_c$) is a promising option to reduce the concrete axial load ratio.



Figure C.1.4 Damage to beam-column joints, losing a building's integrity (2005 Kashmir earthquake)

To realize the seismic retrofit design/construction of existing RC buildings considering the possible loss of the structural integrity because of brittle failure of the above structural components, Chapter 2 presents a flow diagram of the seismic retrofit design which covers several steps to screen a possibility of loss of the structural integrity, to improve the integrity, and to treat nonstructural URM walls for out-of-plane failure. Chapter 3 provides design procedures for several retrofit schemes to improve the structural integrity of the above target components. Chapter 4 verifies the applicability of design equations in the CNCRP/BSPP Manuals to post-installed anchors (one of key devices for the seismic retrofit) in low-strength concrete. Chapter 5 illustrates key points on construction and supervision for the retrofit schemes presented in this Guidelines which are not introduced in the CNCRP/BSPP Manuals. Chapter 6 shows retrofit design samples for two typical existing RC buildings in Bangladesh according to the present Guidelines.

1.3 Definitions

Strength index C : The lateral-load carrying capacity of a member (masonry infill, or RC column) in terms of a shear coefficient, namely the shear capacity normalized by the weight of the building above.

Ductility index F : An index representing the deformation capacity of a structural member.

a_c/h_o ratio: The ratio of contact length of masonry infill to column height.

In-plane failure: A failure mode of masonry infill caused by the load acting horizontally along the wall length.

Out-of-plane failure: A failure mode of masonry infill damaged in a perpendicular direction to the wall surface.

Structural masonry element: An infill that is deemed to contribute to the lateral capacity of a building.

1.4 Notations

Q : ultimate strength of ferrocement strengthened masonry infilled RC frame

Q_1 : Lateral capacity at diagonal compression failure

Q_2 : Lateral capacity at diagonal cracking and sliding failure

Q_3 : lateral capacity at overall flexural failure

Q_4 : lateral capacity at column punching and joint sliding failure

Q_c : Lateral strength of column calculated as the minimum strength of Q_{su} , Q_{mu}

W : The weight of the building including live load for seismic calculation supported by the story concerned

$f_{m,\theta}$: compressive strength of masonry along diagonal

$f_{mor,FC}$: ferrocement mortar strength

f_m : Prism compressive strength of masonry infill

λ_{mas} : relative rigidity factor for masonry

λ_{mas-FC} : relative rigidity factor for ferrocement strengthened masonry

E_{mas} : Young's modulus of masonry infill

E_{FC} : Young's modulus of ferrocement mortar

t_{FC} : thickness of ferrocement mortar layer

t_{mas} : Thickness of masonry infill

n_s : number of surface strengthened with ferrocement

A_{mas} : diagonal area of infill masonry

A_{wm} : Area of mesh reinforcement

S_v : Spacing of horizontal mesh reinforcement
 n_L : number of wire mesh layer in each ferrocement layer
 α : empirical reduction factor
 $f_{y,wm}$: yield strength of mesh reinforcement
 l_w : Length of masonry infill
 d_m : Diagonal length of masonry infill
 θ : Inclination angle of masonry wall's diagonal from the horizontal axis
 E_c : Young's modulus of concrete
 I_c : Moment of inertia of RC column
 M_u : Flexural yield moment of the column calculated based on the Japanese standard (JBDPA, 2001).
 h_o : Clear height of RC column
 h_{mas} : Height of masonry infill
 K_{min} : influence factor considering shear span ratio
 τ_o : basic shear strength of column
 a : shear span
 ρ_g : longitudinal reinforcement ratio of column
 b : width of column
 d : depth of column
 f_c : concrete compression strength
 f_y : yield strength of longitudinal reinforcement
 τ_{mas} : bond strength at masonry top
 $\tau_{mor,FC}$: bond strength at ferrocement top
 $a_{t,col}$: Area of steel of longitudinal reinforcement in tension column.
 l_c : Center to center span length of RC frame
 N : Total axial force on RC columns on both sides of masonry infill wall
 $Q_{mas,cr}$: The contribution of strength of masonry in diagonal cracking
 $Q_{FC,wm}$: The contribution of strength of ferrocement in diagonal cracking failure
 $f_{mas,cr}$: Masonry diagonal cracking strength
 A_{wm} : Area of mesh reinforcement
 $j_s Q_w$: Joint shear capacity
 $\tau_{mor,FC}$: shear strength (cohesion) of mortar in masonry joint and ferrocement
 $a_{wm,v}$: cross sectional area of vertical wire mesh/interface reinforcement
 $\tau_{y,wm}$: shear strength of wire mesh/interface reinforcement
 W_s : Strut width

Chapter 2 Design Flow of the Seismic Retrofit to Improve Structural Integrity

2.1 General

Design of the seismic retrofit for existing RC buildings in Bangladesh shall be performed considering the specific problems on the structural integrity.

C.2.1 [Commentary]

As illustrated in **Figs. C.1.3** and **C.1.4**, existing RC buildings in Bangladesh often have serious problems which may cause the loss of structural integrity under earthquakes. Such specific problems are unique in Bangladeshi buildings; thus, they have not been considered in the *Standard for Seismic Evaluation of Existing Reinforced Concrete Buildings*, *Guidelines for Seismic Retrofit of Existing Reinforced Concrete Buildings*, and *Technical Manual for Seismic Evaluation and Seismic Retrofit of Existing Reinforced Concrete Buildings* (JBDPA 2004) which were developed as “Taishin Shindan Kijun” and “Taishin Kaishu Shishin” in Japan and are the origins of the CNCRP/BSPP Manuals (**Fig. C.1.1**). Therefore, not only in evaluating the seismic performance of a building but also in designing the retrofit plan, the structural integrity shall be considered to prevent unexpected failure because of the above problems. This chapter presents a design flow of the seismic retrofit to improve the structural integrity which is applied along with the conventional retrofit design flow provided in the CNCRP/BSPP Manuals for Seismic Retrofit Design.

References

- [1] Japan Building Disaster Prevention Association (JBDPA) (2004): Standard for Seismic Evaluation of Existing Reinforced Concrete Buildings, 2001, Guidelines for Seismic Retrofit of Existing Reinforced Concrete Buildings, 2001 and Technical Manual for Seismic Evaluation and Seismic Retrofit of Existing Reinforced Concrete Buildings, 2001.

2.2 Design flow considering the structural integrity

Design of the seismic retrofit for existing RC buildings in Bangladesh shall follow **Fig. 2.1**.

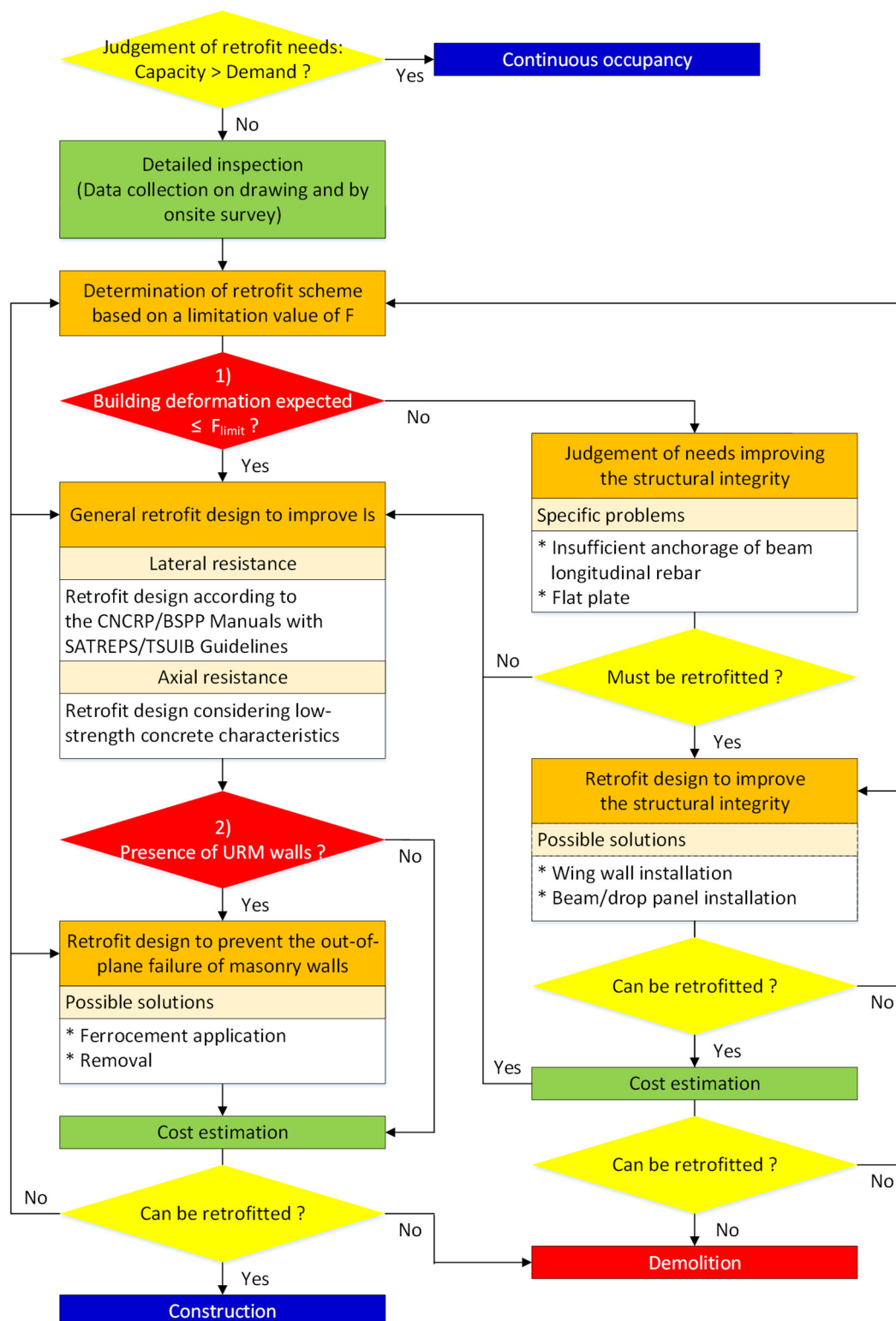


Figure 2.1 General design flow diagram of the seismic retrofit for existing RC buildings in Bangladesh considering the specific problems on the structural integrity

C.2.1 [Commentary]

Figure 2.1 illustrates a general design flow of the seismic retrofit of existing RC buildings in Bangladesh. It particularly includes two specific evaluation processes 1) to judge possible loss of the structural integrity and 2) presence of URM walls that are vulnerable to out-of-plane seismic loads, as shown by red rhombuses in **Fig. 2.1**. The first judgement on the structural integrity covers two specific structural components of the exterior beam-column joint with insufficient anchorage of beam longitudinal rebar and the flat plate-column joint. The possibility of premature failure at these components is evaluated based on the ductility (deformation capacity) limit, F_{limit} which is also adopted in the Guidelines for the seismic evaluation. The second judgement on the presence of URM walls is performed along with the conventional retrofit design process for the structural components. Although they are sometimes regarded nonstructural components, the SATREPS/TSUIB Guidelines present their availability as structural components; thus, the out-of-plane failure should be prevented by retrofit or removal.

1) Exterior beam-column joints may contain insufficient anchorage of beam longitudinal rebar in existing RC buildings in Bangladesh. The insufficiency leads to brittle pullout failure of beam longitudinal rebar, which results in structural collapse because of a loss of structural integrity. A method to screen such buildings is illustrated in the Manual of the seismic evaluation. When a building concerned has a possibility of brittle pullout failure, the structural deformation expected in the seismic retrofit design should be within the ductility limit, F_{limit} of 2.2 (equivalent to the inter-story drift angle of 1.5% rad). Otherwise, the anchorage of beam longitudinal rebar must be improved not to cause the pullout failure beyond the F_{limit} . One of the solutions is introduced in Section 3.1.

Once flat plate-column joints cause punching shear failure, a building concerned may collapse losing the structural integrity. Thus, the SATREPS-TSUIB Guidelines for the seismic evaluation provides how to identify the failure mechanism. When the punching shear failure is expected, the structural deformation assumed in the seismic retrofit design should be within the ductility limit, F_{limit} of 2.6 (equivalent to the inter-story drift angle of 2.0% rad). Otherwise, the flat plate-column joints must be improved to prevent the punching shear failure beyond the F_{limit} . Two solutions are introduced in Section 3.2.

2) URM walls are popular as exterior/partitioning walls in existing RC buildings in Bangladesh but are particularly vulnerable to seismic loads in the out-of-plane direction. The out-of-plane collapse may injure residents and/or the building itself; thus, such brittle components must be removed or strengthened in the retrofit design to prevent the inevitable collapse even though they are regarded as nonstructural components. The present Guidelines for the seismic retrofit introduces one of the promising retrofit schemes in Section 3.3.

Chapter 3 Target Structural Components to be Seismically Retrofitted

The following seismic retrofit methods were developed by the SATREPS-TSUIB project to provide realistic solutions to specific problems commonly found in structural components of RC buildings in Bangladesh.

3.1 Exterior beam-column joint

3.1.1 General

Exterior beam-column joints with a potential risk of pullout failure of beam longitudinal rebar can be retrofitted by installing RC wing walls at the joint.

C.3.1.1 [Commentary]

RC wing wall installation is among the most popular retrofit methods commonly applied to RC buildings in Japan, where RC wall(s) is installed beside existing columns in RC buildings. This method mainly increases the strength of existing columns (and, thus, the overall structure) using concrete and reinforcement without high-tech materials. In the SATREPS-TSUIB project, however, this method was applied to improve the structural integrity of RC exterior beam-column joints with insufficient anchorage of beam longitudinal rebar. Its effectiveness has been verified experimentally. In particular, a design methodology is presented to prevent brittle pullout failure of beam longitudinal rebar from the joints.

3.1.2 Scope

The scope is limited to exterior beam-column joints in RC buildings with insufficient anchorage of beam longitudinal rebar showing brittle pullout failure.

C.3.1.2 [Commentary]

The present method by RC wing wall installation is intended to upgrade RC exterior beam-column joints with insufficient anchorage of beam longitudinal rebar showing brittle pullout failure. Therefore, the scope is mainly limited to those members that are expected to collapse by pullout failure: deformed bars with straight anchorage at the end beyond the ductility limit of pullout failure ($F_{limit} = 2.2$). Such vulnerability details have sometimes been applied to exterior beam-column joints in RC buildings constructed commonly during the period from 1995 to 2006 or later because they contain deformed bars with straight anchorage or inadequate anchorage due to narrow column.

Figure C.3.1.1 shows a close-up of the first judgement (red rhombus) in the general design flow diagram shown in **Fig. 2.1** in Chapter 2. The objectives of the present method is to prevent beam longitudinal rebar from brittle pullout failure which was experimentally found to occur beyond $F_{limit} = 2.2$, as mentioned in detail

below; thus, the method shall be applied when the deformation of a building concerned is expected to exceed the above limitation in the retrofit design. When the possibility of pullout failure is expected, the following design schemes are available and effective. Otherwise, the conventional retrofit design process illustrated in the CNCRP/BSPP Manuals can be applied.

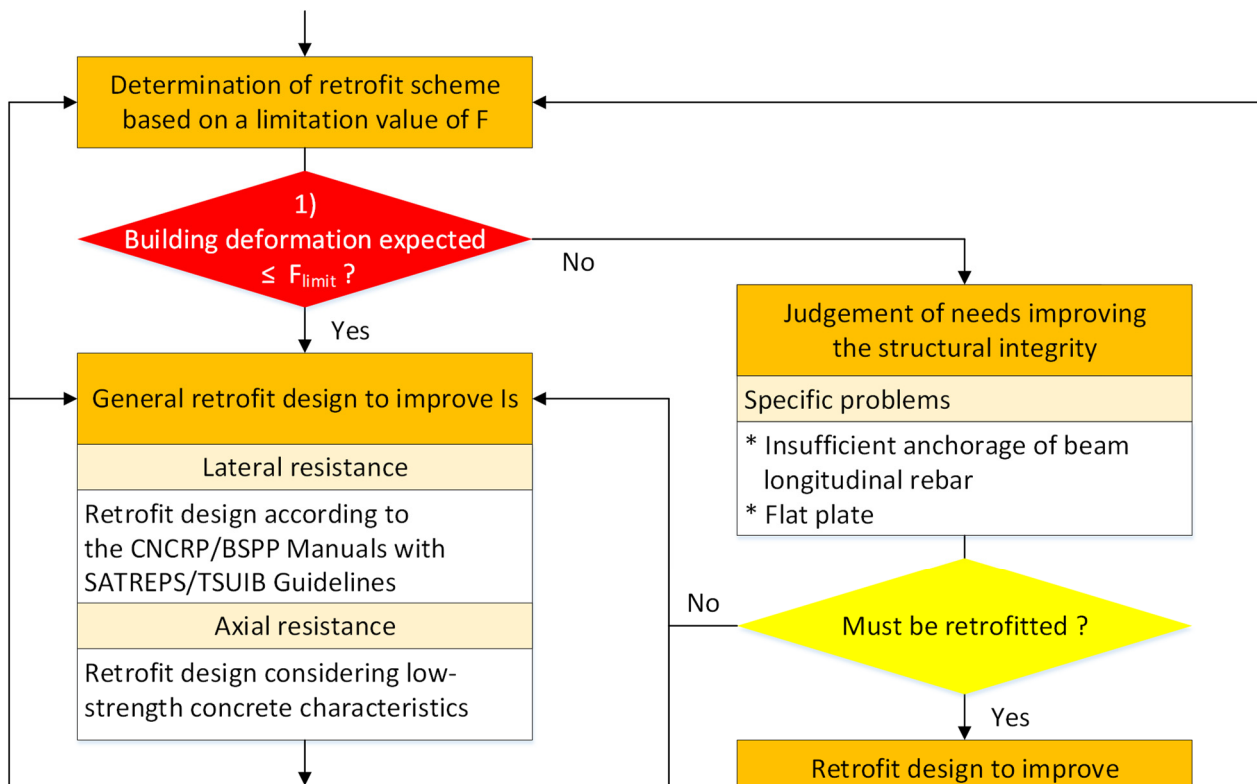


Figure C.3.1.1 Close-up of the first judgement in the general design flow diagram

3.1.3 Design criteria

To prevent brittle anchorage failure of beam longitudinal rebar and to provide appropriate anchorage, the following equation shall be satisfied:

$$l_w \geq l_d - {}_{ex}l_d \quad (3.1.1)$$

where

- l_w : wing wall length for seismic strengthening.
- l_d : demand for anchorage length of beam longitudinal rebar, which can be referred other design standards, such as BNBC and ACI.
- ${}_{ex}l_d$: existing anchorage of beam longitudinal rebar. If there is no information on the anchorage length, use 2/3 times the depth of the column to which the beam longitudinal rebar is anchored.

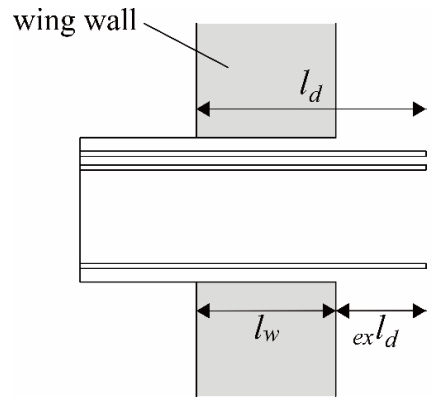


Figure 3.1.1 Wing wall length determination

3.1.4 Failure mechanism identification after wing wall installation

A joint strengthened using the method mentioned above (with the wing wall installation) will be sufficient to prevent pullout failure of beam longitudinal rebar, as well as joint shear failure. The prevention of these failure modes affects the failure mode and shear resistance of an exterior column (with wing wall(s)) connected to the joint. The column failure mode is identified as that showing the minimum of the following shear resistances: ${}_{cw}Q_{mu}$ and ${}_{cw}Q_{su}$, also giving its shear resistance.

${}_{cw}Q_{mu}$ and ${}_{cw}Q_{su}$ are evaluated according to the CNCRP Manual for Seismic Evaluation of Existing Reinforced Concrete Buildings.

3.1.5 Strength index C and Ductility index F of exterior columns with wing wall(s)

The C-index and F-index of exterior columns with wing wall(s) follow those provided by the CNCRP Manual for Seismic Evaluation of Existing Reinforced Concrete Buildings.

C.3.1.3-5 [Commentary]

An experimental study was conducted under the SATREPS-TSUIB project to verify the effectiveness of the wing wall installation to prevent the brittle pullout failure of beam longitudinal rebar.

Two 0.7-scale plane frame replicas of the exterior joint were prepared, namely J1 and J1-W, as shown in **Fig. C.3.1.2**. The specimens were modeled up to the middle points of the upper/lower column and beam; however, the lengths of pin supports attached to the column ends and beam end were included. The specimens were designed with the straight anchorage of beam longitudinal bars into the joint. The existing development length ($_{ex}l_d$) was 235 mm, which was much shorter than the requirement of 579 mm. J1 was the benchmark specimen, representing the original frame without retrofitting. J1-W was the retrofitted specimen featuring wing walls installed along the upper and lower columns. The length of the wing walls was 360 mm, which was determined using Eq. (3.1.1) in Section 3.1.3. The thickness of wing walls was designed according to the Japanese guidelines²⁾ for the seismic retrofit of RC buildings, in which the thickness of wing wall should not be less than 200 mm; hence, the thickness of the wing walls was set to 140 mm for the 0.7-scale model. The post-installed anchors were placed to connect the wing walls and the existing frame. The spacing between the anchors and cover concrete was also based on the Japanese guidelines. The embedment length of the beam and column anchors into the existing frame was 130 mm ($13d_a$). The anchorage length of the anchors into the wing walls was 200 mm ($20d_a$). The vertical and horizontal reinforcements of wing walls used double layers of D10 bars. The reinforcements of wing walls were designed to be not less than a minimum reinforcement ratio based on the Japanese guidelines and to be greater than the total sectional area of the beam/column anchors. To prevent the splitting failure of the concrete, $\phi 6$ spirals were installed at the boundaries between the wing walls and the frame.

Figure C.3.1.3 shows the experimental results of both specimens. J1 reached the maximum strength at $R = +1.5\%$ rad. After that, diagonal cracks increased in the joint region. Then, wide opening of a vertical crack was observed on the beam-column junction, indicating the pullout of bottom beam longitudinal bars. The damage to the benchmark specimen, J1, was concentrated in the joint region. The specimen failed in shear at the joint before beam yielding during positive loading. However, during negative loading, the strength significantly decreased after the cycle to $R = -2\%$ rad due to the pullout of bottom beam longitudinal bars. The strength deterioration during negative loading was much more significant than that which occurred during positive loading, indicating that anchorage failure due to the pullout of beam longitudinal bars exhibited more brittle behavior than joint shear failure.

As for J1-W, during the cycle to $R = +0.5\%$ rad, flexural-shear cracks appeared at the beam end attached to the wing walls, and the bottom beam longitudinal bars at the wall face yielded under negative loading. During the cycle to $R = +1.5\%$ rad, the top beam longitudinal bars at the wall face yielded, and the maximum strength was observed under positive loading. The maximum strength under negative loading was observed during the cycle to $R = +2\%$ rad. J1-W's strength was increased by 2.1 and 1.7 times compared with that of J1 during positive and negative loading, respectively. After that, concrete crushing of the beam was observed at the wing wall end, indicating shear failure of the beam. There was no obvious damage to the wing walls. In the case of

the retrofitted specimen, J1-W, the beam suffered damage at the wing wall ends, indicating a beam yielding mechanism; thus, the joint shear failure and anchorage failure observed in J1 was successfully prevented.

Ductility index F shall be calculated according to the CNCRP/BSPP Manuals which follows the Japanese guidelines. In the Japanese guidelines, the ductility index F of a column with wing wall(s) is limited within $F < 2$. However, the length of wing wall(s) is not so large for satisfying the development length requirement and prevention of pullout failure, as shown in section 3.1.3 of the present guideline. In the case of such short wing wall(s), it might be possible to expect larger ductility. Further research is needed.

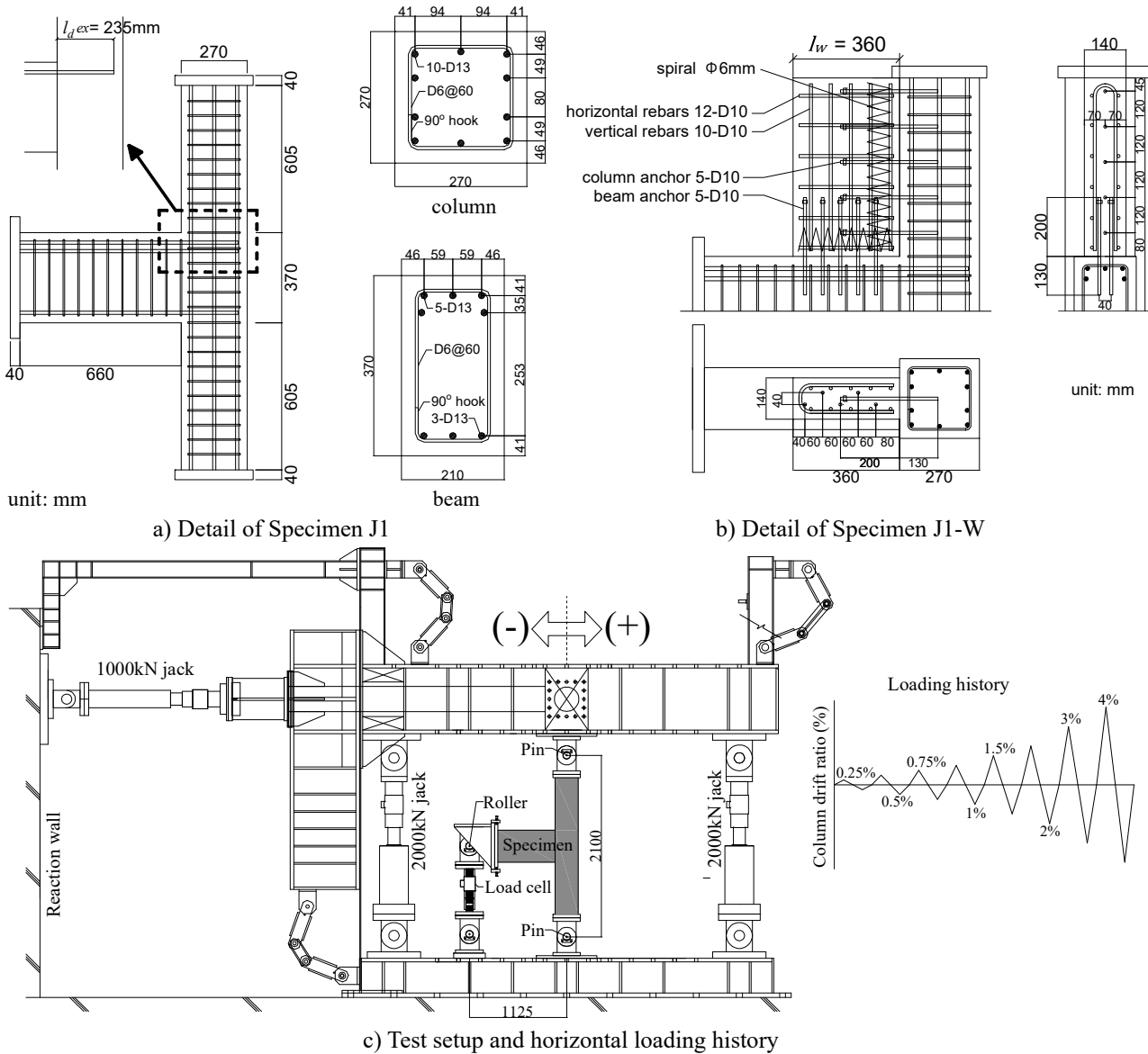
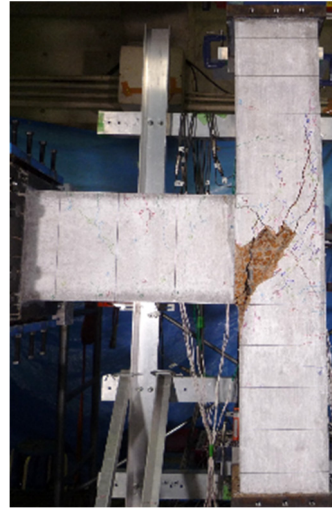
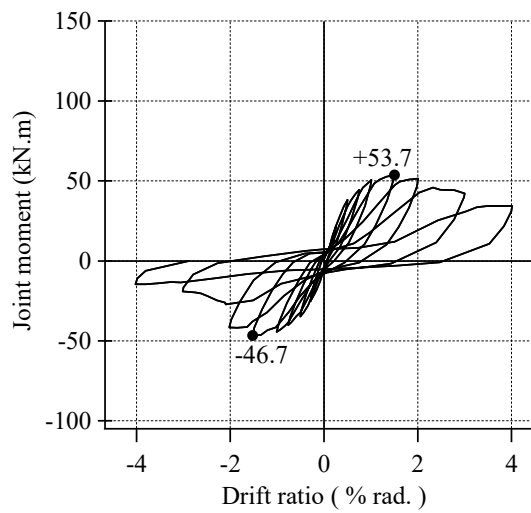
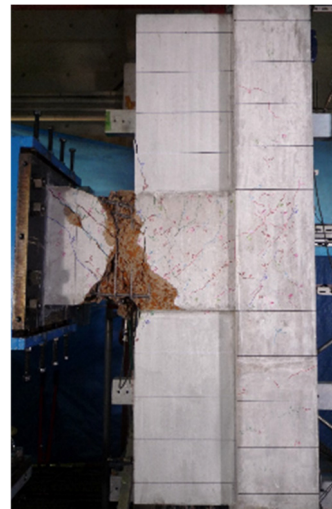
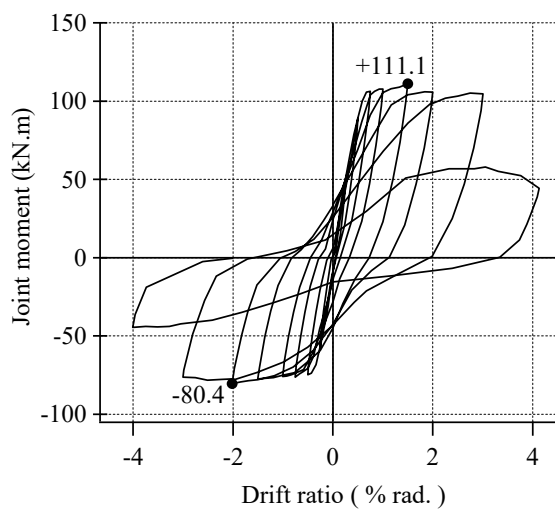


Figure C.3.1.2 Specimens and loading scheme



a) Joint moment–drift ratio relationship and final damage of specimen J1



b) Joint moment–drift ratio relationship and final damage of specimen J1-W

Figure C.3.1.3 Experimental results

References

- [1] Syafri Wardi, Yasushi Sanada, Nandita Saha and Susumu Takahashi: Improving integrity of RC beam-column joints with deficient beam rebar anchorage, *Earthquake Engineering & Structural Dynamics*, Vol. 49, Issue 3, pp. 234-260, March 2020, DOI: 10.1002/eqe.3229
- [2] Japan Building Disaster Prevention Association: English Version, 1st Guidelines for Seismic Retrofit of Existing Reinforced Concrete Buildings, 2001, January 2005

3.2 Flat plate-column joint

3.2.1 General

- (1) This section is to be applied for seismic retrofit of flat plate-column joint.
- (2) Application of wing wall(s) and drop panel prevents flat plate-column joint from punching shear failure.

C.3.2.1 [Commentary]

This section introduces the seismic retrofit of existing RC structures with flat plate-column joints, following the seismic evaluation according to “*Technical Guidelines for Seismic Evaluation of Existing Reinforced Concrete Buildings for Extended Application of BSPP Seismic Evaluation Manual (Chapter 6)*”. Therefore, the scope of application is existing RC structures with flat plate-column joints, which also have beams on their perimeter, as illustrated in the Technical Guidelines.

Fig. 3.2.1.1 shows a flowchart for seismic retrofit of existing RC structures with flat plate-column joints.

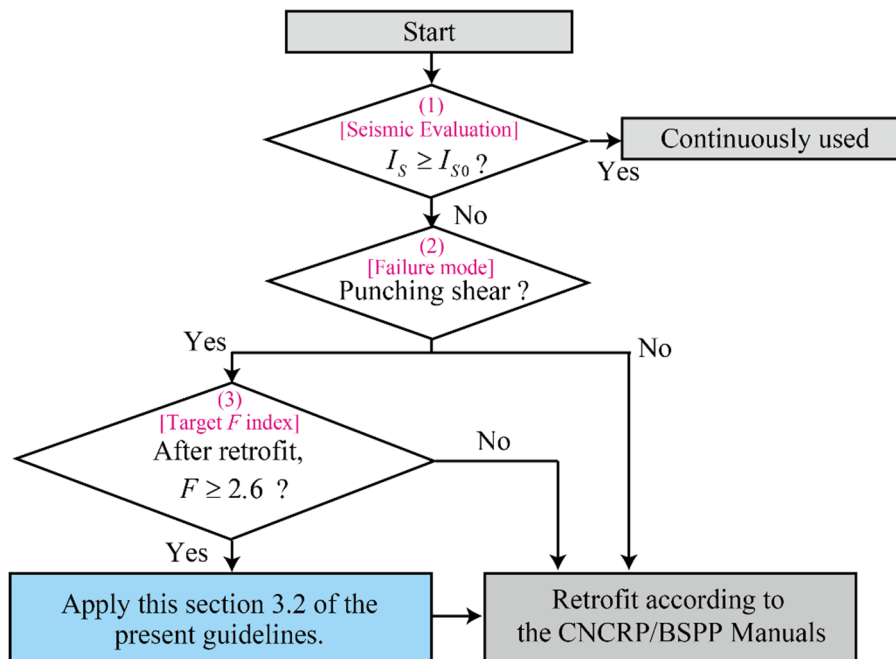


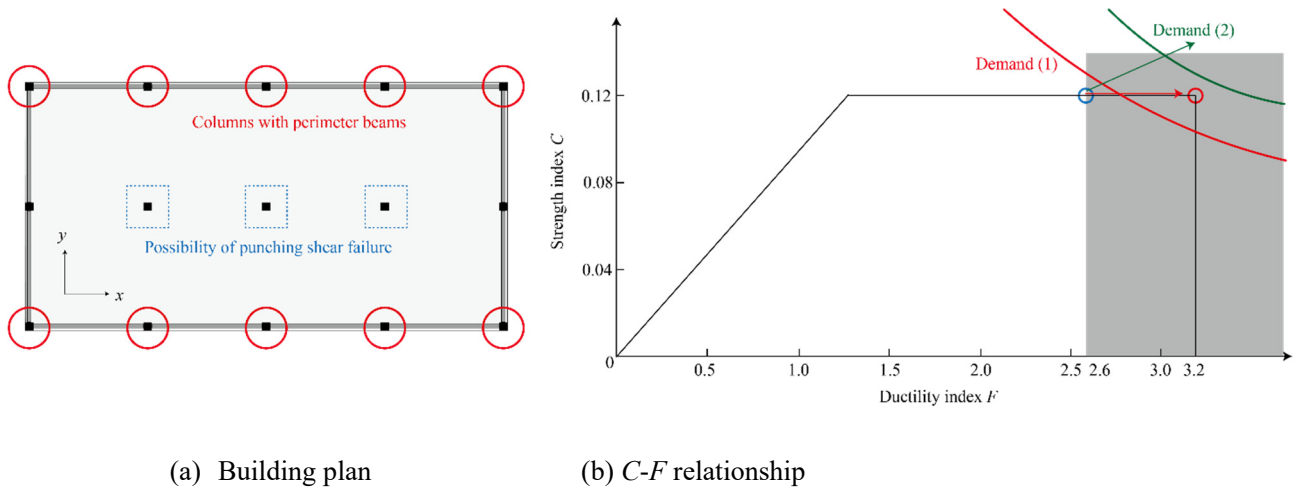
Figure 3.2.1.1 Flowchart for seismic retrofit of existing RC structures with flat plate-column joints

The following illustrates the above flowchart step by step.

(1) The seismic retrofit is needed when the seismic index of an existing RC structure with flat plate-column joints (I_s) does not satisfy the seismic demand (I_{s0}). When the seismic index is evaluated for the structure with flat plate-column joints, as explained in the Technical Guidelines for seismic evaluation, the strength contribution of columns without beam, namely, columns jointed with flat plate, is completely neglected in the seismic evaluation.

(2) If the punching shear failure of the columns without beam is not expected, the seismic retrofit design will be performed according to the CNCRP/BSPP Manuals.

(3) Otherwise, necessity of retrofitting flat plate-column joints according to this section shall be considered based on a target F index after retrofit of the existing RC structure with flat plate-column joints. If the target F index does not exceed 2.6, the punching shear failure will not happen; thus, the retrofitting of flat plate-column joints is not needed. Namely, the seismic retrofit design will be performed according to the CNCRP/BSPP Manuals. On the other hand, if the target F index exceeds 2.6, this section shall be applied. Figure 3.2.1.2 shows an example which represents a typical flat plate structure with perimeter beams. Focusing on the seismic evaluation of x -direction, the contributions of the columns with beams enclosed by the red circles are considered. Figure 3.2.1.2(b) shows the C - F relationship by the black lines and the red circle at $F = 3.2$ in the case that the flat plate-column joints enclosed by the blue squares do not fail in punching shear. In contrast, the blue circle at $F = 2.6$ in **Fig. 3.2.1.2(b)** indicates the upper limit when the flat plate-column joints enclosed by the blue squares fail in punching shear. Then, the seismic indexes of the former and latter cases are $0.12 \times 3.2 = 0.384$ and $0.12 \times 2.6 = 0.312$, respectively. Therefore, if the seismic demand is between 0.312 and 0.384 (the red line in the figure), the seismic retrofit to prevent punching shear failure of the flat plate-column joints is effective to exceed the demand. In this case, drop panel will be adopted for retrofit. If the seismic demand is greater than 0.384 (the green line in the figure), wing wall(s) will be more effective because it contributes not only to prevent punching shear failure but also to increase the strength.



(a) Building plan

(b) C - F relationship

Figure 3.2.1.2 An example of flat plate structure to which this section is applied

3.2.2 Application of wing wall

3.2.2.1 General

- (1) Wing wall(s) can be applied to prevent flat plate-column joint from punching shear failure increasing the lateral load-carrying capacity of the column.
- (2) The contribution of columns without beam retrofitted by wing wall(s) can be considered in the lateral load-carrying capacity according to the present guidelines.
- (3) The contribution of columns with beams retrofitted by wing wall(s) can be evaluated according to the CNCRP/BSPP Manuals.

C.3.2.2.1 [Commentary]

(1) To prevent the punching shear failure of flat plate-column joint, the flowchart shown in **Fig. 3.2.2.1** is applied. First, wing wall(s) is designed; the dimension of wing wall(s) and the reinforcing detail in wing wall(s) are decided. To prevent the punching shear failure, the nodal moments at flexural capacity of slab (M_{slab}) and punching shear capacity (M_{punch}) are compared. The flexural capacity of slab (M_{slab}) is calculated by Eq. (C.3.2.2.1) assuming the moment diagram shown in **Fig. 3.2.2.2**.

$$M_{slab} = \frac{l}{l/2} \times \left(\frac{l}{2} + l_w + \frac{D_c}{2} \right) + \frac{r}{l/2} \times \left(\frac{l}{2} + l_w + \frac{D_c}{2} \right) \quad (C.3.2.2.1)$$

where lM_{slab} and rM_{slab} are calculated according to “*Technical Guidelines for Seismic Evaluation of Existing Reinforced Concrete Buildings for Extended Application of BSPP Seismic Evaluation Manual* (Chapter 6)”.

The punching shear capacity (M_{punch}) is calculated according to the following section. If M_{punch} is smaller than M_{slab} , go back to design of wing wall(s) because the purpose of the installation of wing wall(s) is to prevent punching shear failure.

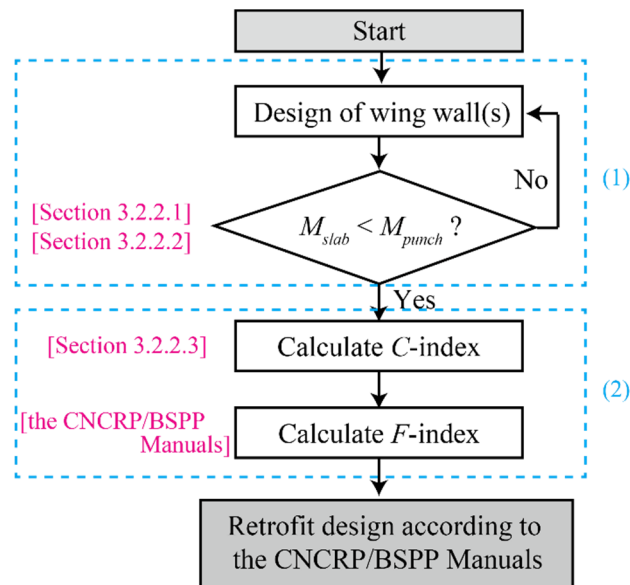


Figure 3.2.2.1 Flowchart of seismic retrofit of existing RC flat plate-column joint by wing wall(s)

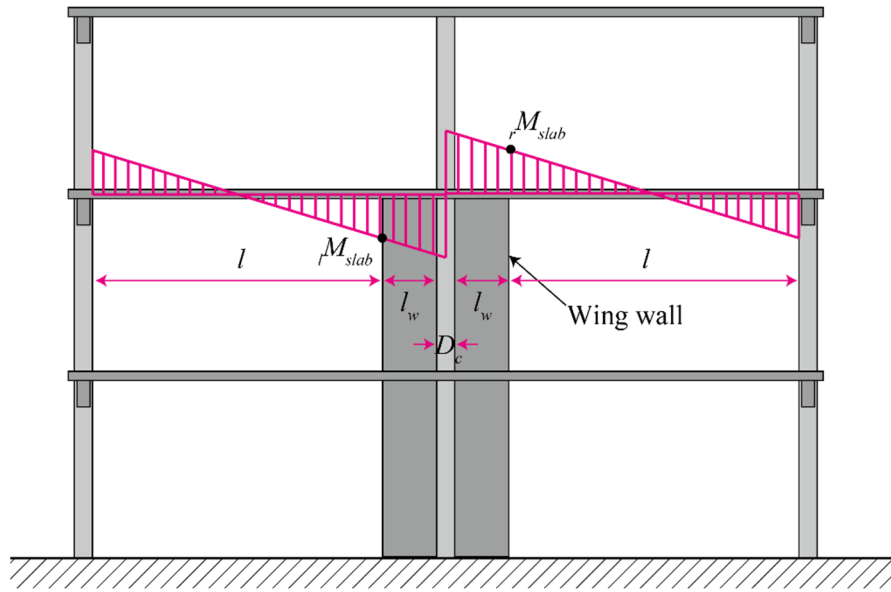


Figure 3.2.2.2 Moment diagram of flat plate retrofitted by wing wall(s)

In the case of the interior column (C5) shown in section 6.2 in the present guidelines, which is expected to fail in punching shear failure, the wing walls of 300 mm length (equal to the column depth) can prevent the column from punching shear failure (**Fig. 3.2.2.3**). The punching shear capacity (M_{punch}) of the column before retrofitting was 278 kNm whereas the nodal moment at the flexural yielding of slab was 301(=105+196) kNm, as shown in **Fig. 3.2.2.4(a)**. After retrofitting by wing walls, the punching shear capacity of the column with wing walls was improved to be 579 kNm. Although the nodal moment at the flexural yielding of slab also increased by the installation of wing walls because the slab yields at the face of the wing walls, as shown in **Fig. 3.2.2.4(b)**, that of 374(=144+230) kNm was smaller than the punching shear capacity. It is found that wing wall(s) immensely increases the punching shear capacity.

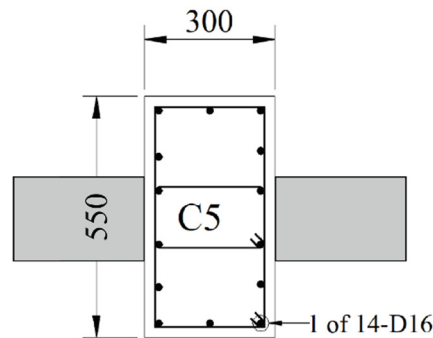


Figure 3.2.2.3 Column with wing walls

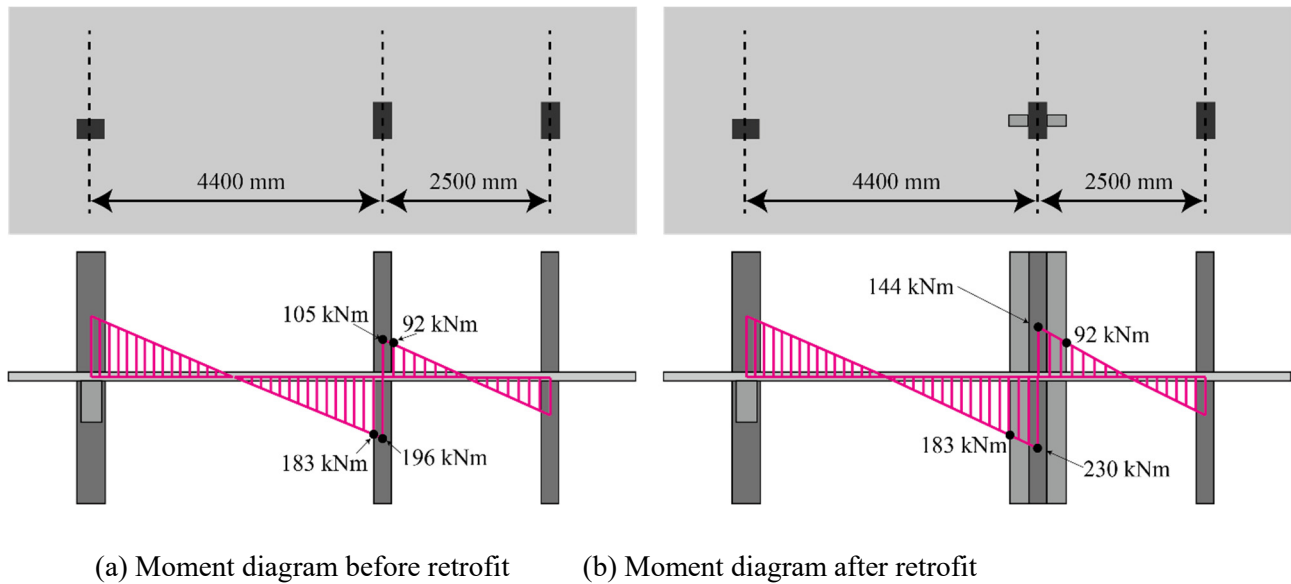


Figure 3.2.2.4 The nodal moment at the flexural yielding of slab

(2) The contribution of columns without beam retrofitted by wing wall(s) can be considered in the lateral load-carrying capacity, therefore, strength index C and ductility index F are calculated according to section 3.2.2.3 of the present guidelines and the CNCRP/BSPP Manuals, respectively.

(3) If wing wall(s) is installed to columns with beams to satisfy the seismic demand, the contribution of columns with beams retrofitted by wing wall(s) can be evaluated according to the CNCRP/BSPP Manuals (section 3.4).

3.2.2.2 Punching shear capacity of a flat plate-column joint with wing wall(s)

(1) In-plane wing wall

When the wing wall(s) is installed parallel to the seismic force direction, the punching shear capacity (M_{punch}) of a flat plate-column with wing wall(s) joint shall be evaluated according to “*Technical Guidelines for Seismic Evaluation of Reinforced Concrete Buildings for Extended Application of BSPP Seismic Evaluation Manual* (Chapter 6)”. The critical section can be $d/2$ distant from the column/wing wall(s) face where d is the effective depth of the slab.

(2) Out-of-plane wing wall

When the wing wall(s) is installed perpendicular to the seismic force direction, the punching shear capacity (M_{punch}) of a flat plate-column with wing wall(s) joint shall be evaluated according to “*Technical Guidelines for Seismic Evaluation of Existing Reinforced Concrete Buildings for Extended Application of BSPP Seismic Evaluation Manual* (Chapter 6)”. The critical section can be $d/2$ distant from the column

C.3.2.2.2 [Commentary]

The critical section of punching shear failure shown in **Fig. 3.2.2.5** can be applied to Eqs.(6.3.9)-(6.3.13) in “*Technical Guidelines for Seismic Evaluation of Reinforced Concrete Buildings for Extended Application of*

BSPP Seismic Evaluation Manual (Chapter 6)” which is based on the experimental study conducted in the SATREPS-TSUIB project (Samdani et al., 2021).

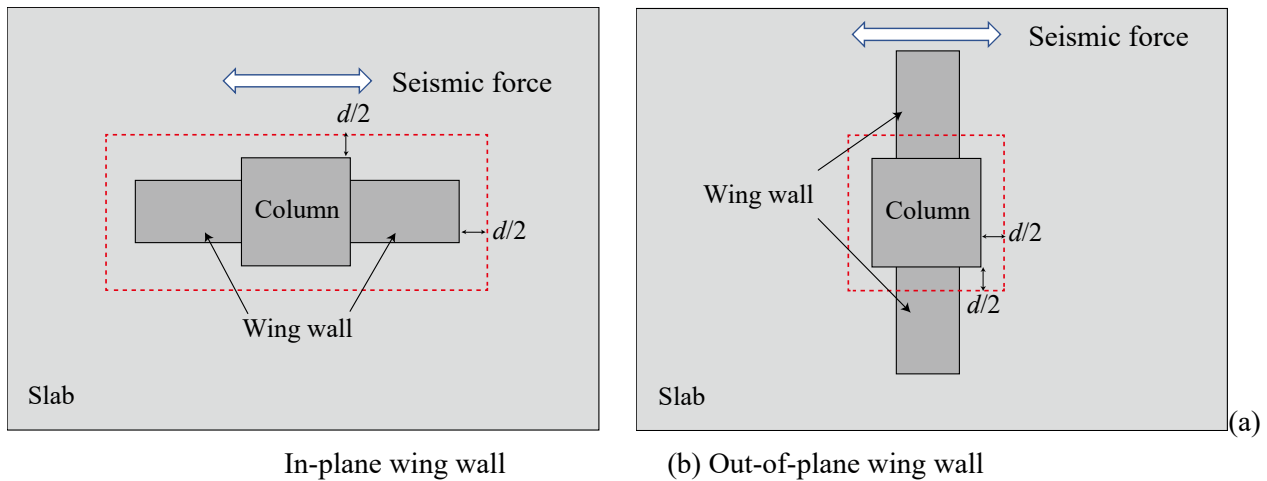
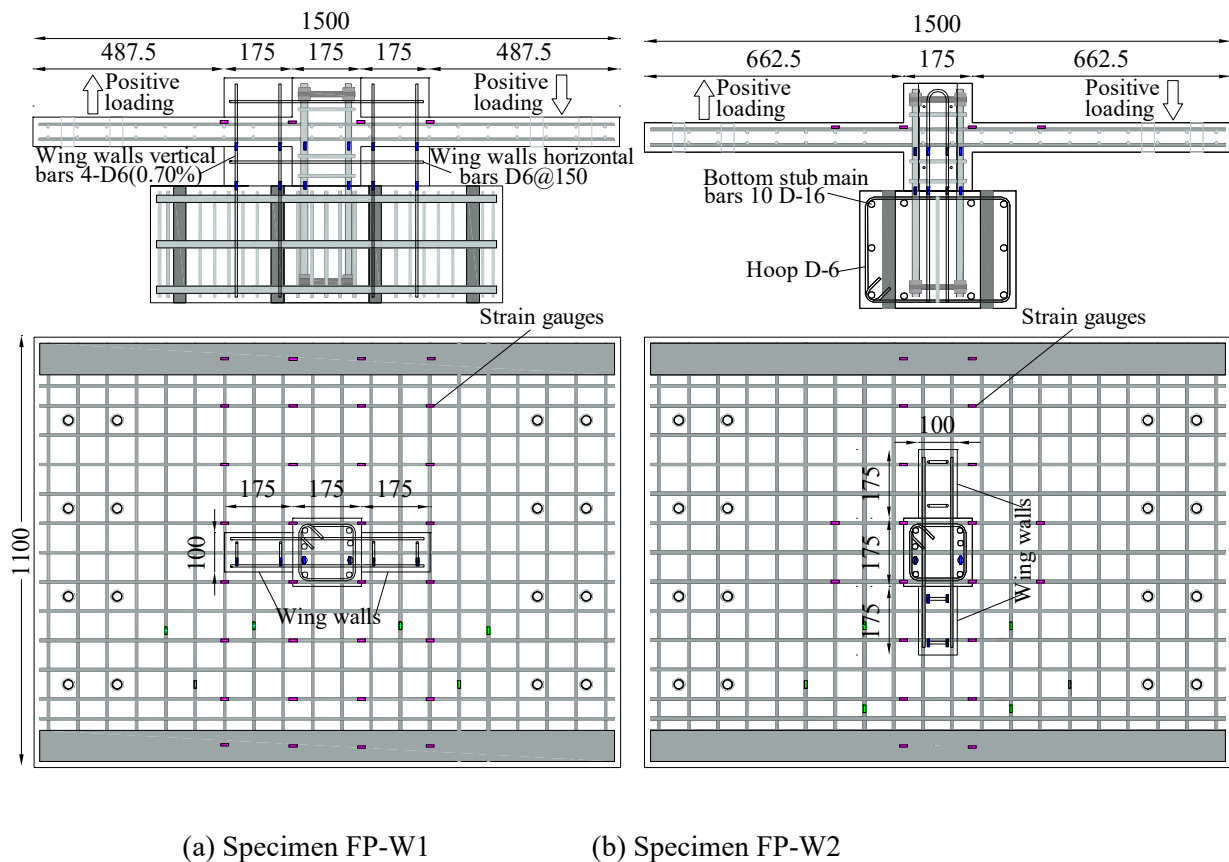


Figure 3.2.2.5 Critical section of punching shear failure

The experimental study was conducted to verify the effectiveness of wing wall(s) installation to prevent the punching shear failure of the flat plate-column joints. Figure 3.2.2.6 shows the specimens of flat plate-column joint retrofitted by wing walls. A schematic view of the experimental setup of the flat plate specimen is shown in **Fig. 3.2.2.7**. Vertical reversed cyclic loads with increasing amplitude were applied to the plate ends, which represented the bending moment distribution near the plate and column junction under earthquake loading.



(a) Specimen FP-W1

(b) Specimen FP-W2

Figure 3.2.2.6 Specimens

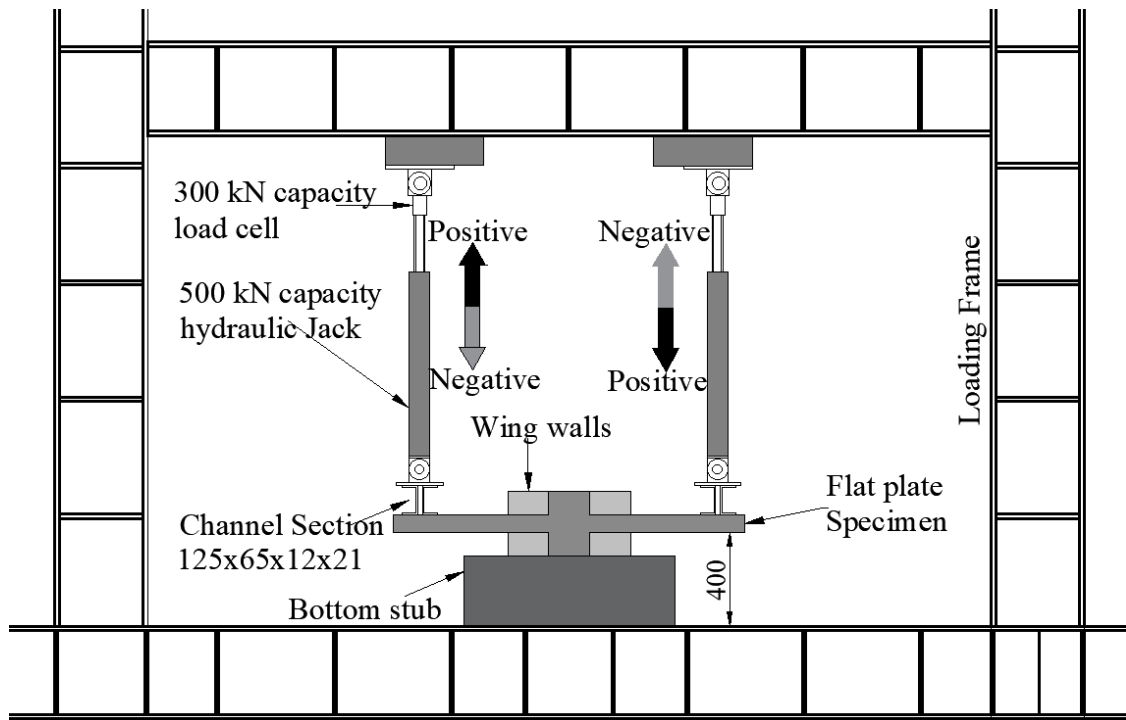
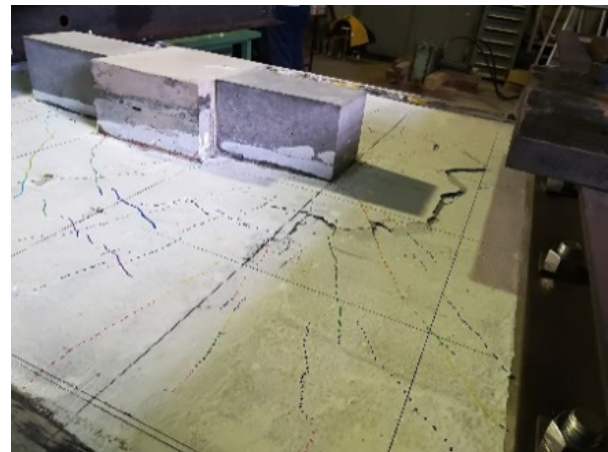
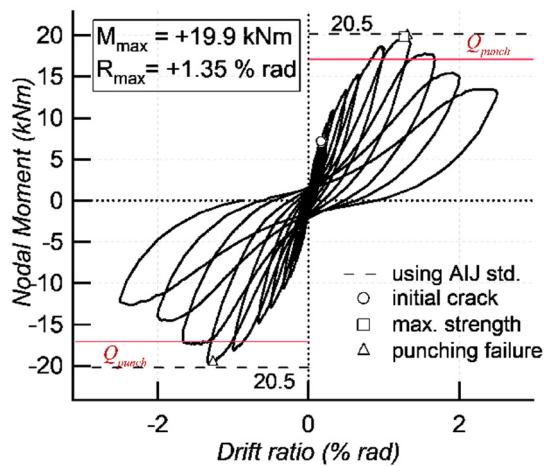
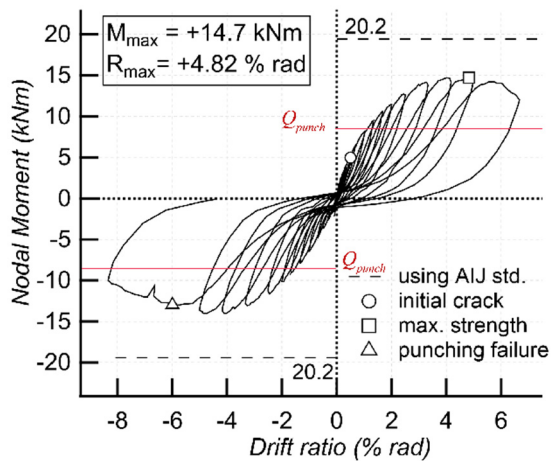


Figure 3.2.2.7 Outline of experiment



(a) Load-drift relationship (b) Punching shear failure

Figure 3.2.2.8 Experimental result (Specimen FP-W1)



(a) Load-drift relationship (b) Punching shear failure

Figure 3.2.2.9 Experimental result (Specimen FP-W2)

The maximum moment strength of specimen FP-W1, which was strengthened with wing walls installed along the loading direction of the column (in-plane wing walls), was 19.9 kNm (**Fig. 3.2.2.8**) and was 1.15 times the calculated strength based on the critical section shown in **Fig. 3.2.2.5(a)**. The failure area almost agreed with the critical section shown in **Fig. 3.2.2.5(a)**. The maximum moment strength of specimen FP-W2, which was strengthened with wing walls along the orthogonal loading direction of the column (out-of-plane wing walls), was 14.7 kNm (**Fig. 3.2.2.9**) and was 1.77 times the calculated strength based on the critical section shown in **Fig. 3.2.2.5(b)** because the wing walls were not considered for the conservative estimation. In the case of specimen FP-W2, the yielding of slab reinforcements was observed before the punching shear failure, which indicated that the punching shear capacity of this specimen was not fully obtained from this experiment. Therefore, the conservative estimation shown in **Fig. 3.2.2.5(b)** is adopted in the present guidelines. Further research is needed.

3.2.2.3 Strength index C and ductility index F of a column connected to flat plate retrofitted by wing wall(s)

(1) Lateral load-carrying capacity

Lateral load-carrying capacity of a column without beam retrofitted by with wing wall(s) installed parallel to the seismic force direction can be considered under the condition of $M_{slab} < M_{punch}$. In the present guidelines, it shall be evaluated by the following equation.

$$Q_u = \frac{{}_cM_w}{h} = \frac{{}_cM_w + N \cdot M_{slab}}{H} \leq \frac{2{}_cM_w}{H} \quad (3.2.2.1)$$

where, ${}_cM_w$: the flexural capacity of a column without beam retrofitted by with wing wall(s),

h : inflection height from the bottom of wing wall(s),

N : the number of stories installed wing wall(s),

H : the total height of wing wall(s).

(2) Strength index C

Strength index C shall be calculated following the CNCRP/BSPP Manuals (Chapter 3) by using Q_u from Eq. (3.2.2.1).

(3) Ductility index F

Ductility index F shall be calculated following the CNCRP/BSPP Manuals (Chapter 3).

C.3.2.2.3 [Commentary]

(1) In the calculation of lateral load-carrying capacity of a column without beam retrofitted by with wing wall(s), the moment diagram shown in **Fig. 3.2.2.10** is assumed because the column with wing wall(s) is likely to form a flexural hinging at the bottom considering the slender shape as exemplified above. As shown in the

figure, assuming uniform shear force distribution along the height, Eq. (3.2.2.1) is derived and the obtained Q_u is applied to multi-stories concerned (namely, the first and second stories in the figure). When the flexural capacity of slab is large enough, a flexural hinging is formed at the top of the wing wall(s), therefore, Q_u cannot exceed $2c_w M_w/H$. In the present guidelines, the wing wall(s) installed parallel to the seismic force direction is only considered because the flexural capacity of a column with wing wall(s) will much larger than that of a column when the wing wall(s) is installed to this direction.

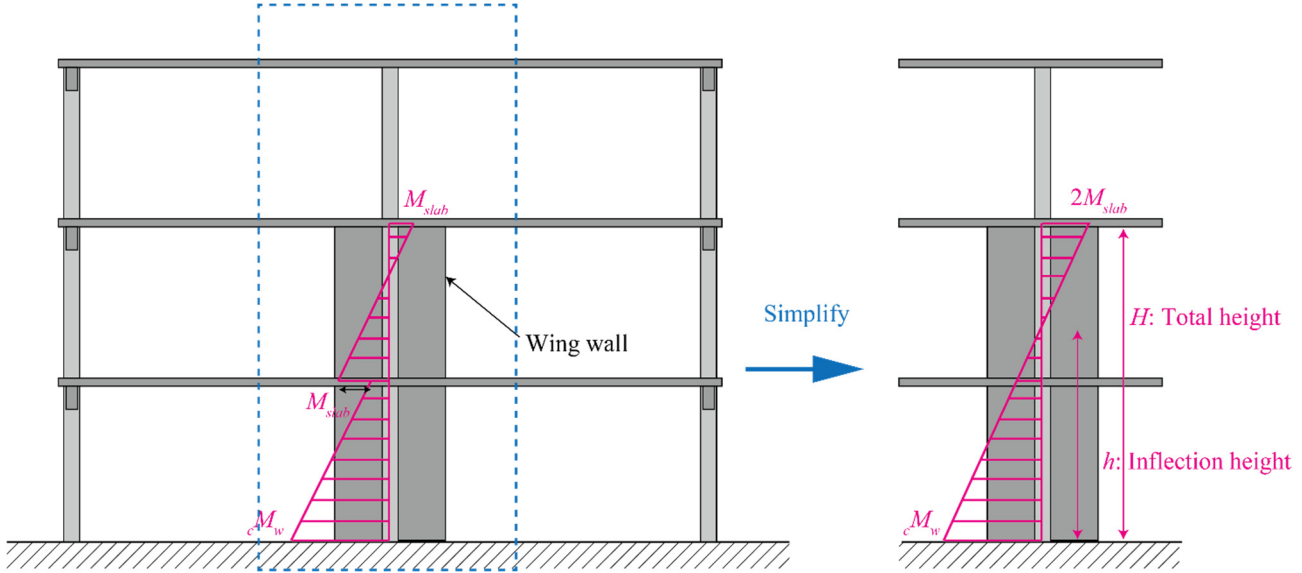


Figure 3.2.2.10 Assumed moment diagram

(2) Strength index C shall be calculated by $C = Q_u / \Sigma W$, where Q_u is calculated from Eq. (3.2.2.1) and ΣW is the weight of the building including live load for seismic calculation supported by the story concerned.

(3) Ductility index F shall be calculated according to the CNCRP/BSPP Manuals (Chapter 3) which follows the Japanese guidelines. In the Japanese guidelines, the ductility index F of a column with wing wall(s) is limited within $F < 2$, which is smaller than the upper limit due to punching shear failure in the present guidelines. However, the length of wing wall(s) is not so large for preventing punching shear failure, as shown in section C.3.2.2.1 of the present guidelines. In the case of such short wing wall(s), it might be possible to expect larger ductility. Further research is needed.

3.2.3 Application of drop panel

3.2.3.1 General

- (1) Drop panel can be applied to prevent flat plate-column joint from punching shear failure.
- (2) The contribution of columns without beams retrofitted by drop panel can not be considered in the lateral load-carrying capacity.
- (3) The upper limit of ductility index F can be removed by preventing flat plate-column joint from punching shear failure.

C.3.2.3.1 [Commentary]

(1) To prevent the punching shear failure of flat plate-column joint, the flowchart shown in **Fig. 3.2.3.1** is applied. First, drop panel is designed; the dimensions of drop panel and the reinforcing detail in drop panel are planned. To identify the failure mode, the flexural capacity of slab (M_{slab}) and punching shear capacity (M_{punch}) are compared. The flexural capacity of slab (M_{slab}) is calculated by assuming the moment diagram shown in **Fig. 3.2.3.2**.

$$M_{slab} = \frac{l}{l/2} \times \left(\frac{l}{2} + \frac{l_d}{2} \right) \times \frac{r}{l/2} \times \left(\frac{l}{2} + \frac{l_d}{2} \right) \quad (C.3.2.3.1)$$

where, lM_{slab} and rM_{slab} are calculated according to the SATREPS-TSUIB Seismic Evaluation Guidelines (Chapter 6).

The punching shear capacity (M_{punch}) is calculated according to the following section. If M_{punch} is smaller than M_{slab} , go back to design of drop panel because the purpose of the installation of drop panel is to prevent punching shear failure.

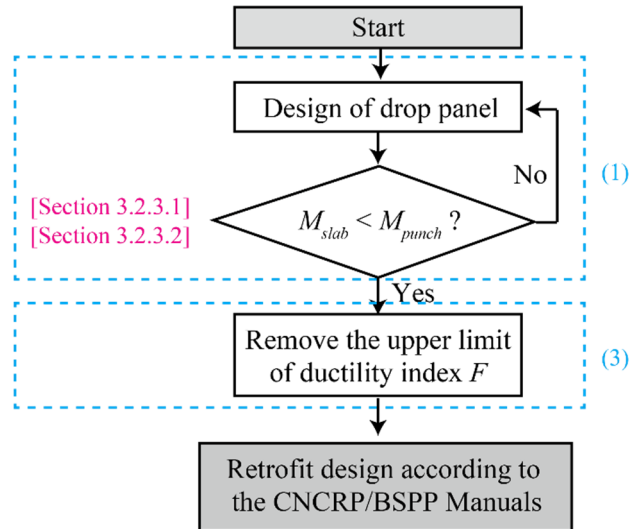


Figure 3.2.3.1 Flowchart of seismic retrofit of existing RC flat plate-column joint by drop panel

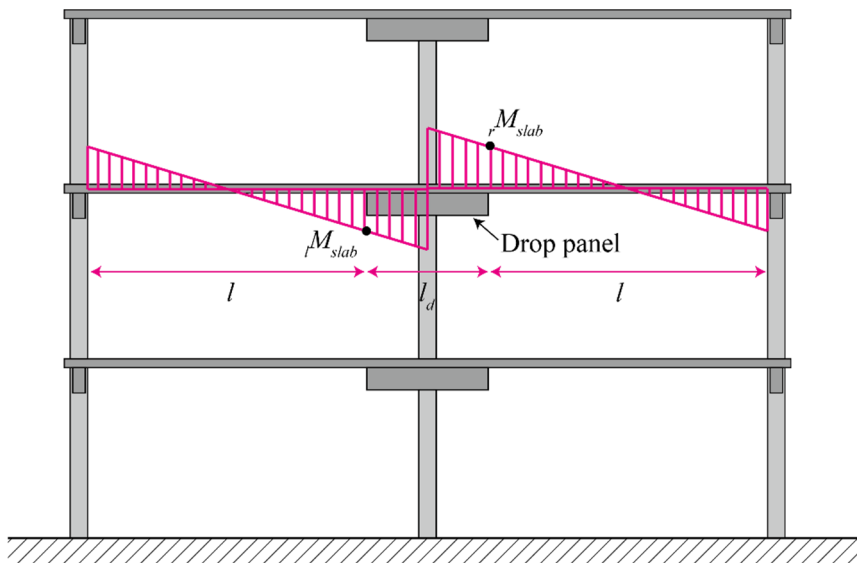


Figure 3.2.3.2 Moment diagram of flat plate retrofitted by drop panel

3.2.3.2 Punching shear capacity of flat plate-column joint with drop panel

- (1) The punching shear capacity (M_{punch}) of a flat plate-column joint with drop panel shall be evaluated according to “*Technical Guidelines for Seismic Evaluation of Existing Reinforced Concrete Buildings for Extended Application of BSPP Seismic Evaluation Manual* (Chapter 6)”. The critical section can be $d/2$ distant from the drop panel face where d is the effective depth of the slab.

C.3.2.3.2 [Commentary]

The critical section of punching shear failure shown in **Fig. 3.2.3.3** can be applied to Eqs.(6.3.9)-(6.3.13) in “*Technical Guidelines for Seismic Evaluation of Existing Reinforced Concrete Buildings for Extended Application of BSPP Seismic Evaluation Manual* (Chapter 6)” which is based on the experimental study conducted in the SATREPS-TSUIB project (Samdani et al., 2020).

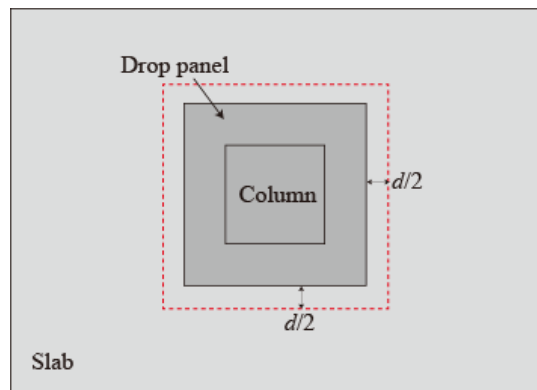
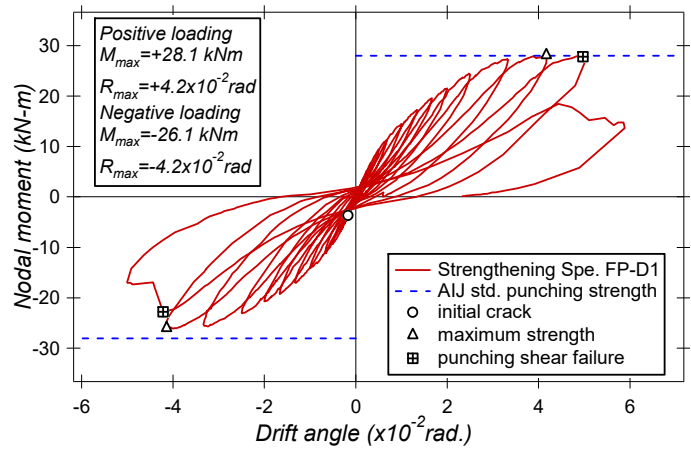


Figure 3.2.3.3 Critical section of punching shear failure

The experimental study was conducted to verify the effectiveness of drop panel installation to prevent the punching shear failure of the flat plate-column joints. A half scaled flat plate specimen (specimen FP-D1) was constructed, and the dimensions of drop panel were $380 \times 380 \times 75$ mm (length \times width \times thickness).

The maximum moment strength of specimen FP-D1, which was strengthened with drop panel, was 28.1 kNm and the calculated strength based on the critical section shown in **Fig. 3.2.2.4** was 28.0 kNm. The punching shear strength was appropriately evaluated. The observed failure surface was also similar to the critical section shown in **Fig. 3.2.2.3**.



(a) Specimen

(b) Load-drift relationship

Figure 3.2.3.4 Experimental result (Specimen FP-D1)

References

- [1] H. M. Golam Samdani, Susumu Takahashi, Rokhyun Yoon, Yasushi Sanada(2021): Strengthening seismically vulnerable reinforced concrete flat plate-column connections by installing wing walls, *Japan Architecture Review*, Vol. 4, Issue 3, pp. 442-454
- [2] H. M. Golam Samdani, Susumu Takahashi, Rokhyun Yoon, Yasushi Sanada (2020): Experimental Study on Flat Plate-Column Connection Made with Low-Strength Concrete Part 5 Effect of Drop Panel, *AIJ Summaries of Technical Papers of Annual Meeting*, pp. 331-332

3.3 Masonry infill wall

3.3.1 General

- (1) This section is to be applied for the structural design of masonry infilled RC frame strengthened with ferrocement (FC), with a view to upgrade the in-plane strength, and construction work.
- (2) Strengthening by ferrocement lamination shall be applied to a masonry infill wall which is judged as a structural element by seismic evaluation.

Definitions

Strength index C : The lateral-load carrying capacity of a member (masonry infill, or RC column) in terms of a shear coefficient, namely the shear capacity normalized by the weight of the building above.

Ductility index F : An index representing the deformation capacity of a structural member.

a_c/h_o ratio: The ratio of contact length of masonry infill to column height.

In-plane failure: A failure mode of masonry infill caused by the load acting horizontally along the wall length.

Out-of-plane failure: A failure mode of masonry infill damaged in a perpendicular direction to the wall surface.

Structural masonry element: An infill that is deemed to contribute to the lateral capacity of a building.

Notations

Q : Ultimate strength of ferrocement strengthened masonry infilled RC frame

Q_1 : Lateral capacity at diagonal compression failure

Q_2 : Lateral capacity at diagonal cracking and sliding failure

Q_3 : Lateral capacity at overall flexural failure

Q_4 : Lateral capacity at column punching and joint sliding failure

Q_c : Lateral strength of column calculated as the minimum strength of Q_{su} , Q_{mu}

W : The weight of the building including live load for seismic calculation supported by the story concerned

$f_{m,\theta}$: Compressive strength of masonry along diagonal

$f_{mor,FC}$: Ferrocement mortar strength

f_m : Prism compressive strength of masonry infill

λ_{mas} : Relative rigidity factor for masonry

λ_{mas-FC} : Relative rigidity factor for ferrocement strengthened masonry

E_{mas} : Young's modulus of masonry infill

E_{FC} : Young's modulus of ferrocement mortar

t_{FC} : Thickness of ferrocement mortar layer

t_{mas} : Thickness of masonry infill

n_s : Number of surface strengthened with ferrocement

A_{mas} : Diagonal area of infill masonry

A_{ym} : Area of mesh reinforcement

S_v : Spacing of horizontal mesh reinforcement

n_L : Number of wire mesh layer in each ferrocement layer
 α : Empirical reduction factor
 $f_{y,wm}$: Yield strength of mesh reinforcement
 l_w : Length of masonry infill
 d_m : Diagonal length of masonry infill
 θ : Inclination angle of masonry wall's diagonal from the horizontal axis
 E_c : Young's modulus of concrete
 I_c : Moment of inertia of RC column
 M_u : Flexural yield moment of the column calculated based on the Japanese standard (JBDPA, 2001).
 h_o : Clear height of RC column
 h_{mas} : Height of masonry infill
 K_{min} : Influence factor considering shear span ratio
 τ_o : Basic shear strength of column
 a : Shear span
 ρ_g : Longitudinal reinforcement ratio of column
 b : Width of column
 d : Depth of column
 f_c : Concrete compression strength
 f_y : Yield strength of longitudinal reinforcement
 τ_{mas} : Bond strength at masonry top
 $\tau_{mor,FC}$: Bond strength at ferrocement top
 $a_{t,col}$: Area of steel of longitudinal reinforcement in tension column.
 l_c : Center to center span length of RC frame
 N : Total axial force on RC columns on both sides of masonry infill wall
 $Q_{mas,cr}$: The contribution of strength of masonry in diagonal cracking
 $Q_{FC,wm}$: The contribution of strength of ferrocement in diagonal cracking failure
 $f_{mas,cr}$: Masonry diagonal cracking strength
 A_{wm} : Area of mesh reinforcement
 $j_s Q_w$: Joint shear capacity
 $\tau_{mor,FC}$: Shear strength (cohesion) of mortar in masonry joint and ferrocement
 $a_{wm,v}$: Cross sectional area of vertical wire mesh/interface reinforcement
 $\tau_{y,wm}$: Shear strength of wire mesh/interface reinforcement
 W_s : Strut width

C.3.3.1 [Commentary]

C.3.3.1.1 Scope of application

- Ferrocement strengthening method is intended to be used for low rise masonry infilled RC frame buildings.
- Ferrocement should be applied to solid infill masonry, which is bounded by RC frame in four sides, to increase in-plane shear strength.

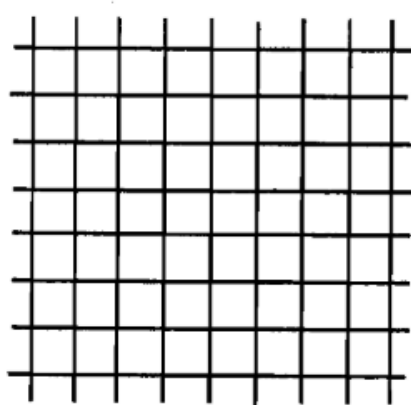
- The strength upgradation of masonry infill with openings (doors, windows etc.) is out of the scope of this guideline.
- This guideline assumed adequate connection between masonry and wire mesh, therefore delamination can be precluded.
- Ferrocement strengthening might not be effective when the contact length ratio (a_c/h) ≤ 0.2 , therefore in that case application of ferrocement is not recommended.
- This evaluation manual should not be applied for RC frames with extremely short column and with extremely high axial load column, where column ductility is very low ($F=0.8$).

3.3.2 Introduction to ferrocement

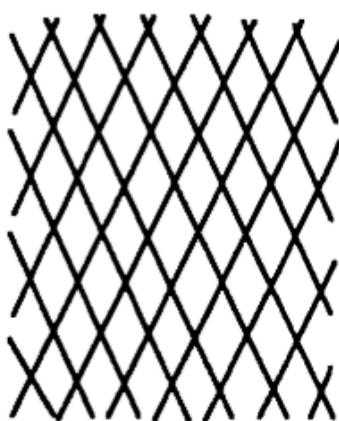
Ferrocement consists of a thin layer of cementitious composite where relatively small size wire meshes, as shown in **Fig. 3.3.1**, are embedded in mortar matrix. In this Guideline, material specifications, as reported in **Table 3.3.1**, are recommended to be used for strengthening of masonry infilled RC frame. General idea of ferrocement strengthening is illustrated in **Fig. 3.3.2**. Initially, mortar layer (1st layer) is applied on both sides of the existing infill masonry, and then wire mesh is placed and fixed to infill masonry by nails. This is followed by the application of 2nd mortar layer. Connection of wire mesh to surrounding RC frame is recommended to prevent delamination and out-of-plane failure in the early stage of shaking during earthquakes.

Table 3.3.1 Material specification

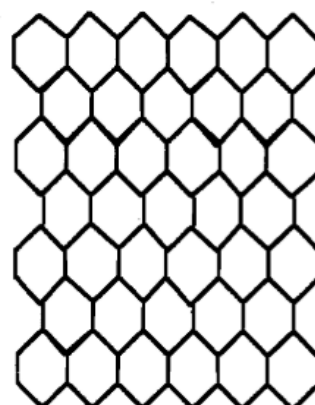
Material	Mortar		Wire mesh	Connection with infill
	Sand to cement ratio (s/c)	Water to cement ratio (w/c)	Type	
Specification	1.4 ~ 2.5	0.3 ~ 0.5	Woven square or rectangular mesh	9 nails/sqm. or more



(a) Square wire mesh



(b) Expanded wire mesh



(c) Hexagonal wire mesh



(d) Section: Woven mesh



(e) Section: Welded mesh

Figure 3.3.1: Different types of wire mesh (Naaman, 2000)

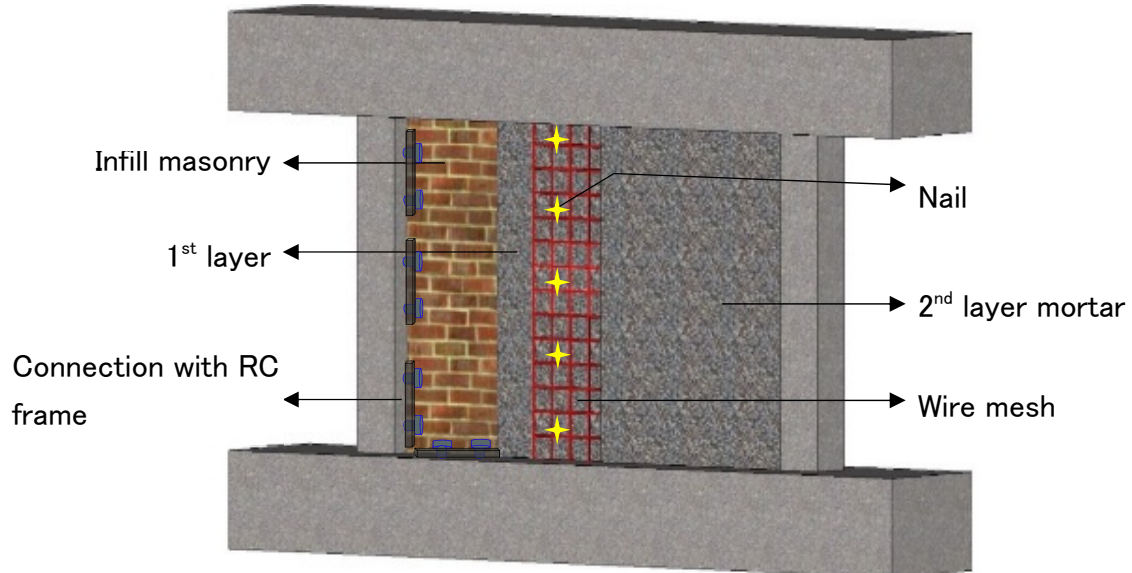


Figure 3.3.2 Schematic diagram of ferrocement strengthened masonry infill

C.3.3.2 [Commentary]

In general, ferrocement refers to a thin layer of cementitious composite where closely spaced layers of continuous and relatively small size wire meshes are embedded in mortar matrix. The mortar matrix of ferrocement consists of Portland cement and sand. The sand to cement ratio is in a range of 1.4 to 2.5 and water to cement ratio (mass basis) of mortar vary between 0.3 and 0.5 (ACI 549R-97, 1997). The reinforcing wire meshes embedded in mortar can be woven mesh, expanded wire mesh, and chicken mesh (hexagonal shape) etc. as shown in **Fig. 3.3.1**. Ferrocement strengthening of masonry refers to application of an initial mortar layer on the both faces of masonry wall which is followed by the placement of steel wire mesh and a second mortar layer, as shown in **Fig. 3.3.2**. Application of cement slurry on the initial mortar layer has been suggested in a retrofitting report in India (Arya & Agarwal, 2007) to have a good bond between first and second mortar layer. On the other hand, several field practice reports (Clarke & Sharma, 1998; Shahzada, 2007) suggested to attach wire mesh directly on infill masonry, which is followed by application of total mortar layer. Generally, nails or clamps are used to attach wire mesh with the masonry, as shown in **Fig. C.3.3.1**. There is no established guideline to calculate the number of connection required to attach wire mesh with masonry, however, Alcocer and Flores (2001) investigated on the effect of number of connectors and suggested nine connectors per square meter of masonry for clay brick masonry strengthening. At the same time dowel connection between existing RC frame and ferrocement layer is also evident in literature.

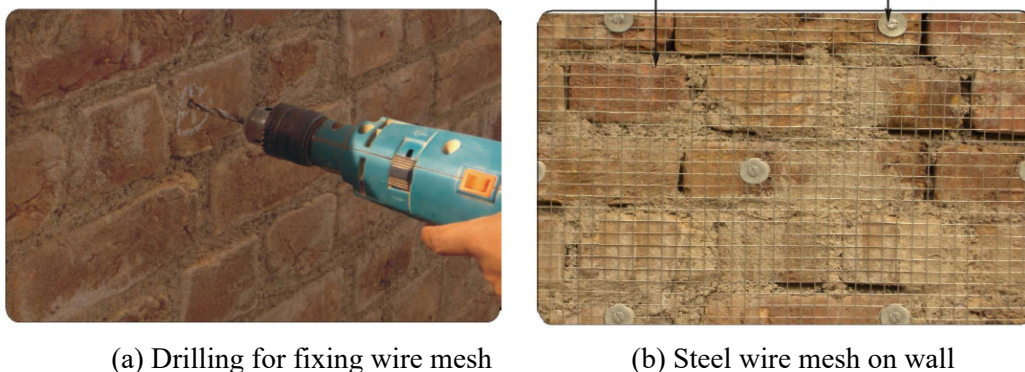


Figure C.3.3.1 Wire mesh attachment process suggested in field of practice in Pakistan (Shahzada, 2007)

3.3.3 General flow of structural design of ferrocement strengthening

Structural design of the ferrocement strengthening for infill masonry shall be conducted by considering following steps. The flow diagram of the design process is also shown in **Fig. 3.3.3**.

(1) **Step-1:** Judgement of applicability of ferrocement (FC) strengthening (Section 3.3.4) shall be made depending on the expected failure mechanism of existing masonry infilled RC frame. The failure mechanism of masonry infill before strengthening is judged by contact length ratio (a_c/h) according to Chapter-4 of “Technical Guidelines for Seismic Evaluation of Existing Reinforced Concrete Buildings in Bangladesh for Extended Application of BSPP Seismic Evaluation Manual”. Seismic in-plane capacity improvement by ferrocement is expected and thus ferrocement can be applied when expected failure mechanism of existing infilled masonry is “diagonal compression” or “sliding-diagonal cracking”.

(2) **Step-2:** Structural design of ferrocement strengthening

Step 2-1: Selection of target failure mechanism (see Section 3.3.5)

Step 2-2: Decide dimension and material of ferrocement (see Section 3.3.6)

Step 2-3: Evaluation Strength Index-C (see Section 3.3.7)

Step 2-4: Evaluation ductility Index-F (see Section 3.3.8)

Step 2-5: Re-confirm of requirement (check capacity and demand)

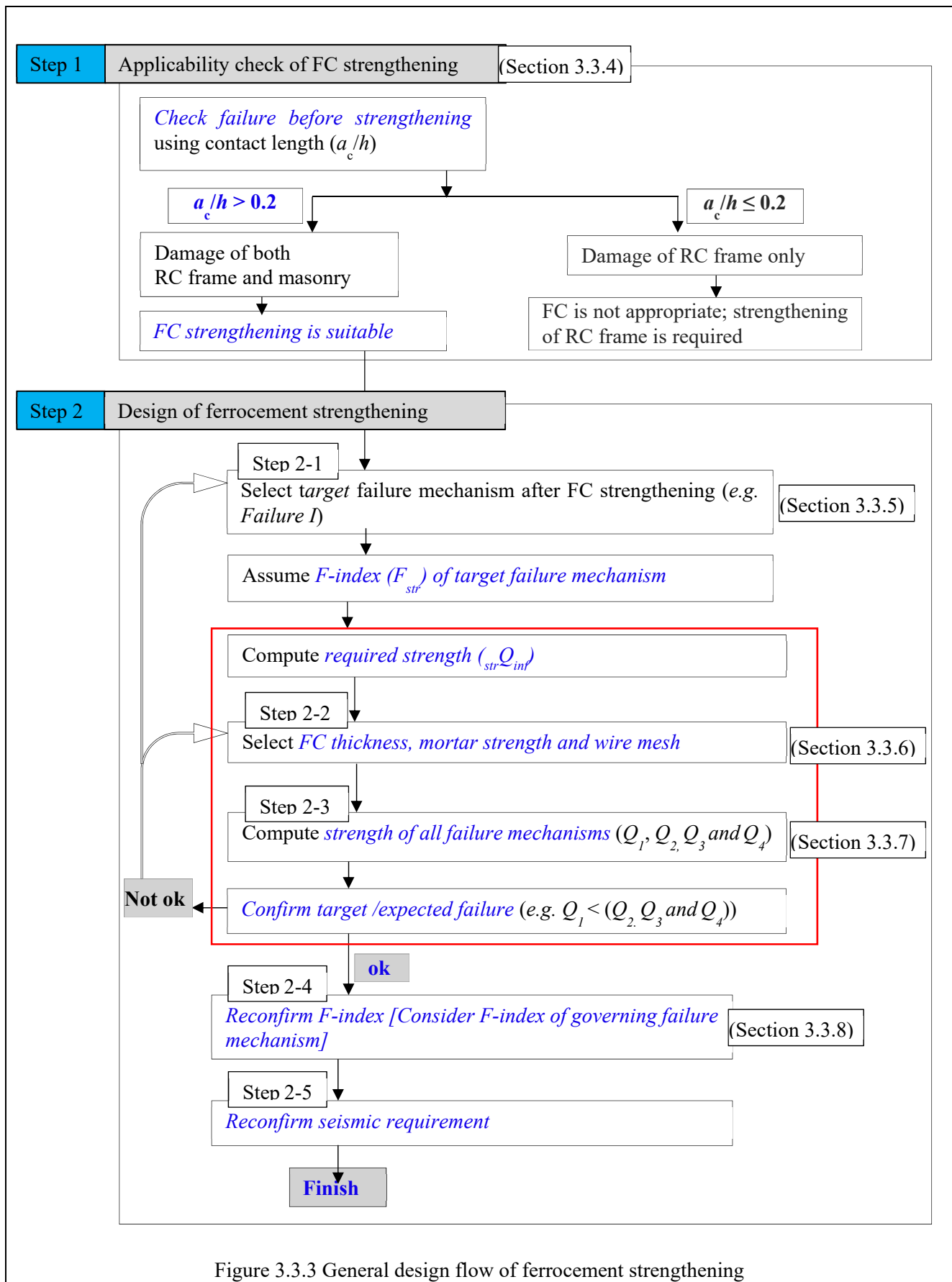


Figure 3.3.3 General design flow of ferrocement strengthening

3.3.4 Judgement of applicability of ferrocement retrofit

(1) Possible failure mechanisms

Failure mechanisms of masonry infill walls with ferrocement strengthening are classified into four types (i.e. Type I to Type IV) as follows, also shown in **Fig. 3.3.4** (Sen 2020):

Type I: Diagonal compression failure

Type II: Diagonal cracking-sliding failure

Type III: Overall flexural failure

Type IV: Column punching- joint sliding failure

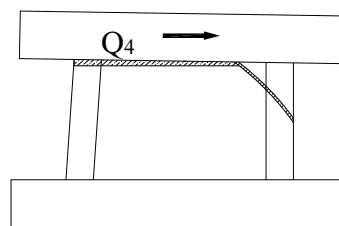
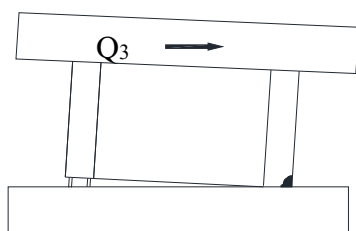
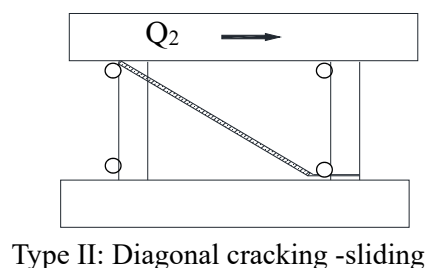
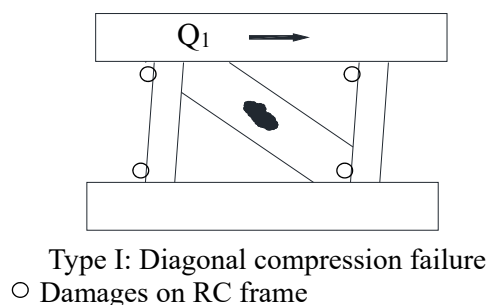


Figure 3.3.4 Failure mechanisms after ferrocement strengthening of masonry infilled RC frame

(2) Applicability of Ferrocement for strengthening of infill masonry

Ferrocement strengthening can be applied on masonry infill with all of the failure mechanisms (Type I to IV) possible for un-strengthened masonry infilled RC frame. However, the extend of capacity improvement is different according to failure mechanism that likely to occur before ferrocement strengthening. When expected failure mechanism of un-strengthened masonry infill is Overall flexural (Type III) or Column punching-joint sliding (Type IV), the expected increase in strength, after ferrocement strengthening, is rather limited because the un-strengthened masonry infill is strong and stiff enough to form major damage or failure in RC frame (yielding of tension column reinforcement and shear failure, respectively) even without ferrocement (**Fig. 3.3.5**). On the contrary, in case of Type I (Diagonal compression) or Type II (Diagonal cracking) failure, where un-strengthened masonry infill is expected to fail, a remarkable improvement is possible as shown in **Fig. 3.3.6**. Therefore, identification of failure mechanism of un-strengthened masonry infilled RC frame is important to judge the application of the ferrocement. “Technical Guidelines for Seismic Evaluation of Existing Reinforced Concrete Buildings in Bangladesh for Extended Application of BSPP Seismic Evaluation Manual” proposes a contact length ratio (a_c/h) as a judging criteria for failure mechanism and border has been set at 0.2. In this Guideline, ferrocement lamination is recommended to apply to masonry infill when contact length ratio is greater than 0.2 ($a_c/h > 0.2$).

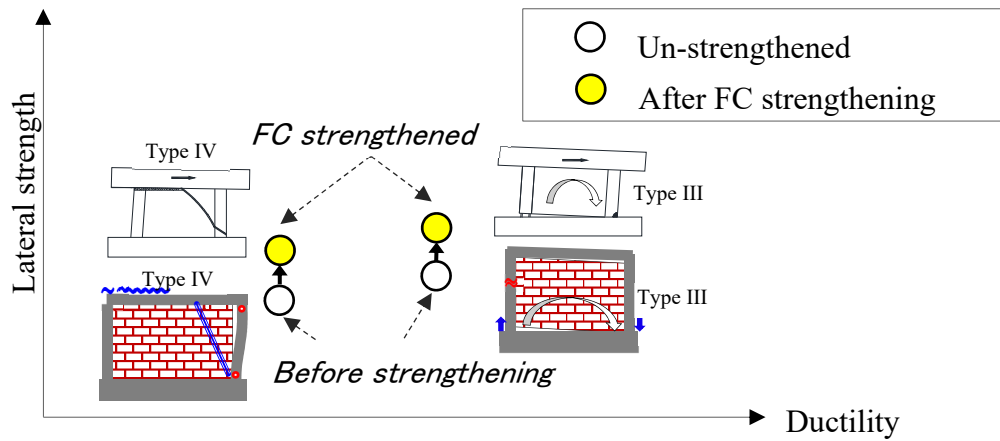


Figure 3.3.5 Schematic diagram of impact of ferrocement strengthening of un-strengthened masonry infilled RC frame having less contact length ($a_c/h \leq 0.2$)

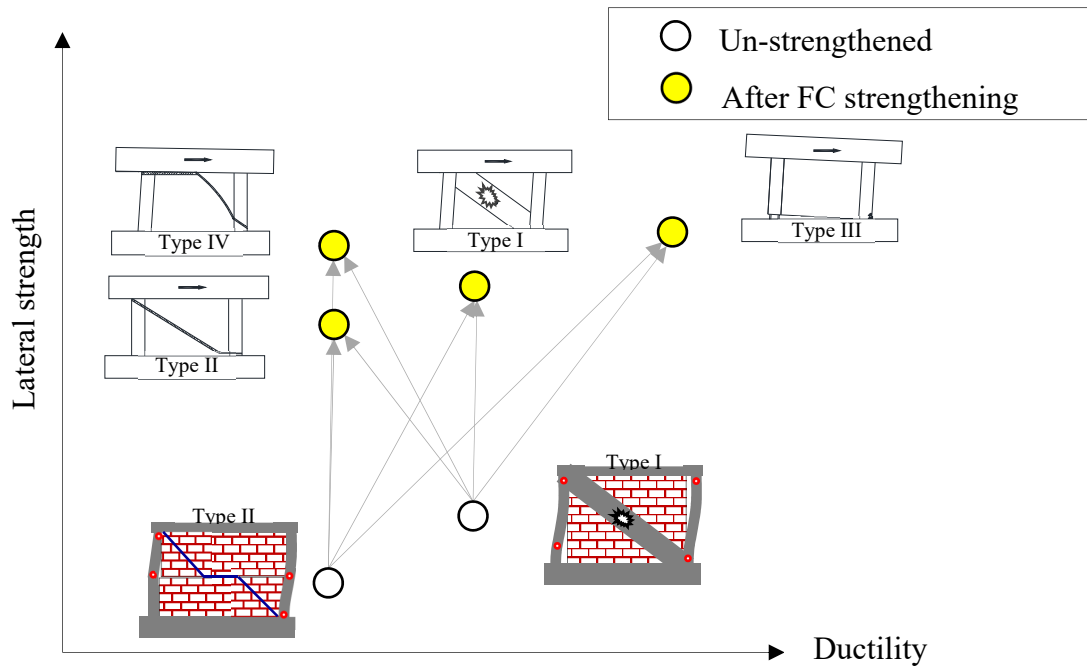


Figure 3.3.6 Schematic diagram of the impact of ferrocement strengthening on un-strengthened masonry infilled RC frame having larger contact length ($a_c/h > 0.2$) [Schematic diagram]

C.3.3.4 [Commentary]

C.3.3.4.1 Damage associated with different failure mechanisms

The major damages on different components of ferrocement strengthened masonry infilled RC frame for each failure mechanism are shown in **Table C.3.3.1**.

Table C.3.3.1 Failure mechanisms of masonry infilled RC frame strengthened with ferrocement

Failure mechanism	Existing RC frame	Strengthened masonry	Joint at top beam soffit
Type I Diagonal compression	- Flexural failure of column or beams - Shear failure of column or beams	- Compression failure of diagonal strut	- No damage
Type II Diagonal cracking-sliding	- Flexural failure of column or beams - Shear failure of column or beams	- Major diagonal shear cracks on masonry and mortar layer	- No damage
Type III Overall flexural failure	- Tensile yielding of tension column - Compressive failure of compression column	- No failure	- No damage
Type IV Column punching and joint sliding	- Punching/ direct shear failure of tension column - Flexural or shear failure of compression column	- No failure	- Bond failure

C.3.3.4.2 Contact length ratio (a_c/h) of un-strengthened masonry infill

The contact length ratio is defined as the ratio of contact length of un-strengthened masonry infill (a_c) to the RC column height (h). The contact length (a_c) shall be calculated as per Eq. 3.3.1, where relative stiffness ratio (λ_{mas}) shall be calculated using Eq. 3.3.2.

$$a_c = \frac{\pi}{4\lambda_{mas}} \quad (3.3.1)$$

$$\lambda_{mas} = \sqrt[4]{\frac{E_{mastmas} \cos^2 \theta}{4E_c I_c d_m}} \quad (3.3.2)$$

C.3.3.4.3 Identification of failure mechanism

The failure mechanism of the un-strengthened masonry infilled RC frames is classified in “Technical Guidelines for Seismic Evaluation of Existing Reinforced Concrete Buildings in Bangladesh for Extended Application of BSPP Seismic Evaluation Manual”. According to that manual, when contact length ratio is less than or equal 0.2 ($a_c/h \leq 0.2$) the failure mechanism is likely to be “Overall flexural failure” or “Column punching-joint sliding failure” where infill masonry is very strong compared to the surrounding RC frame. On the contrary, the failure mechanism is likely to be “Diagonal compression” or “Sliding-diagonal cracking” when contact length ratio is greater than 0.2 ($a_c/h > 0.2$) i.e. masonry is relatively weak.

3.3.5 Selection of target failure mechanism

Target failure mechanism of ferrocement strengthened masonry infilled RC frame is need to be selected in consideration of target seismic behavior of overall building structure. Following three strategies, namely (1), (2) and (3), shall be employed to select target failure mechanism.

- (1) Lateral strength improvement with the same deformation capacity
- (2) Improvement of both of strength and deformation capacity
- (3) Lateral strength improvement with decrease in deformation capacity

The concept of the target failure selection is illustrated in **Fig. 3.3.7**. When un-strengthened infill masonry is likely to have a failure Type I or Type II then ferrocement is recommended to apply, as described in section 3.3.4.

According to strategy- (1), after ferrocement strengthening similar failure mechanism (Type I or II) can be made as target failure with same F-index as before. If ductility (F-index) improvement is required for retrofitting, Type III (Overall flexural) is preferable failure mechanism which is strategy- (2). On the contrary, when reduction of F-index is possible (i.e. acceptable), Type IV (Column punching-joint sliding) can also be selected as strategy-(3).

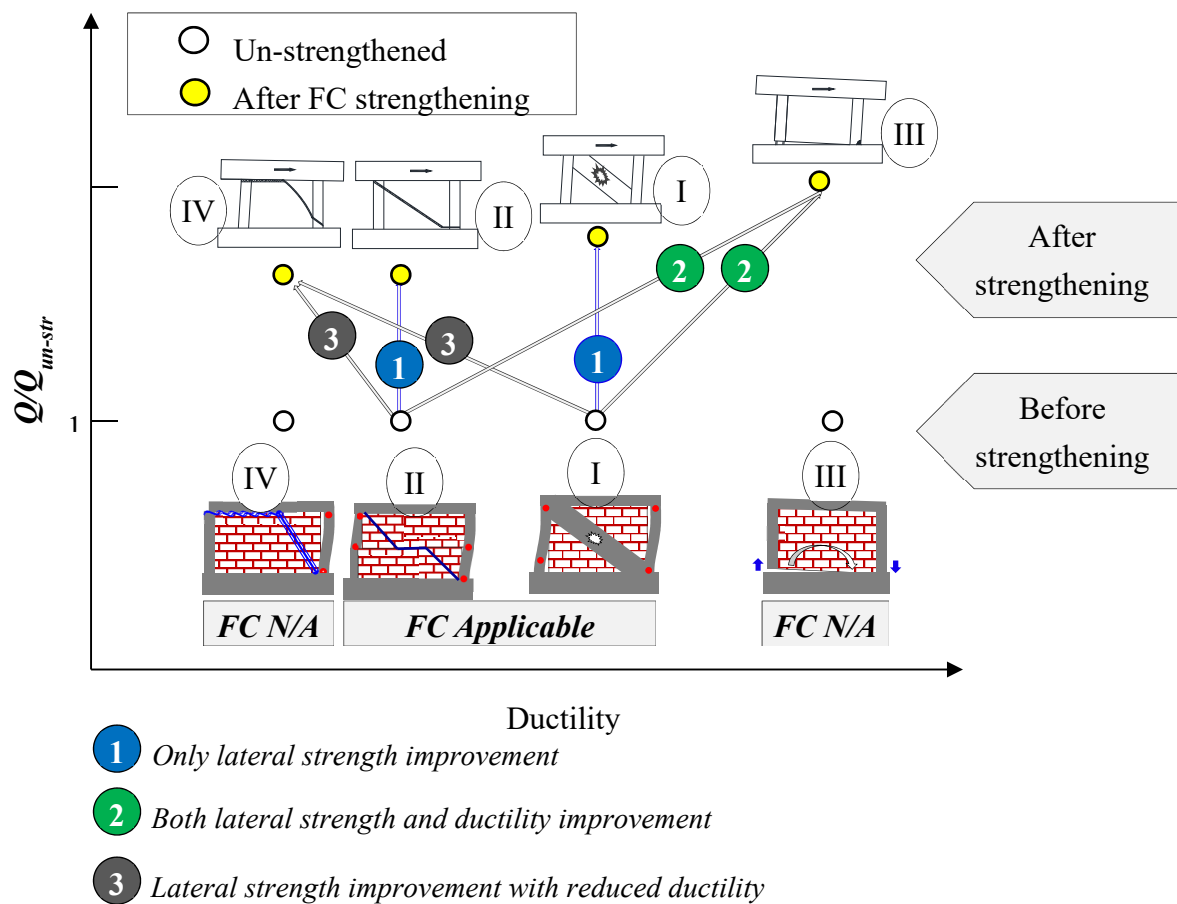


Figure 3.3.7 Conceptual diagram of target failure mechanism selection procedure

3.3.6 Selection of ferrocement configuration

- Thickness and material strength of mortar and wire mesh is selected according to target failure mechanism and required capacity improvement.
- Maximum two layers of wire mesh can be used, in one ferrocement mortar layer, to avoid de-bonding between 1st and 2nd layer mortar.

- Thickness should be considered as per design requirement. However, thickness should be minimum 25 mm (keeping wire meshes at center) to provide a cover for mesh reinforcement.
- Mortar strength should be of medium to high strength (>10MPa), since it is a strengthening procedure.

3.3.7 Strength index C

(1) General

The lateral strength index (C) indicates the base shear coefficient that can be resisted by non-linear ferrocement strengthened masonry infilled RC frame, which can be estimated as per Eq. 3.3.3.

$$C = \frac{Q}{W} \quad (3.3.3)$$

where, Q = ultimate strength of ferrocement strengthened masonry infilled RC frame (calculated in Eq. 3.3.4),
 W = total weight of the structure.

$$Q = \min (Q_1, Q_2, Q_3, \text{ and } Q_4) \quad (3.3.4)$$

where, Q_1 = lateral capacity at diagonal compression failure; Q_2 = lateral capacity at diagonal cracking and sliding failure; Q_3 = lateral capacity at overall flexural failure; and Q_4 = lateral capacity at column punching and joint sliding failure.

(2) Type I (Diagonal compression failure)

Lateral strength at diagonal compressive failure (Q_1) shall be determined using Eq. 3.3.5 ~ Eq. 3.3.8.

$$Q_1 = 2Q_c + 0.5f_{m,\theta}W_s t_{mas} \cos\theta + 0.5f_{mor,FC}W_s n_s t_{FC} \cos\theta \quad (3.3.5)$$

$$W_s = 2a_c \cos\theta \quad (3.3.6)$$

$$a_c = \frac{\pi}{4\lambda_{mas-FC}} \quad (3.3.7)$$

$$\lambda_{mas-FC} = \sqrt[4]{\frac{(E_{mas}t_{mas} + E_{FC}n_s t_{FC}) \cos^2\theta}{4E_c I_c d_m}} \quad (3.3.8)$$

where, Q_c = lateral strength of RC column; $f_{m,\theta}$ = compressive strength of masonry along diagonal ($= 0.5f_m$, f_m = masonry prism strength); $f_{mor,FC}$ = ferrocement mortar strength; W_s = strut width; a_c = contact length; λ_{mas-FC} = relative rigidity factor for ferrocement strengthened masonry; E_c , E_{mas} , E_{FC} = Young's modulus of concrete, masonry, ferrocement mortar ($E_{mas} = 550f_m$ and $E_{mor} = 200f_{mor,FC}$ [Kaushik 2007]); t_{mas} , t_{FC} = thickness of masonry, ferrocement mortar layer; n_s = number of surface strengthened with ferrocement; I_c = moment of inertia of RC column; d_m = diagonal length of infill panel; and θ = inclination of loaded diagonal with horizontal.

(3) Type II (Diagonal cracking-sliding)

Lateral strength at diagonal cracking-sliding failure (Q_2) shall be determined using Eq. 3.3.9.

$$Q_2 = 2Q_c + 0.05f_m A_{mas} \sin\theta + \alpha \cdot n_s n_L \frac{A_s}{S_v} \cdot f_{y,wm} \cdot h_{mas} \quad (3.3.9)$$

where, Q_c =lateral strength of RC column; f_m = compressive strength of masonry prism; A_{mas} = diagonal area of infill masonry (diagonal length x thickness); θ = angle of diagonal with horizontal; A_{wm} = Area of mesh reinforcement; S_v = Spacing of horizontal mesh reinforcement; $f_{y,wm}$ = yield strength of mesh reinforcement; h_{mas} = height of masonry infill; α = empirical reduction factor (=0.7 [Sen et al 2020]); n_s = number of surface strengthened with ferrocement; and n_L =number of wire mesh layer in each ferrocement layer.

(4) Type III (Overall flexural failure)

Lateral strength at overall flexural failure (Q_3) shall be determined using Eq. 3.3.10 ~Eq. 3.3.11.

$$Q_3 = M_u / h_o \quad (3.3.10)$$

$$M_u = a_t f_y l_c + 0.5 N l_c \quad (3.3.11)$$

where, M_u = ultimate moment capacity of RC frame; h_o = clear height of column; a_t = cross sectional area of column longitudinal reinforcements; f_y = yield strength of column longitudinal reinforcement; l_c = center to center distance of boundary columns, and N = total axial load on RC columns (summation of the axial loads employed on both columns).

(5) Type IV (Column punching and joint sliding)

Lateral strength at column punching and joint sliding failure (Q_4) shall be determined using Eq. 3.3.12 ~ Eq. 3.3.16.

$$Q_4 = k_{min} \tau_o b d + \tau_{mas} l_w t_{mas} + \tau_{mor,FC} l_w n_s t_{FC} + Q_c \quad (3.3.12)$$

$$\tau_o = 0.98 + 0.1 f_c + 0.85 \sigma \quad \text{in case } 0 \leq \sigma \leq 0.33 f_c - 2.75 \quad (3.3.13)$$

$$= 0.22 f_c + 0.49 \sigma \quad \text{in case } 0.33 f_c - 2.75 \leq \sigma \leq 0.66 f_c$$

$$= 0.66 f_c \quad \text{in case } 0.66 f_c \leq \sigma$$

$$\sigma = \rho_g f_y + \sigma_0 \quad (3.3.14)$$

$$\sigma_0 = \frac{N'}{b d} \quad (3.3.15)$$

$$k_{min} = \frac{0.34}{0.52 + a/d} \quad (3.3.16)$$

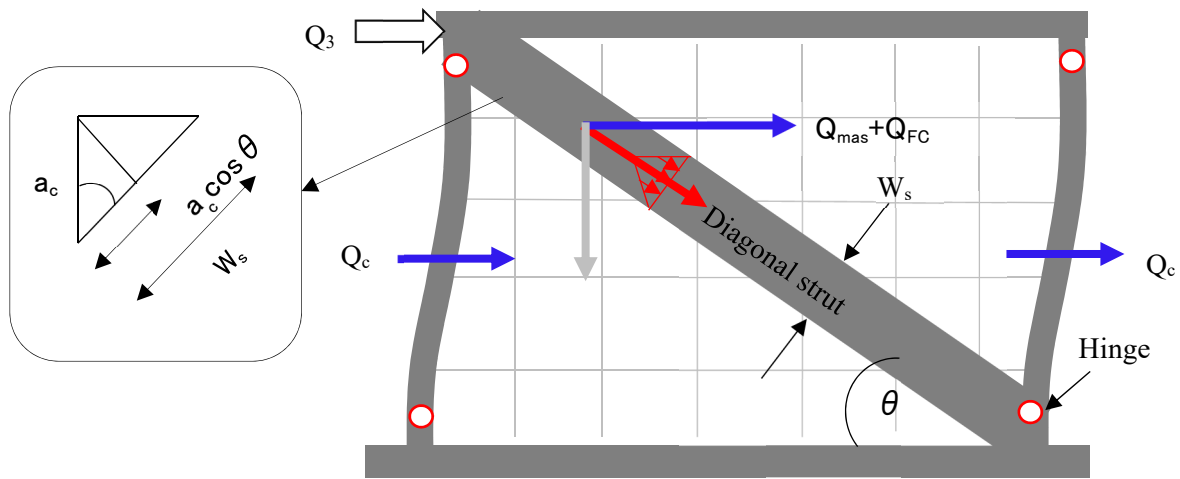
where, K_{min} =influence factor considering shear span ratio; τ_o = basic shear strength of column; b and d = width and depth of column; a = shear span = $d/3$; ρ_g = longitudinal reinforcement ratio of column, f_c = concrete compression strength, f_y = yield strength of longitudinal reinforcement, N' = axial load on column; τ_{mas} = bond strength at masonry top (= $0.17 \sqrt{f_{joint,mor}}$, $f_{joint,mor}$ = compressive strength of masonry joint mortar); $\tau_{mor,FC}$ = bond strength at ferrocement top (= $0.17 \sqrt{f_{mor}}$), l_w = length of masonry wall; t_{mas} , t_{FC} = thickness of masonry and ferrocement layer; n_s = number of surface strengthened with ferrocement and Q_c = lateral capacity of compression column.

C.3.3.5 [Commentary]

C.3.3.5.1 General

The failure modes (Type I to Type IV) mentioned in Sec. 3.3.4 are considered in this Guidelines. The lateral strength of the RC frame with FC strengthened masonry infill at different failure mechanisms shall be evaluated as described in the following sub-sections.

C.3.3.5.2 Diagonal compression failure



* $Q_{mas} + Q_{FC}$ = summation of horizontal components of masonry and FC mortar strut

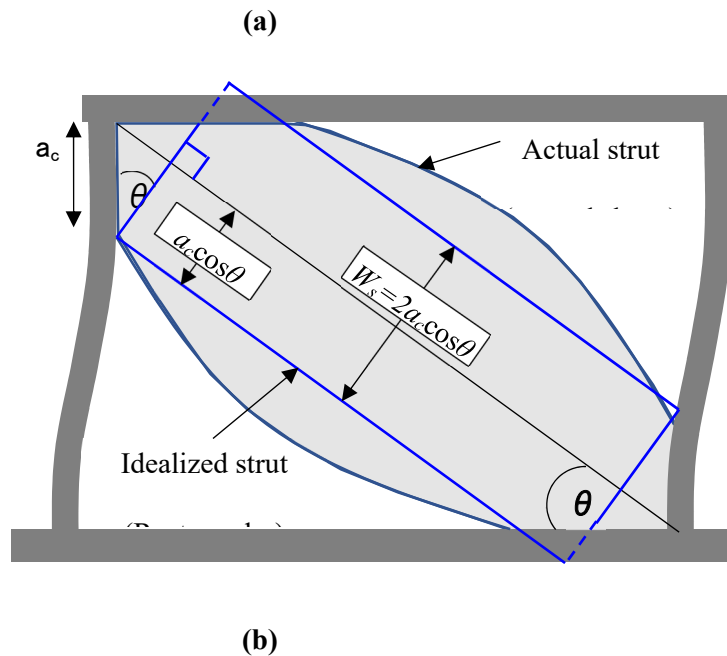


Figure C.3.3.2: (a) Idealized load transfer mechanism of diagonal compression (Type I) (Sen 2020) and (b) concept of idealized diagonal strut width

Diagonal compression failure at peak strength is idealized as illustrated in **Fig. C.3.3.2(a)** considering the formation of a diagonal strut on infill panel. The strut width depends on the relative rigidity of infill material

in comparison to surrounding RC column. Under lateral loading, RC column is considered as a beam element resting on infill material, as shown in **Fig. C.3.3.3(a)**, where infill material would act a foundation of the loaded beam element. The lateral deflection (y) and curvature (ϕ) of the RC column could be evaluated considering it is analogous to a beam on elastic foundation. According to the theory of elasticity, general solution of beam deflection (y) resting on an elastic foundation can be expressed by Eq. 3.3.17 [Hetneyi 1946], where, relative rigidity (λ) of foundation with respect to beam has been defined as Eq. 3.3.18.

$$y = \frac{P\lambda}{2bk_o} e^{-\lambda x} (\sin\lambda x + \cos\lambda x) \quad (3.3.17)$$

$$\lambda = \sqrt[4]{\frac{bk_o}{4EI}} \quad (3.3.18)$$

where, P = lateral load; b = foundation thickness; k_o = modulus of foundation i.e. pressure required to get unit deflection of foundation; E = Young's modulus of beam element i.e. concrete, and I = moment of inertia of beam element i.e. column.

Considering the flexural rigidity of RC column (EI) and modulus of ferrocement laminated masonry strut following relative rigidity factor (λ_{mas-FC}) for ferrocement laminated masonry is defined here as Eq.3.3.19.

$$\lambda_{mas-FC} = \sqrt[4]{\frac{(E_{mas}t_{mas} + E_{FC}n_s t_{FC}) \cos^2 \theta}{4E_c I_c d_m}} \quad (3.3.19)$$

where, E_c , E_{mas} , E_{FC} = young's modulus of concrete; masonry, ferrocement mortar; t_{mas} , t_{FC} = thickness of masonry, ferrocement mortar layer; n_s = number of surface retrofitted with ferrocement; I_c = moment of inertia of RC column; d_m = diagonal length of infill panel, and θ = inclination of loaded diagonal with horizontal.

It is evident from the column deflection shape, as shown in **Fig. C.3.3.3(b)**, that the lower portion of RC column exhibits flexure deflection whereas the deflection mode of upper part is changed from flexural shape due to presence of infill masonry, which actually causes the separation between masonry and RC frame. Based on the deflection shape, it has been considered that the infill panel of the upper part of inflection point is attached with RC frame effectively and considered as contact length (a_c) of diagonal strut. The height of inflection point i.e. effective length (a_c) has been evaluated from the condition of zero curvature at inflection point, as shown in **Fig. C.3.3.3(c)**, using Eq. 3.3.20. The curvature of RC column, as shown in **Fig. C.3.3.3(c)**, has been determined from the second derivative of column deflection (y).

The diagonal strut width (W_s) is considered in reference to **Fig. C.3.3.2(b)**. Actual infill strut is funnel shaped, as discussed by Crisafuli (1997) using stress distribution on masonry diagonal, however the width of strut is considered constant along the diagonal length in capacity evaluation for simplicity. The strut width is considered perpendicular to the diagonal of infill masonry. The half of the strut width is determined as $a_c \cos \theta$ considering the contact length of infill, a_c (as per Eq. C3.3.20) with column. Subsequently, width of the diagonal strut (W_s) has been calculated by using Eq. C.3.3.21, as shown in **Fig. C.3.3.2(b)**. It is to be noted that the considered strut width would overestimate strut width, shown as dotted line in **Fig. C.3.3.2(b)**, at the ends of diagonal strut. However, at center of diagonal strut it will give a conservative strut width. The simplified strut width (W_s) can give a fair agreement with experimental results that will be discussed in section C.3.3.5.6.

$$a_c = \frac{\pi}{4\lambda_{mas-FC}} \quad (3.3.20)$$

$$W_s = 2a_c \cos\theta \quad (3.3.21)$$

where, a_c = contact length of ferrocement strengthened masonry infill; W_s = strut width; λ_{mas-FC} = relative rigidity factor for ferrocement laminated masonry, and θ = inclination of loaded diagonal with horizontal.

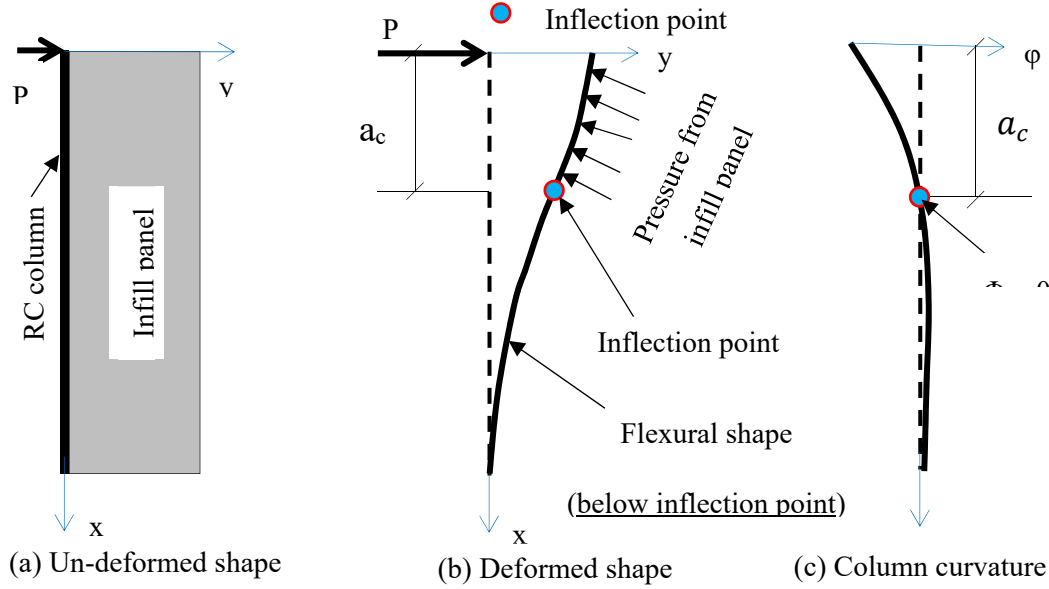


Figure C.3.3.3 Surrounding RC column (a) un-deformed shape, (b) deformed shape and (c) curvature distribution

C.3.3.5.3 Diagonal cracking-sliding failure

Diagonal cracking –sliding failure at peak strength is idealized as illustrated in **Fig. C.3.3.4** considering the formation of a diagonal crack on infill panel. Sliding occurred after the peak strength, as observed in Seki et al (2017), following the diagonal cracking, therefore sliding is not considered at the peak strength evaluation. The contribution of masonry and wire mesh in the diagonal cracking strength is discussed herein.

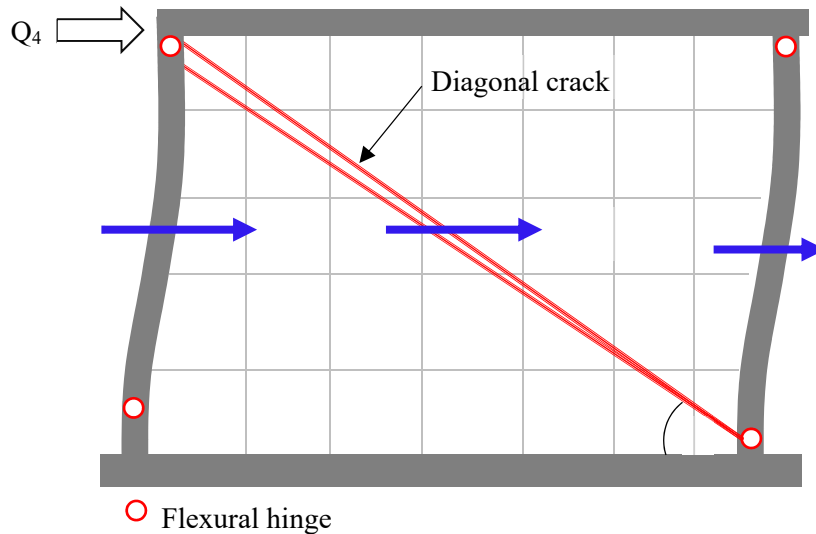


Figure C.3.3.4 Idealized load transfer mechanism of diagonal cracking and sliding (Type II) (Sen 2020)

[Cracking strength of masonry]

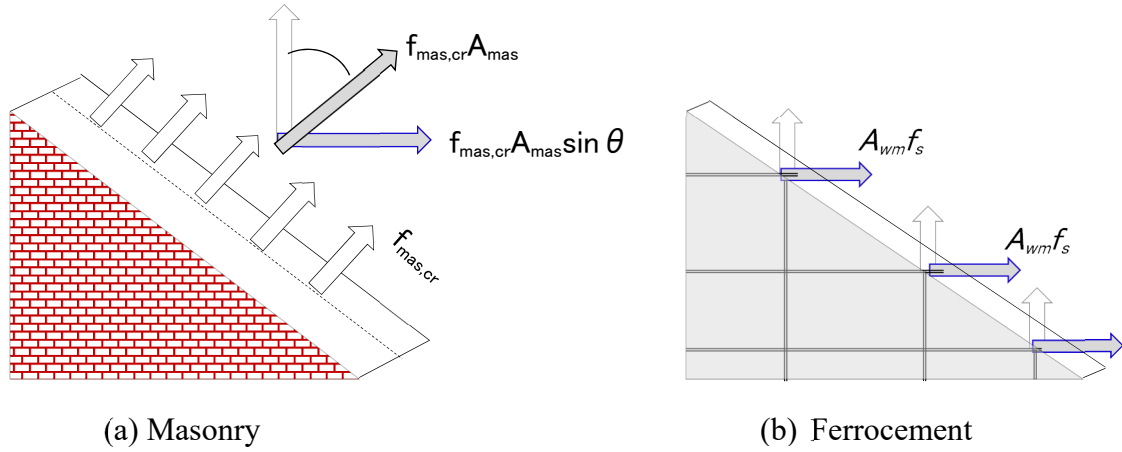


Figure C.3.3.5 a) masonry infill, and b) ferrocement layer at diagonal cracking

The contribution of infill masonry due to diagonal cracking has been evaluated using Eq. 3.3.22, in reference to Figure C 3.3.5(a).

$$Q_{mas,cr} = f_{mas,cr} A_{mas} \sin \theta \quad (3.3.22)$$

where, $f_{mas,cr}$ = cracking strength of infill masonry, A_{mas} = diagonal area of infill masonry (diagonal length x thickness), θ = angle of diagonal with horizontal.

Masonry diagonal cracking strength ($f_{mas,cr}$) is explained in reference to diagonal masonry wallet test as shown in **Fig. C.3.3.6(a)**. Under diagonal loading (P_d), the center of masonry wallet is in pure shear state and generally the crack is formed in loaded diagonal direction. The formation of diagonal crack is due to tension as explained in **Fig. C.3.3.6(a)** through stress transformation. The Mohr's circle of the stress transformation is also shown in **Fig. C.3.3.6(b)** from where it is evident that shear stress should be equal to principal normal stresses (σ_1 and σ_2). At diagonal cracking, shear strength ($\tau_{d,mas}$) should be equal to the tensile strength ($f_{mas,cr}$) of masonry. Therefore, the cracking strength has been evaluated from diagonal masonry wallet test. Several diagonal test of masonry wallet have been investigated to correlate shear strength of masonry i.e. cracking strength with masonry compressive prism strength. The correlation is shown in **Fig. C.3.3.7** and the diagonal shear strength (as well as diagonal cracking strength, $f_{mas,cr}$) can be considered as $0.05f_m$ by linear regression with correlation coefficient of 0.55.

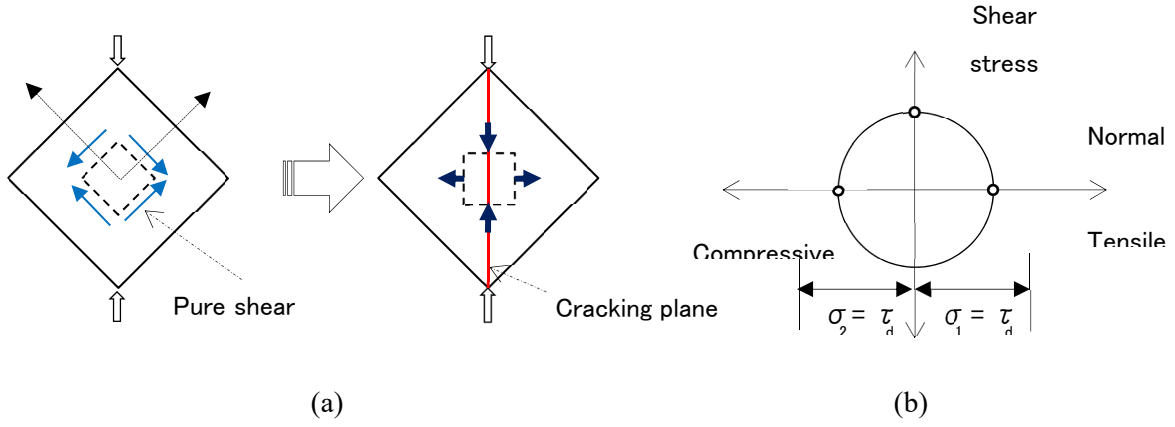


Figure C.3.3.6 a) State of stress on diagonal wallet and b) Corresponding Mohr's circle representation

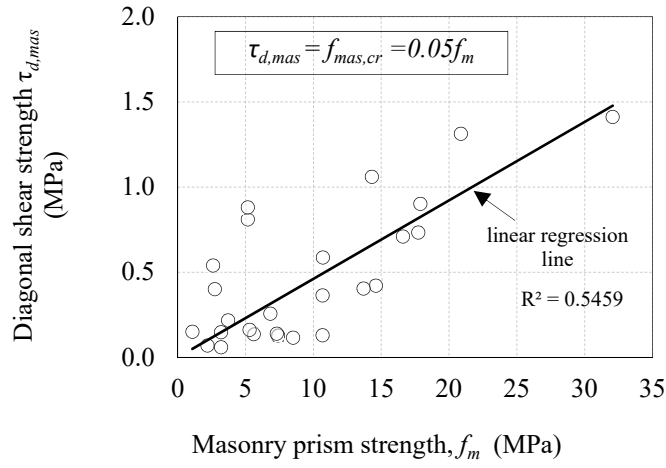


Figure C.3.3.7 Relationship between diagonal shear strength and masonry prism strength (Sen 2020)

[Contribution of wire mesh]

The contribution of ferrocement or reinforced mortar has been assumed to be equal to the shear capacity provided by the horizontal mesh reinforcement as shown in Eq. 3.3.23.

$$Q_{FC,wm} = \alpha \cdot n_s n_L \frac{A_{wm}}{S_v} \cdot f_{y,wm} \cdot h_{mas} \quad (3.3.23)$$

where, A_{wm} = Area of mesh reinforcement; S_v = Spacing of horizontal mesh reinforcement; $f_{y,wm}$ = yield strength of mesh reinforcement; h_{mas} = height of masonry infill; α = empirical reduction factor; n_s = number of surface strengthened with ferrocement, and n_L = number of wire mesh layer in each FC layer.

Conceptually, the contribution of horizontal steel area is considered similar to the reinforcement in RC shear wall. However, Alcocer et al. (2003) addressed that the strain in reinforcement at the center portion of reinforced masonry wall is larger compared to the strain near the corner, which indicates that all of the horizontal reinforcements of diagonal crack might not reach to yield condition. It is to be noted that, in reinforced masonry, reinforcements are built inside the masonry during construction, whereas, in ferrocement strengthening, mesh reinforcements are embedded into surface mortar later after masonry construction. ferrocement studies are very few and different from reinforced masonry walls. However, for simplicity, ferrocement could be considered to have similar behaviour to reinforced masonry infill, therefore, studies for

reinforced masonry are referred in this section. Assuming the same behavior for the ferrocement strengthened masonry, an empirical reduction factor (α) has been imposed in Eq. 3.3.23 to accommodate the less effectiveness of mesh reinforcement compared to contribution in RC shear wall. The less effectiveness might happen due to the less development length provided for reinforcements in masonry. Anderson and Priestley (1992) observed that the strength of shear reinforcement in reinforced masonry wall is approximately half than that of in RC shear wall. Several building codes e.g. MSJC (2011); CSA-S304.1-04 (2004) and NZS 4230 (2004) have also taken account less effectiveness of horizontal reinforcement for internally reinforced masonry. The range of the reduction factor varies in between 0.5 ~ 0.8. In this study, the empirical reduction factor (α) has been assumed as 0.7 for ferrocement lamination as suggested by Sen et al (2020).

C.3.3.5.4 Overall flexural failure

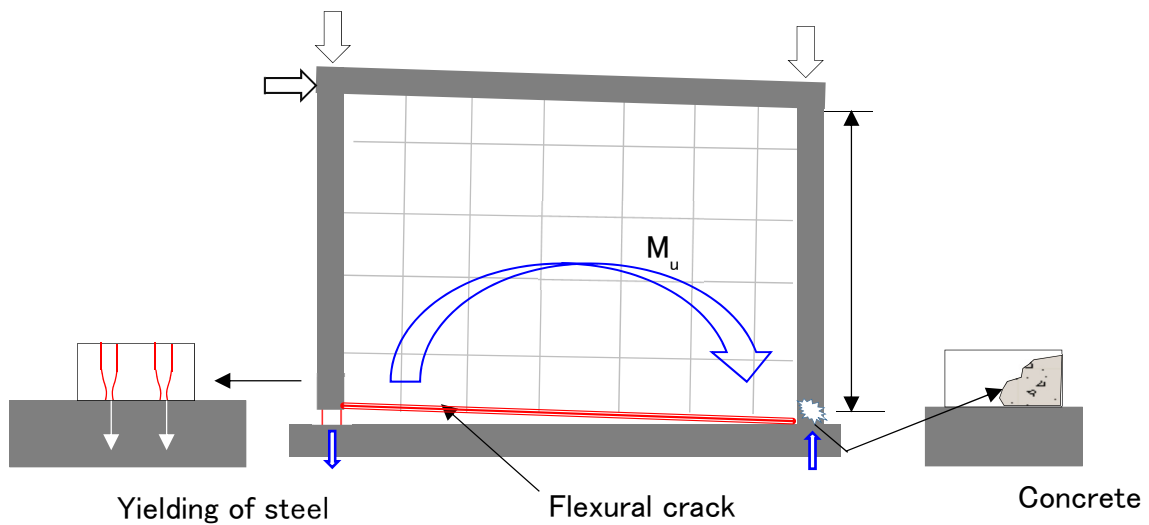


Figure C.3.3.8 Idealized load transfer mechanism of overall flexural failure (Type III) (Sen 2020)

The idealized load transfer mechanism by overall flexural yielding is shown in **Fig. C.3.3.8**. The lateral capacity at flexural yielding of RC frame (Q_3) is computed from flexural theory, using Eq. 3.3.10 and Eq. 3.3.11. It is to be noted that, in ultimate moment calculation (Eq. 3.3.11) the contribution of mesh reinforcement is not considered because mesh reinforcements would not connected firmly (i.e. not having enough development length to sustain stretching/yielding) with stub/foundation beam. In addition, if dowel bars are used, it might not contribute like shear wall reinforcement because of discontinuity of those bars. Therefore, the lateral capacity of the cantilever wall is thought to be provided by the only RC frame.

C.3.3.5.5 Column punching and joint sliding failure

Column punching and joint sliding failure at peak strength is idealized as illustrated in **Fig. C.3.3.9** considering the punching shear failure of tension column top, joint failure at the interface of infill panel top and beam soffit, and the failure of compression column as per design (i.e. flexural or shear). The bond failure at joint is discussed herein for clarification of the effect of connection on the bond strength.

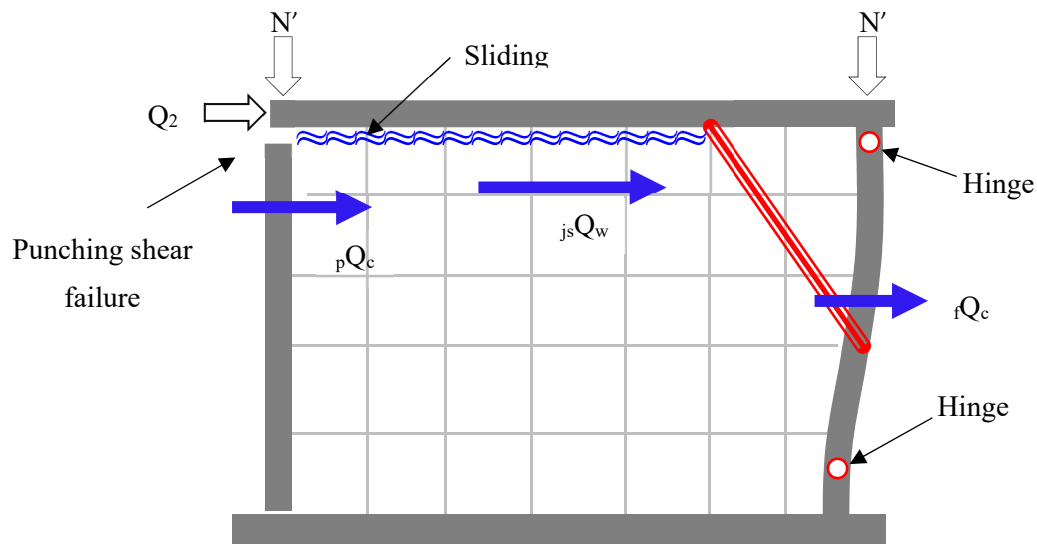


Figure C.3.3.9 Idealized load transfer mechanism of column punching and joint sliding (Type IV) (Sen 2020)

[Top joint shear capacity]

The top joint of ferrocement strengthened masonry infilled RC frame is considered as a horizontal construction joint. In general, the main sources of horizontal construction joint capacity are the bond strength, shear friction, and dowel action- as suggested by Paulay et al. (1974). The interaction of these shear resisting components are suggested by FIB (2013). At the lower shear slip, bond strength works to resist shear. At the failure of the bond, with increasing slip, interlocking effect i.e. shear friction decreases quickly. While the shear friction resistance declines, the bending resistance i.e. dowel action of the connectors increases with larger slips. The interaction of all sources can be shown graphically as shown in **Fig. C.3.3.10**. If, interface reinforcement is not present, obviously the joint capacity will be the bond strength (Q_{bond}). While interface connectors are present, the peak strength is the summation of the contribution of bond strength (Q_{bond}) and a fraction of dowel strength (αQ_{dowel}) as shown in **Fig. C.3.3.10**. However, the contribution of dowel is relatively less compared to the contribution of bond strength. To understand the contribution of dowel action at peak shear resistance, the study by Paulay et al. (1974) is considered herein. In that study, two concrete joint specimens, one with both bond and 10mm diameter interface reinforcement (namely troweled) and another with only similar interface reinforcements (namely troweled: no bond - dowel action), were subjected to direct interface shear loading. The interface reinforcement was 0.69%. The shear stress – slip relation is shown in **Fig. C.3.3.11**. It is evident that at the peak resistance the contribution of dowel action is about 23%, which is considerably less than the bond strength. Therefore, if interface reinforcement is relatively low then the contribution of interface reinforcement can be overlooked as a conservative approach. However, if interface reinforcement is very high, then the contribution of interface reinforcement at peak resistance might be considered.

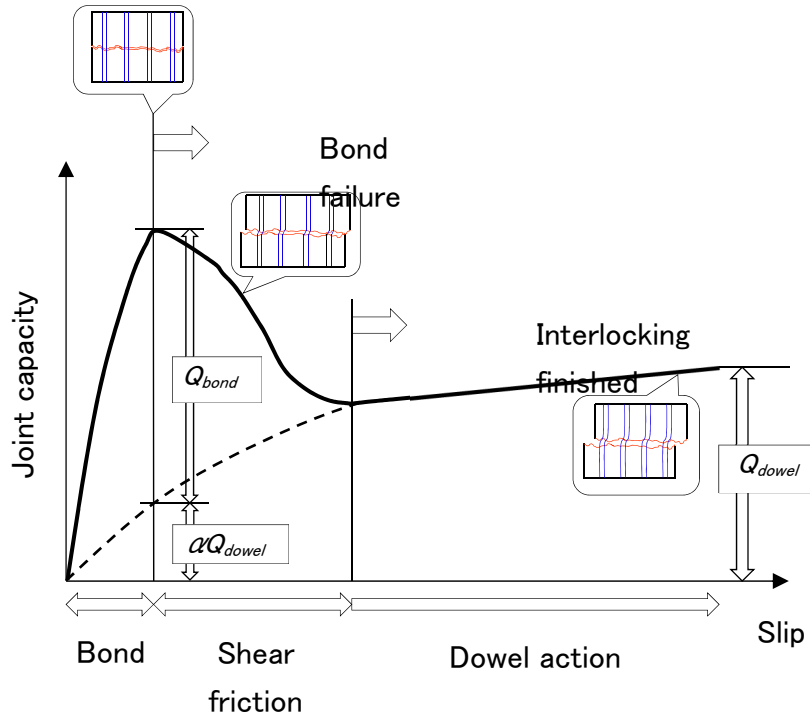


Figure C.3.3.10 Typical shear-slip relationship of construction joint

In this study, the joint shear capacity is investigated considering two stages i.e. *a*) before sliding and *b*) after sliding at the top constriction joint. At initial stage, before any slippage at the interface of infill top and soffit, shear capacity is considered as bond strength (cohesion) of mortar at interface. In initial joint capacity, wire mesh/interface reinforcement might have some contribution in addition to mortar cohesion however, as discussed above the contribution is ignored as a conservative approach. After the occurrence of slippage wire mesh or interface reinforcement will be subjected to shearing force i.e. dowel action hence considered as the source of residual shear capacity at the interface. After slippage, friction might also work, however, is not been considered here for simplicity. The joint shear capacity is evaluated from Eq. 3.3.24.

$$j_s Q_w = \tau_{mas} l_w t_{mas} + \tau_{mor,FC} l_w n_s t_{FC} \quad (3.3.24)$$

τ_{mas} , $\tau_{mor,FC}$ = shear strength (cohesion) of mortar in masonry joint and ferrocement; l_w = length of infill; t_{mas} , t_{FC} = thickness of masonry wall and ferrocement layer; n_s = number of ferrocement surface; $a_{wm,v}$ = cross sectional area of vertical wire mesh/interface reinforcement; $\tau_{y,wm}$ = shear strength of wire mesh/interface reinforcement ($f_{y,wm}/\sqrt{3}$). It is to be noted that cohesion capacity of mortar, for both masonry and ferrocement layer, has been considered as $0.17\sqrt{f_{mor}}$ (where f_{mor} = compressive strength of mortar), which has been suggested by Mander and Nair 1994; Naaman 2000 as shear strength of FC. The yield strength of wire mesh, ($f_{y,wm} = 0.925*f_{u,wm}$) has been considered as per AS/NZS 2001.

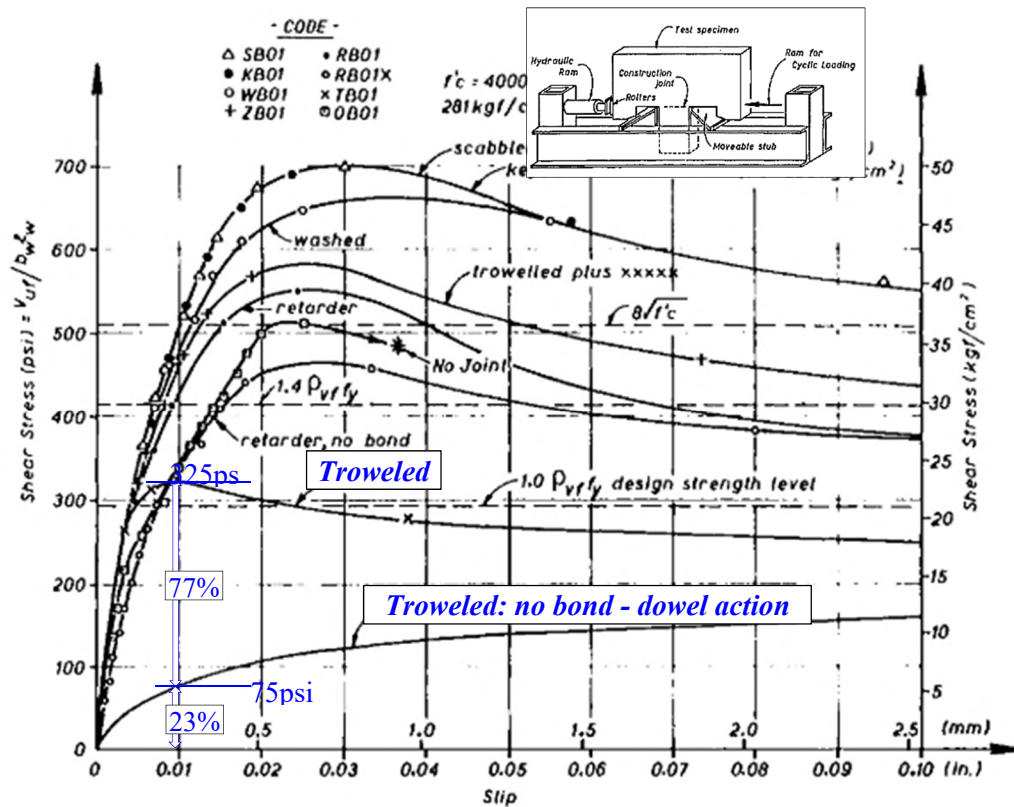


Figure C.3.3.11 Typical shear-slip relationship of construction joint (Paulay et al. 1974)

C.3.3.5.6 Comparison between experimental results and calculation

The experimental and calculated lateral strength of nine ferrocement strengthened masonry infilled RC frame specimens are used herein, as listed in **Table C.3.3.2**, to check the performance of the suggested capacity evaluation method. The calculated lateral strength is the minimum capacity of the four considered failure mechanisms in consideration. **Fig. C.3.3.12** shows a comparison of experimental and predicted capacity, which implies a fair prediction having average ratio of predicted to experimental capacity of 0.8 with a coefficient of variation of 0.2.

Table C.3.3.2 Summary of the experimental and calculated lateral strengths (Sen 2020)

Specimen		Experimental		Calculated capacities					Predicted capacity	
		Observed failure	Q_{exp}	Q_1	Q_2	Q_3	Q_4		Q	Q/Q_{exp}
			kN	kN	kN	kN	kN		kN	
IM-FC-1 (Sen D. 2020)	Mixed		538	612	337	494	487		337	0.63
IM-FC-2 (Sen D. 2020)	Overall flexural		593	649	502	494	492		492	0.83
IM-FC-3 (Sen D. 2020)	Column punching		942	1322	557	1332	832		557	0.59
IM-FC-4 (Sen D. 2020)	and joint sliding		176	137	142	260	178		137	0.78
Sp-5 (Kaya et al. 2018)	Diagonal		155	110	200	212	174		110	0.71
SMF (Demirel et al. 2015)	compression		181	136	-	700	280		136	0.75
S5-FMFC (Seki et al. 2018)			330	302	300	680	334		300	0.91
Sp-4 (Altin et al. 2010)	Diagonal crackin		191	237	114	217	136		114	0.59
M3 (Zarnic and Tomazevic 1985)	and sliding		333	472	375	1300	427		375	1.12
									Average =	0.77
									Coefficient of variation (CoV) =	0.21

* Mixed failure refers to flexural yielding then column punching and joint sliding

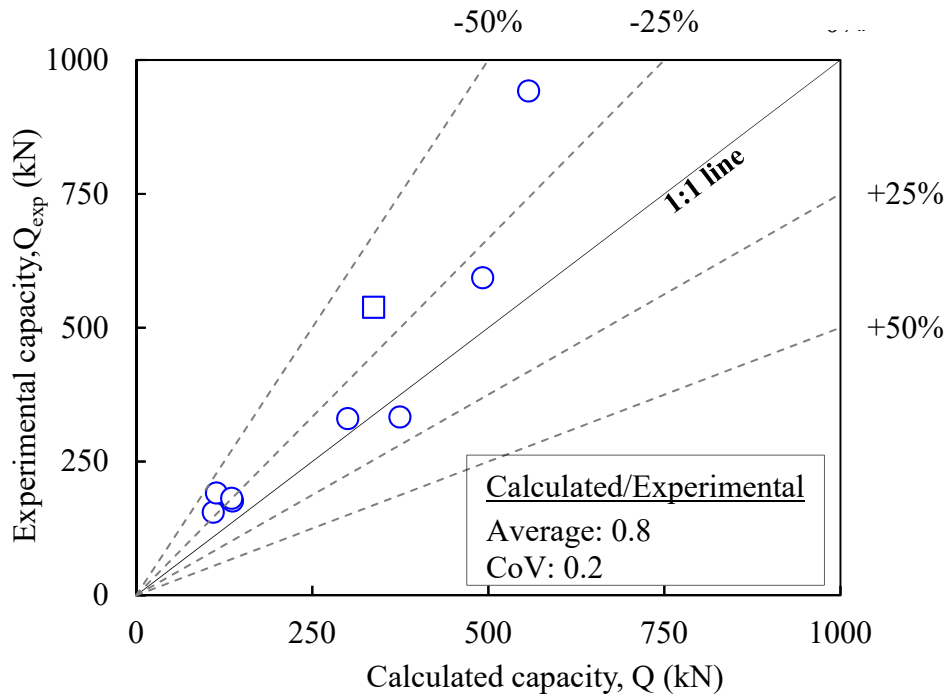


Figure C.3.3.12 Calculated and experimental capacities of all investigated specimens (Sen 2020)

3.3.8 Ductility index F

Ductility index for each failure mechanism is given below considering FC strengthened masonry infilled RC frame as a unit and surrounding columns are flexural column. However, when surrounding column is a shear column, ductility index should be considered as unity ($F = 1.0$), irrespective to the failure mechanism. In case of overall flexural failure with shear column, the strength contribution factor, α is to be considered as 0.7. The overall idea is summarized in **Table 3.3.2**.

Table 3.3.2 Suggested F -index for different failure mechanisms

<i>Failure mechanism</i>	<i>F-index</i>
Diagonal compression (Type I)	1.75
Sliding-diagonal cracking (Type II)	1.27
Overall flexural (Type III)	1.75
Column punching-joint sliding (Type IV)	1.00

C.3.3.8 [Commentary]

The F -index is taken based on experimental observation for each failure mode as shown in Figure C 3.3.13. The lower bound of F -index of diagonal compression failure as well as overall flexural failure is considered as 1.75, which indicates relatively ductile behavior. On the other hand, the lower bound of F -index of diagonal cracking-sliding is considered as 1.27. In case of column punching-joint sliding failure, the F -index is considered to be a unity ($F=1$), since the failure is governed by shear and the lower bound of F -index is below 1.27. Idealized C-F relationship of each failure mechanism is shown in **Table C.3.3.3**.

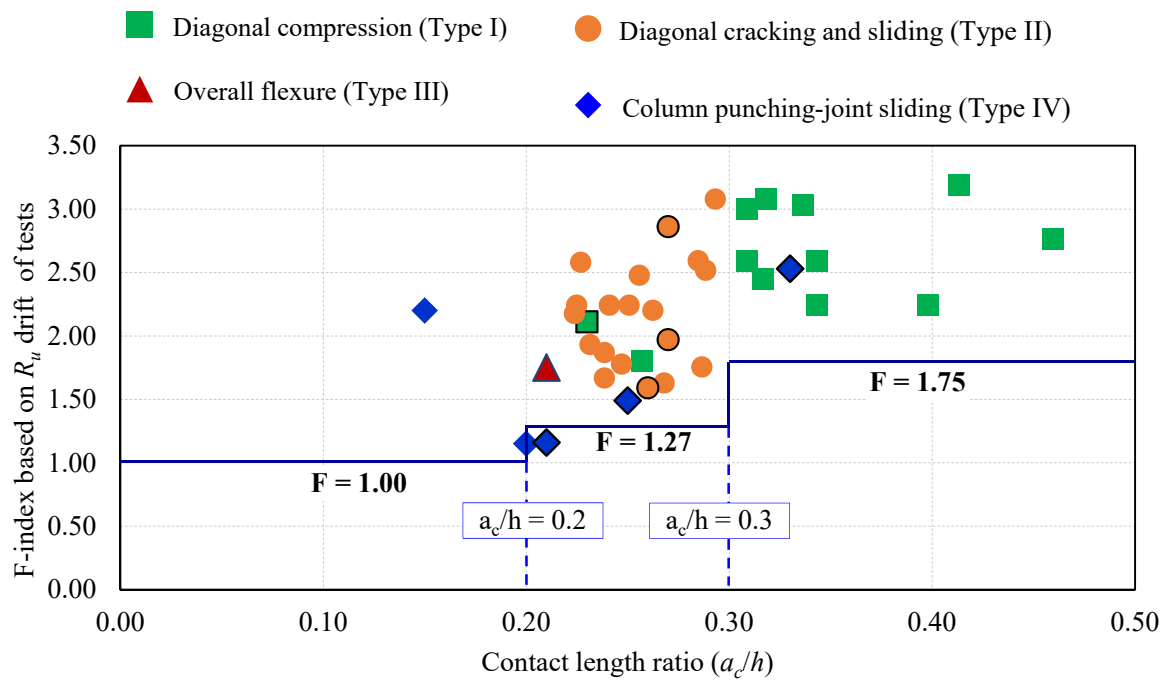
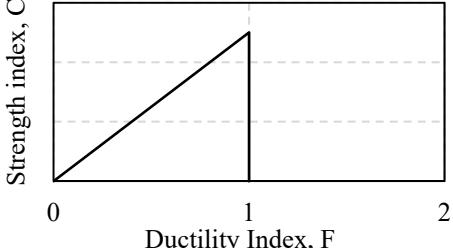


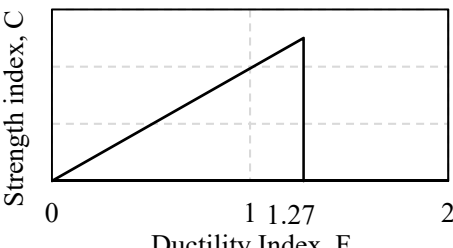
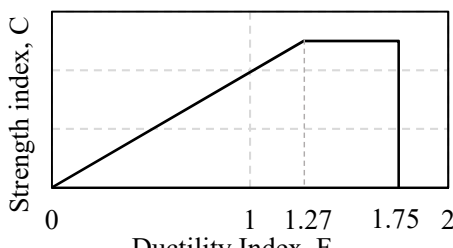
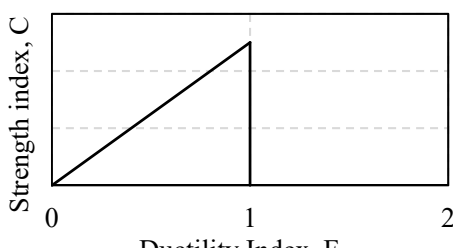


Figure C.3.3.13 F-indices for test specimens

Table C.3.3.3 Idealized C-F relationship of FC laminated Masonry infilled RC frame

Column type	Failure mode	Idealized C and F relationship
Shear column	Diagonal compression (Type I), Diagonal cracking-sliding (Type II), and Column punching-joint sliding (Type IV)	
	Overall flexural (Type III)	
Flexural column	Diagonal compression (Type I)	
	Diagonal cracking-sliding (Type II)	
	Overall flexural (Type III)	
	Column punching-joint sliding (Type IV)	

3.3.9 Application Example

1) Introduction/overview of building

An example of detailed procedure has been described in following section. A 3 storied residential building is considered. A general view and other information are shown in Figure 3.3.8-3.3.9.

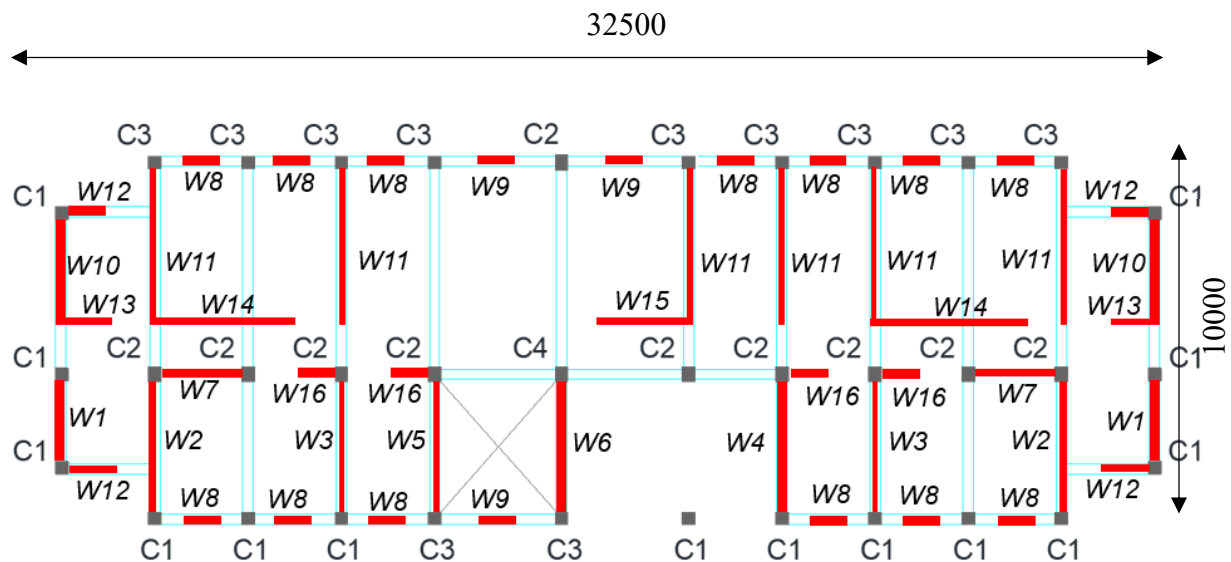


Figure 3.3.8 Architectural plan (dimensions are in mm)

Table 3.3.3 Column dimension

Legend for column	Dimension(mm)
Column (C1,C3)	300×300
Column (C2,C4)	300×375

Table 3.3.4 Masonry infill-wall properties

Wall ID	Number	Length (mm)	Thickness (mm)	Surrounding frame	Opening area %	Opening or Solid	Structural wall (yes/no)
W1	2	2750	250	Yes	0%	Solid	Yes
W2	2	3875	125	Yes	0%	Solid	Yes
W3	2	3875	125	Yes	0%	Solid	Yes
W4	1	3875	250	Yes	0%	Solid	Yes
W5	1	3875	125	Yes	0%	Solid	Yes
W6	1	3875	250	Yes	0%	Solid	Yes
W7	2	2400	125	Yes	0%	Solid	Yes
W8	13	2400	250	Yes	>40%	Opening	No
W9	3	3875	250	Yes	>40%	Opening	No
W10	2	2750	250	Yes	>40%	Opening	No
W11	6	4750	125	Yes	>40%	Opening	No
W12	4	2750	250	No	-	Opening	No
W13	2	2750	125	No	-	Opening	No
W14	2	2750	125	No	-	Opening	No
W15	1	2350	125	No	-	Opening	No
W16	4	2750	125	Yes	>40%	Opening	No

2) Seismic evaluation results:(from SATREPS seismic evaluation manual)

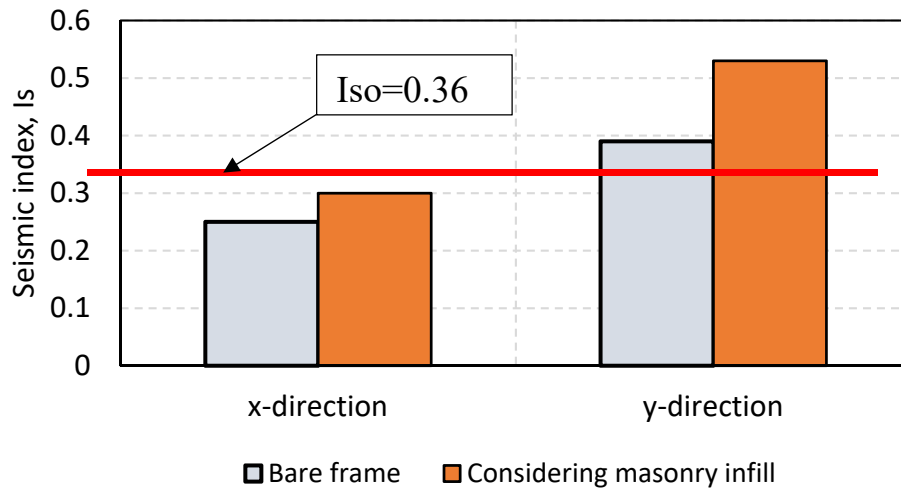


Figure 3.3.9 Seismic index (I_s) of the investigated building

From the above Figure 3.3.10, Seismic strengthening in X-direction is required

3) Required strength

Seismic Index in x-direction, $I_s=0.30$ (from evaluation, page,)

Seismic demand index, $I_{so}=0.36$,

Deficiency of seismic index, $\Delta I_s = 0.36 - 0.30 = 0.06$

4) Check the applicability of ferrocement strengthening (Step 1)

In x-direction, there is 2 masonry infills,

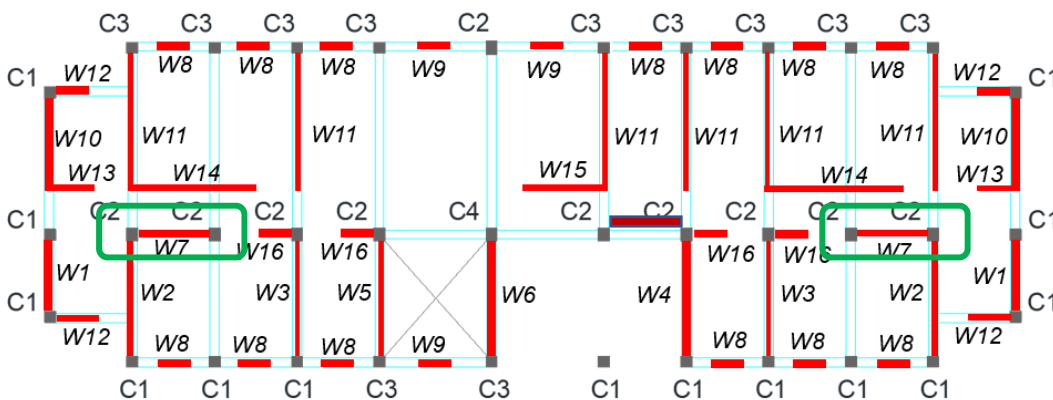


Figure 3.3.10 Showing masonry infill used for FC lamination

From seismic evaluation, (SATREPS manual)

Contact length ratio, $a_o/h_o=0.3$ for both wall.

Failure mode: Diagonal compression failure (Before retrofitting)

Since, $a_c/h_o > 0.20$, the masonry infill is considered for retrofitting.

5) Design of ferrocement strengthening (Step 2)

Target failure mechanism: **Consider diagonal compression (Step 2-1)**

Ductility index, $F=1.75$

Required strength = $\Delta I_s * W/F$

Deficiency of seismic index, $\Delta I_s = 0.06$

W = building weight = 10904 kN (from, evaluation)

Required strength = 373.05 kN

Material properties (Step 2-2)

Masonry properties:

Prism strength, $f_m = 8$ MPa

Young Modulus, $E_{mas} = 550 * f_m = 4400$ Mpa

Thickness of masonry infill, $t_{mas} = 125$ mm

Ferrocement properties,

Number of surface, $n_s = 2$ (two side)

Mortar strength, $f_{mortar} = 20$ Mpa

Young Modulus, $E_{FC\ mortar} = 200 * f_{mortar} = 21019$ MPa (Kaushik et al. 2007)

Ferrocement thickness, $t_{FC} = 25$ mm (one side thickness)

Moment of inertia, $I_c = 84375000$ mm⁴

Note: Minimum I_c should be considered in case of different column size

Wiremesh properties:

Number of layer, $n_l = 2$ (one side)

Diameter of wire mesh = 1 mm

Wire mesh spacing, $S_v = 5$ mm

Yield strength of wire mesh, $f_y = 300$ Mpa

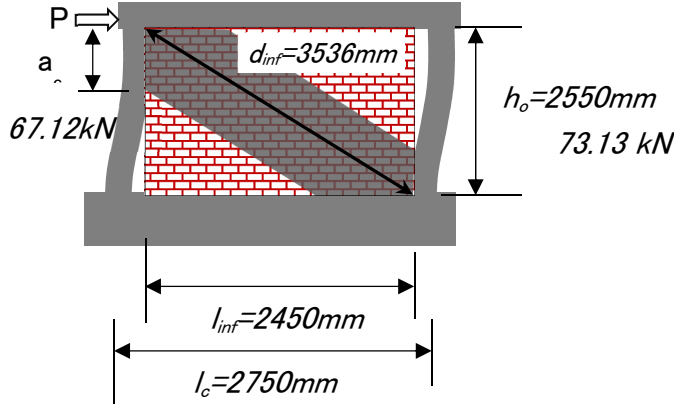
Concrete properties:

Concrete strength, $f_c = 17$ MPa

Young Modulus, $E_c=19500$ MPa

Reinforcement properties, $f_y=276$ MPa

Masonry infill dimension:



C- index evaluation (Step 2-3)

Strength index, $C = Q/W$

$Q = \min (Q_1, Q_2, Q_3 \text{ and } Q_4)$

a) Diagonal compression

$$Q_1 = 2Q_c + 0.5f_{m,\theta}W_s t_{mas} \cos\theta + 0.5f_{mor,FC}W_s n_s t_{FC} \cos\theta$$

$$\lambda_{mas-FC} = \sqrt[4]{\frac{(E_{mas}t_{mas} + E_{FC}n_s t_{FC}) \cos^2\theta}{4E_c l_c d_m}} \quad (3.3.19)$$

$$\lambda_{mas-FC} = 0.001115 / \text{mm}$$

Contact length, $a_c=704$ mm

Strut width, $W_s=2a_c \cdot \cos\theta=2 \cdot 704 \cdot 0.69= 975$ mm

$$(i) 2Q_c=140.25 \text{ kN}$$

$$(ii) 0.5f_{m,\theta} \cdot W_s \cdot t_{mas} \cdot \cos\theta=168.94 \text{ kN}$$

$$(iii) 0.5 \cdot f_{mor,FC} \cdot W_s \cdot n_s \cdot t_{FC} \cdot \cos\theta=337.87 \text{ kN}$$

Total lateral forces: $Q_1=647.06 \text{ kN}$

b) Diagonal cracking-sliding

$$Q_1 = 2Q_c + f_{mas,cr}A_{mas} \sin\theta + \alpha \cdot n_s n_L \frac{A_{wm}}{S_v} \cdot f_{y,wm} \cdot h_{mas}$$

$$A_{mas}=125 \cdot 3536=442030.1 \text{ mm}^2$$

$$\sin\theta=0.7211$$

$$\alpha = 0.70$$

Area of one wire mesh, $A_s = 0.8 \text{ mm}^2$ (1 mm dia)

Spacing, $S_v = 5 \text{ mm}$

Wire mesh, $f_y = 300 \text{ MPa}$

Total lateral forces: $Q_2 = (140.25 + 127.5 + 334.15) = 601.90 \text{ kN}$

c) Overall flexure

$$Q_3 = M_u / h_o$$

$$M_u = a_t f_y l_c + 0.5 N l_c$$

Column rebar area, $a_t = 1701 \text{ mm}^2$

Note: Min^m value should be considered in case different rebars

Length of wall center to center, $l_c = 2750 \text{ mm}$

$N' = 406.56 \text{ kN}$ (Summation of two columns axial load)

Clear height, $h_o = 2550 \text{ mm}$

Total lateral forces, $Q_3 = 944.80 \text{ kN}$

d) Column punching and joint sliding failure

$$K_{min} = 0.40$$

$$\sigma_0 = 3.61$$

$$\sigma = 7.79$$

$$\tau_0 = 7.56 \text{ MPa}$$

$$\tau_{mas} = 0.17 \sqrt{f_{mor,FC}} = 0.76 \text{ MPa}$$

$$\tau_{mortar} = 0.76 \text{ MPa}$$

$$Q_4 = k_{min} \tau_o b d + \tau_{mas} l_w t_{mas} + \tau_{mor,FC} l_w n_s t_{FC} + Q_c$$

Total forces, $Q_4 = 338.68 + 232.83 + 93.13 + 70.13 = 734.77 \text{ kN}$

Lateral capacity considered, $Q = \min (Q_1, Q_2, Q_3, Q_4) = 602 \text{ kN}$

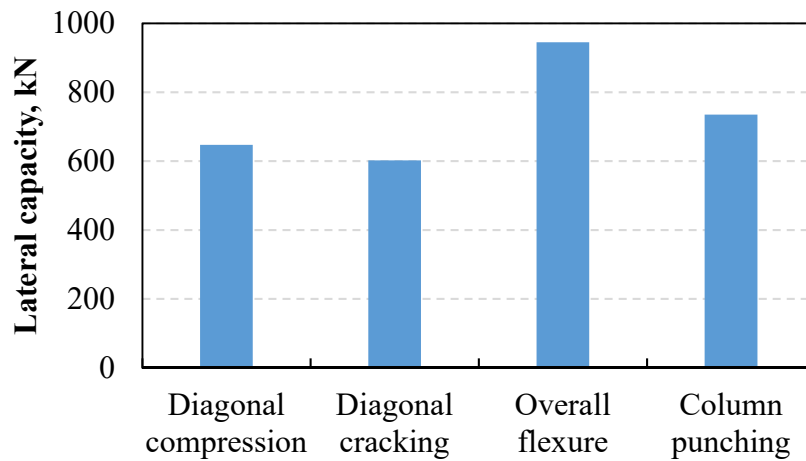


Figure 3.3.11 Different failure modes

The minimum value of Q is 602kN, Diagonal cracking- sliding type failure

Ductility index, $F=1.27$ (Step 2-4)

Contact length ratio, $a_c/h_o=0.27$, hence diagonal cracking failure is confirmed.

6) Recalculate the required strength (Step 2-5)

Target failure mechanism: Consider diagonal cracking, Ductility index, $F=1.27$

Before retrofit

Whole building, $I_s=0.30$, $C=0.181$, $F=1.75$

Building weight= 10904 kN

Total strength, $Q_B=0.181*10904=1973$ kN

After retrofit

Strength of one retrofitted wall=602 kN

Strength of one masonry infill wall before retrofit= $(Q_{frame}+Q_{infill})= (140.25+122)=260.25$ kN

Considering two infill wall retrofitting,

Strength improvement, $\Delta Q = (602-260.25)*2=342*2=684$ kN

Total strength of Building=1973+684=2933 kN

C- index=2657/10904=0.25

F- index=1.27 (Diagonal cracking and sliding failure, II)

Seismic index after retrofitting, $I_s= 0.32$

Considering two infill wall retrofitting + one infill wall insertion and then retrofitting,

Strength improvement, $\Delta Q = (602-260.25)*2 + (602-140) = 684+462=1146$ kN

Total strength of building= $1973+1146=3119$ kN

C- index = $3119/10904=0.29$

F- index =1.27 (Diagonal cracking and sliding failure, II)

Seismic index after retrofitting, $I_s=0.37$

Comment: For retrofitting, 2 existing masonry infill have been selected. One additional infill wall is to be inserted and retrofitting to meet the requirement.

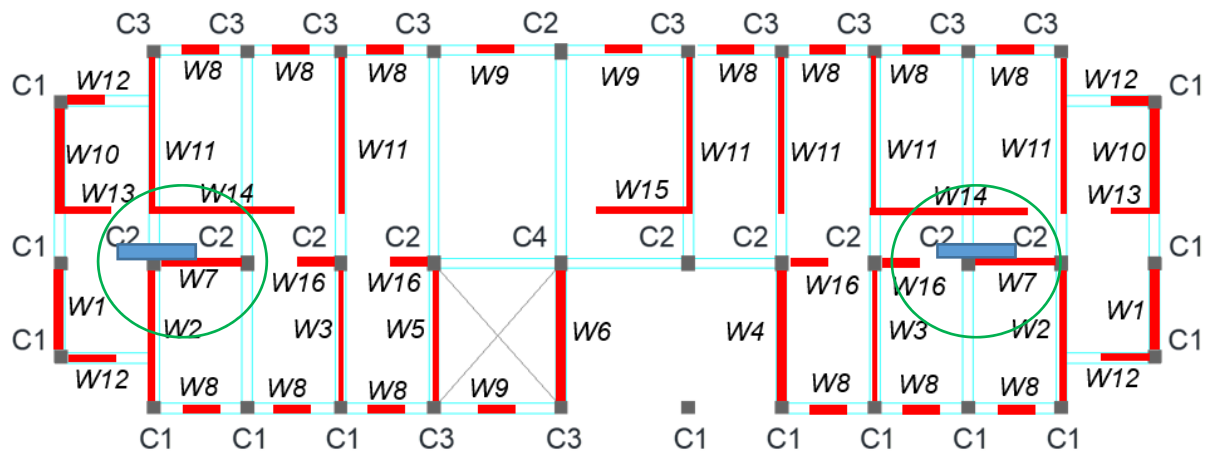


Figure 3.3.12 Showing location of ferrocement strengthening

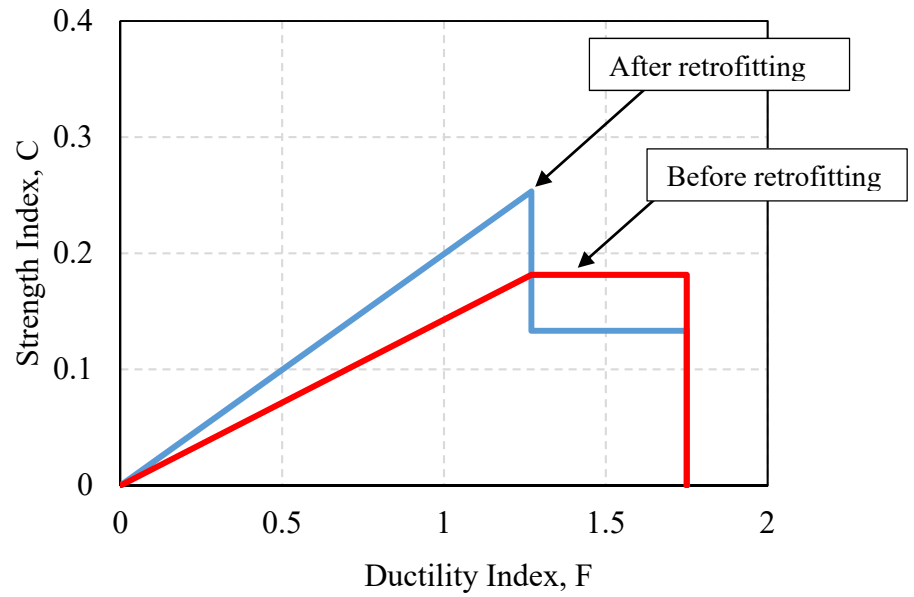
7) Seismic evaluation after retrofitting:

Evaluation of C index considering 2 retrofitting wall.

C-index=0.25

F-index=1.27

$I_s=0.32$



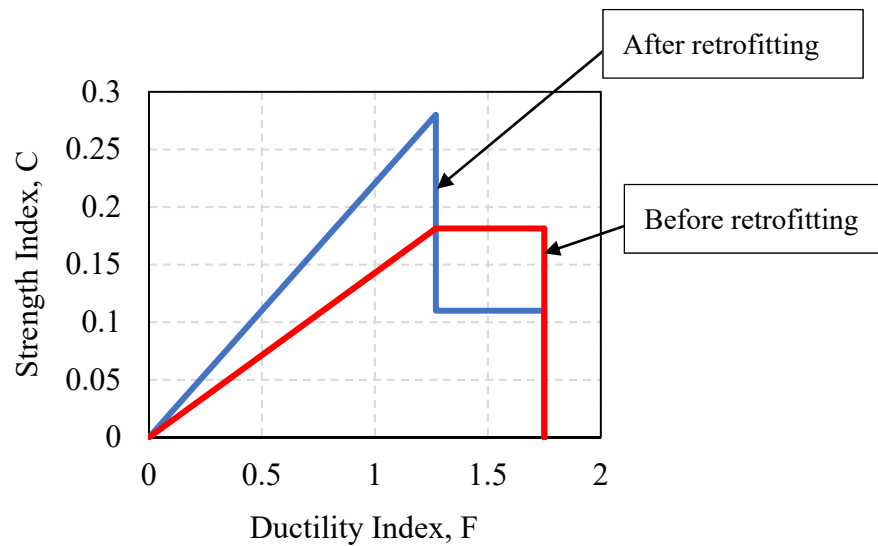
Since, the capacity is less than the demand ($I_s=0.32 < I_{so}=0.36$), in this example, 3 wall is considered for FC strengthening.

In case of 3 infill walls:

C-index=0.29,

F-index=1.27

$I_s=0.37$



Since, the capacity is equal to the demand ($I_s=0.36 = I_{so}=0.36$), in this example, 3 wall is considered for FC strengthening.

Comment: For retrofitting, 2 existing masonry infill have been selected. One additional infill wall is to be inserted and retrofitting to meet the requirement.

References

- [1] Alcocer, S. M., and Flores, L. (2001). Tests on connectors for seismic retrofitting of concrete and masonry structures in Mexico. *In International RILEM Symposium on Connections between Steel and Concrete*, (pp. 481–490). RILEM Publications SARL
- [2] Alcocer, S. M., Cesín, J., Flores, L. E., Hernández, O., Meli, R., Tena, A., and Vasconcelos, D. (2003, June). The New Mexico City building code requirements for design and construction of masonry structures. *In Proceedings of the 9th North American Masonry Conference*, South Carolina, USA (No. 4B3)
- [3] Altin, S., Anil, Ö., Kopraman, Y., and Belgin, Ç. (2010). Strengthening masonry infill walls with reinforced plaster. *Proceedings of the Institution of Civil Engineers: Structures and Buildings*, 163(5), 331–342. <https://doi.org/10.1680/stbu.2010.163.5.331>
- [4] Anderson, D. L., and Priestley, M. J. N. (1992). In Plane Shear Strength of Masonry Walls.” *In 6th Canadian Masonry Symposium*, Canada (pp. 223–234)
- [5] Arya, A. S., and Agarwal, A. (2007). *Simple retrofitting details for improving earthquake resistance of brick masonry buildings of Delhi and the NCR*. Government of India, Disaster Risk Management Programme
- [6] Canadian Standards Association. (2004). *Design of masonry structures (CSA S304.1-04)*. Mississauga, Canada.
- [7] Clarke, R. P., and Sharma, A. K. (1998). *The earthquake strengthening of single story unreinforced block masonry houses in Trinidad and Tobago using ferrocement*. Trinidad and Tobago: The University of West Indies
- [8] Crisafulli, F. J. (1997). Seismic behaviour of reinforced concrete structures with masonry infills. Civil Engineering. (Doctoral dissertation, University of Canterbury)
- [9] Demirel, I. O., Yakut, A., Binici, B., and Canbay, E. (2015, November). An experimental investigation of infill behaviour in RC frames. *In Proceedings of the 10th Pacific Conference on Earthquake Engineering Building an Earthquake-Resilient Pacific*, Australia (pp. 1-8)
- [10] Fédération internationale du béton (FIB). (2013). *Fib Model Code for Concrete Structures 2010*. Ernst and Sohn, Wiley.
- [11] Hetenyi, M. (1946). *Beams On Elastic Foundation Theory with applications in the fields of civil and mechanical engineering* (1st ed.). Michigan, USA: The university of Michigan Press
- [12] Kaushik, H. B., Rai, D. C., and Jain, S. K. (2007). Stress-strain characteristics of clay brick masonry under uniaxial compression. *Journal of Materials in Civil Engineering*, 19(9), 728-739
- [13] Kaya, F., Tekeli, H., and Anil, Ö. (2018). Experimental behavior of strengthening of masonry infilled reinforced concrete frames by adding rebar-reinforced stucco. *Structural Concrete*, 19(6), 1792–1805. <https://doi.org/10.1002/suco.201700210>
- [14] Mander, J B, and B Nair. 1994. Seismic resistance of brick-infilled steel frames with and without retrofit. *The masonry Journal*, 12(2), 24–37

- [15] Masonry Standards Joint Committee., American Concrete Institute., Structural Engineering Institute., and Masonry Society (U.S.). (2011). *Building code requirements and specification for masonry structures: Containing Building code requirements for masonry structures (TMS 402-11/ACI 530-11/ASCE 5-11) [and] Specification for masonry structures (TMS 602-11/ACI 530.1-11/ASCE 6-11) and companion commentaries*. Boulder, CO: Masonry Society.
- [16] Naaman, A. E. (2000). *Ferrocement and laminated cementitious composites* (1st ed.). Michigan, USA: Techno Press. <https://doi.org/10.1007/BF02484171>
- [17] New Zealand Society for Earthquake Engineering (NZSEE). (2017). *The Seismic Assessment of Existing Buildings - Section C7 – Moment Resisting Frames with Infill Panels*. Wellington.
- [18] Paulay, T., Park, R., and Phillips, M. H. (1974). Horizontal construction joints in cast-in-place reinforced concrete. *ACI Special Publication*, 42, 599-616
- [19] Seki, M., Popa, V., Lozinca, E., Dutu, A., and Papurcu, A. (2018). Experimental Study on Retrofit Technologies for RC Frames with infilled brick masonry walls in developing countries. *In Proceedings of the 16th European Conference on Earthquake Engineering*, Greece (pp. 1–12)
- [20] Sen D (2020) Identification of failure mechanism and seismic performance evaluation of masonry infilled RC frame strengthened by ferrocement. Dissertation, Tohoku University
- [21] Sen D, Alwashali H, Islam MS, Maeda M (2020) Investigation of the lateral capacity of ferro-cement investigation of the lateral retrofitted masonry capacity masonry in RC frame and simplified prediction approach. *AIJ Journal of Technology and Design* 26(62):159–63
- [22] Shahzada, E. K. (2007). *Field Practicing Manual*. Peshawar, Pakistan: Earthquake Engineering Center, NWFP University of Engineering and Technology
- [23] Standards Australia/Standards New Zealand. (2001). *Steel Reinforcing Materials, AS/NZS 4671: 2001*.
- [24] Zarnic, R., and Tomazevic, M. (1985). Study of the Behaviour of Masonry Infilled Reinforced Concrete Frames Subjected to Seismic Loading. *In Proceedings of the 7th International Conference on Brick Masonry*, Australia (pp. 1315–1326)

3.4 Column Jacketing using Carbon Fiber Reinforced Plastics

3.4.1 General

In this section, column retrofitting using carbon fiber sheets and epoxy resin is mentioned in terms of lateral strength evaluation. CFRP retrofitting provides increase of shear strength of column Q_{su} and ductility index F because F is a function of Q_{su}/Q_{mu} . However, since the weight of buildings is generally very large, the contribution of CFRP retrofit to strength index $C (=Q_u/\Sigma W)$ is quite small. Therefore, CFRP retrofit is generally used for the purpose of improving the ductility. CFRP retrofit is effective when small number of low-ductility (small F) columns are critical and they govern the building ductility. When CFRP retrofit is appropriately planned and applied to such low-ductility columns, the building performance will be significantly improved.

3.4.2 Shear strength (Q_{su})

Shear strength of RC columns jacketed by CFRP (Carbon Fiber Reinforced Plastics) shall be calculated by the following Eq. (3.4.1).

$$Q_{su} = \left\{ \frac{0.053 p_t^{0.23} (F_c + 18)}{M / Qd + 0.12} + \alpha_L \sqrt{p_w \sigma_{wy} + P_{wf} \sigma_{fd}} + 0.1 \sigma_0 \right\} b j \quad (3.4.1)$$

$$\alpha_L = 0.038 F_c \leq 0.85 \quad (3.4.2)$$

Q_{su} : shear strength of column

p_t : tensile reinforcement ratio (%)

F_c : concrete compressive strength

d : effective depth of column. $D - 50$ mm shall be applied.

M/Q : Shear span length. $h_0/2$ shall be applied. $1.0 \leq M/Qd \leq 3.0$

b : width of column

D : depth of column

j : distance between centroids of tension and compression forces, $0.8D$ shall be applied.

p_w : transverse reinforcement ratio

σ_{wy} : yield strength of transverse reinforcing bars in column

P_{wf} : transverse reinforcement ratio of carbon fiber sheet

σ_{fd} : Design tensile strength of carbon fiber sheet, calculated using Eq. (3.4.3).

σ_0 : axial stress in column, not exceeding 7.8MPa

α_L : reduction factor for low strength concrete

h_0 : clear height of column

$$\sigma_{fd} = \min(E_{fd} \varepsilon_{fd}, \frac{2}{3} \sigma_f) \quad (3.4.3)$$

E_{fd} : nominal elastic modulus of carbon fiber sheet

ε_{fd} : effective strain of carbon fiber sheet. 0.70% shall be applied.

σ_f : nominal tensile strength of carbon fiber sheet

3.4.3 Flexural strength (M_u)

Flexural strength M_u shall be calculated same as existing RC columns.

3.4.4 Construction

Construction of CFRP jacketing should be made by well-trained worker. It is necessary to properly follow manuals and instructions provided by CFRP Supplier.

C.3 [Commentary]

C.3.1 Introduction of a CFRP retrofit test example in Bangladesh

In Japan, jacketing whole existing column body is required for seismic retrofit by CFRP. In this case, the CFRP sheets are pasted without any gaps. Equation (3.4.1) is examined by test results of such columns.

Although number of examinations are limited, there is an example of experimental study of stripe jacketing¹ in Bangladesh. Bangladesh University of Engineering and Technology (BUET) tested eight column specimens retrofitted by partially jacketed CFRP sheet as shown in **Fig. 3.4.1**. In this case, CFRP sheet is pasted at where transverse reinforcements do not exist and there are some gaps in between CFRP sheets. Those column specimens are tested under axial compression and cyclic shear.

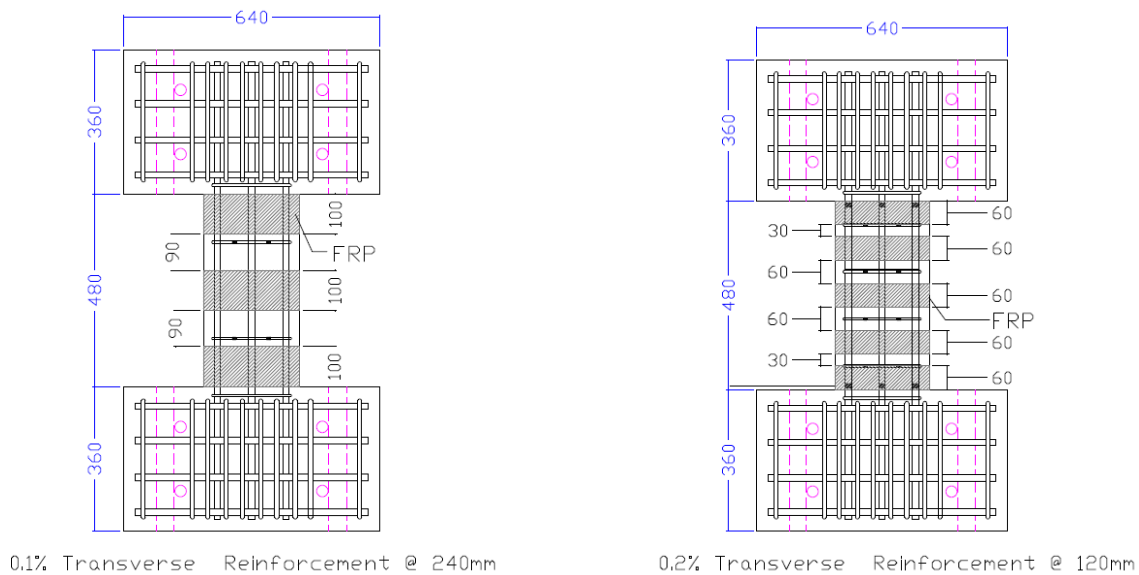


Figure 3.4.1 Drawings of CFRP retrofitted specimens

The Equation (3.4.1) is examined using those column specimens. The results are shown in **Fig. 3.4.2**. Even though several specimens did not reach their maximum strength due to the capacity limitation of testing facilities, however, Equations (3.4.1) could capture the lower bound of shear strength.

¹ This research on stripe jacketing is under developing, and careful discussions are further expected for their practical applications.

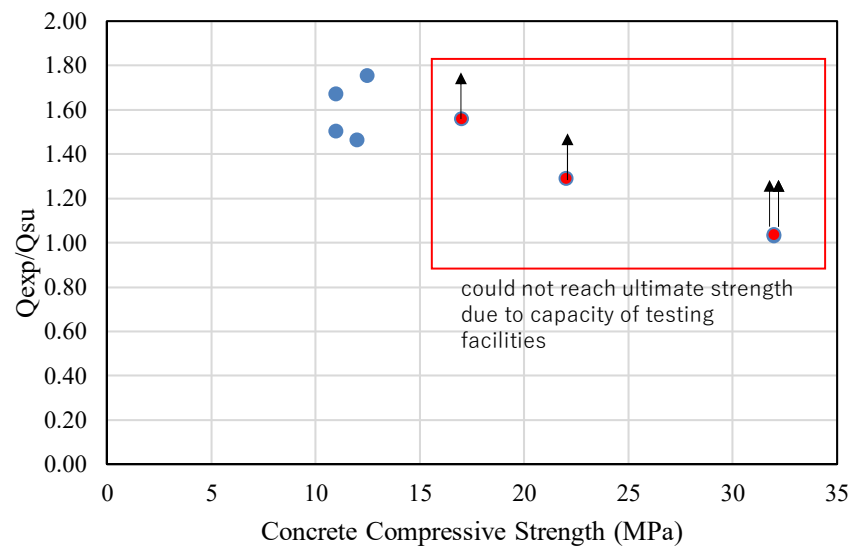
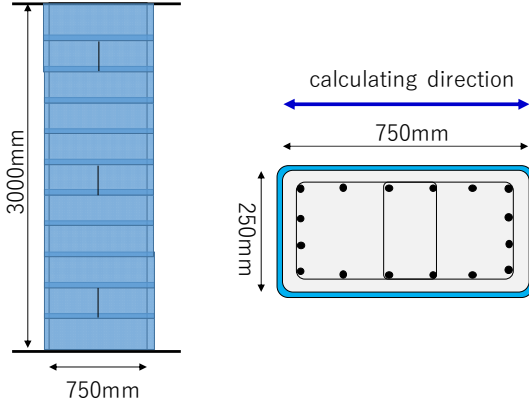


Figure 3.4.2 Ratio of tested Q_{su} to calculated Q_{su} of CFRP retrofitted specimens

3.4.5 Example of application: An RC column of a five-story office building in Dhaka constructed in 1985

A single RC column with the following dimensions is shown as an example for shear and flexural strength calculation.



Column
 Long. bars: 16-φ20
 Ties: 2-φ10
 Clear height: 3.0m
 Axial load: 1,000kN
 Concrete compressive strength: 16MPa
 Tensile strength of rebar (σ_y , σ_{wy}): 275 MPa

CFRP
 Nominal thickness: 0.167 (mm)
 Nominal tensile strength: 3,400 (N/mm²)
 Elastic modulus: 230 (kN/mm²)
 Effective strain: 0.0070
 double layer, sufficient overlapping, whole jacketing is assumed.

Shear strength Q_{su} :

$$Q_{su} = \left\{ \frac{0.053 p_t^{0.23} (F_c + 18)}{M / Qd + 0.12} + \alpha_L \sqrt{p_w \sigma_{wy} + P_{wf} \sigma_{fd} + 0.1 \sigma_0} \right\} bj \quad (3.2.1)$$

where

p_t : tensile reinforcement ratio (%)

F_c : concrete compressive strength (MPa)

M/Q : shear span length (mm). $h_0/2$ shall be applied. $1.0 \leq M/Qd \leq 3.0$.

d : effective depth of column (mm). $D - 50$ mm shall be applied.

D : depth of column (mm)

σ_{wy} : yield strength of transverse reinforcing bars in columns (MPa)

σ_0 : axial stress in column (MPa), not exceeding 8 MPa

α_L : reduction factor for low strength concrete

b : width of column (mm)

j : distance between centroids of tension and compression forces (mm), $0.8D$ shall be applied.

h_0 : clear height of column (mm)

a_t : total area of tensile longitudinal reinforcement (mm²)

P_{wf} : transverse reinforcement ratio of carbon fiber sheet

σ_{fd} : design tensile strength of carbon fiber sheet.

E_{fd} : nominal elastic modulus of carbon fiber sheet

ϵ_{fd} : effective strain of carbon fiber sheet. 0.70% shall be applied.

σ_f : nominal tensile strength of carbon fiber sheet

$$p_t = a/bD = 314.2 \text{ mm}^2 \times 4\text{nos.} / 750 \text{ mm} \times 250 \text{ mm} \times 100(\%) = 0.67\%$$

$$F_c = 16.0 \text{ MPa}$$

$$d = 750 \text{ mm} - 50 \text{ mm} = 700 \text{ mm}$$

$$M/Qd = h_0/2/d = 3000 \text{ mm}/2/700 \text{ mm} = 2.14, < 3, \text{ therefore } M/Qd = 2.14.$$

$$p_w = a_w/b/s = 78.54 \text{ mm}^2 \times 2\text{nos.} / 250 \text{ mm}/250 \text{ mm} = 0.00251$$

$$\sigma_{wy} = 275 \text{ MPa}$$

$$P_{wf} = 2(\text{front and back}) \times 2(\text{double layer}) \times 0.167/250 = 2.67 \times 10^{-3}$$

$$\sigma_{fd} = \min(E_{fd}\epsilon_{fd}, 2/3\sigma_f) = \min(230 \times 10^3 \times 0.7 \times 10^{-2}, 2/3 \times 3,400) = \min(1610, 2267) = 1610 \text{ N/mm}^2$$

$$\sigma_0 = N/bD = 1000 \times 10^3 \text{ N}/750 \text{ mm}/250 \text{ mm} = 5.33 \text{ MPa} < 8 \text{ MPa}$$

$$\alpha_L = 0.038F_c = 0.608 < 0.85$$

Before CFRP retrofit, Q_{su} is calculated as:

$$Q_{su} = \left\{ \frac{0.053 \cdot 0.66^{0.23} (16 + 18)}{2.14 + 0.12} + 0.608 \sqrt{0.00251 \cdot 275} + 0.1 \cdot 5.33 \right\} 750 \cdot 0.8 \cdot 250$$

$$= 270.9 \text{ kN}$$

After retrofit, the shear strength Q_{su} is calculated as:

$$Q_{su} = \left\{ \frac{0.053 \cdot 0.66^{0.23} (16 + 18)}{2.14 + 0.12} + 0.608 \sqrt{0.00251 \cdot 275 + 0.00167 \cdot 1610} + 0.1 \cdot 5.33 \right\} 750 \cdot 0.8 \cdot 250$$

$$= 398.8 \text{ kN}$$

Regarding F -index, because $Q_{mu} = 304.9 \text{ kN}$, Q_{su}/Q_{mu} ratios before and after retrofit are 0.89 and 1.31, respectively. F -index for the column before retrofit is 1.0 and that of after retrofit is 3.2.

Chapter 4 Post Installed Bonded Anchor

4.1 General

The tensile and shear capacity of post installed bonded anchor in low strength concrete shall be evaluated according to the CNCRP/BSPP Manuals for the seismic retrofit.

C.4.1[Commentary]

Post-installed anchor is one of key elements for retrofit of existing buildings. It connects the existing RC buildings with the newly installed strengthening members in order to transmit the load smoothly. The design and application process of post installed anchors are also simpler than most other available retrofitting techniques resulting its increased popularity in building strengthening. Post installed anchors can be generalized in two categories as bonded anchor (also known as adhesive anchor) and mechanical/expansion anchor. The tensile capacity and the shear capacity of post installed bonded anchor shall be basically evaluated according to the CNCRP/BSPP Manuals for the seismic retrofit. However, the CNCRP/BSPP Manuals do not cover the cases associated with low strength concrete and this is a barrier to retrofit existing buildings with low strength concrete. In order to overcome this problem and to facilitate the seismic retrofitting of existing RC buildings this manual aimed to set out the design guidelines to evaluate the tensile capacity and shear capacity of post installed bonded anchor in low strength concrete. In this chapter “low strength concrete” refers to concrete with a 28 days compressive strength between 10 N/mm^2 to 15 N/mm^2 . This chapter is intended to be a guideline required to design the tensile capacity and shear capacity of bonded anchor in low strength concrete with brick chips (which is quite common in Bangladesh), based on concepts of the Japanese Seismic Evaluation Standard of Existing Reinforced Concrete Buildings (JBDPA, 2001).

Bonded anchors are frequently used in both new constructions such as microwave towers, industrial buildings and repair of retrofit projects (N. Subramanian and R.A. Cook, 2002).

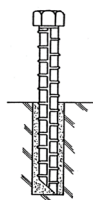


Figure C.4.1 Bonded anchor (JBDPA, 2001)

An adhesive or bonded anchor is simply a reinforcement bar or a threaded rod inserted into a predrilled hole in the hardened concrete, whose diameter is slightly greater than the diameter of the anchor. **Fig. C.4.1** shows a typical bonded anchor. Typically, the drill hole diameter is only 10 to 25 percentage larger than the diameter of the reinforcing bar or threaded rod.

The gap between the drill hole surface and the anchor surface is filled with an adhesive to be acting as a bonding agent between the concrete and the steel after setting and hardening. The material, shape, and size of post-installed bonded anchor shall be carefully examined before installation. **Fig. C.4.2** shows an example of application of post installed bonded anchor in retrofitting beam-column joint with wing-wall(s).

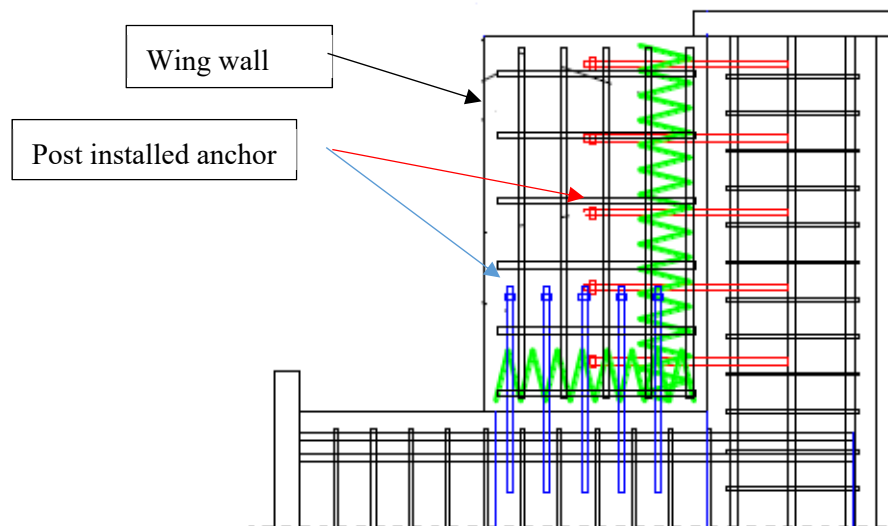


Figure C.4.2 Application of post installed bonded anchor in retrofitting

4.2 Scope

The followings will be the main scopes of this guideline,

- (1) Compressive strength of concrete should be between 10 N/mm² to 36 N/mm² (15-36 N/mm² for CNCRP/BSPP Manuals) and this will cover the low strength concrete (10-15N/mm²). Too high strength (i.e. strength greater than 36 N/mm²) is not covered in this guideline.
- (2) Lightweight concrete which is a mixture made with lightweight coarse aggregates such as shale, clay, or slate, which give it its characteristic low density is not applicable.
- (3) Only chemically bonded anchors are the target, mechanical anchors are not applicable.
- (4) Group anchors in pure concrete specimen are out of the scope of this guideline. Only single anchor is covered.
- (5) It also covers the pullout test and shear test guidelines of single bonded anchor in base materials like low strength pure concrete or reinforced concrete.

C.4.2[Commentary]

This guideline will enhance the scope of the CNCRP/BSPP Manuals for the evaluation of tensile and shear capacity of post installed bonded single anchor for concrete with brick chips. The present CNCRP/BSPP Manuals are basically prepared based on the Japanese Seismic Evaluation Standard of Existing Reinforced Concrete Buildings (JBDPA, 2001). The application range of equations in Japanese Guidelines is defined for

compressive strength between 15 and 36 N/mm². Low strength concrete is originally out of scope of those equations. However, the CNCRP/BSPP Manuals which are originally based on Japanese standards show promising calculation and for predicting the possible failure patterns of a varieties of specimens with concrete strength starting from as low as 10N/mm² enhancing the scope to deal with a wide variety of specimens with different concrete strength (N. Saha et al, 2020) as described in C.4.3.1[Commentary]. For this reason, this guideline is intended to be used to design the bonded anchor considering tension and shear following the CNCRP/BSPP Manuals. The procedures specified in this guideline should be used in evaluating the tensile and shear capacity of single bonded anchor only. Performance evaluation of bonded anchor with below 10 N/mm² concrete specimens and the performance evaluation of mechanical anchors are out of scope. The supporting experimental data used in this chapter will be helpful to calculate the required embedment length of bonded anchor (which plays a vital role in retrofitting RC buildings) to avoid the brittle failure as well as concrete cone failure.

4.3 Design guidelines for post installed single bonded anchor in low strength concrete

4.3.1 Tensile capacity

The tensile capacity of post installed bonded anchors in concrete with compressive strength between 10-15 N/mm² cannot be evaluated according to the existing CNCRP/BSPP Manuals provided by PWD. This guideline extended the scope of application to low strength concrete ranged between 10-15 N/mm². The tensile capacity of single bonded anchor, T_a is determined by three basic failure modes, as shown in **Fig. 4.1** T_a shall be the smallest value of T_{a1} which is determined by steel strength, T_{a2} which is determined by concrete cone failure, and T_{a3} which is determined by bond strength. T_{a1} , T_{a2} and T_{a3} can be evaluated by the following equations:

$$T_a = \min(T_{a1}, T_{a2}, T_{a3}) \quad (4.3.1)$$

$$T_{a1} = \sigma_y \cdot a_o \quad (4.3.2)$$

$$T_{a2} = 0.23 \sqrt{\sigma_B} \cdot A_c \quad (4.3.3)$$

$$T_{a3} = \tau_a \cdot \pi \cdot d_a \cdot l_e \quad (4.3.4)$$

$$\tau_a = 10 \sqrt{(\sigma_B/21)} \quad (4.3.5)$$

where,

σ_B : Compressive strength of concrete (N/mm²)

σ_y : Yield stress of steel (N/mm²)

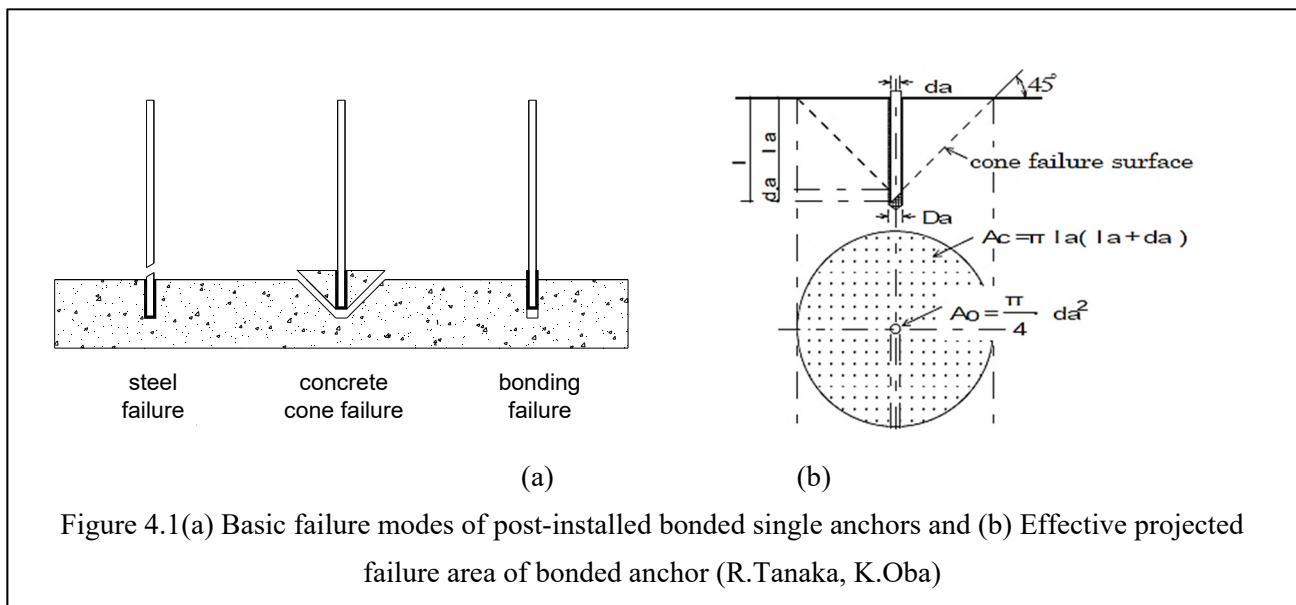
a_o : Nominal cross-sectional area of anchorage bar (mm²)

A_c : Projected area of concrete cone failure (mm²) $A_c = \pi \cdot l_e \cdot (l_e + d_a)$ assuming 45° cone failure surface to the horizontal/vertical.

d_a : Anchor diameter (mm)

l_e : Effective embedment length of anchor (mm)

τ_a : Bond strength of bonded anchor against pullout force (N/mm²)



C.4.3.1 [Commentary]

Design parameters of tensile capacity of post installed bonded single anchor and expected failure modes of the anchor

The design tensile capacity mainly varies along a number of parameters. These parameters include concrete strength, anchor diameter as well as effective embedment length of the anchor. C.4.3.1 [Commentary] shows an example of an experimental study of evaluation process of possible failure modes as well as the calculation of design tensile capacity of anchor specimen.

The material requirements are as follows,

- Steel bar shall be deformed bar, unless specified. Anchor diameter below 6mm and above 20mm are out of scope.
- Epoxy resin and resin mortar can be used for post-installed anchors, crack repair, and bonding new and old concrete when they have sufficient durability and fire resistance. Epoxy resin shall be used for the strengthening with continuous fiber reinforcement.

Post-installed anchors shall be installed in accordance with the standard construction procedure. Compressive strength of existing concrete should be above 10 N/mm² and up to 36 N/mm². Too high strength should be out of range. The compressive strength of concrete and material strength of post-installed anchors found in the experimental reports need to be higher than the design strength.

In experimental studies on pullout test, anchor and rebar specimens were tested in RC slab as well as pure concrete block specimens. In case of pure concrete block, seven types of anchor specimens were designed using equations provided by this guideline for tensile test of single bonded anchor. The parameters of the specimens were anchor diameter, concrete strength and embedment length. Concrete strength of as low as 10 N/mm², 20 N/mm² and 30 N/mm² strength specimen were selected for this experiment (the real concrete

strength of a varieties of specimens was found to be 10.65 N/mm², 11.07 N/mm², 11.56 N/mm², 12.2 N/mm², 24 N/mm² and 33.23 N/mm²). 10mm, 16mm and 20mm diameter of rebar with varying embedment length of $7d_b$, $10d_b$ and $13d_b$ were selected for this study. Sample calculation of design tensile capacity of the specimens and expected failure modes of post installed rebar specimens of diameter d_b , effective embedment length l_e and concrete of strength of σ_B is as follows,

$$d_a = 10\text{mm}$$

$$\sigma_B = 12.2 \text{ N/mm}^2$$

$$l_e = 7d_b = 7 \text{ times the rebar diameter which is } (7 \times 10) = 70\text{mm.}$$

$$\sigma_y = \text{the yield strength of the rebar specimen} = 560\text{N/mm}^2$$

According to this guideline which follows the CNCRP/BSPP Manuals,

$$T_a = \min [T_{a1}, T_{a2}, T_{a3}]$$

Now, T_{a1} is the product of the yield strength of the rebar specimen and the nominal cross-sectional area(a_o) of the rebar implying,

$$T_{a1} = \sigma_y a_o$$

$$= 39.94 \text{ kN}$$

σ_y (N/mm ²)	a_o (mm ²)
560	71.33

Now, T_{a2} is the product of 0.23 with the square root of the concrete compressive strength (σ_B) and the projected concrete cone failure area A_c . Therefore,

$$T_{a2} = 0.23\sqrt{\sigma_B} \cdot A_c$$

$$= 14.13 \text{ kN}$$

σ_B (N/mm ²)	d_a (mm)	l_e (mm)	A_c (mm ²)
12.2	10	70	17592.92

$$A_c = \text{Projected area of concrete cone failure} = \pi \cdot l_e \cdot (l_e + d_a)$$

T_{a3} refers to the steel strength which can be calculated by multiplying bond strength of bonded anchor against pullout force (τ_a) with π , d_a and l_e .

$$T_{a3} = \tau_a \pi \cdot d_a \cdot l_e$$

$$= 16.71 \text{ kN}$$

τ_a (N/mm ²)	d_a (mm)	l_e (mm)
7.6	10	70

$$\tau_a = 10 \sqrt{\frac{\sigma_B}{21}} = 7.6 \text{ N/mm}^2$$

$$T_a = \min [T_{a1}, T_{a2}, T_{a3}]$$

$$= T_{a2} = 14.13 \text{ kN}$$

Therefore, as per this guideline, this rebar will have a failure of concrete cone type failure and its tensile capacity will be 14.13 kN. Assuming 45° cone failure surface to the horizontal/vertical as per this guideline and Fig C.4.3, the concrete cone diameter of the failure surface should be 150mm.

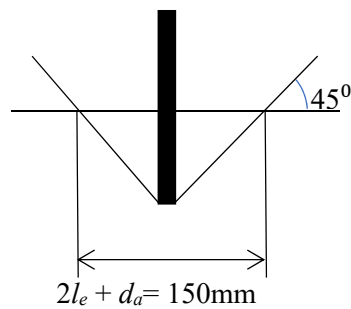


Figure C.4.3 Calculated diameter of concrete cone failure surface

The summary of the above calculation can be shown in the **Table C.4.1** as follows,

Table C.4.1 Summary of the calculation of design tensile capacity of a sample specimen

Strength	Calculated values	Remarks
Tensile strength at yielding (T_{a1})		
σ_y (N/mm ²)	560	
a_o (mm ²)	71.33	
T_{a1} (kN)	39.94	Eq. 4.3.2
Tensile strength at concrete failure (T_{a2})		
σ_B (N/mm ²)	12.2	
d_a (mm)	10	
l_e (mm)	70	
A_c (mm ²)	17592.92	
T_{a2} (kN)	14.13	Eq. 4.3.3
Tensile strength at bond failure (T_{a3})		
τ_a (N/mm ²)	7.6	Eq. 4.3.5
d_a (mm)	10	
l_e (mm)	70	
T_{a3} (kN)	16.71	Eq. 4.3.4
Tensile strength T_a (kN)	14.13	Eq. 4.3.1

All other specimens were designed following the above-mentioned calculation process.

In case of a “Test series-1” of anchors in RC slab, 2 types of anchor specimens of 6mm and 8mm diameter were designed using above-mentioned equations. The parameters of these specimens were anchor diameter and varying embedment length. Concrete strength of the RC slab was found to be 11.7 N/mm². Embedment

length of $7d_b$, $8d_b$, $9.4d_b$, $9.8d_b$, and $12.5d_b$ were selected for this “Test series-1”. All of the specimen were designed following the above-mentioned sample calculation process.

Specimen preparation and test set up of pullout test of post installed bonded anchor

As mentioned at section 4.3.1 the tensile capacity can be determined by performing pullout test of the anchor. This part of the commentary C.4.3.1 will mainly describe the detailed example of performing pullout test starting from the specimen preparation, test set up and loading system. To prepare the specimen for the pullout test, a regular drill bit can be used to drill the holes in RC member/pure concrete member for anchor insertion. However, if the concrete is of low strength (i.e. 10 N/mm^2) then the diamond core drill bit should be used instead of regular drill bit.



Figure C.4.4 Temporary wooden supports of anchor and rebar (from left)

Dust should be removed from the holes by flushing compressed air followed by cleaning using a wire brush to sustain adequate bond strength. After the cleaning, the holes should be filled with adhesive (i.e. HILTI HIT-RE 500V3 epoxy resin) as bonding material for the anchors. The tip of the anchor should be cut at a 45° angle at the bottom (JBDPA, 2001). The anchor should be inserted into the adhesive filled holes in a circular downward motion to ensure no void in it. The anchors then need to be kept in vertical position till it gets hard and therefore temporary supports must be built. **Fig. C.4.4** shows some examples of temporary supports of anchor.

Loading set up of pullout test of post installed bonded anchor

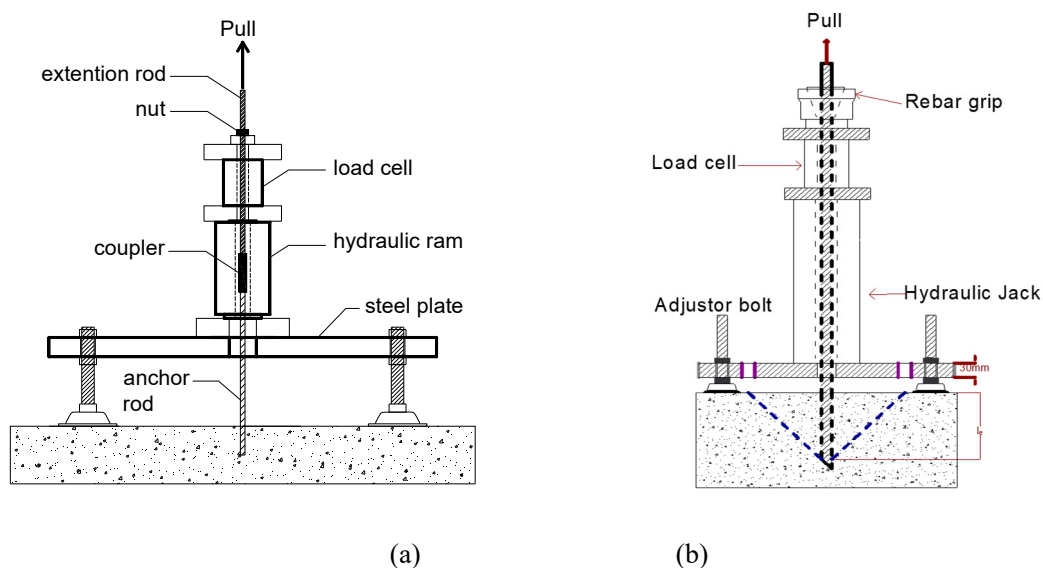


Figure C.4.5 Test set up of pullout test to determine tensile capacity of (a) anchor in RC slab and (b) rebar in pure low strength concrete

The loading equipment as shown in **Fig. C.4.5** can be used for the pullout test in case of RC slab or RC concrete block or in pure concrete block. The reaction frame should be designed strong enough so that it does not fail before the tensile failure of the anchor specimen or rebar occurs. Therefore, thickness of the steel plate and adjuster bolts as supporting legs should be selected carefully. The distance between the supports of reaction frame and anchor rod must be kept equal or greater to the effective embedment depth of the anchor in order to allow concrete cone failure to develop.

The loading should be applied through center hole hydraulic ram operated by a manual pump or automatic pump. A center hole load cell can be placed above the hydraulic ram to measure loads during the test.

Validation of CNCRP/BSPP Manuals for pullout test of post installed bonded anchor in low strength concrete

Following the above-mentioned test set up and loading system and after performing the pullout test of the sample specimen designed in section C.4.3.1, the experimental study found the tensile capacity of the sample rebar to be 21.32kN. This refers that the design capacity of the anchor calculated by this guideline is conservative and safe (N. Saha et al., 2020).

The experimental failure mode of the above-mentioned sample specimen shows a concrete cone failure which matches totally with the predicted failure modes by this guideline. However, as the experimental tensile capacity was more than the design calculations, the concrete cone failure area observed in the experiment also

exceeded the design assumption in this guideline, as shown in **Fig. C.4.6**. All other specimens from the experimental study having concrete cone failure showed similar characteristics.

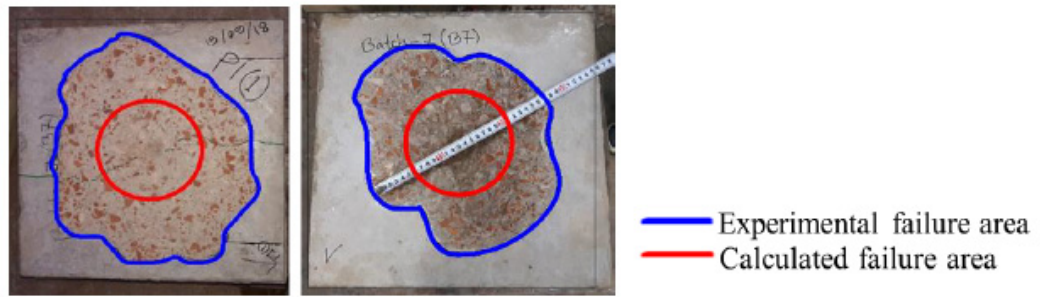


Figure C.4.6 Experimental failure area vs calculated failure area of pullout test of post installed bonded rebar in pure 12.2 N/mm² concrete block (N. Saha et al., 2020)

Two categories of bond failure occurred as shown in **Fig. C.4.7 (a)** have been observed from the experiment performed in pure concrete specimen. These categories are bond failure of adhesive/concrete interface and bond failure of steel/adhesive interface. In the case of bond failure of adhesive/concrete interface the experimental tensile capacity was more than 18% higher and for the specimens having bond failure of steel/adhesive interface the tensile capacity was 19% higher than that of the design tensile capacity for most of cases of this experimental study.

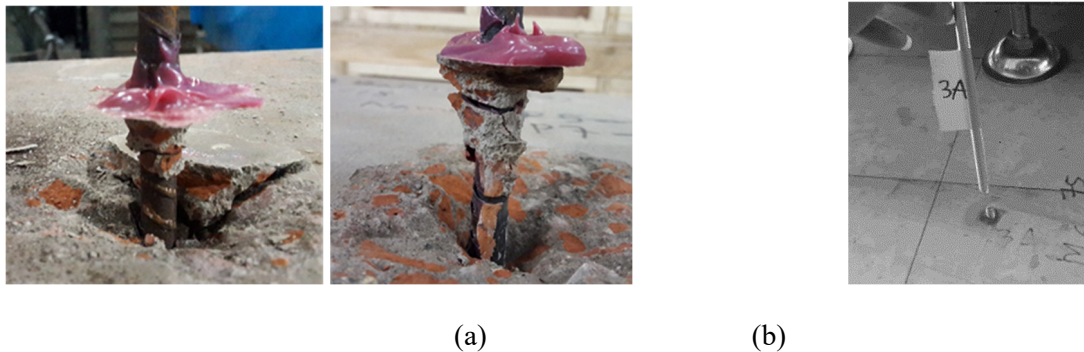


Figure C.4.7 (a) Bond failure of steel/adhesive interface and adhesive/concrete interface (from left) (N. Saha et al., 2020) and (b) Anchor specimen with tensile fracture

The expected failure modes of the “Test series-1” test specimen where the anchor specimens of 6mm and 8mm diameter were in the RC slab of low strength concrete matched with the experimental failure modes. Steel failure occurred only in case of “Test series-1” test specimen as shown in **Fig. C.4.7(b)**. The following **Fig. C.4.8** shows the test results from the “Test series-1” of pullout test of the anchor specimen.

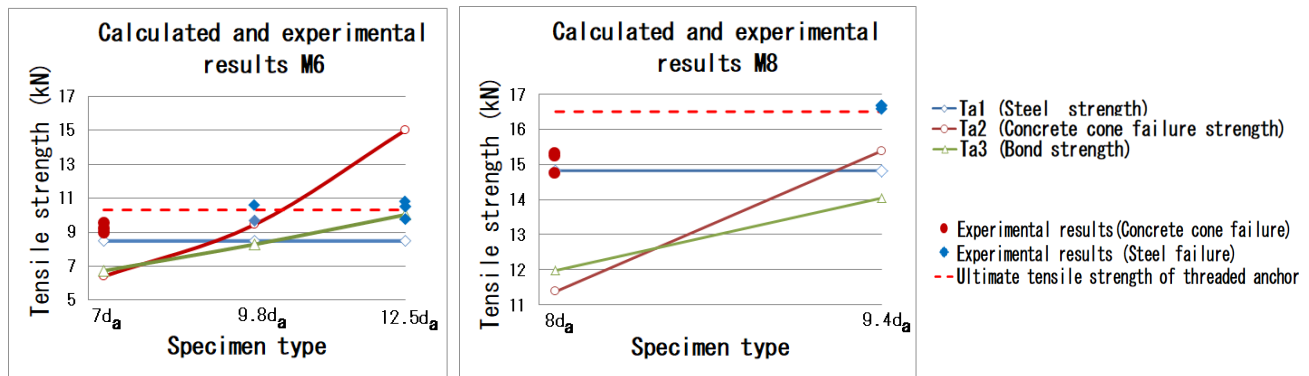
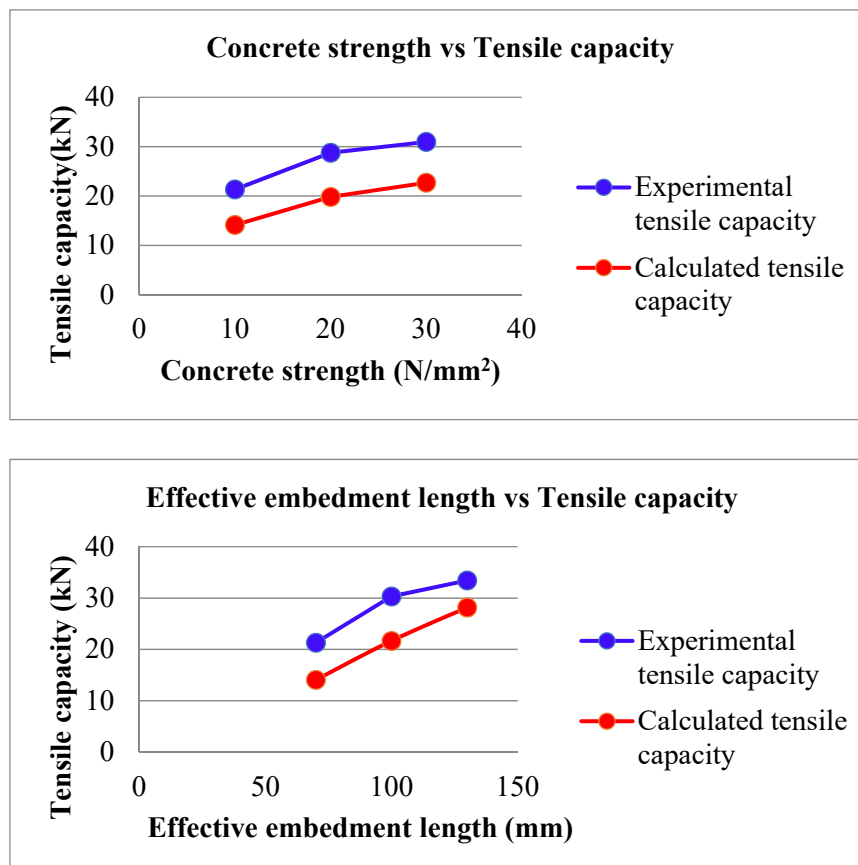


Figure C.4.8 Experimental tensile capacity of anchors compared to the design calculations (N. Saha, 2018)

However, the tensile capacity of anchors with steel fracture was also higher than the design calculations. The tensile capacity was observed at the ultimate tensile strength beyond yielding. This refers that if Ta_1 is calculated using the ultimate tensile strength (dashed red line in Fig. C.4.8) instead of yield strength (blue line in Fig. C.4.8), the calculated tensile capacity of anchors with steel fracture agrees with experimental results.

The experimental studies also show that if the effective embedment length is kept at least or larger than ten times the anchor diameter ($10d_b$) then the brittle type failure of concrete can be avoided (N. Saha, 2018). Therefore, for retrofitting purpose while selecting the effective embedment length must be selected greater than or equal to $10d_b$ for a rebar with diameter d_b .

From the experimental studies the effects of the change in concrete strength, rebar diameter and embedment length can be seen as shown in Fig. C.4.9.



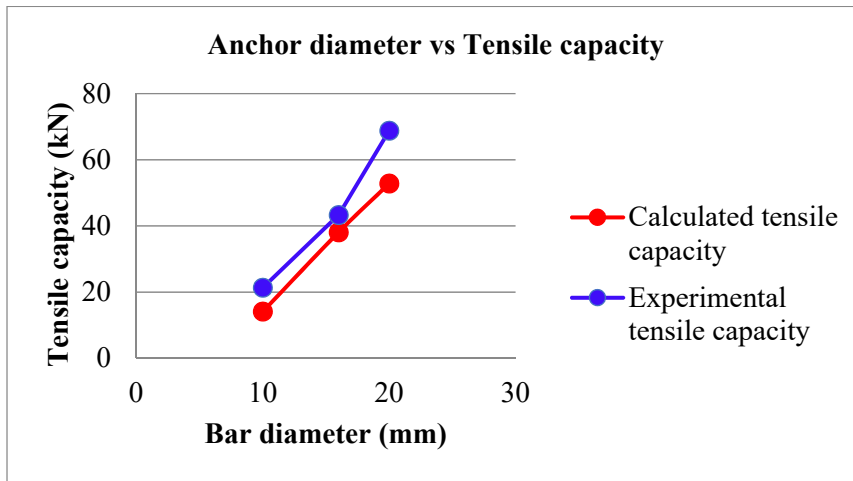


Figure C.4.9 Effects of concrete strength, rebar diameter and embedment length on tensile capacity of post installed single bonded anchors (N. Saha et al.,2020)

From the graphs of **Fig. C.4.9** it can be concluded that the tensile capacity increases with the increase in concrete strength, rebar diameter and embedment length and experimental results exceeded the design capacity in all cases.

From the graph of **Fig. C.4.10** it can be found that, the mean (Ta_{exp} / Ta_{cal})=1.31 and the coefficient of variation (CoV) =0.10 (N. Saha et al.,2020). Results obtained from this study, it can be seen that the tensile capacity calculated by this guideline is lower than the experimental results.

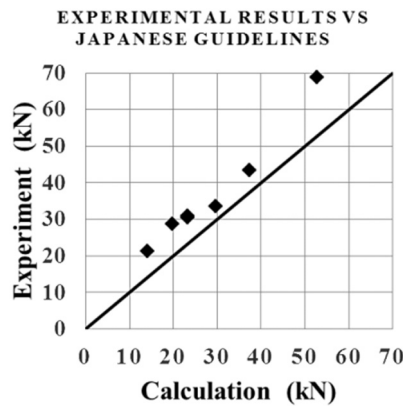


Figure C.4.10 Experimental results versus design data by this guideline (N. Saha et al., 2020)

From the graphs of **Fig. C.4.9** and **Fig. C.4.10** it is proved that this guideline (as well as CNCRP/BSPP Manuals) evaluated the tensile capacity of post installed single bonded anchor in low strength concrete with brick chips conservatively.

4.3.2 Shear Test

The shear capacity of post installed bonded anchors in concrete with compressive strength between 10-15 N/mm² cannot be evaluated according to the existing CNCRP/BSPP Manuals provided by PWD. This guideline extended the scope of application to low strength concrete ranged between 10-15 N/mm². The shear capacity Q_a is defined as the capacity resisted by a single anchor at the concrete interface. Shear capacity shall be the smaller value of Q_{a1} and Q_{a2} , which are determined by steel strength and bearing strength of concrete, respectively.

For bonded anchor in case of $l_e \geq 7d_a$

$$Q_{a1} = 0.7 \cdot \sigma_y \cdot s a_e \quad (4.3.6)$$

$$Q_{a2} = 0.4 \sqrt{E_c \sigma_B} \cdot s a_e \quad (4.3.7)$$

However, bond stress, $\mathcal{T} = \frac{Q_a}{s a_e} \leq 294 \text{ N/mm}^2$

where,

σ_B = Compressive strength of existing concrete. In general, the strength shall be obtained by compression test of concrete cores. When the test value is larger than specified concrete strength F_c , σ_B shall be determined according to the standard.

$s a_e$ = Cross-sectional area of the anchor specimen.

E_c = Young's modulus calculated based on σ_B . The test value can be used when measured during compression test.

C.4.3.2 [Commentary]

Design of shear capacity of post installed bonded anchor in low strength concrete and expected failure modes of the anchor

The design shear capacity mainly varies mainly along with concrete compressive strength and the yield stress of steel. C.4.3.2 [Commentary] of this guideline show an example of evaluation process of possible failure modes as well as the calculation of design shear capacity of anchor specimen. Sample calculation of design shear capacity of the specimens and expected failure modes of post installed rebar specimens of diameter d_b , concrete strength of σ_B and yield stress of σ_y is as follows,

$$d_a = 10 \text{ mm.}$$

$$s a_e = 78.54 \text{ mm}^2$$

$$\sigma_B = 12.2 \text{ N/mm}^2$$

$$\sigma_y = \text{the yield strength of the rebar specimen} = 560 \text{ N/mm}^2$$

$$Q_{a1} = 0.7 \cdot \sigma_{y,s} a_e$$

$$= 0.7 \cdot 560 \cdot 78.54$$

$$= 30.79 \text{ kN}$$

σ_y (N/mm ²)	$s a_e$ (mm ²)
560	78.54

$$Q_{a2} = 0.4 \sqrt{E_c \sigma_B} \cdot s a_e$$

$$= 16.03 \text{ kN}$$

σ_B (N/mm ²)	$s a_e$ (mm ²)	γ (kN/m ³)	E_c (N/mm ²)
12.96	78.54	24	20100

$$Q_a = \min \{Q_{a1}, Q_{a2}\}$$

$$= 16.03 \text{ kN}$$

$$\frac{Q_a}{s a_e} \leq 294 \text{ N/mm}^2$$

As for this specimen the calculated value of Q_{a2} is smaller than Q_{a1} , therefore for this shear test of post installed bonded single anchor, concrete bearing failure will occur.

Example of shear test of post installed bonded anchor

For the specimen designed in C.4.3.2 the shear test loading set up can be done as per ASTM E 488-96. The anchor rebar of shear test was installed at the side of the RC specimen. Installation of anchor rebar for shear test can be done in a way similar with the anchor installation of post installed anchor rebar for pullout test as described on section C.4.3.1 of this guideline. Holes were created on the side of the RC slab/block specimens and then the holes were filled with epoxy resin. Then the anchor specimens were inserted inside the hole by a clockwise rotation. The specimens were kept twenty-four hours untouched or without any movement till the adhesive gets hard. The test set up of shear test along with its failure mode are shown in **Fig. C.4.11**(N. Saha et al.,2020).

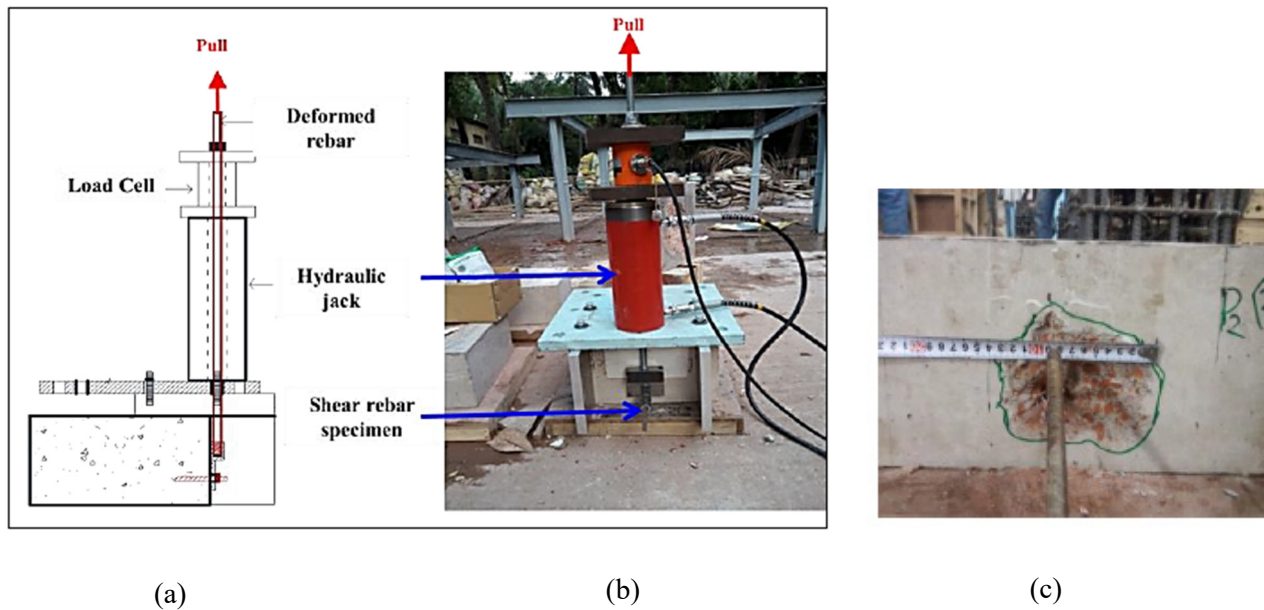


Figure C.4.11 Experimental shear test loading set up on concrete block (a) side view, (b) front view and (c) concrete bearing failure of shear test (N. Saha et al. ,2020)

From **Fig. C.4.11 (a)** the side view of the shear test set up and from **Fig. C.4.11 (b)** the front view of the shear test of post installed single bonded anchor in concrete block can be seen. The loading equipment included the same steel plate, center hole hydraulic ram, center hole load cell along with the additional equipment which were used for the pullout test.

After performing the shear test, experimental result shows that the shear capacity of the rebar specimen which was designed in C.4.3.2 is 21.70 kN (N. Saha et al., 2020). This value is higher than the expected shear capacity calculated by this guideline. The experimental failure mode is concrete bearing failure which is shown in **Fig. C.4.11(c)**. This fully matches with the expected failure mode predicted by this guideline. From the above discussion it is clear that this guideline calculates the value of shear capacity and shear failure modes of post installed single bonded anchor with accuracy.

4.4 Limitations

Post-installed anchors shall be installed in accordance with the standard construction procedure carefully. Anchor diameter which are greater than 20mm are not covered by this guideline. Too high strength (greater than 36 N/mm²) are out of scope of this guideline.

References

- [1] JBDPA (2001): Standard for Seismic Evaluation of Existing Reinforced Concrete Buildings; Guidelines for Seismic Retrofit of Existing Reinforced Concrete Buildings.
- [2] N. Subramanian and R.A. Cook (2002): Installation, behavior and design of bonded anchors, *Indian Concrete Journal* 76(1): pp.47-56

- [3] Reizi Tanaka, Koichi Oba, "Experimental study on seismic performance of beam members connected with post installed anchors", Figure: 6, pp. 583.
- [4] N.Saha, Y. Sanada, S. Takahashi, M.M. Rahman, A.F.M.S. Amin (2020): *INVESTIGATION ON TENSILE AND SHEAR CAPACITY OF POST INSTALLED BONDED REBAR IN BRICK-AGGREGATE CONCRETE*, 17th World Conference on Earthquake Engineering, 17WCEE Sendai, Japan - September 13th to 18th 2020,3f-0014
- [5] Saha Nandita, Wardi Syafri, Susumu Takahashi, Yasushi Sanada: Report on Pullout Test of Post Installed Anchors in Low Strength Concrete with Brick Chips, Architectural Institute of Japan (AIJ) conference,2018
- [6] ASTM E488-96, American Association for Testing and Materials, "Standard Test Methods for Strength of Anchors in Concrete and Masonry Elements", *ASTM*, June 2003, pp. 1-8.

Chapter 5 Instruction on Retrofit Construction

The construction procedure for retrofit is different from the general new building construction work. In this chapter, the construction procedures of the proposed retrofitting techniques in the SATREPS-TSUIB project are introduced.

5.1 Drop panel installation

Installing drop panels is a popular method to prevent punching shear failure of flat plate structures (**Fig. 5.1.1**) because a drop panel is effective to increase the joint area of flat plate structures.

Drop panel can be installed by using post-installed anchors as shown in **Fig. 5.1.2**. The anchorage length of post-installed anchors is governed by the thickness of flat plate, therefore, it is necessary to confirm that the thickness of flat plate is enough for the anchorage referring Chapter 4.

The construction flow is shown in **Fig. 5.1.3**. After removal of plaster, concrete surface is chipped. Afterwards, flat plate is drilled to install post-installed anchors. Post-installed anchors are vertically installed as shown in **Fig. 5.1.2**, and are fixed by epoxy. Reinforcing bars in a drop panel are arranged as shown in **Fig. 5.1.2**. Subsequently, a formwork is set up for casting concrete of the drop panel. After the curing of concrete, the formwork is removed.

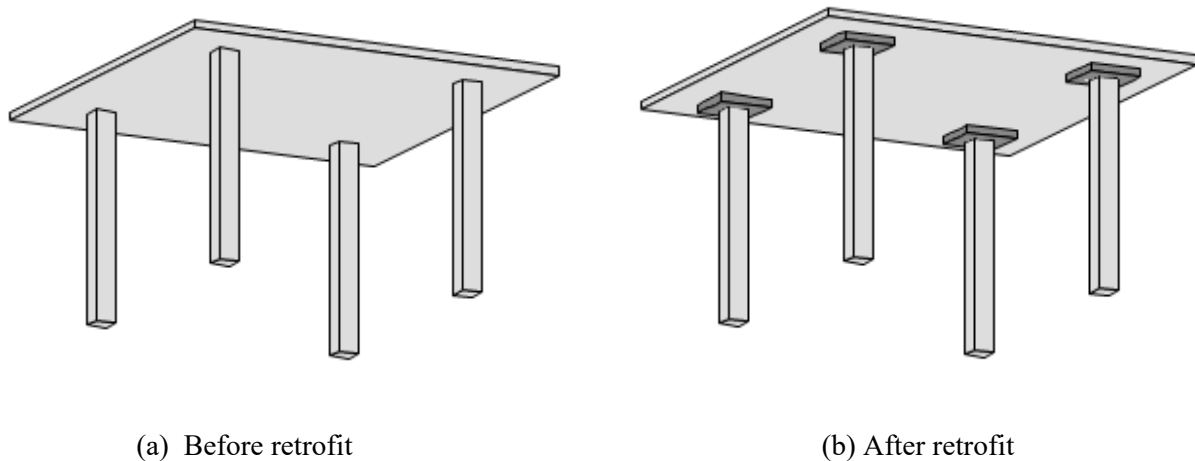


Figure 5.1.1 Retrofit of flat plate structures by drop panel

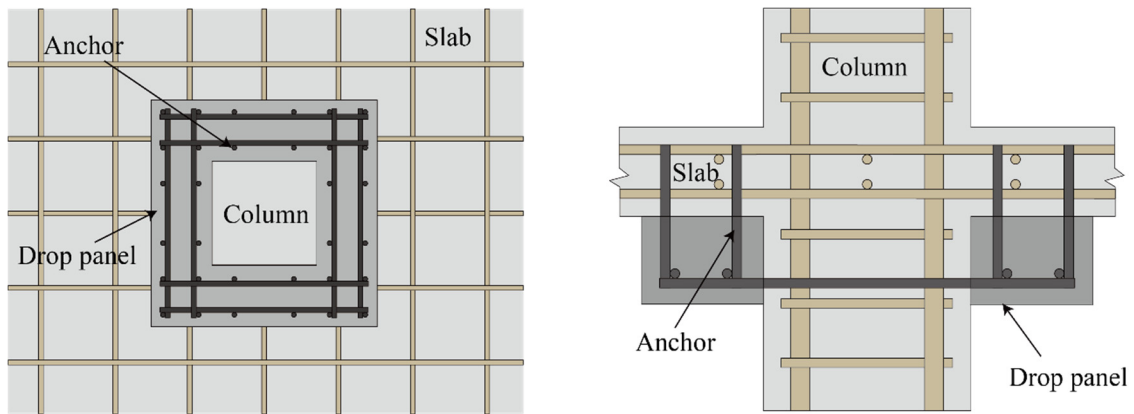


Figure 5.1.2 Drop panel installation

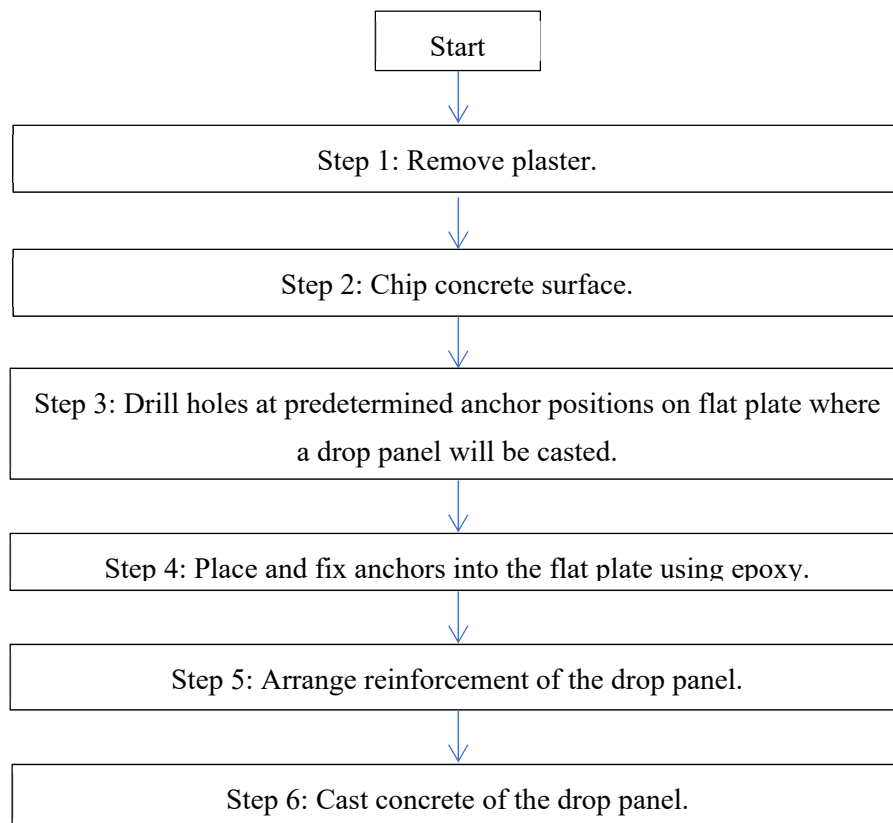


Figure 5.1.3 Construction flow chart for drop panel installation

Step 1: Remove plaster.

- The plaster of slab should be removed and the surface will be exposed.
- The plaster removing work should be carried out carefully to ensure that it does not produce any crack on the slab.
- A blower shall be used to clean dust and fine powders from the slab surface.

Step 2: Chip concrete surface.

- A chipping device or a metal brush shall be used to chip the surface of the slab.
- Chipped surface should be 2-5 mm roughness. (JBDPA, 2001)

Step 3: Drill holes at predetermined anchor positions on flat plate where a drop panel will be casted.

- The depth of holes should be marked on the drill (**Fig. 5.1.4**).
- Drill holes as shown in **Fig. 5.1.5**.



Figure 5.1.4 Mark a drill

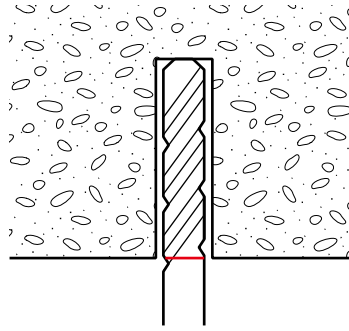


Figure 5.1.5 Drill a hole

Step 4: Place and fix anchors into the flat plate using epoxy.

- Insert glue into the drilled holes (**Fig. 5.1.6**).
- Install anchors as shown in **Fig. 5.1.7**.

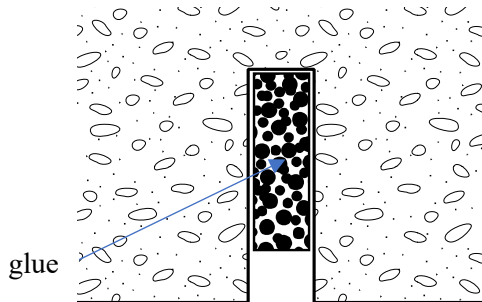


Figure 5.1.6 Insert glue

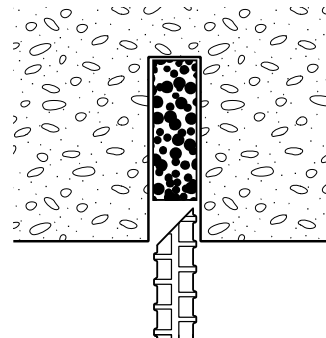


Figure 5.1.7 Install an anchor

Step 5: Arrange reinforcement of the drop panel.

- Arrange reinforcement of the drop panel as shown in **Fig. 5.1.8**.
- Reinforcements can be fixed by connecting with the anchors.

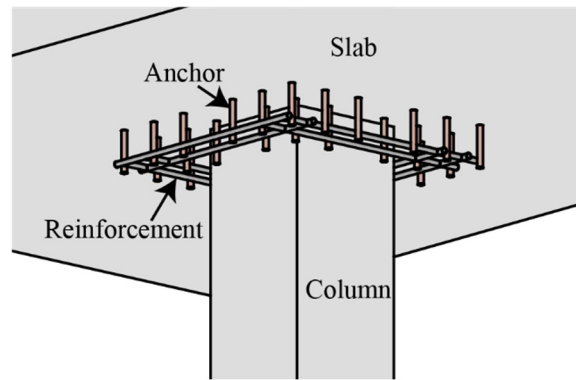


Figure 5.1.8 Arrangement of reinforcement

Step 6: Cast concrete of the drop panel.

- Make formwork to cast concrete of the drop panel as shown in Fig. 5.1.9.
- Cast concrete of the drop panel.

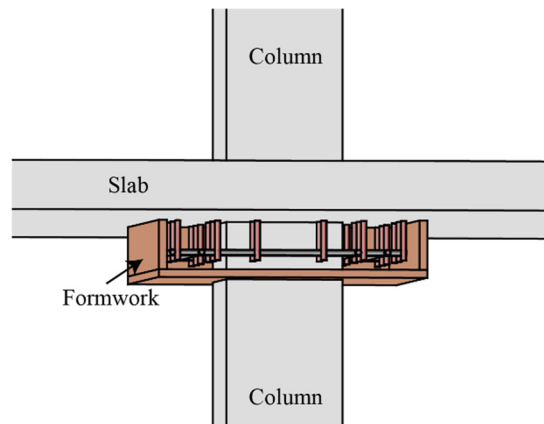


Figure 5.1.9 Formwork of the drop panel

5.2 Ferrocement application to masonry infill walls

The flow of construction procedure in detail as shown in Figure 5.2.1:

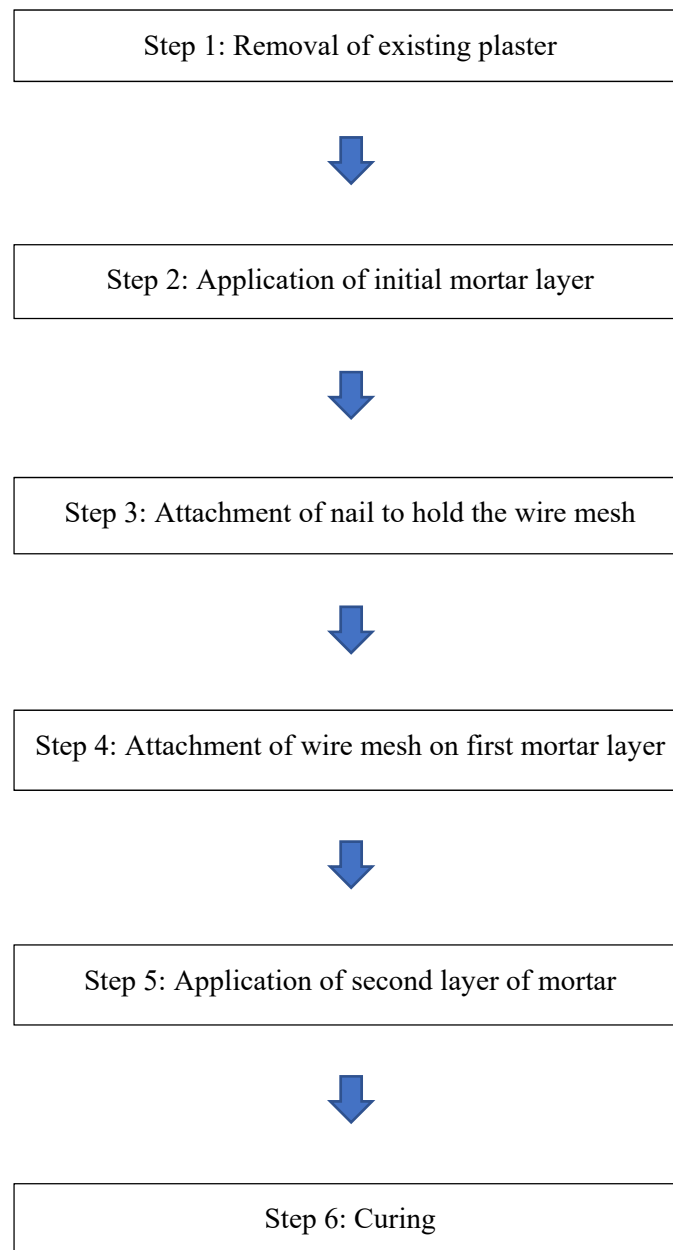


Figure 5.2.1 Construction procedure for FC lamination

Construction procedure in detail:

Step 1: Removal of existing plaster

- To facilitate the retrofit work, adjacent fixtures, decoration, etc. should be removed carefully.

- Appropriate measures should be taken to minimize the noise, vibration, and dust generated by the construction work.
- The plaster of masonry surface to be retrofitted should be removed completely and the surface will be exposed as shown in the Figure 5.2.2.
- The plaster removing work should be carried out carefully to ensure that no crack inside the joint mortar or it does not produce any crack on brick.
- A blower and suction devise should be used to clean dust and fine powders from the masonry surface.
- Repair the cracks if any on masonry infill and inside mortar joint.

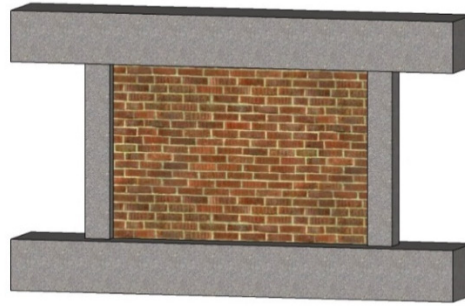


Figure 5.2.2 Removal of existing mortar (plaster) from infill masonry

Step 2: Application of initial mortar layer

- Confirm the mixing method of mortar with appropriate water to cement ratio to get a target mortar strength.
- Mortar placing as per specification (mortar placing section, amount of mortar placing in a single portion) as shown in Figure 5.2.3 (in the figure 5.2.3, mortar is shown on a portion of wall to demonstrate the mortar layer and masonry wall. In practical case full wall surface shall be covered with mortar.
- Level should be maintained by marking both end with string controlling the same thickness of mortar over the masonry infill wall.

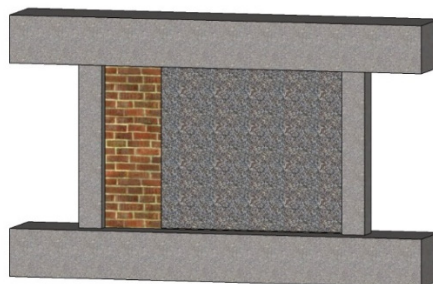


Figure 5.2.3 Application of initial mortar layer

Step 3: Attachment of nail to hold wire mesh

- At least 9 nails/sqm. should be applied on each masonry surface, a schematic image is shown in Figure 5.2.4.
- Marking the point on the infill wall for nail insertion, it is preferable to make a hole on bricks to avoid

joint mortar. It is better to mark the line of each joint mortar level on the column before application of the initial mortar.

- Drilling on initial mortar layer, drilling depth should be satisfying as per judgment. In that case, drilling depth should be marked to confirm the drilling depth.
- Cleaning of drilling holes should be carried out carefully by using a blower and brushes. If there is some dust, the epoxy material will not get sufficient bonding.
- Install nail using epoxy resin glue: The application method shall be done according to the instruction of the chemical manufacture's guideline.
- The nail shall be installed with sufficient care by skilled worker.

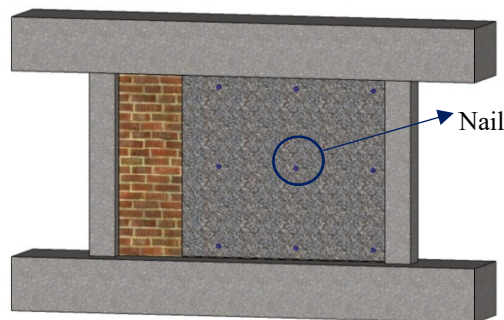


Figure 5.2.4 Attachment of nail after drilling

Step 4: Attachment of wire mesh on first mortar layer

- Cut the wire mesh into same size of masonry infill panel.
- Keep 100mm overlapping of wire mesh, when it is necessary to join wire mesh to cover full masonry infill wall surface.
- Put wire mesh on initial plaster mortar as shown in Figure 5.2.5 (in the figure 5.2.5, FC is shown on a portion of wall to demonstrate the layers only. In practical case full wall surface shall be covered with FC).
- Bind the wire mesh with the attached nails in the earlier step.
- In the case of multilayers, the first layers should be put and attached with nails and the following layer will be attached and tied with nails consecutively.

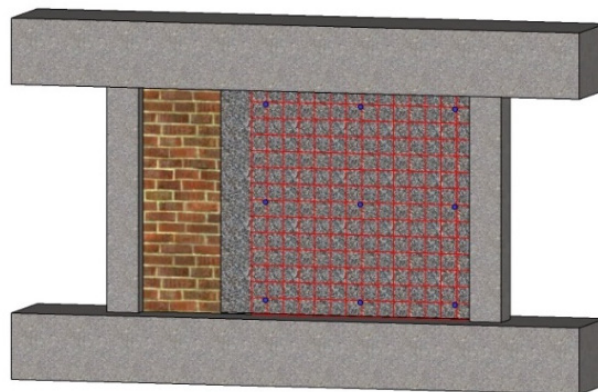


Figure 5.2.5 Attachment of wire mesh

Step 5: Application of second layer of mortar

- Confirm the mixing method of mortar with appropriate ratio to get a target mortar strength.
- Mortar placement of second mortar layer as shown in Figure 5.2.6 (in the figure 5.2.6, FC is shown on a portion of wall to demonstrate the layers only. In practical case full wall surface shall be covered with FC).
- The level should be maintained by marking both ends with string controlling the same thickness of mortar over the masonry infill wall.
- Use the wooden Patta (instrument made from wood) for smoothing and leveling the mortar surface until smooth.

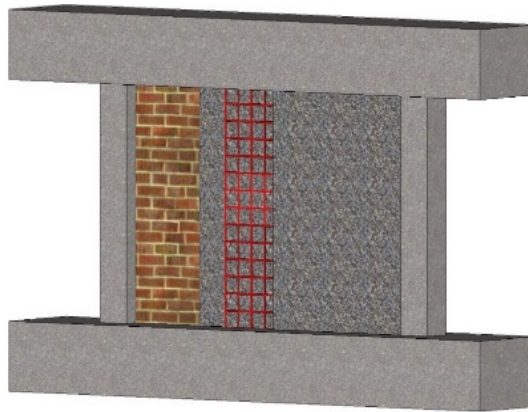


Figure 5.2.6 Application of second layer of mortar

Step 6: Curing

- Confirm the curing method (for example using gunny bag and pouring water.)
- Use a gunny bag for curing and pour water to confirm sufficient moisture.

Appendix: Pro forma

1. Checklist pro forma for construction work
2. Photographic monitoring in construction work
2. Material testing work

Chapter 6 Examples of Seismic Retrofit

6.1 Moment-resisting frame structure

6.1.1 General

The procedure of the seismic retrofit is illustrated through an example of existing moment-resisting frame building which is outlined in this section. The main purpose of this example calculation is to show the process of determining the seismic performance based on CNCRP/BSPP Manuals & SATREPS-TSUIB Guidelines and to show how to apply the present guidelines for seismic retrofit. The subject building selected for retrofitting is same as the one shown in section 7.2 of SATREPS-TSUIB seismic performance evaluation guideline.

6.1.2 Scope

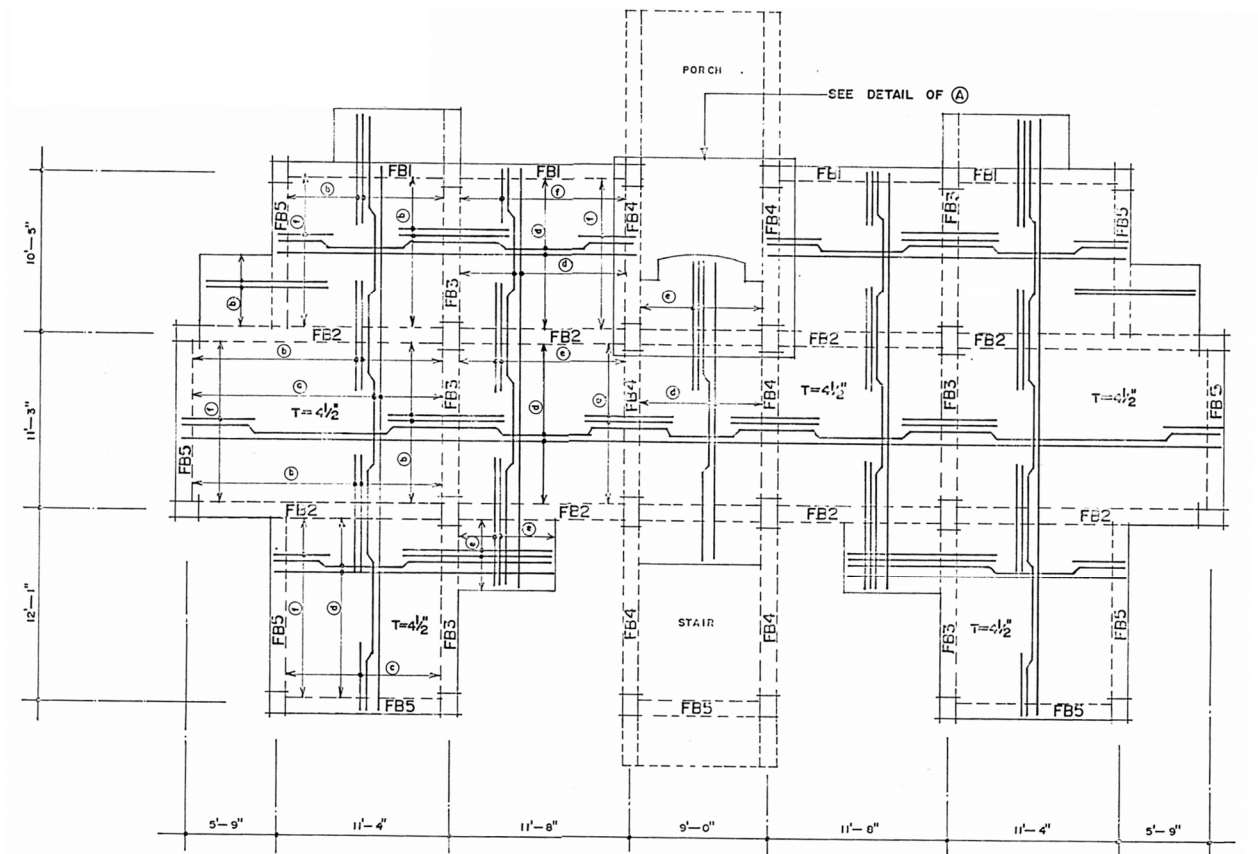
The following sample calculation flow mainly focuses on and illustrates several new procedures and/or schemes presented in both SATREPS-TSUIB Guidelines for the seismic evaluation and retrofit; thus, conventional calculation details according to CNCRP/BSPP Manuals are mostly skipped. Assumptions of evaluation are made according to CNCRP/BSPP Manuals & SATREPS-TSUIB Guidelines.

6.1.3 Outline of the structure

The example building is a multi-storey RC building located in Dhaka city. The structure has no load-bearing infill walls. It represents a typical Bangladeshi moment-resisting frame structure. The building is used for residential purposes. The floor plan, column schedule and material property are shown in the following tables and figures.

Table 6.1.1 Summary

Usage	Residential building
Number of stories	Six
Structure type	Moment-resisting frame
Foundation type	Pile foundation
Construction year	2002
Building constructor	GoB PWD (Public)
Building location	Dhaka city



Unit: Feet-inch

Figure 6.1.1 Typical floor plan

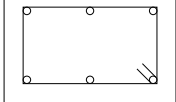
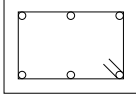
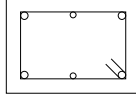
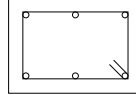
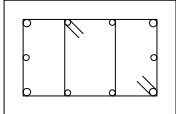
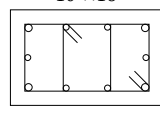
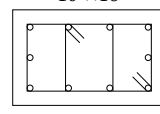
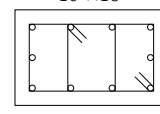
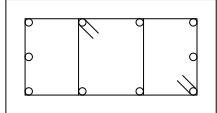
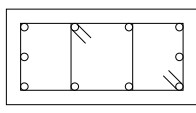
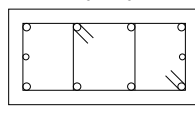
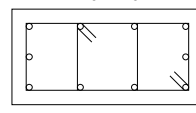
	UP TO F.G.L	UP TO 2 ND FLOOR	UP TO 4 TH FLOOR	UP TO ROOF LEVEL
C1	12"×16"  6 – 20 mm ϕ	10"×14"  6 – 20 mm ϕ	10"×14"  4 – 20 mm ϕ (corner) 2 – 16 mm ϕ	10"×14"  6 – 16 mm ϕ
C2	12"×18"  4 – 20 mm ϕ (corner) 6 – 16 mm ϕ	10"×16"  4 – 20 mm ϕ (corner) 6 – 16 mm ϕ	10"×16"  10 – 20 mm ϕ	10"×16"  10 – 16 mm ϕ
C3	12"×22"  10 – 20 mm ϕ	10"×20"  10 – 20 mm ϕ	10"×20"  4 – 20 mm ϕ (corner) 6 – 16 mm ϕ	10"×20"  10 – 16 mm ϕ

Figure 6.1.2 Column schedule

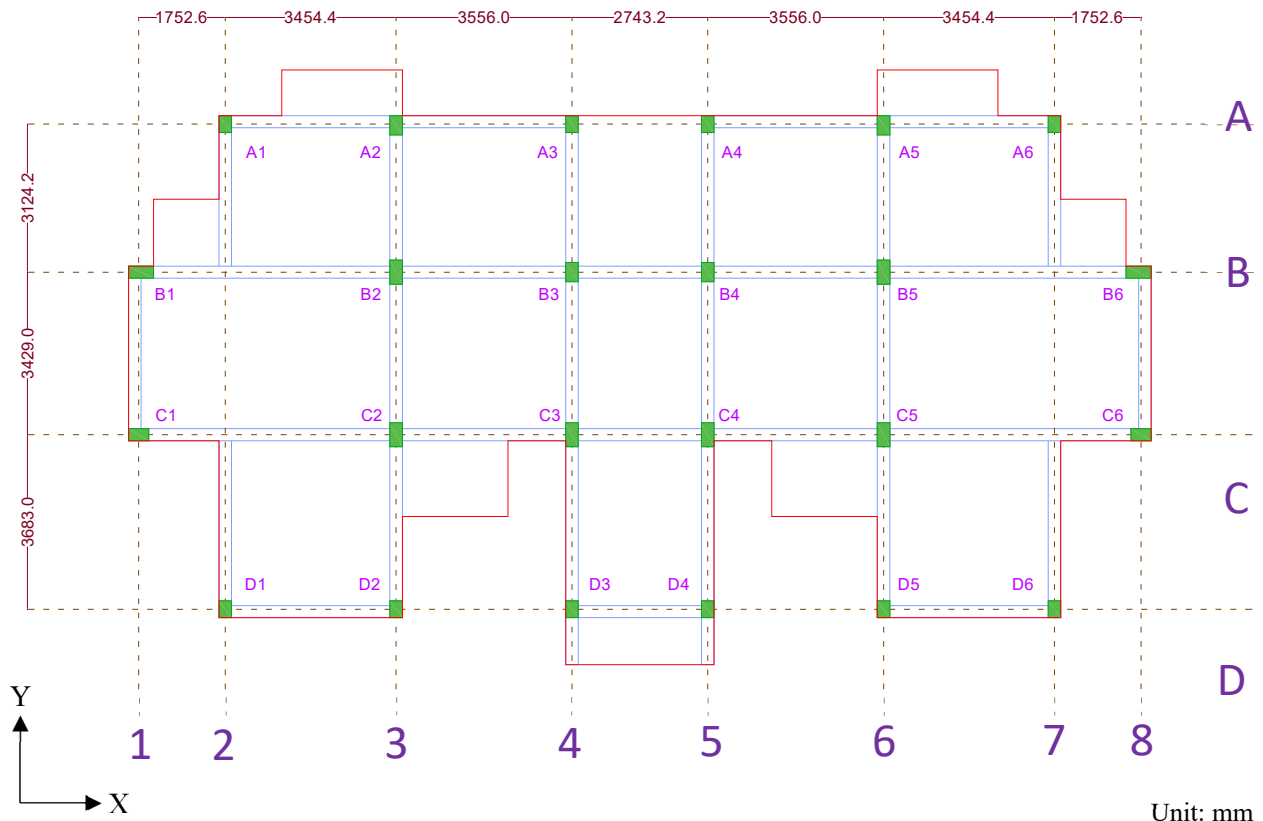


Figure 6.1.3 Column layout

Table 6.1.2 Column Layout

Column Layout						
Frame	1	2	3	4	5	6
A	A1	A2	A3	A4	A5	A6
B	B1	B2	B3	B4	B5	B6
C	C1	C2	C3	C4	C5	C6
D	D1	D2	D3	D4	D5	D6

Table 6.1.3 Material property

Type of concrete	Normal strength concrete
Concrete strength	25 MPa (28 days cylinder test)
Type of rebar	Deformed
Rebar yield stress	415 MPa (billet steel)

6.1.4 Seismic evaluation of the building

The subject building selected is the same as the one shown in the SATREPS-TSUIB evaluation guideline. The detailed seismic performance evaluation process is shown in the SATREPS-TUSIB seismic evaluation guideline and skipped in this guideline. Summary of the structural performance of the building is as following.

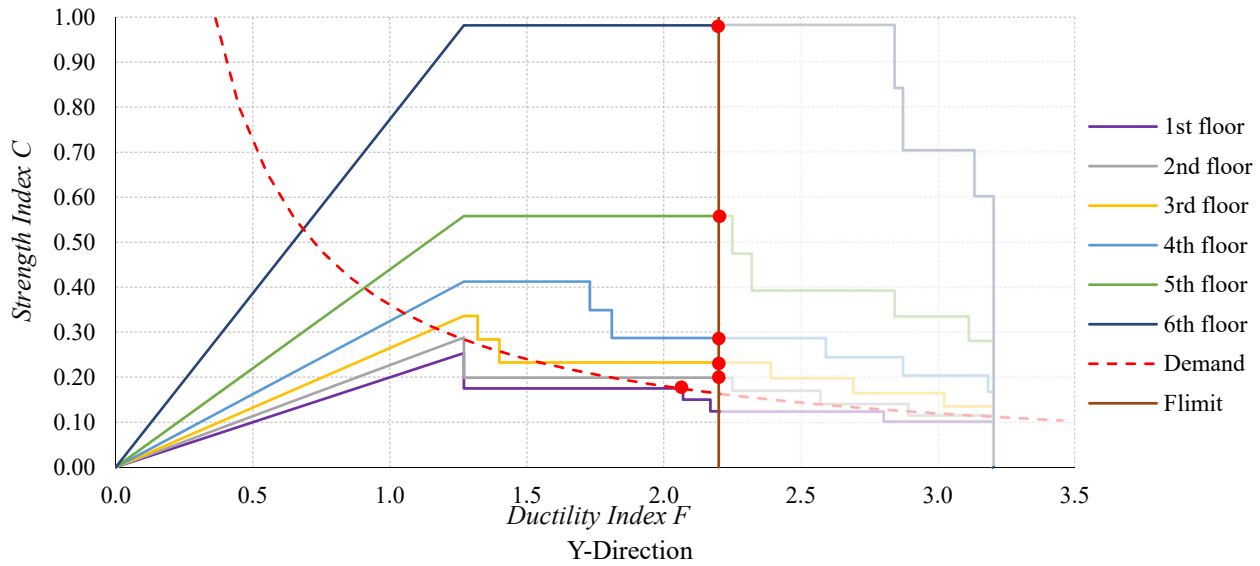
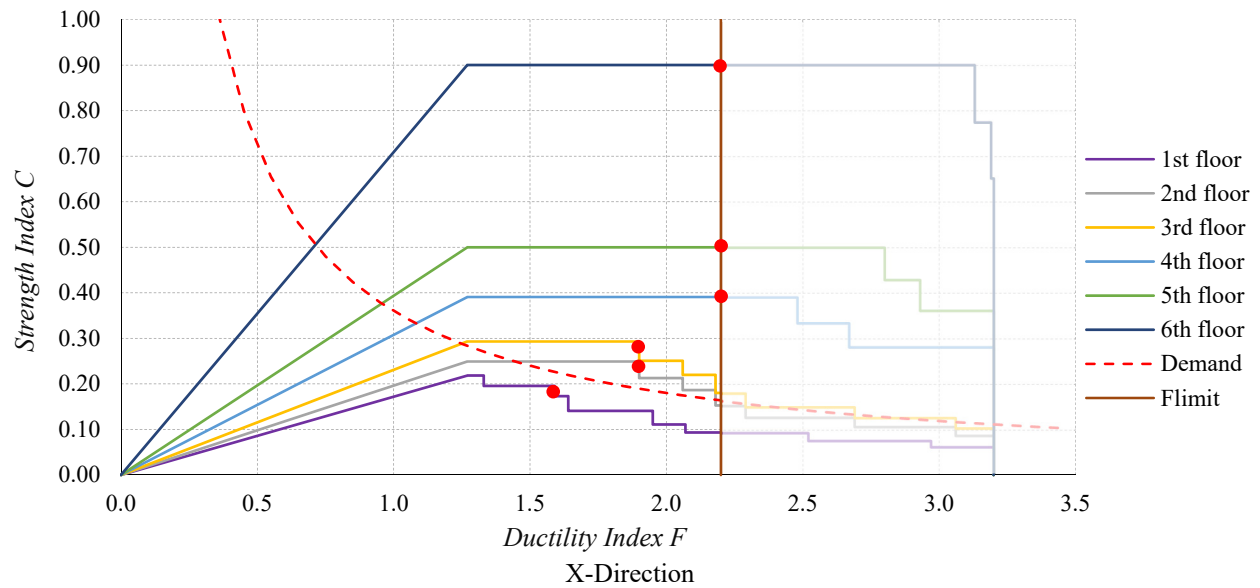


Figure 6.1.6 Structural performance curve

6.1.5 Seismic retrofit of the building

Seismic retrofit is required for the 1st floor in the X-direction. In this example, masonry infill wall strengthened with ferrocement was selected to highlight the new retrofitting technique described in the SATREPS-TSUIB Guidelines for retrofitting.

Deformation capacity of the structure after strengthening was targeted as ductility index, $F = 1.27$ to minimize the damage to the structure.

Note: The target F index after retrofit should be selected based on careful judgement of engineers.

According to the CNCRP/BSPP Seismic Retrofit Design Manual.

For 1st floor X-direction:

$$\Delta I_S = I_{S0} - I_S = 0.36 - 0.311 = 0.049$$

$$E = \frac{n+1}{n+i} \times C \times F$$

$$I_s = E \cdot S_D \cdot T = \frac{n+1}{n+i} \times C \cdot F \cdot S_D \cdot T$$

$$\text{or, } C \cdot F = \frac{n+i}{n+1} \times \frac{I_s}{S_D \cdot T} \text{ where, } C = \frac{Q}{\Sigma W}$$

$$\text{Then required, } Q = \frac{n+i}{n+1} \times \frac{I_{s0} \times \Sigma W}{(F \cdot S_D \cdot T)} - \frac{n+i}{n+1} \times \text{original } C \text{ (at } F = 1.27) \times \Sigma W$$

$$\text{For the case of 1}^{\text{st}} \text{ floor, } \Delta Q = \frac{I_{s0} \times \Sigma W}{(F \cdot S_D \cdot T)} - \text{original } C \text{ (at } F = 1.27) \times \Sigma W$$

$$= \frac{0.36 \times 13485.1}{1.27 \times 1 \times 1} - 0.218 \times 1.27 \times 13485.1$$

$$= 191.11 \text{ kN}$$

Four masonry infill walls strengthened with ferrocement are considered to be installed on the 1st floor of the structure to maintain the symmetry of the structure and keep it balanced. **Figure 6.1.7** shows the location of the infill wall strengthened with ferrocement.

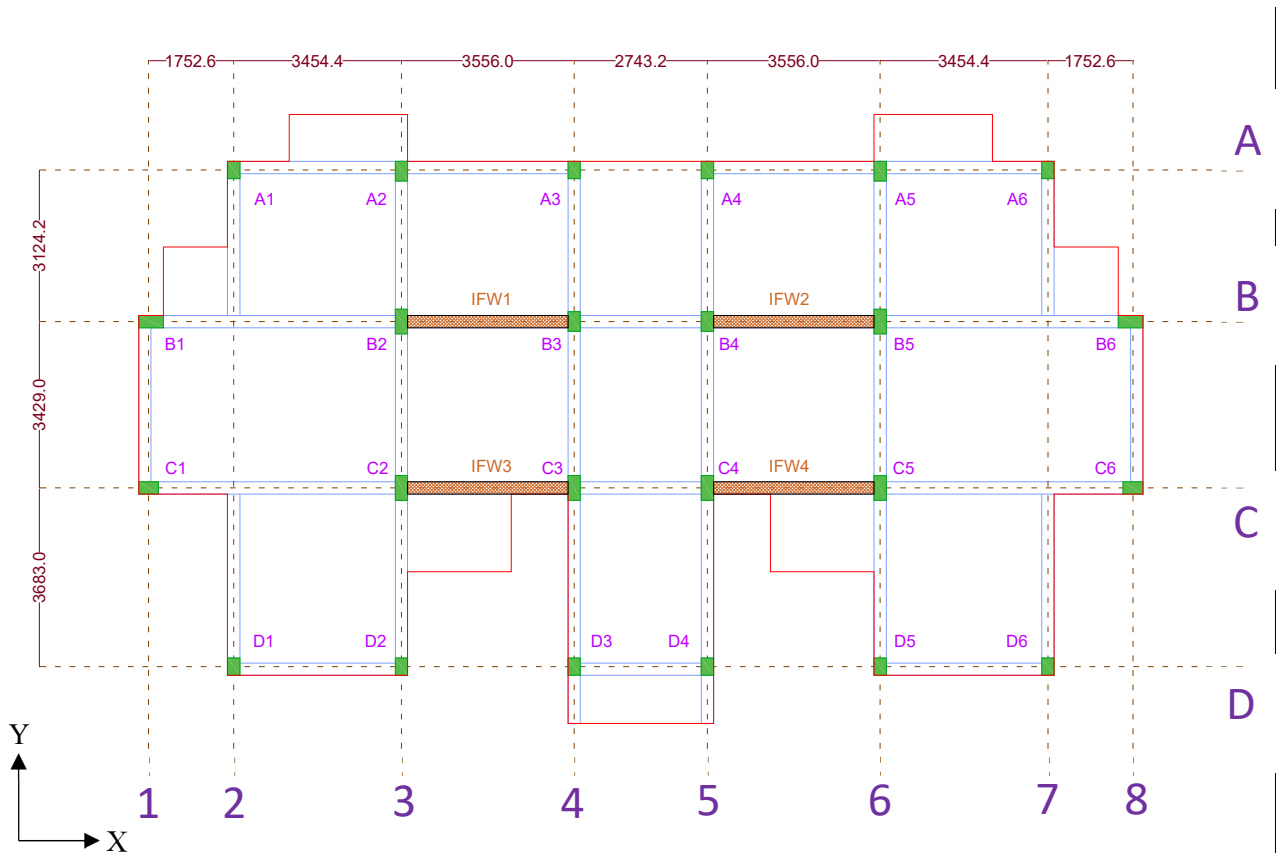


Figure 6.1.7 Strengthening proposal 1st floor

Member strength after strengthening

The following retrofit was done according to the process described in section 3.3 of this guideline. Furthermore, the material property for the strengthening process was taken same as described in section 3.3 of this guideline.

Masonry property:

Prism strength, $f_m = 8 \text{ MPa}$

Young Modulus, $E_{mas} = 550 \times f_m = 4400 \text{ MPa}$

Thickness of masonry infill, $t_{mas} = 125 \text{ mm}$

Ferrocement property:

Number of surfaces, $n_s = 2$ (two side)

Mortar strength, $f_{mortar} = 20 \text{ MPa}$

Young Modulus, $E_{FC \text{ mortar}} = 4700\sqrt{f_{mortar}} = 21019 \text{ MPa}$

Ferrocement thickness, $t_{FC} = 25 \text{ mm}$ (one side thickness)

Wiremesh property:

Number of layers, $n_l = 2$ (one side)

Area of wiremesh, $A_s = 1.0 \text{ mm}^2$

Wire mesh spacing, $S_y = 5 \text{ mm}$

Yield strength of wire mesh, $\sigma_y = 300 \text{ MPa}$

Concrete & Reinforcement property:

Concrete strength, $f_c' = 300 \text{ MPa}$

Young Modulus, $E_c = 4700\sqrt{f_c'} = 23500 \text{ MPa}$

Reinforcement properties, $\sigma_y = 415 \text{ MPa}$

For IFW1 ferrocement strengthened masonry infill wall,

Frame diagonal length, $d_{inf} = 4399.7 \text{ mm}$

Inclination angle of diagonal from the horizontal axis, $\theta \text{ (rad)} = 0.63$

$Q_{frame} = Q_{left \text{ col.}} + Q_{right \text{ col.}} = 151.33 + 119.07 = 270.4 \text{ kN}$

$$\lambda_{mas-FC} = \sqrt[4]{\frac{(E_{mas}t_{mas} + E_{FC}n_s t_{FC})\cos^2\theta}{4E_C I_C d_{inf}}} = 0.00115489$$

$$a_c = \frac{\pi}{4\lambda_{mas-FC}} = 680.063 \text{ mm}$$

$$W_s = 2a_c \cos\theta = 1099.02 \text{ mm}$$

$$f_{m,\theta} = 0.5f_m = 4 \text{ MPa}$$

a) diagonal compression

$$\begin{aligned} Q_1 &= Q_{frame} + 0.5f_{m,\theta}W_s t_{mas} \cos\theta + 0.5f_{mor,FC}W_s n_s t_{FC} \cos\theta \\ &= 936.43 \text{ kN} \end{aligned}$$

b) diagonal cracking

$$A_{mas} = d_{inf} t_{mas} = 549962.5$$

$$\alpha = 0.7; h_{mas} = h_0$$

$$\begin{aligned} Q_2 &= Q_{frame} + 0.5f_m A_{mas} \sin\theta + \alpha n_s n_l \frac{A_s}{S_y} \sigma_y h_{mas} \\ &= 748.2 \text{ kN} \end{aligned}$$

c) Overall flexure

$$M_u = a_t \sigma_y l_w + 0.5N l_w = 4718.58 \text{ kN} \cdot \text{m}$$

$$Q_3 = M_u / h_0 = 1821.28 \text{ kN}$$

d) Column punching and joint sliding failure

$$K_{min} = \frac{0.34}{0.52 + a/D} = 0.40$$

$$\sigma = \rho_g \cdot \sigma_y + \sigma_0 = 17.128$$

$$\tau_0 = 0.66f_c' = 16.5$$

$$\tau_{mas} = 0.17\sqrt{f_{c,mor}} = 0.7603$$

$$\tau_{mas,FC} = 0.17\sqrt{f_{c,mor}} = 0.7603$$

$$\begin{aligned} Q_4 &= K_{min} \tau_0 bD + \tau_{mas} l_w t_{mas} + \tau_{mor,FC} l_w n_s t_{FC} + Q_c \\ &= 1273.47 \text{ kN} \end{aligned}$$

$$\text{Frame strength, } Q = \min(Q_1, Q_2, Q_3, Q_4) = 748.2 \text{ kN}$$

The minimum value of Q is 748.2 kN , Diagonal cracking type failure, hence ductility index, $F = 1.27$ according to section 3.3 of this guideline.

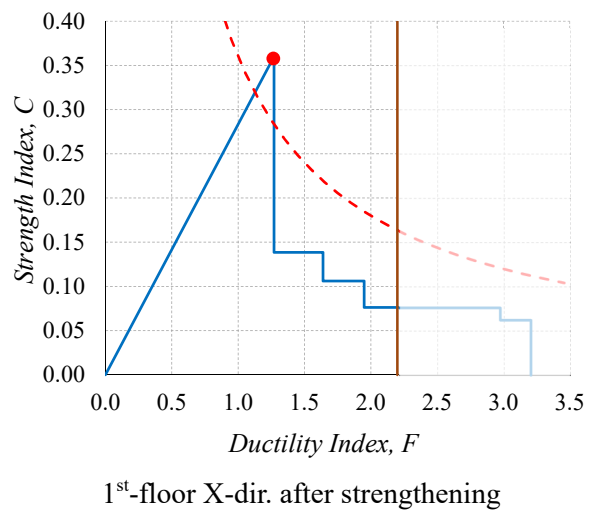
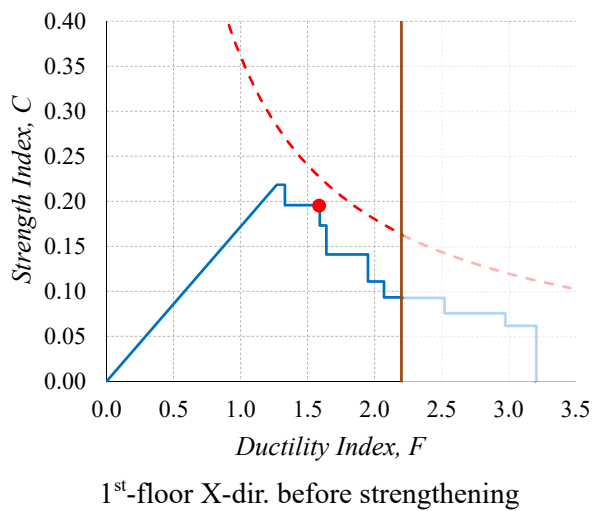
Similarly, the member strength of ferrocement strengthened infill masonry wall can be calculated for the other masonry infill walls.

Table 6.1.7 Summary of strengthened member performance

Member ID	Frame Strength Q_{min}	Failure type	Storey weight (kN)	Strength index, C	Ductility index, F
IFW1	748.2	Diagonal Cracking	13485.1	0.055	1.27
IFW2	748.2	Diagonal Cracking		0.055	1.27
IFW3	746.29	Diagonal Cracking		0.055	1.27
IFW4	746.29	Diagonal Cracking		0.055	1.27

Seismic performance after strengthening

C-F relationship for the example structure after strengthening:



After strengthening the max E_0 value in the X-direction is 0.457 at $F = 1.27$

The seismic capacity of the 1st floor in the X-direction after strengthening is, $I_s = 0.457 > I_{s0}$.

Thus, the seismic performance capacity of the structure was improved beyond the seismic demand.

Seismic performance of the structure after strengthening:

Table 6.1.8 Seismic performance of 1st floor in the X-Direction

Storey	Seismic demand I_{S0}	Before retrofit			After retrofit		
		Seismic capacity I_S	Corresponding ductility index	Judgment	Seismic capacity I_S	Corresponding ductility index	Judgement
1	0.360	0.311	1.59	Not Good	0.457	1.27	OK

Thus, the installation of ferrocement strengthened infill masonry wall was adequate to increase the seismic performance of the structure to meet the seismic demand.

References

- [1] Technical Guidelines for Seismic Evaluation of Existing Reinforced Concrete Buildings in Bangladesh for Extended Application of BSPP Seismic Evaluation Manual, 2021.
- [2] Public Works Department (PWD). Manual for seismic evaluation of existing reinforced concrete buildings, Manual for seismic retrofit design of existing reinforced concrete buildings, Manual for seismic design of existing reinforced concrete buildings (CNCRP manual). Published online 2015.
- [3] JBDPA. Standard for seismic evaluation of existing reinforced concrete buildings, 2001, Guidelines for seismic retrofit of existing reinforced concrete buildings, 2001 and Technical manual for seismic evaluation and seismic retrofit of existing reinforced concrete. Published online 2005.
- [4] HBRI. Bangladesh National Building Code (BNBC 2020).

Table 6.2.1 Summary of materials

Concrete Strength	24 (N/mm ²) for column and 20 (N/mm ²) for slab
Rebar yield stress	400 (N/mm ²)
Rebar type	Deformed

(B) Result of seismic evaluation:

The seismic evaluation result is shown in **Table 6.2.2** for each major direction and each building floor. The seismic demand I_{s0} is 0.36 for buildings located in Dhaka based on soil type SD of BNBC 2020. However, it was evaluated that the building was not safe in any direction. Therefore, it is desirable to establish some retrofit plans that will ensure $I_s > 0.36$ is achieved at each floor level and in each direction. Hence, strengthening should be carried out, either installing by wing walls or drop panel, or shear wall as much as needed and possible. Therefore, the following retrofit is done according to the process described in the section 3.2 of this guideline.

Table 6.2.2 Summary of the seismic evaluation

Storey	Seismic demand index I_{s0}	X-direction			Y-direction		
		Seismic capacity I_s	Corresponding ductility index	Judgement	Seismic capacity I_s	Corresponding ductility index	Judgement
6	0.36	0.405	2.59	OK	0.330	2.59	Not OK
5		0.279	2.59	Not OK	0.215	2.59	Not OK
4		0.239	2.59	Not OK	0.179	2.59	Not OK
3		0.310	2.59	Not OK	0.222	2.59	Not OK
2		0.305	2.59	Not OK	0.214	2.59	Not OK
1		0.303	2.59	Not OK	0.189	2.59	Not OK

6.2.2 Seismic retrofit using drop panel

In the example building, the failure mode of an interior column was identified as punching shear failure, which is a brittle failure mode that is undesirable to this structural system. Therefore, the post-installed drop panel shall be installed to change the failure mode from brittle punching to ductile flexural failure, possibly leading to the improvement of the seismic capacity. The seismic retrofit flow chart using drop panel is shown in **Fig. 6.2.2**.

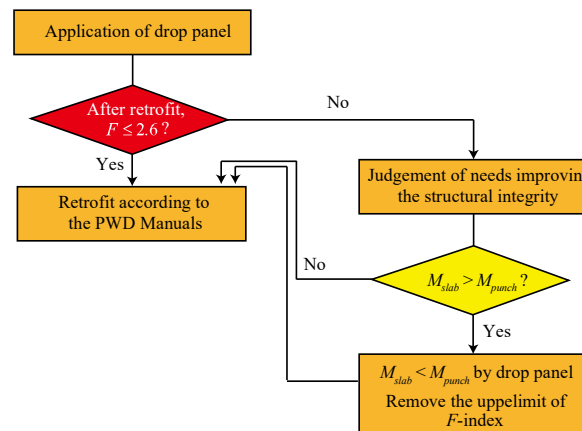


Figure 6.2.2 Flow Diagram of Seismic Retrofit using drop panel

Calculation procedure according to this guideline (section 3.2)

The interior columns of C5 and C8 required to be strengthened using drop panel to prevent the punching shear failure. Here, the calculation procedure of seismic evaluation after installing the drop panel is shown step by step as follows:

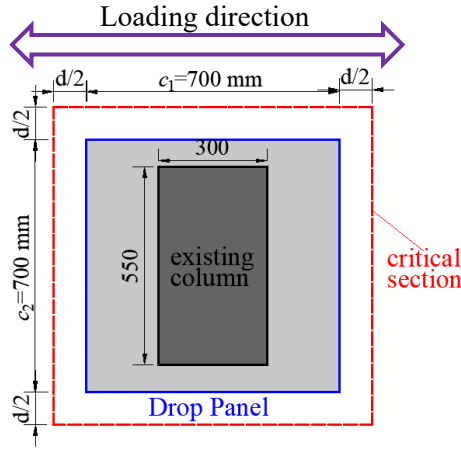


Figure 6.2.3 Assumed critical section of the column with drop panel

Reinforcement of slab: D12@200

Total length of slab span = $4400/2 + 2500/2 = 3450$ (mm).

The minimum size of drop panel is $= 1/5^{\text{th}}$ of span length $= 1/5 \times 3450 = 690$ (mm), considering BNBC (2020) requirement.

Here, the assumed drop panel size is $700 \text{ mm} \times 700 \text{ mm}$. The thickness of drop panel is 200 mm (considering same as slab thickness). The assumed critical section of the column with drop panel is shown in Figure 6.2.3.

Here, $Q_{mu} = 137.3$ (kN), and $Q_{su} = 282.7$ (kN) [From Section 7.3.3 of SATREPS-TSUIB Evaluation Manual]

Q_{slab} :

Q_{slab} : column shear resistance based on the flexural yielding of slab

$$Q_{slab} = \frac{M_{slab}}{h_0}$$

where, M_{slab} : flexural yielding capacity of slab perspective with the nodal moment

h_0 : clear height of column

The flexural capacity of slab (M_{slab}) is calculated by assuming the moment diagram shown in Figure 6.2.4 and using the following equation based on section 3.2 of this guideline.

$$M_{slab} = \frac{l M_{slab}}{l/2} \times \left(\frac{l}{2} + \frac{l_d}{2} \right) + \frac{r M_{slab}}{l/2} \times \left(\frac{l}{2} + \frac{l_d}{2} \right)$$

where, $l M_{slab} / r M_{slab}$: flexural yielding capacity of the slab in the corresponding side

l : clear span of the length in the corresponding side

l_d : length of the drop panel

Flexural yielding capacity of slab, M_{slab} :

$$lM_{slab} = 0.9a_t\sigma_y d = 0.9 \times 32 \times 113.1 \times 275 \times 182 = 163.0 \text{ (kN} \cdot \text{m)}$$

$$rM_{slab} = 0.9a_t\sigma_y d = 0.9 \times 16 \times 113.1 \times 275 \times 182 = 81.5 \text{ (kN} \cdot \text{m)}$$

Therefore,

$$M_{slab} = \frac{163}{3825/2} \times \left(\frac{3825}{2} + \frac{700}{2} \right) + \frac{81.5}{1800/2} \times \left(\frac{1800}{2} + \frac{700}{2} \right) = 306 \text{ (kN.m)}$$

$$\therefore Q_{slab} = M_{slab}/h_0 = 306/3.025 = 101.1 \text{ (kN)}$$

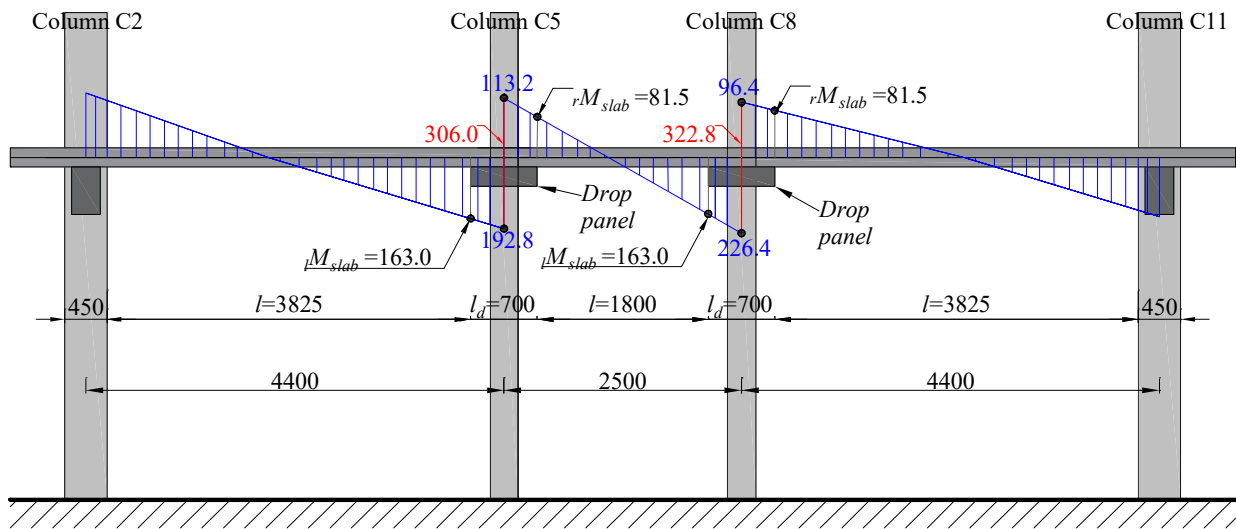


Figure 6.2.4 Nodal moment of slab (Grid Y2)

Q_{punch} :

The thickness of drop panel is 200mm

c_1 = drop panel depth = 700 (mm)

c_2 = drop panel width = 700 (mm)

σ_y : 275 (N/mm²) for slab (400 N/mm²) for column

F_c : 20 (N/mm²) for slab

d : effective depth = 200 - 18 = 182 (mm)

$$\begin{aligned} M_f &= 0.9a_{ot} \cdot \sigma_y \cdot d \cdot \frac{c_2 + d}{x_t} + 0.9a_{ob} \cdot \sigma_y \cdot d \cdot \frac{c_2 + d}{x_b} \\ &= 0.9 \times 113.1 \times 275 \times 182 \times \frac{700+182}{100} + 0.9 \times 113.1 \times 275 \times 182 \times \frac{700+182}{200} \\ &= 67.4 \text{ (kN} \cdot \text{m)} \end{aligned}$$

$$\begin{aligned}
M_s &= \tau_u \cdot (c_2 + d) \cdot d \cdot (c_1 + d) \\
&= 0.335 \times \sqrt{20} \times (700 + 182) \times 182 \times (700 + 182) \\
&= 212.1 \text{ (kN} \cdot \text{m)}
\end{aligned}$$

$$\begin{aligned}
M_t &= \tau_{tu} \frac{d^2}{2} \left\{ (c_1 + d) - \frac{d}{3} \right\} \cdot 2 \\
&= 6 \times 0.335 \times \sqrt{20} \times \frac{182^2}{2} \left\{ (700 + 182) - \frac{182}{3} \right\} \cdot 2 \\
&= 244.5 \text{ (kN} \cdot \text{m)}
\end{aligned}$$

$$M_0 = M_f + M_s + M_t = 67.4 + 212.1 + 244.5 = 524.1 \text{ (kN} \cdot \text{m)}$$

$$\begin{aligned}
V_0 &= \tau_u A_c = 0.335 \sqrt{20} \times \{(700 + 182) \times 2 + (700 + 182) \times 2\} \times 182 \\
&= 962 \text{ (kN)}
\end{aligned}$$

$$\frac{V_u}{V_0} + \frac{M_u}{M_0} = \frac{149}{962} + \frac{M_u}{524.1} = 1$$

$$M_u = 442.9 \text{ (kN} \cdot \text{m)}$$

$$\therefore Q_{punch} = \frac{442.9}{3.025} = 146.4 \text{ (kN)} > 101.1 \text{ (kN)}$$

Therefore, the failure mode of the interior column was changed to slab flexure. The calculation procedure of ductility index F shall be the same as the normal moment-resisting structure.

From the previous calculation:

$${}_c R_{max} = \min \left\{ \frac{1}{33}, \frac{1}{30}, \frac{1}{30}, \frac{1}{30}, \frac{1}{30} \right\} = 1/33$$

Since the failure mode of interior column was not punching, the value of ${}_c R_{max}$ will not be bound for 1/50.

Therefore, ${}_c R_{max} = 1/33$

The ductility index:

Since $R_{mu} \geq R_y$

Therefore, $F = \frac{\sqrt{2R_{mu}/R_y - 1}}{0.75(1 + 0.05R_{mu}/R_y)} \leq 3.2$ for $R_{mu} \geq R_y$

$$F = \frac{\sqrt{2 \times \frac{1}{33} / \frac{1}{150} - 1}}{0.75(1 + 0.05 \times \frac{1}{33} / \frac{1}{150})} = 3.1 \leq 3.2$$

[**Note:** The columns without being connected to beams are flexible in their respective directions; thus, only the contributions of perimeter columns with beams can be considered to evaluate the seismic capacity of the structure. For example: in this sample building, C2 and C11 columns are not connected with beams in the X-direction; thus, their contributions shall be ignored along with the interior columns of C5, and C8]

The strength index C and ductility index F of each exterior column can be calculated in the same procedure. The calculated index of each member in X-direction is listed in **Table 6.2.3** as below.

Table 6.2.3 Ductility index F and strength index C

Column ID	Storey	Weight of the building	Q_u (kN)	C	Q_{su}/Q_{mu}	F	Remarks
C1	1	10476	171.7	0.0164	1.66	3.1	Ext. column with beam
C2	1		Ignoring shear resistance				Ext. column without beam
C3	1		179.0	0.0171	1.63	3.1	Ext. column with beam
C4	1		135.0	0.0129	1.96	3.1	Ext. column with beam
C5	1		-	-	-	-	Int. column
C6	1		117.4	0.0113	1.96	3.1	Ext. column with beam
C7	1		135.0	0.0129	1.96	3.1	Ext. column with beam
C8	1		-	-	-	-	Int. column
C9	1		117.4	0.0113	1.96	3.1	Ext. column with beam
C10	1		169.8	0.0162	1.67	3.1	Ext. column with beam
C11	1		Ignoring shear resistance				Ext. column without beam
C12	1		177.1	0.0169	1.64	3.1	Ext. column with beam

Therefore, the summation of C from all contributed columns is 0.1168.

Here, $E_0 = C * F = 0.1168 * 3.1 = 0.361$, as shown in **Fig. 6.2.5**.

Therefore, the seismic index, $I_s = E_0 * S_d * T = 0.361 * 1 * 1 = 0.361$

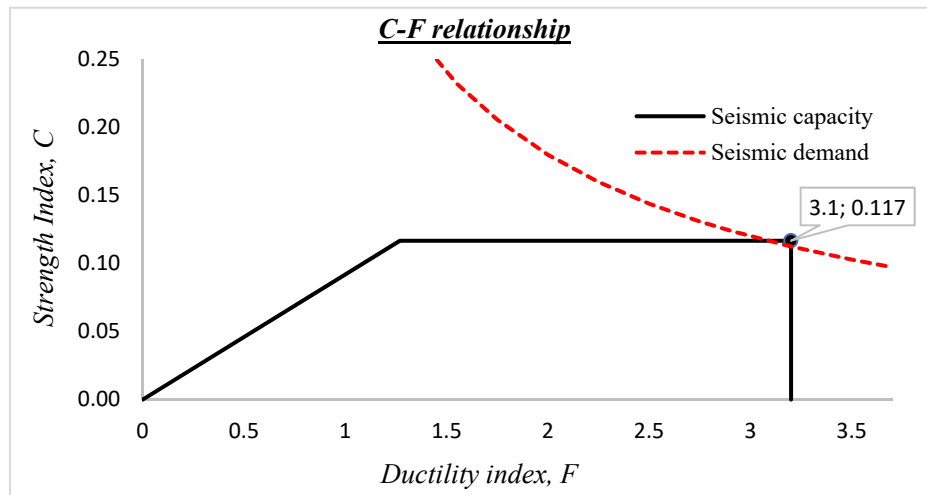


Figure 6.2.5 Relationship between strength index C and ductility index F

Therefore, the seismic index of this building in X-direction of the 1st-floor level was $I_s = 0.361 > I_{s0} = 0.36$ (**Safe**). Though the building satisfied the seismic demand (minimum requirement), the large drift was expected to exhibit the seismic capacity with F of 3.1. In general, a drift of the structure is recommended to be kept as small as possible to prevent damage to the structure under large deformation. For such purpose, another option is recommended by applying post-installed wing walls to increase/decrease the C/F index at the maximum performance in the following section.

Furthermore, it was evaluated that the building was not safe on the 1st to 5th floors in the Y-direction and on the 4th and 5th floors in the X-direction by using drop panels (as listed in **Table 6.2.4** and **Fig. 6.2.6**). Drop panels typically improve the ductility of the structure by preventing the punching shear failure of the interior slab, but they do not increase the lateral resistance of the column. Therefore, further strengthening is necessary to improve the seismic performance of the building in consideration of both directions. As a result, strength-oriented retrofit schemes are recommended (for example, wing walls, shear walls etc.).

Table 6.2.4 Summary of the seismic evaluation using drop panel

Storey	Seismic demand index I_{s0}	X-direction			Y-direction		
		Seismic capacity I_s	Corresponding ductility index	Judgement	Seismic capacity I_s	Corresponding ductility index	Judgement
6	0.36	0.483	3.1	OK	0.393	3.1	OK
5		0.332	3.1	Not OK	0.257	3.1	Not OK
4		0.286	3.1	Not OK	0.213	3.1	Not OK
3		0.370	3.1	OK	0.264	3.1	Not OK
2		0.364	3.1	OK	0.255	3.1	Not OK
1		0.361	3.1	OK	0.225	3.1	Not OK

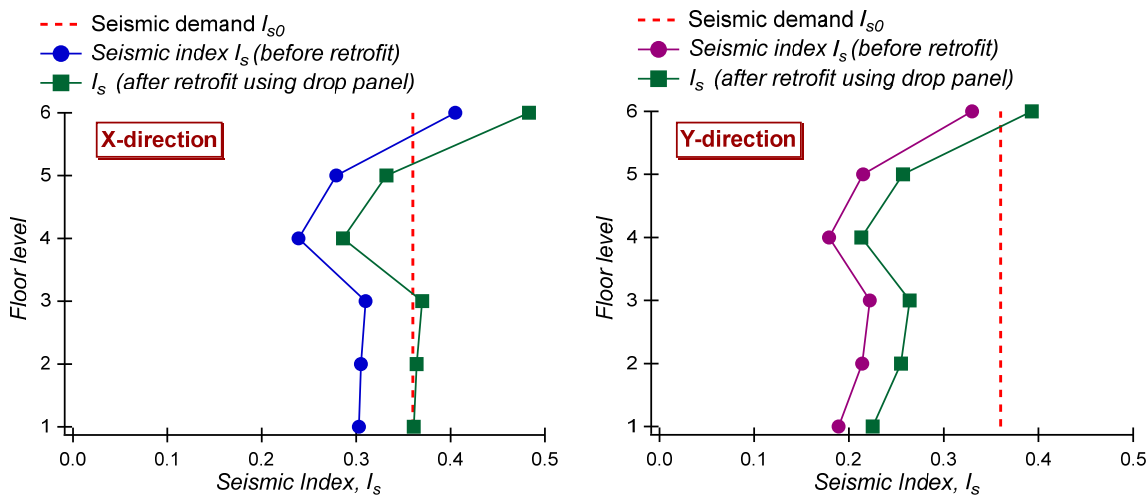


Figure 6.2.6 Comparison between seismic demand and capacity

[Note: The building was considered to be safe in both directions on the 6th-floor level only after retrofitted using post-installed drop panels. As a result, wing walls were planned to be installed from the 1st to 5th-floor level in the following section, considering the continuous installation of wing walls from the bottom of the building and lower values of I_s compared to those in the 6th floor].

6.2.3 Seismic retrofit using wing walls

The seismic retrofit flow chart using wing wall is shown in **Fig. 6.2.7**. The wing walls were planned to be installed to increase/decrease the C/F index showing a strength-type retrofit design. The layout and dimensions of wing walls are shown in **Fig. 6.2.8**. The wing walls were intended to be installed from the 1st to 5th-floor level of the building because the drop panel is sufficient to increase the seismic index in both X & Y-direction on the 6th floor. The detailed calculation of wing walls with beams is available in the CNCRP manual. Therefore, the calculation of wing walls without beam (interior column) is explained in this section.

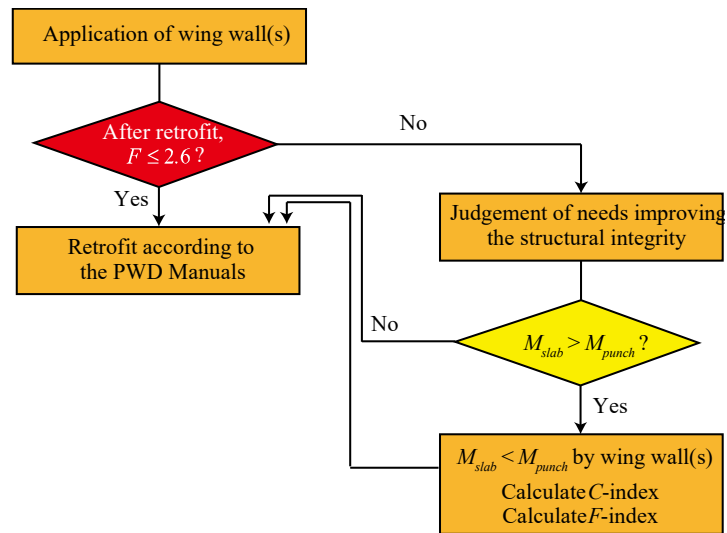


Figure 6.2.7 Flow Diagram of Seismic Retrofit using wing wall

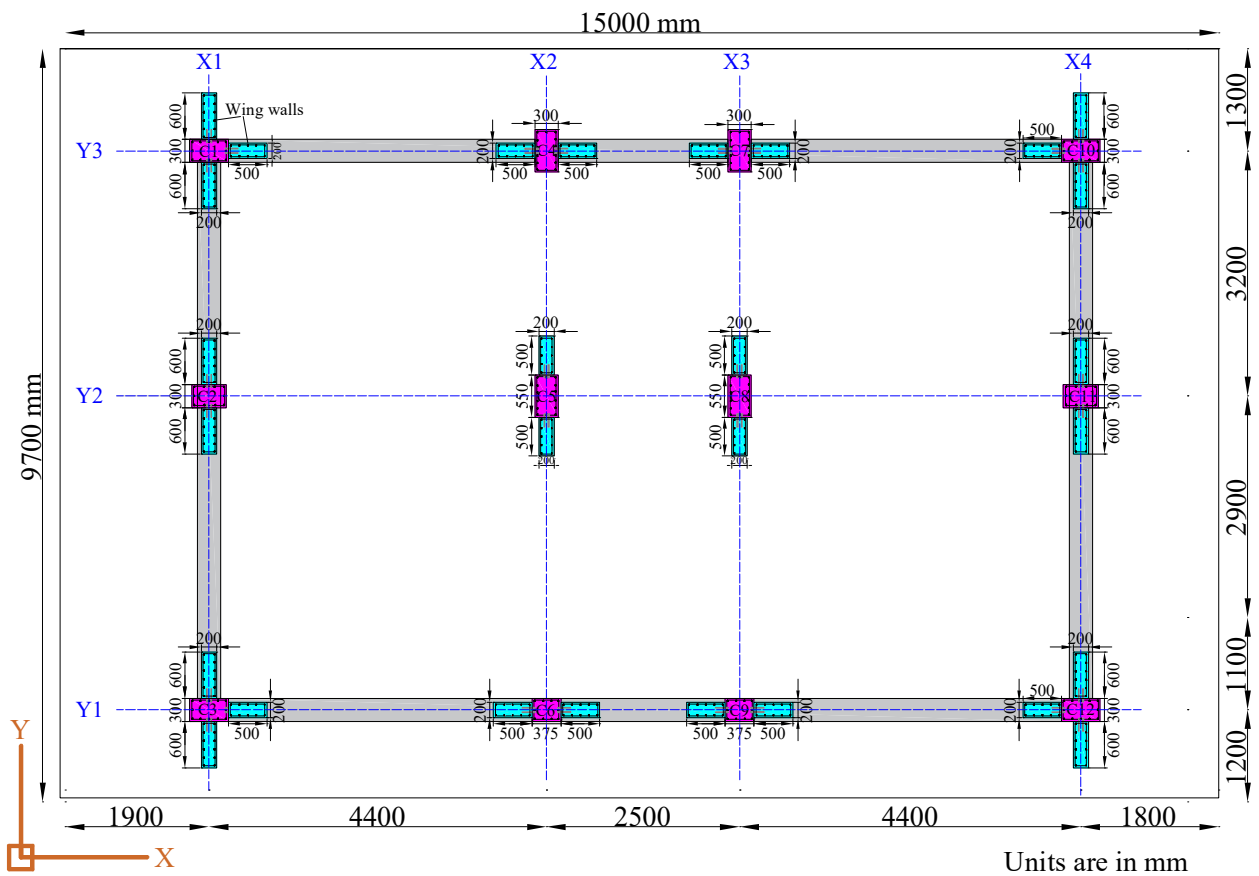


Figure 6.2.8 Layout of the wing wall after installation

Detailed calculation procedure of column with wing walls (C₅) in Y-direction (1st floor):

Original column:

Size = 300 (mm) × 550 (mm)

Tie bar = D10@200c/c

$F_c = 20$ (N/mm²)

$\sigma_y = 400$ (N/mm²)

Specification of wing walls:

Wing wall (thickness × length) = 200 (mm) × 500 (mm)

Additional vertical rebar = 10-D13

Hoop spacing = D10@100 c/c

$F_{c1} = 30$ (N/mm²)

$\sigma_y = 500$ (N/mm²)

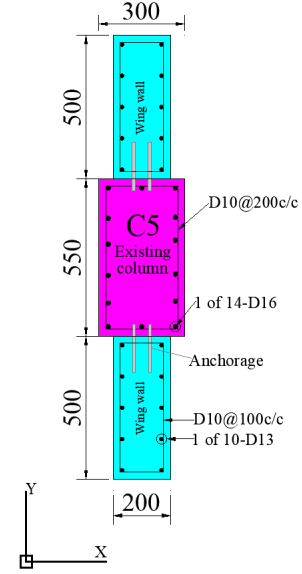


Figure 6.2.9 Plan of Column with wing walls

Fig. 6.2.9 shows the detailed plan of the C5 column retrofitted with wing walls. The lateral load-carrying capacity of a column without beam retrofitted using wing wall installed parallel to the seismic force direction can be considered under the condition of $M_{slab} < M_{punch}$. According to Section 3.2 in the current guideline, it shall be evaluated by the following equation.

$$Q_u = \frac{cM_w}{h} = \frac{cM_w + N \cdot M_{slab}}{H} \leq \frac{2}{H} \frac{cM_w}{H}$$

where, cM_w : the flexural capacity of a column without beam retrofitted by with wing wall(s),

h : inflection height from the bottom of wing wall(s),

N : the number of stories installed wing wall(s),

H : the total height of wing wall(s).

The nodal moments at the flexural capacity of slab (M_{slab}) and the punching shear capacity (M_{punch}) are compared to prevent punching shear failure.

Calculation of M_{slab} :

The flexural capacity of slab (M_{slab}) is calculated by assuming the moment diagram shown in Figure 6.2.10 and using the following equation based on section 3.2.

$$M_{slab} = \frac{lM_{slab}}{l/2} \times \left(\frac{l}{2} + l_w + \frac{D_c}{2} \right) + \frac{rM_{slab}}{l/2} \times \left(\frac{l}{2} + l_w + \frac{D_c}{2} \right)$$

where, lM_{slab} / rM_{slab} : flexural yielding capacity of the slab in the corresponding side

l : clear span of the length in the corresponding side

l_w : length of the wing wall

D_c : depth of the column

Reinforcement: D12@200 alt. with extra top 1-D12@200

Number of reinforcement = transverse span length / spacing of rebar = $6900/2 \times 100 = 35 + 1 = 36$ rebar for top slab and 18 rebar for bottom slab.

The flexural yielding capacity of slab, M_{slab} :

$$\begin{aligned} {}_l M_{slab} (left) &= 0.9 a_t \sigma_y d = 0.9 \times 36 \times 113 \times 275 \times 182 \\ &= 183243060 \text{ (N} \cdot \text{mm)} = 183.2 \text{ (kN} \cdot \text{m)} \end{aligned}$$

$$\begin{aligned} {}_r M_{slab} (right) &= 0.9 a_t \sigma_y d = 0.9 \times 18 \times 113 \times 275 \times 182 \\ &= 91621530 \text{ (N} \cdot \text{mm)} = 91.6 \text{ (kN} \cdot \text{m)} \end{aligned}$$

$$\begin{aligned} \text{Therefore, } M_{slab} &= \frac{{}_l M_{slab}}{\frac{l}{2}} \times \left(\frac{l}{2} + l_w + \frac{D_c}{2} \right) + \frac{{}_r M_{slab}}{\frac{l}{2}} \times \left(\frac{l}{2} + l_w + \frac{D_c}{2} \right) \\ &= \frac{183.2}{1537.5} \times \left(\frac{3075}{2} + 500 + \frac{550}{2} \right) + \frac{91.6}{1075} \times \left(\frac{2150}{2} + 500 + \frac{550}{2} \right) \\ &= 433.2 \text{ (kN.m)} \end{aligned}$$

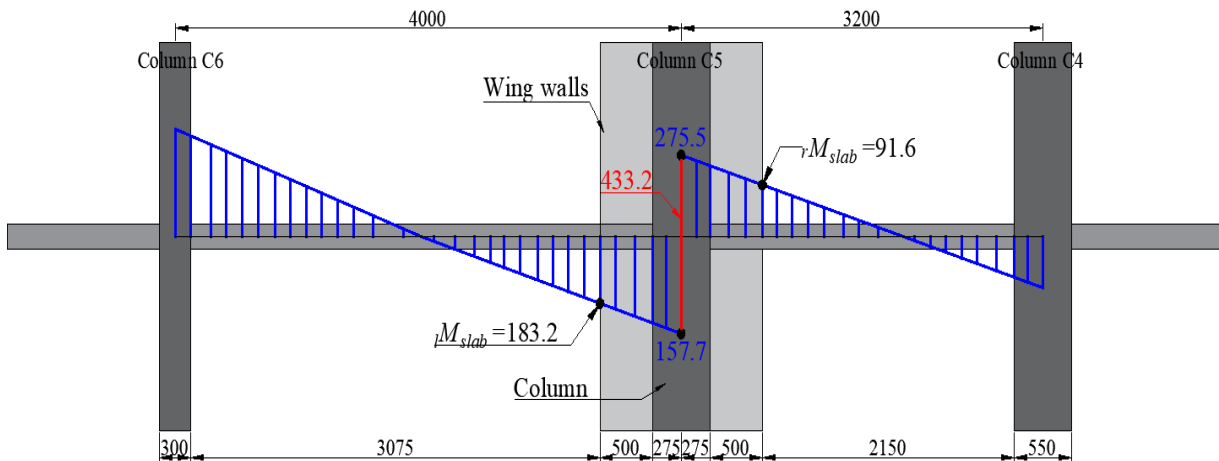


Figure 6.2.10 Assumed moment diagram after retrofitting by wing walls (X2 Grid)

Calculation of M_{punch} :

c_1 = column depth with wing walls = 1550 (mm)

c_2 = column width with wing walls = 300 (mm)

σ_y : 275 (N/mm²) for slab, 400 (N/mm²) for column

F_c : 20 (N/mm²) for slab

Axial load (one storey) V_u = 149.0 (kN)

d : effective depth = 200 - 18 = 182 (mm)

$$\begin{aligned}
M_f &= 0.9a_{0t} \cdot \sigma_y \cdot d \cdot \frac{c_2+d}{x_t} + 0.9a_{0b} \cdot \sigma_y \cdot d \cdot \frac{c_2+d}{x_b} \\
&= 0.9 \times 113.1 \times 275 \times 182 \times \frac{300+182}{100} + 0.9 \times 113.1 \times 275 \times 182 \times \frac{300+182}{200} \\
&= 36.8 \text{ (kN} \cdot \text{m)}
\end{aligned}$$

$$\begin{aligned}
M_s &= \tau_u \cdot (c_2 + d) \cdot d \cdot (c_1 + d) \\
&= 0.335 \times \sqrt{20} \times (300 + 182) \times 182 \times (1550 + 182) \\
&= 227.6 \text{ (kN} \cdot \text{m)}
\end{aligned}$$

$$\begin{aligned}
M_t &= \tau_{tu} \frac{d^2}{2} \left\{ (c_1 + d) - \frac{d}{3} \right\} \cdot 2 \\
&= 6 \times 0.335 \times \sqrt{20} \times \frac{182^2}{2} \left\{ (1550 + 182) - \frac{182}{3} \right\} \cdot 2 \\
&= 497.6 \text{ (kN} \cdot \text{m)}
\end{aligned}$$

$$M_0 = M_f + M_s + M_t = 36.83 + 227.6 + 497.6 = 762.1 \text{ (kN} \cdot \text{m)}$$

$$\begin{aligned}
V_0 &= \tau_u A_c \\
&= 0.335 \sqrt{20} \times \{ (300 + 182) \times 2 + (1550 + 182) \times 2 \} \times 182 \\
&= 1207.4 \text{ (kN)}
\end{aligned}$$

$$\frac{V_u}{V_0} + \frac{M_u}{M_0} = \frac{149}{1207.4} + \frac{M_u}{762.1} = 1$$

$$M_u = M_{punch} = 668.0 \text{ (kN} \cdot \text{m)} > 433.2 \text{ (kN} \cdot \text{m)}, \text{ slab flexural failure mode}$$

Therefore, $M_{slab} < M_{punch}$. The assumed dimension of the wing wall is enough to prevent punching shear failure.

The flexural capacity (cM_w) of the column with wing wall cast-in-place shall be calculated as follows. If only one wing wall is attached to the column, the contribution of the wing wall in the tension side shall be ignored. For details of wing wall Sec-3.2 of Japanese Guidelines is referred.

$$\text{So, } cM_w = (0.9 + \beta)a_t \cdot \sigma_y \cdot D + 0.5N \cdot D \left\{ 1 + 2\beta - \frac{N}{\alpha_e \cdot b \cdot D \cdot F_{c1}} \left(\frac{a_t \cdot \sigma_y}{N} + 1 \right) \right\}$$

where,

a_t = gross sectional area of longitudinal reinforcing bars of column in tension side (mm^2) = $3 \times 201 \text{ (mm}^2\text{)}$

σ_y =yield stress of the longitudinal reinforcing of column (N/mm^2) = $400 \text{ (N/mm}^2\text{)}$

b = width of column = 300 (mm)

D = depth of column = 550 (mm)

t = wall thickness of installed wing wall (mm) = 200 (mm)

$$\alpha = t/b = 0.67$$

$$\beta = \text{wing wall length in compressive side divided by } D = L_w/D = 500/550 = 0.909$$

$$\text{Now, } \alpha_e = \frac{1+2\alpha\beta}{1+2\beta} = \frac{1+2 \times 0.67 \times 0.909}{1+2 \times 0.909} = 0.785$$

$$N = \text{axial force of C5 column} = (3.45 \times 3.6 \times 6 \times 12) = 894.2 \text{ (kN)}$$

$$F_{cl} = \text{specified design strength of concrete for wing wall (N/mm}^2\text{)} = 30 \text{ (N/mm}^2\text{)}$$

Therefore,

$$\begin{aligned} {}_cM_w &= (0.9 + \beta) a_t \cdot \sigma_y \cdot D + 0.5 N \cdot D \left\{ 1 + 2\beta - \frac{N}{\alpha_e \cdot b \cdot D \cdot F_{cl}} \left(\frac{a_t \cdot \sigma_y}{N} + 1 \right) \right\} \\ {}_cM_w &= (0.9 + 0.909) \times 3 \times 201 \times 400 \times 550 + 0.5 \times 894.2 \times 1000 \times 550 \\ &\quad \times \left\{ 1 + 2 \times 0.909 - \frac{894.2 \times 1000}{0.785 \times 300 \times 550 \times 30} \cdot \left(\frac{3 \times 201 \times 400}{894.2 \times 1000} + 1 \right) \right\} \\ &= 861.1 \text{ (kN.m)} \end{aligned}$$

$$\begin{aligned} \text{Therefore, } Q_u &= \frac{{}_cM_w}{h} = \frac{{}_cM_w + N \cdot M_{slab}}{H} \leq \frac{2 \cdot {}_cM_w}{H} \\ &= \frac{861.1 + 5 \times 433.2}{15.6} \leq \frac{2 \times 861.1}{15.6} = 110.4 \text{ (kN)} \end{aligned}$$

$$\text{Total weight of the building} = 15 \times 9.7 \times 12 \times 6 = 10476 \text{ (kN)}$$

The column's load-carrying capacity with wing wall = 99.2 kN and the flexural yielding precedes the shear failure.

$$C\text{-Index, } C = 99.2/10476 = 0.0947$$

Calculation of column with wing wall ductility index F according to CNCRP manual:

The ductility index calculation of the vertical member after installation of wing wall shall follow as CNCRP manual. Therefore, the ductility Index, F of C_5 column with wing walls in Y-direction is 2.0; (since $Q_{su}/Q_{mu} = 564.9/99.2 = 5.69 \geq 1.3$).

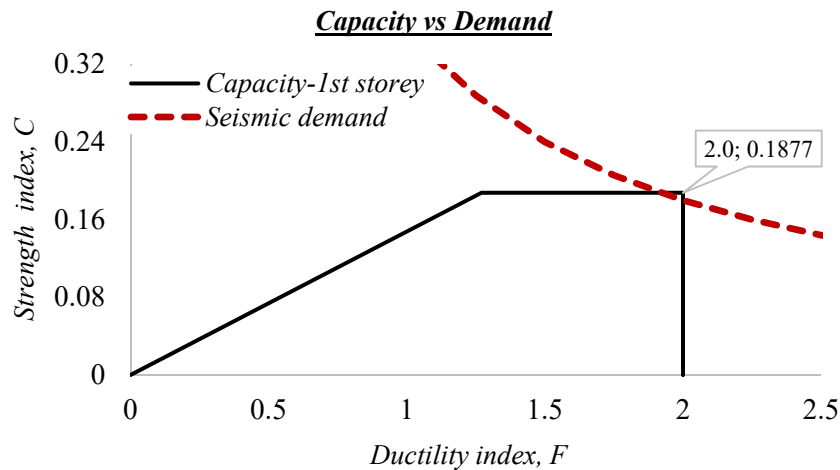
The strength index C and ductility index F of each exterior column with wing walls can be calculated in the same procedure. The calculated index of each member is listed below.

Table 6.2.5 Ductility index F and strength index C

Column ID	Storey	Weight of the building	Q_u (kN)	C	Q_{su}/Q_{mu}	F	Remarks
C1	1	10476	265.2	0.0253	1.95	2.0	Installed wing walls in Y-direction (both side)
C2	1		284.8	0.0272	2.16	2.0	Installed wing walls in Y-direction (both side)
C3			340.1	0.0324	1.53	2.0	Installed wing walls in Y-direction (both side)
C4	1		Ignoring shear resistance				Exterior column without beam
C5	1		110.4	0.0105	5.69	2.0	Int. column installed wing walls in Y-direction (both side)
C6	1		Ignoring shear resistance				Exterior column without beam
C7	1		Ignoring shear resistance				Exterior column without beam
C8	1		110.4	0.0105	5.69	2.0	Int. column installed wing walls in Y-direction (both side)
C9	1		Ignoring shear resistance				Exterior column without beam
C10	1		261.5	0.0250	1.97	2.0	Installed wing walls in Y-direction (both side)
C11	1		284.8	0.0272	2.16	2.0	Installed wing walls in Y-direction (both side)
C12	1		309.4	0.0295	1.64	2.0	Installed wing walls in Y-direction (both side)

Therefore, the summation of C from all contributed columns is 0.1877.

Here, $E_0 = C \cdot F = 0.1877 \cdot 2 = 0.375$, as shown in Figure 6.2.11.

Figure 6.2.11 Relationship between strength index C and ductility index F

Here, the seismic index, $I_s = E_0 \times S_d \times T = 0.375 \times 1 \times 1 = 0.375$, as shown in **Fig. 6.2.9**. Therefore, the seismic index of this building after the application of the wing wall retrofit scheme was 0.375 ($I_s = 0.375 > I_{s0} = 0.36$ (Safe)).

Finally, seismic evaluation is done for each major direction and each floor of the building (shown in **Table 6.2.6** and **Fig 6.2.12**. In this case, the seismic capacity on the 5th floor level has been over strengthened in the

Y-direction; however, it is possible to reduce the capacity but simple retrofitting strategy is the main objective for ease of understanding. The building is considered satisfactory after retrofitting wing walls up to the 5th-floor level and using drop panels on the 6th floor.

Table 6.2.6 Summary of the seismic evaluation using wing walls

Storey	Seismic demand index I_{s0}	X-direction			Y-direction			Remarks (retrofit scheme)
		Seismic capacity I_s	Corresponding ductility index	Judgement	Seismic capacity I_s	Corresponding ductility index	Judgement	
6	0.36	0.484	3.1	OK	0.408	3.1	OK	Drop panel
5		0.590	2.0	OK	0.729	2.0	OK	Wing wall
4		0.456	2.0	OK	0.534	2.0	OK	Wing wall
3		0.459	2.0	OK	0.496	2.0	OK	Wing wall
2		0.403	2.0	OK	0.438	2.0	OK	Wing wall
1		0.371	2.0	OK	0.375	2.0	OK	Wing wall

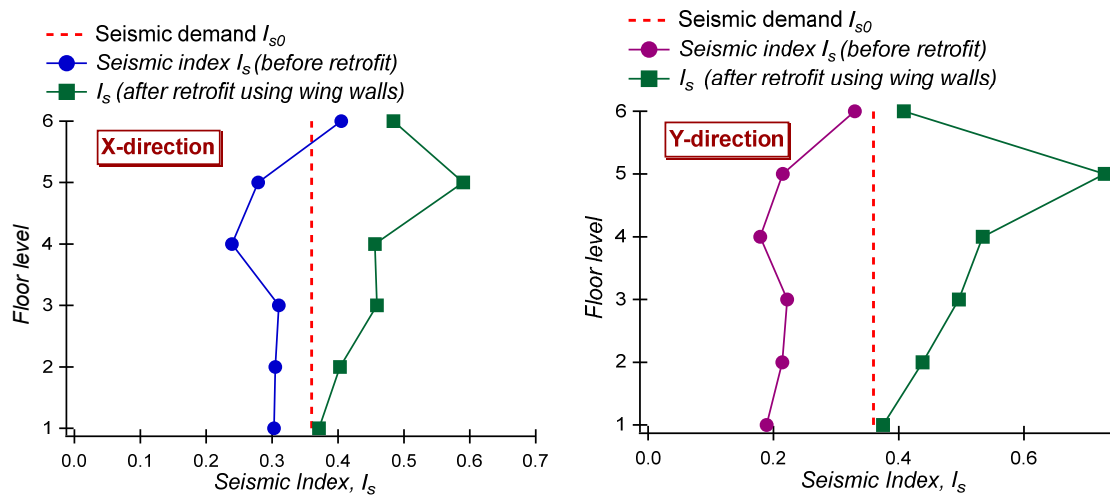


Figure 6.2.12 Comparison between seismic demand and capacity

References:

- [1] Technical guidelines for seismic evaluation of existing reinforced concrete buildings in Bangladesh for extended application of BSPP seismic evaluation manual, 2021.
- [2] JBDPA. Standard for seismic evaluation of existing reinforced concrete buildings, 2001, Guidelines for seismic retrofit of existing reinforced concrete buildings, 2001 and Technical manual for seismic evaluation and seismic retrofit of existing reinforced concrete. Published online 2005.
- [3] Public Works Department (PWD). Manual for seismic evaluation of existing reinforced concrete buildings, Manual for seismic retrofit design of existing reinforced concrete buildings, Manual for seismic design of existing reinforced concrete buildings (CNCRP manual). Published online 2015.
- [4] Samdani HMG, Takahashi S, Yoon R, Sanada Y: Strengthening seismically vulnerable reinforced concrete flat plate-column connections by installing wing walls, *Japan Architectural Review*, Vol. 4; Issue 3, pp. 442–454, June 2021, <https://doi.org/10.1002/2475-8876.12232>.

- [5] Samdani HMG, Sanada Y, Takahashi S, Suzuki S, Yoon R, Anam I: Experimental study on a new Strengthening technique of flat plate-column connections using wing walls, *Proceedings of the 17th World Conference on Earthquake Engineering*, Sendai, Japan, Sep. 2020, Paper No. 3b-0059.
- [6] Samdani HMG, Takahashi S, Yoon R, Sanada Y. “Experimental study on flat plate-column connection made with low-strength concrete Part 5: Effect of drop panel” *Summaries of Technical Papers of Annual Meeting of AIJ*, pp. 331–332, Structures-IV, Chiba, Japan, Sep. 2020.
- [7] AIJ. AIJ Standard for structural calculation of reinforced concrete structures, revised 2010; 2010 (in Japanese).
- [8] HBRI. Bangladesh National Building Code (BNBC 2020)

Appendix Pilot Project for Ferrocement Retrofit Construction in Bangladesh

Contents

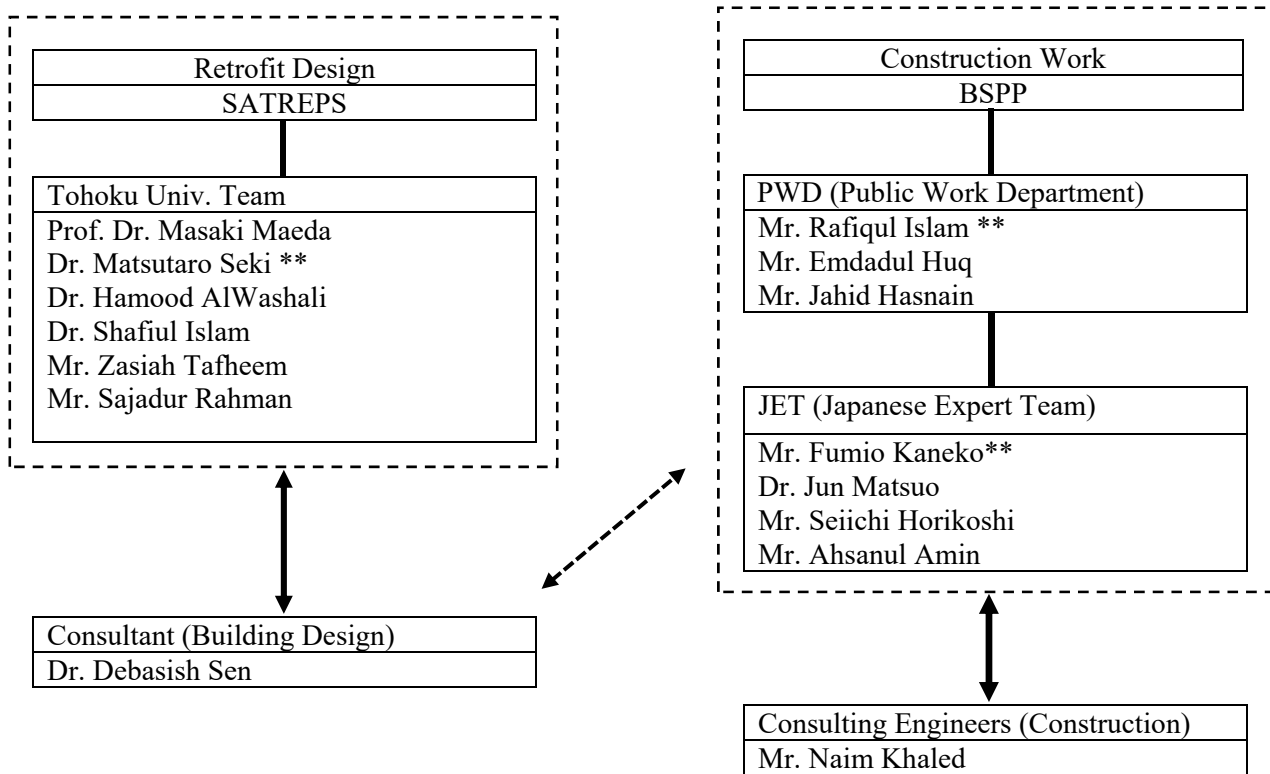
Background of this pilot project	A-2
Formation of pilot project for ferrocement retrofit	A-2
A.1 Retrofit Design	
A.1.1 Target site	A-3
A.1.2 Assumption of material properties	A-5
A.1.3 Recognition of failure mechanism of existing masonry infilled frame	A-5
A.1.4 Check for out-of-plane failure	A-7
A.1.5 Selection of failure mechanism after FC strengthening	A-8
A.1.6 Proposed FC configuration	A-9
A.1.7 Lateral capacity after FC strengthening	A-9
A.1.8 Structural drawing	A-10
A.1.9 Construction steps	A-15
A.1.10 Summary	A-17
A.1.11 Site survey and testing list	A-17
A.2 Construction Work	
A.2.1 Plan of ferrocement work	A-18
A.2.2 Issues of work	A-20
A.2.3 Steps of work	A-22
A.2.4 Comparison between work plan and execution	A-50
A.2.5 Report of compressive mortar strength of cube test	A-53
A.2.6 Report of wire mesh test	A-54
A.2.7 Comparison of Costing and Duration in between SATREPS- TSUIB, Wall-A and PWD-BSPP, Wall-B	A-55
A.2.8 Conclusion	A-55

Pilot Project for Ferrocement Retrofit Construction in Bangladesh

Background of this pilot project

This pilot project was conducted in collaboration with the SATREPS-TSUIB project and the BSPP project. The SATREPS-TSUIB project was in charge of the retrofit design using ferrocement lamination, and the BSPP project was in charge of the retrofit work. It is considered useful that the retrofit design and construction work were carried out on one building for the purpose of future practical application.

Formation of pilot project for ferrocement retrofit



**Contact Person

A.1 Retrofit Design
A.1.1 Target site
(a) Target building



Figure A.1.1: Picture of overall building



Target infill wall for
ferrocement retrofit

Figure A.1.2: Photos of the target building

Architectural drawings of a building's exterior wall and floor slab.

The main drawing shows a cross-section of a wall with a height of 3800 mm. It includes a 10" Brick wall on the left, a 5" Brick wall on the right, and a central Column. Dimensions for wall thicknesses, column widths, and slab heights are provided. A red dashed line highlights the top section of the wall.

To the right, a detail of the "1st Floor Slab" shows its connection to the wall and column. The slab is 483 mm thick and is supported by the wall and column. The wall is 5" Brick wall.

Below the main drawing, a plan view of the wall shows its overall dimensions: 338 x 1050 mm for the outer wall and 550 x 550 mm for the inner core. The plan view also shows the wall's position relative to the floor slab and the ground floor.

Figure A.1.3: Plan and elevation of the target site (*bricks are schematic*)

A.1.2 Assumption of material properties

Table A.1.1: Material Properties

Concrete		
Compressive strength, f'_c (MPa)	13	-
Shear strength, τ_c (MPa)	1 for $ho/D \leq 6$ 0.7 for $ho/D > 6$	JBDPA (2001)
Mod. of Elasticity, E_c (MPa)	16946	ACI code = $4700\sqrt{13}$ (MPa)
Masonry		
Compressive strength, f_m (MPa)	5	-
Mod. of Elasticity, E_m (MPa)	3750	$750f_m$ [BNBC 2020]

A.1.3 Recognition of failure mechanism of existing masonry infilled frame

Table A.1.2: Geometric and Structural Properties

Left Column	
Cross section (mm x mm)	338 x 1050
Height (clear)	2975
Long reinforcement	
Shear reinforcement	
Moment of inertia, I_{LC} (mm ⁴)	3.3×10^{10}
Moment capacity, M_{LC} (kN-m)	
Shear capacity at flexural yielding, $Q_{mu,LC}$ (kN)	
Shear capacity, $Q_{su,LC}$ (kN)	
Simplified shear capacity, $Q_{s,LC}$ (kN)	354.9 (1x 338 x 1050)
Right column	
Cross section (mm x mm)	550 x 550
Height (clear)	2975
Long reinforcement	
Shear reinforcement	
Moment of inertia, I_{LC} (mm ⁴)	7.6×10^9
Moment capacity, M_{LC} (kN-m)	
Shear capacity at flexural yielding, $Q_{mu,LC}$ (kN)	
Shear capacity, $Q_{su,LC}$ (kN)	
Simplified shear capacity, $Q_{s,LC}$ (kN)	302.5 (1 x 550 x 550)
Masonry	
Length, l_{mas} (mm)	3025
Height, h_{mas} (mm)	2975
Thickness, t_{mas} (mm)	125 (w/o plaster)
	150 (w/ plaster)
Diagonal length, d_m (mm)	4242.8
Inclination, θ (°)	44.5

Table A.1.3: Failure mechanism recognition parameters

Contact length		Remarks
Stiffness parameter $\lambda_{mas} = \sqrt[4]{\frac{E_{mas} t_{mas} \cos^2 \theta}{4 E_c I_c d_m}}$	5.7 x10 ⁻⁴	Masonry thickness w/o plaster is considered
Contact length ratio (a_c/h_{mas}) $\frac{a_c}{h} = \frac{\pi}{4 \lambda_{mas} h_{mas}}$	0.45	-
<i>Expected failure mechanism</i>	<i>Diagonal compression</i>	<i>$a_c/h > 0.3$</i>
Relative strength		
RC frame capacity, Q_{fr} (kN)	657.4	$Q_{s,LC} + Q_{s,RC}$
Masonry capacity, Q_{mas} (kN)	94.5	$Q_{mas} = 0.05 f_m l_{mas} t_{mas}$
Relative strength, β	6.96	-
<i>Expected failure mechanism</i>	<i>Diagonal compression</i>	<i>$\beta > 1$</i>
<i>Result : Failure mode of infilled wall is Diagonal compression.</i>		

A.1.4 Check for out-of-plane failure

Table A.1.4: Out-of-plane check

	Parameters		Remarks
New Zealand (2017) Section C7.6	α	50	$\alpha = \frac{1}{h_{inf}} (E_c I_c h_{inf}^2)^{0.25} \leq 50$ Considering average of two columns = 78.8
	β	46.7	$\beta = \frac{1}{l_{inf}} (E_b I_b l_{inf}^2)^{0.25} \leq 50$
	γ	0.624	$\gamma = 1.1 \left(1 - \frac{h_{inf}}{55 \cdot t_{inf}} \right) \leq 1.0$
	Out of plane pressure, q_{ult} (kPa)	4.66	$q_u = 730 \cdot \gamma \cdot (f_m)^{0.75} t_{inf}^2 \cdot (\alpha / l_{inf}^{2.5} + \beta / l_{inf}^{2.5})$ - Valid for the four side bounded infill
	Capacity (kN)	42.1	$q_u \cdot l_{inf} \cdot h_{inf}$
ASCE/SEI 41-06 (2007)	h/t	23.8	Slenderness ratio
	λ	0.015	From slenderness table
	Out of plane pressure, q_{ult} (kPa)	2.21	$q_u \cdot l_{inf} \cdot h_{inf}$
	Capacity (kN)	19.9	
BNBC 2020 Section 2.5.15.3 (Also suggested in CNCRP Seismic Retrofit manual section 3.6)	Demand (kN)	2.9 (at GF)	$F_c = \frac{\alpha_c a_h W_c I_c}{R_c} \left(1 + 2 \frac{z}{h} \right)$ <p> $[0.75 a_h W_c I_c \leq F_c \leq 1.5 a_h W_c I_c]$ $\alpha_c = 1, R_c = 1.5, z = 1.8m, h = 12.5m$ $W_c = (2975 \times 3025 \times 125 \times 19.2 / 1000^3) = 21.6 \text{ kN}$ $a_h = 0.67 Z S = 0.67 * 0.2 * 1.15 = 0.1541$ </p> <p>- 2.9 kN demand at Ground Floor (GF), even we consider the demand at 5th floor demand would be 7.4 kN</p>
Result: Might be safe from out-of-plane failure as the demand is less than the capacity.			

A.1.5 Selection of failure mechanism after FC strengthening

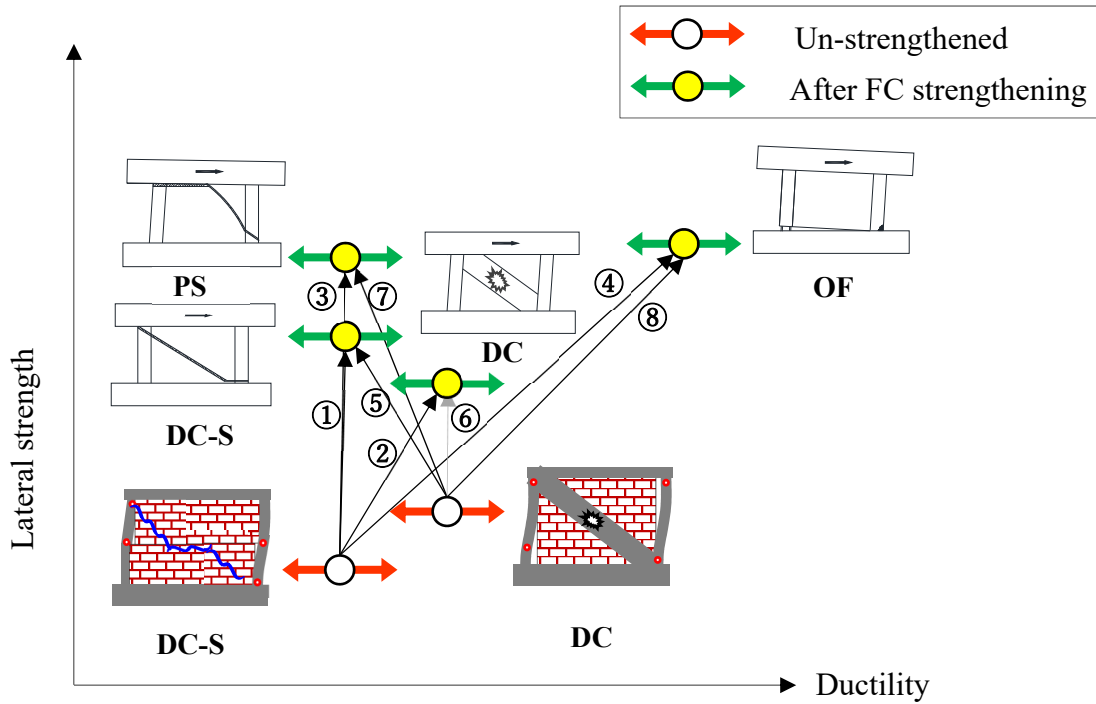


Figure A.1.4: Selection of failure mechanism after FC strengthening

Table A.1.5: Selection of failure mechanism

No.	Before retrofit	After retrofit	How to retrofit	Possibility of technical realization	Recommendation	Comment
①	DC-S	DC-S	Wire mesh is connected to surrounding RC Frame	○	○	
②		DC	Adjustment of FC mortar thickness	○	△	Final failure mode and F-index? (β , a/h become smaller.)
③		PS	-	×	×	
④		OF	-	×	×	
⑤	DC	DC-S	Wire mesh is connected to surrounding RC Frame	○	×	F-index becomes smaller.
⑥		DC	Adjustment of FC mortar thickness	○	○	Adopted in this report
⑦		PS	-	×	×	
⑧		OF	-	×	×	
Result: No. ⑥ (DC→DC) retrofit method is selected.						

DC-S: Diagonal cracking-sliding, DC: Diagonal compression, PS: Punching shear, OF: Overall flexure

A.1.6 Proposed FC configuration

Table A.1.6: Ferrocement configuration

		Remarks
Ferrocement composition		
Thickness (mm)	25	As a minimum thickness
Side of FC application	1	Obligatory as per client
Wire mesh diameter (mm)	1.0	
Wire mesh spacing (mm)	13	
No. of wire mesh layer	1	
FC Mortar strength (MPa)	15	BNBC (2020) recommends 30 MPa for FC structural members. However, there is no guideline for strengthening purpose. 30 MPa is hard to achieve in field, therefore 15MPa is considered.
Yield strength (tensile) of wire mesh (MPa)	275	BNBC (2020) says 60 Grade for FC, however in experimental tests we found tensile yield strength around 275 MPa (40 Grade).

A.1.7 Lateral capacity after FC strengthening

Table A.1.7: Lateral capacity of FC laminated masonry infilled RC frame

		Remarks
Lateral capacity of existing infilled RC frame (kN)	870	$\circ Q_{fr,un-str} = Q_{fr} + Q_{mas}$ $= 657.4 + 212.8 = 870.2 \text{ kN}$
Target lateral capacity after retrofitting (kN)	1083	\circ Considering two times capacity improvement of masonry capacity $\circ Q_{fr,str} = Q_{fr} + 2Q_{mas} = 1083 \text{ kN}$
Diagonal compression capacity (kN)	1124	$\circ Q_{fr,un-str} = Q_{fr} + Q_{mas} + Q_{FC}$ $= 657.4 + 212.8 + 254.2 = \mathbf{1124.4 \text{ kN}}$

A.1.8 Structural drawing

Table A.1.8: Connection details of FC laminated masonry infilled RC frame

Connection details		
Dowel diameter, d_b (mm)	12	*CNCRP manual (2015) specification - Dowel diameter (d_b): 12 to 22mm - Spacing, $S > 7.5d_b$ or $S < 300\text{mm}$
Spacing, S (mm)	300	○ Considering equal amount of wire mesh and connection reinforcement per unit length ○ $\frac{\pi(0.5)^2}{13} \times 1000 = \frac{\pi(6)^2}{S} \times 1000$ $S = 1872 \text{ mm}$ [$S > 7.5 \times 12 = 90\text{mm}$ and $S < 300\text{mm}$] (*CNCRP manual 2015) = 300 mm
Embedment length, l_e (mm)	84	○ Embedment length, $l_e = 7d_b$ [*CNCRP 2015]

*CNCRP (2015): *Manual for Seismic Retrofit Design of Existing Reinforced Concrete Buildings*, Public Works Department

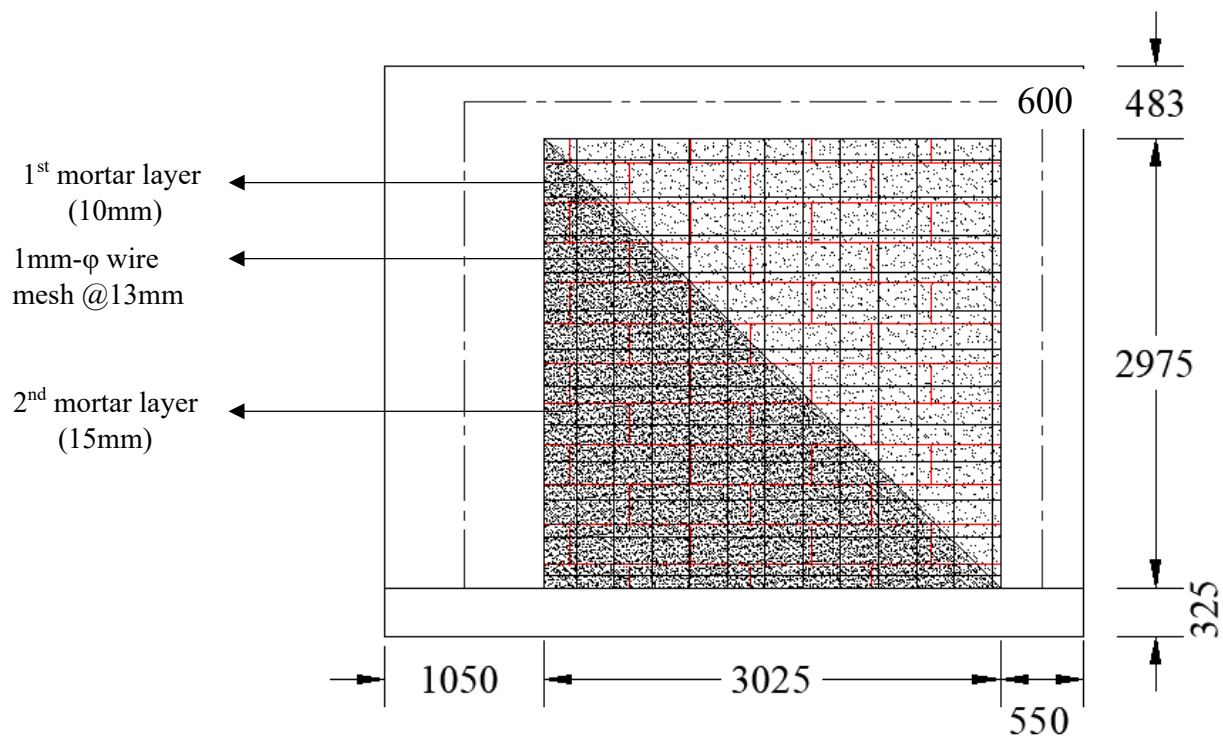


Figure A.1.5: Overall layout of ferrocement
(Connections are not shown here, and bricks and wire meshes are schematic)

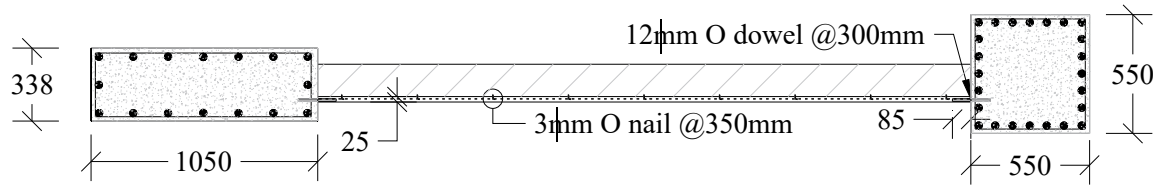


Figure A.1.6: Cross section of infill panel with necessary nail and dowel connections

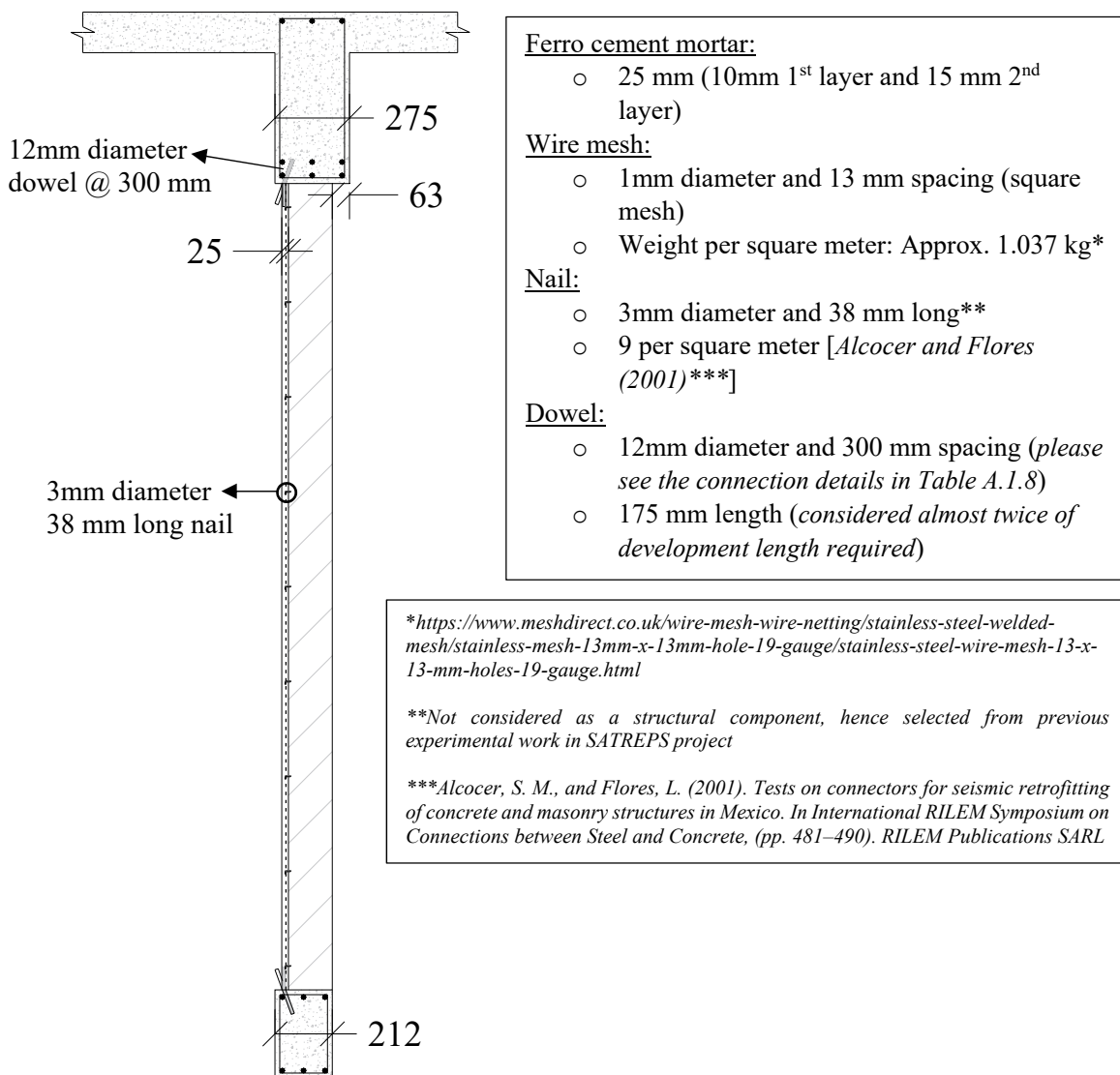


Figure A.1.7: Section of the retrofitted infill wall

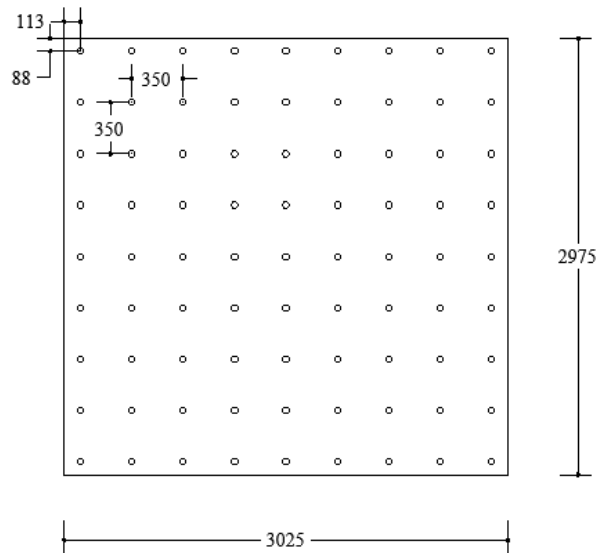
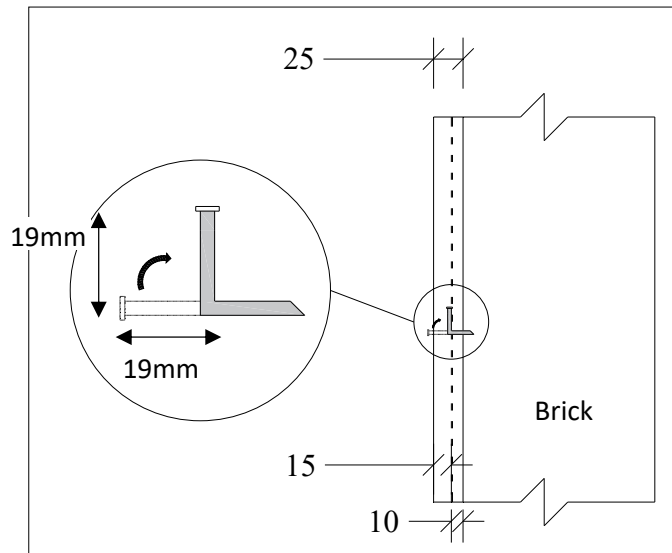


Figure A.1.8: Locations of nail connections on infill panel (9 nails/square meter)

Nail Insertion: There are three kinds of insertion and the appropriate method will be selected after detail investigation.

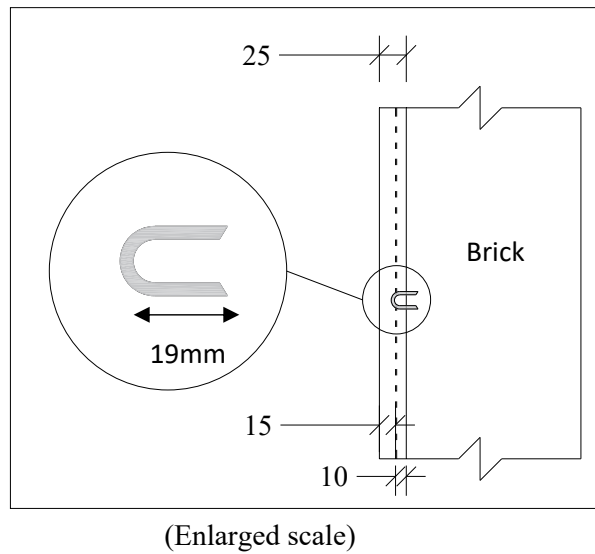
Nail insertion (Idea 1)

1. Hammering of the 3mm nail (38 mm long)
2. Bending of the nail top/extended portion upward



Nail insertion (Idea 2)

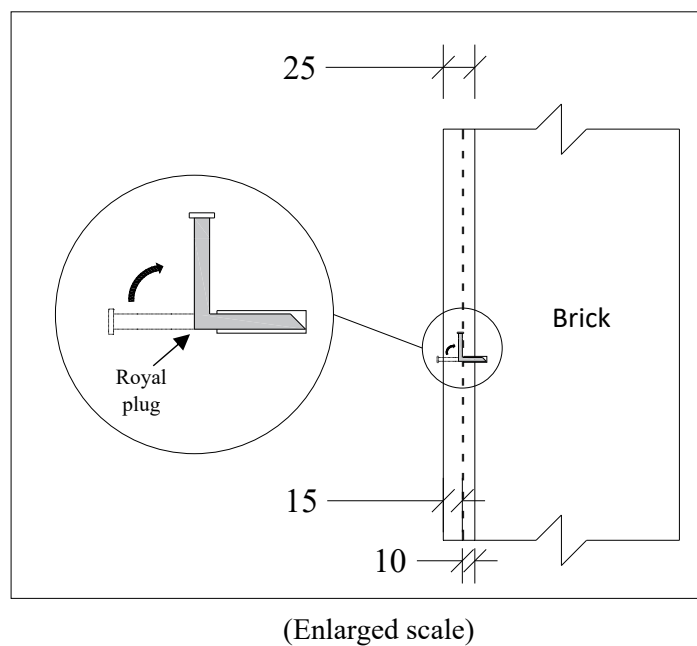
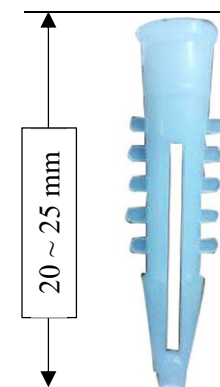
- ### 1. Hammering of the 3mm U-shaped hook



Nail insertion (Idea 3) Drilling of infill after 1st layer of mortar application

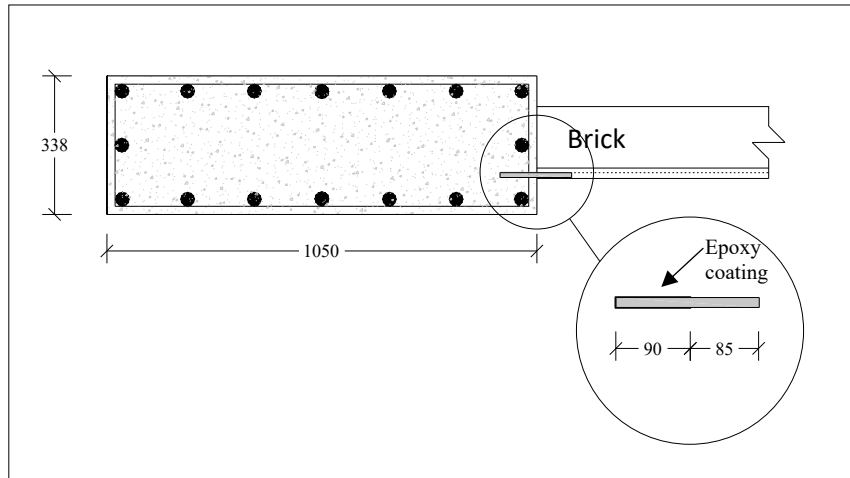
1. Insertion of royal plugs
2. Hammering of the 3mm nail (38 mm long)
3. Bending of the nail top/extended portion

Royal plug (3mm inner diameter)

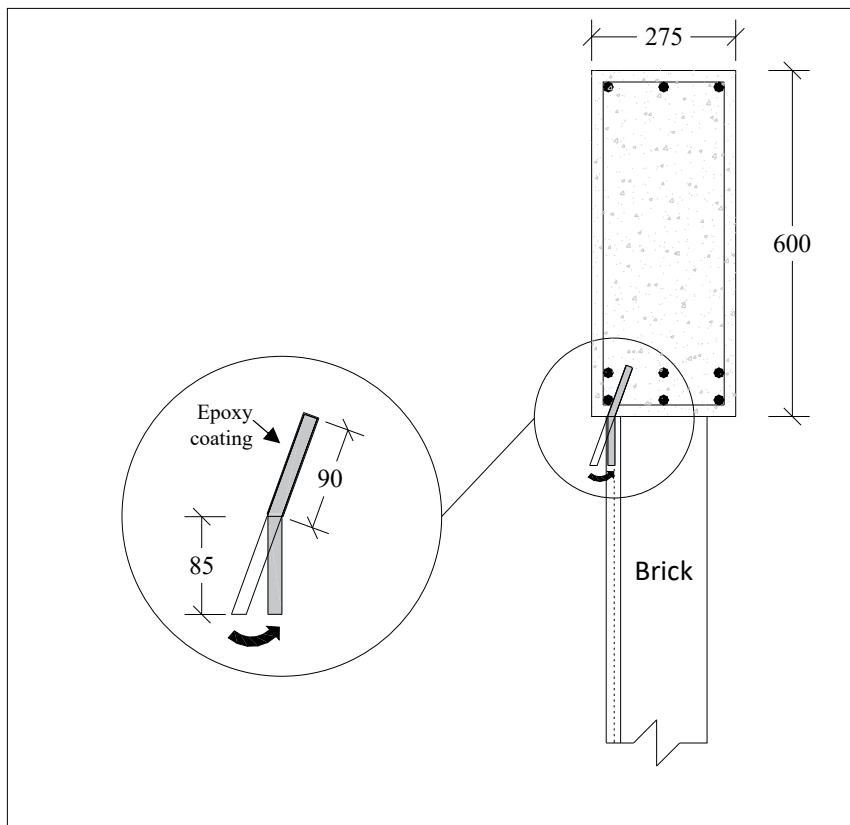


Dowel bar insertion

Case 1: Offset of column/ beam edge is enough for dowel insertion



Case 2: Offset of column/ beam edge is not enough for dowel insertion



A.1.9 Construction steps

The flow of construction procedure in details:

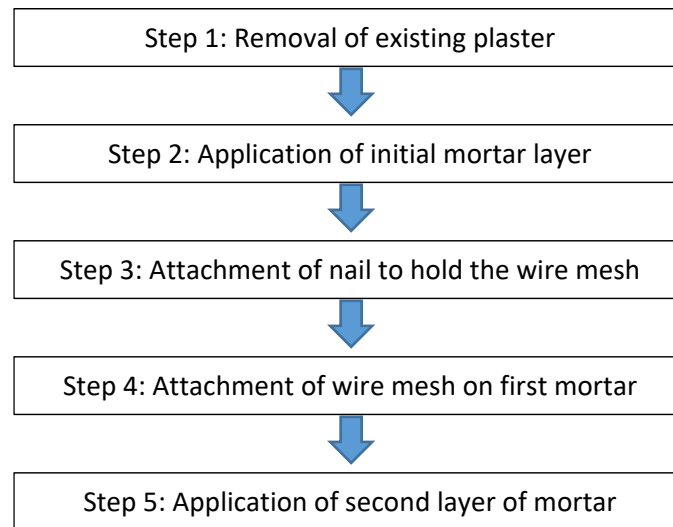


Figure A.1.9: Construction procedure for ferrocement lamination

Construction procedure in details:

Step 1: Preparation of retrofitting works: removal of existing plaster from infill masonry

- To facilitate the retrofit work, adjacent fixtures, decoration etc. should be removed carefully.
- Appropriate measure should be taken to minimize the noise, vibration and dust generated by the construction work.
- Special attention should be paid for safety issue of labor and manpower.
- Plaster of masonry surface to be retrofitted should be removed completely and the surface will be exposed.
- The plaster removing work should be carried out carefully to ensure that no crack inside joint mortar or it does not produce any crack on brick.
- Blower and suction devise should be used to clean dust and fine powders from masonry surface.
- Repair the cracks if any on masonry infill and inside mortar joint.

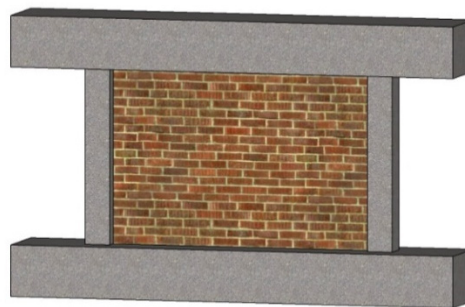


Figure A.1.10: Removal of existing mortar (plaster) from infill masonry

Step 2: Application of initial mortar layer

- Confirm the mixing method of mortar with appropriate water to cement ratio.
- Mortar placing specification (mortar placing section, amount of mortar placing in a single portion)
- Level should be maintained by marking both end with string controlling the same thickness of mortar over the wall.

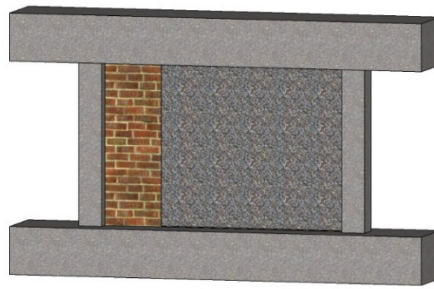


Figure A.1.11: Application of initial mortar layer

Step 3: Attachment of nail

- At least 9 nails/sqm. should be applied on each masonry wall side.
- Marking the point on the infill wall, it is preferable to make hole on bricks avoid joint mortar. It is better to mark the line of each joint mortar level on column before application of initial mortar. At least wait 5~7 days after first mortar layer application.
- Drilling/hammering on initial mortar layer, drilling depth should be satisfying the requirement. In that case, drilling depth should be marked to confirm the drilling depth.
- Cleaning of drilling hole should be carried out carefully by using blower and brushes. If there is some dust, the epoxy material will not get sufficient bonding.
- Alternatively, nail can also be installed by hammering
- The nail shall be installed with sufficient care by skilled worker.

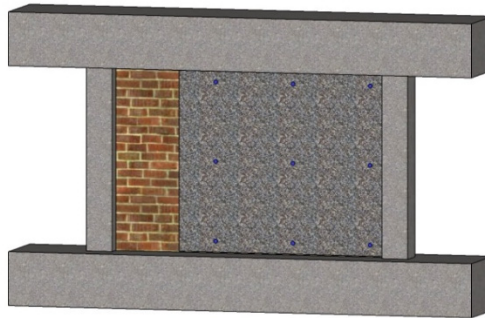


Figure A.1.12: Attachment of nail after drilling

Step 4: Placement of wire mesh mortar

- Cut the wire mesh into same size of masonry infill panel.
- Keep 100mm overlapping of wire mesh, when it is necessary to join wire mesh to cover full masonry wall surface.
- Put wire mesh on initial plaster mortar.
- Bind the wire mesh with the attached nails in the earlier step.
- In case of multilayers, first layers should be put and attached with nails and following layer will be attached and tied with nail consecutively.

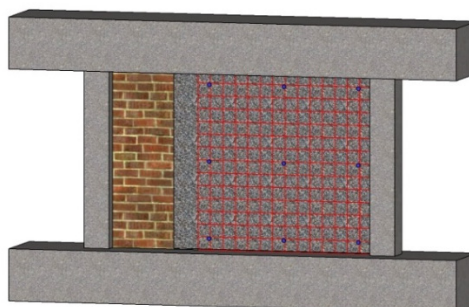


Figure A.1.13: Attachment of wire mesh

Step 5: Connection with CR frame

- Drilling of the RC columns and beams at appropriate spacing
- Cleaning of the holes
- Use epoxy coating to before insertion of the dowel in the hole

Step 6: Application of final layer of mortar.

- Confirm the mixing method of mortar with appropriate ratio.
- Mortar placing specification (mortar placing section, amount of mortar placing in a single portion)
- Level should be maintained by marking both end with string controlling the same thickness of mortar over the wall.
- Use the wooden patta (instrument made from wood) smoothing and leveling the mortar surface until smooth.

Step 7: Curing

- Use gunny bag for curing and pour water to confirm sufficient moisture.

A.1.10 Summary

1) Target site:

- The target site is a building inside the campus of PWD
- The target is the wall of the garage. The retrofit is planned on one side of wall facing inside.

2) Failure mechanism of existing infill wall

- The failure mechanism of existing infilled wall is diagonal compression (DC) failure.

3) The out-of-plane failure mechanism

- Strength of out of plane is larger than the required demand strength. The retrofit is not necessary.

4) Failure mechanism of retrofitted infill wall

- The selected failure mechanism of retrofitted infill wall is the diagonal compression (DC) failure.
- The target strength of infill panel after the ferrocement retrofit is designed as twice of the existing infill wall panel.

5) Structural drawings

- According to the evaluation of out of plane strength, the retrofit for out of plane failure is not necessary. But the dowel connection between the surrounding RC frame and the ferrocement layer was added for demonstration to general engineers.

6) Construction work

- According to the BSPP policy, the construction will not be completed as the ordinal construction in order to show the construction process to general engineers. In this report, this specification is not included.

A.1.11 Site survey and testing list

item		Nos.	comments	
(1) Material, etc. of RC frame				
1)	Concrete strength (column)	3	If impossible: rebound hammer test	
2)	Location of rebar (column) (Longitudinal bar and tie bar)	2	Rebar scanning test	
3)	Size of section, height of column, span length, etc.	1	Measuring scale, laser scale, etc.	
(2) Material etc. of Infilled masonry				
1)	Size of brick	3	Measuring scale	
(3) Material of wire mesh and mortar				
1)	Tensile strength of wire mesh	1	If the tensile strength is unknown, tensile test shall be conducted	
2)	Compressive strength of mortar	3	Compressive strength test	

A.2 Construction Work

Note: The construction work was performed in addition to the portion covered by SATREPS-TSUIB, plus the construction portion of BSPP-PWD. Since there are many different ways to install a ferrocement lamination on an existing RC frame or existing brick wall, and none of them have been established at this time, this project was undertaken to compare the installation methods.

A.2.1 Plan of ferrocement work

The two design plans for Ferrocement work procedures for the two walls of Wall-A and Wall-B respectively at the target location of test work in PWD-HQ were prepared by SATREPS-TSUIB and PWD-BSPP. In this chapter, plan and test result are shown.

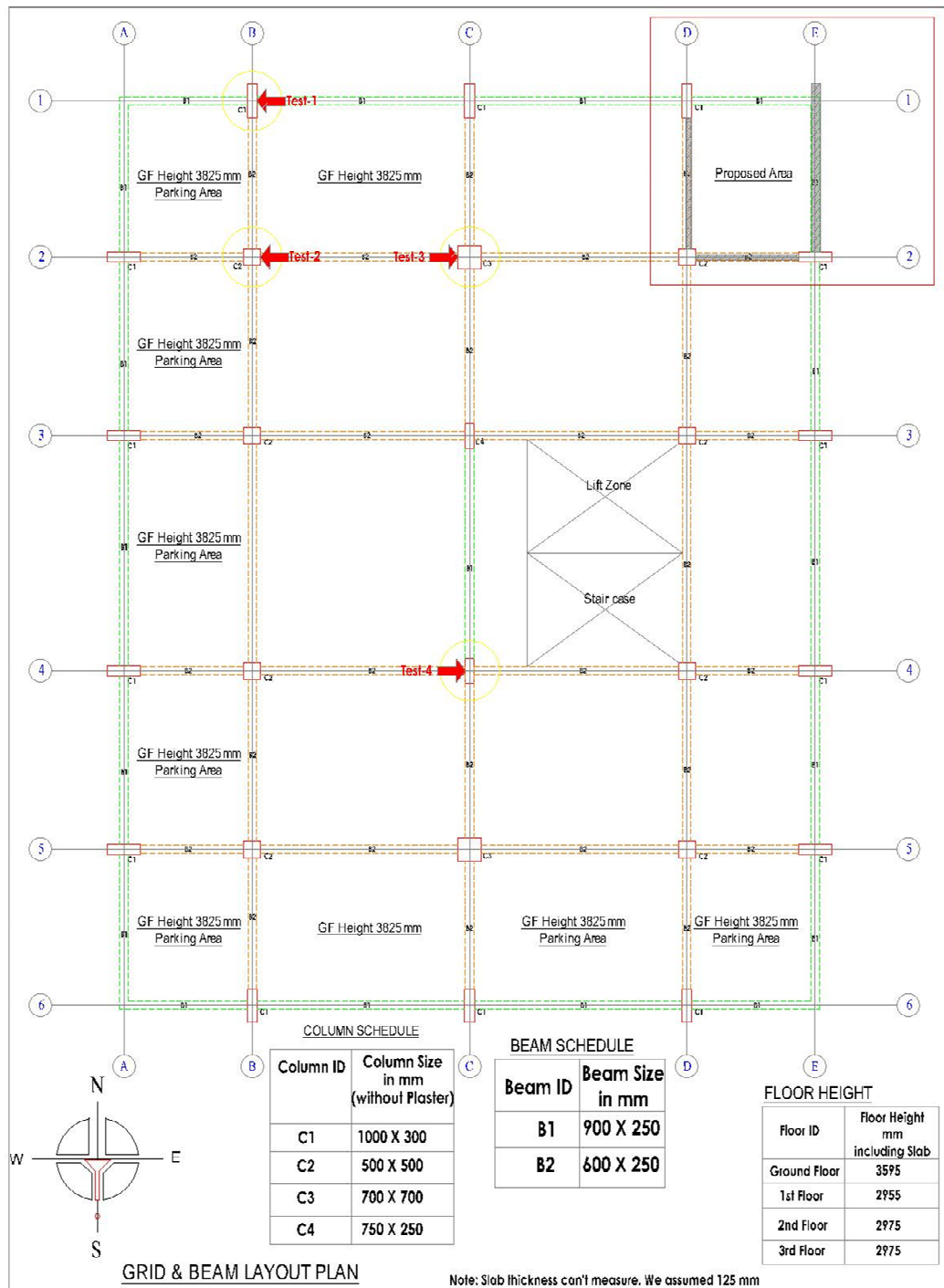


Figure A.2.1: Target Location of test work in PWD-HQ

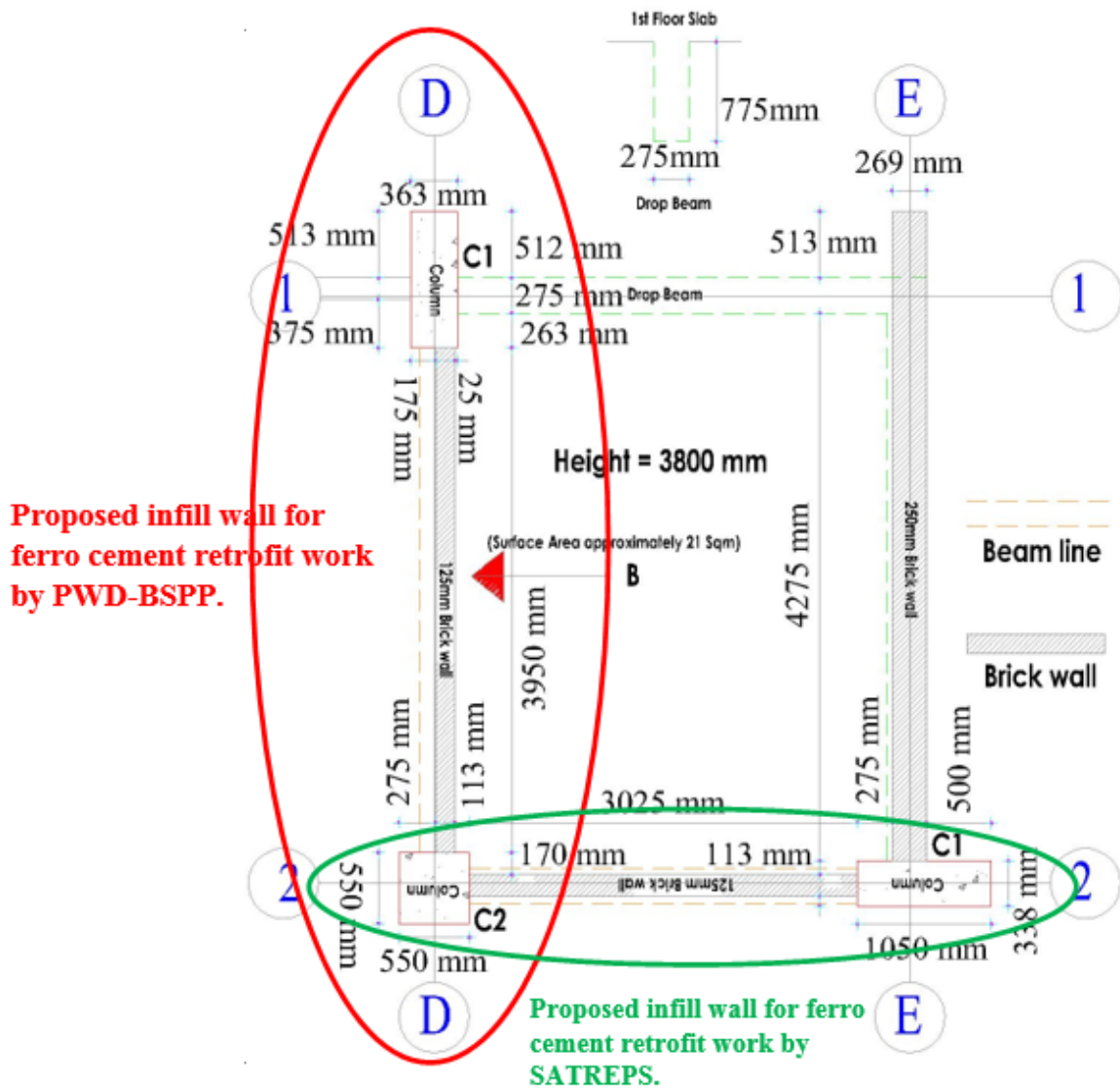


Figure A.2.2: Target location blowup (All dimensions include plaster thickness)

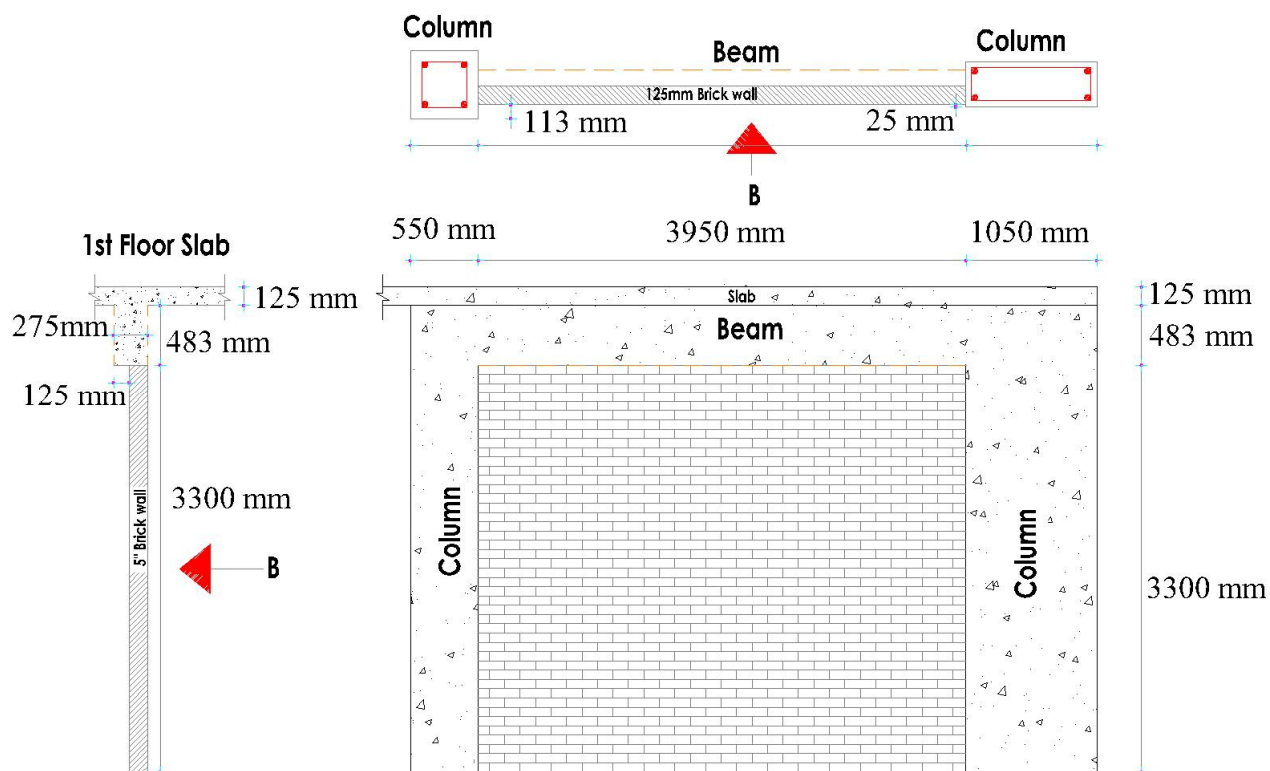


Figure A.2.3: Plan, Section and elevation of the target infill wall (All dimensions are included plaster thickness)

A.2.2 Issues of work

(1) For wire mesh:

- 13 mm X 13 mm X 1 mm (19 number wire) generally 18 number and 20 number are locally found. 18 number has a thickness of 1.26 mm while 20 number has a thickness of 0.91 mm. it can generally be suggested to use locally available 20 number instead of using 19 number wire if the design permits.

(2) For nail installation:

SATREPS- TSUIB	Specification	Spacing
Plan	Thickness: 3mm, Length: 38 mm	350 mm
Actual	Thickness: 2.8 mm, Length: 38 mm	250-275 mm.

PWD-BSPP	Specification	Spacing
Plan	Thickness: 2mm, Length :75 mm	610 mm
Actual	Thickness: 2.9~3 mm, Length: 50 mm	250-275 mm.

Nail to nail distance minimization:

To avoid swelling /sag of wire mesh, the planned spacing of nail was changed for both methods. The changed spacing in between two nails were 250-275 mm.

Nail installation process:

Initially, it was planned for PWD-BSPP to use nail in brick joint by hammering. However, it was found that inserting nail via hammering had few hindrances.

- 30-40% nail could be wasted even following the marking of brick joint line.
- Insert of required length could not achieved accurately.
- This process was time consuming compare to drilling and inserting rawl plug.

(3) Desired FM of Sand:

During casting work, it was found that the available sand (local/white) was finer than the requirement and the Fineness Modulus (FM) was below 1. To fulfil the requirement of FM (1.2) 20 percent of coarse sand was added with local sand and tested at lab which is around 1.2 to 1.3.

(4) Thickness of final layer mortar work for SATREPS- TSUIB:

- a. Planned: 15 mm
- b. Actual: 20 mm (approximately)

Reason for changing the thickness:

- 15 mm mortar work could not cover the anchored rebar. The diameter of rebar was 12 mm. During drilling work at horizontally, 2-3 mm (approx.) additional spacing was needed. In addition to that, the diameter of wire at wire mesh was 1 mm. As a result, the top surface of rebar was around 16-17 mm from previous mortar work. To cover it properly, 19-20 mm (approx.) thickness of mortar work was needed.
- Mortar work was performed in two layers. 10-12 mm mortar work was performed at first. After completion of first layer, 1-2 hours gap were provided and 2nd layer mortar work was done in the same day.
- To recover this large thickness, it is suggested to use 8 mm rebar instead of 12 mm.

(5) 2nd layer 6 mm mortar work for BSPP-PWD (after first layer wire mesh installation):

Accurate 6 mm mortar could not be performed as the thickness is less and to maintain proper measurement is quite difficult. The thickness of this layer is in between 6-6.5 mm.

(6) Frame connection in BSPP- PWD: using rawl plug and bolt instead of rawl bolt:

- 12 mm dia Rawl plug was used to install 10 mm nut-bolt. After installing nut bolt, additional length along with head was cut down.
- One nut-bolt is used instead of two at case 01 as per site condition. (fig: 63)
- Initially, it was planned to used rawl bolt to install angle and flat bar in joint area. But proper tightening and installing could not be performed. On contrary, installing rawl plug with nut bolt was easier than rawl bolt.

(7) Frame connection in BSPP- PWD: change of flat bar thickness due to market unavailability:

- Flat bar information: 38 mm X 150 mm X 4 mm (thickness) flat bar was used instead of 50 mm X 150 mm X 3 mm (thickness).

A.2.3 Steps of work

Step no	Work breakdown	Duration in days (for 15 to 20 sqm mortar work)
01	Removing existing plaster work	1
02	Cleaning brick surface	1
03	Pointing/ marking the existing brick layer	1
04	First layer 8 to10 mm mortar work (rough plaster)	1
05	Curing work	7
Total days (approx.)		11 days

Option 01 (after step 05)-single layer with epoxy resin anchorage

Step no	Work breakdown	Duration (for 15 to 20 sqm mortar work)
06.	Drill work for frame connection (both beam and column joint with brick surface and wire mesh)	2
07.	First layer wire mesh (vertical laying)	1
08.	Nail work to fix the wire mesh	(same day)
09.	Epoxy resin anchorage work	2
10.	Final layer 15 mm wire mesh	1
11.	Curing work	7
12.	Paint work	7
13.	Display work	3
Total days for option 01(approx.)		23 days

Option 02 (after step 05)-double layer with angle, flat bar and bolt

Step no	Work breakdown	Duration (for 15 to 20 sqm mortar work)
06.	First layer wire mesh (horizontal laying)	1
07.	Nail work to fix the wire mesh	(same day)
08.	Second layer 6 mm plaster work	1
09.	Curing work	7
10.	Drill work for frame connection (both beam and column joint with brick surface and wire mesh)	1
11.	second layer wire mesh (vertical laying)	1
12.	Nail work to fix the wire mesh	(same day)
13.	Frame connection	1
14.	Final layer 10 mm mortar work	1
15.	Curing work (7 days)	7
16.	Paint work	7
17.	Display work	3
Total days for option 02 (approx.)		30 days

A.2.3.1 Steps of work for SATREPS- TSUIB, WALL-A

Step 01: The first step of ferrocement plaster work is to remove existing plaster work.



Figure A.2.4: *Plaster removal for existing brick wall*



Figure A.2.5: *Plaster removal for brick joint*

Step 02: Cleaning brick surface



Figure A.2.6: *Cleaning brick surface with steel brush*



Figure A.2.7: *Cleaning brick work for next work phase*

Step 03: Pointing/ marking the existing brick layer



Figure A.2.8: *Marking brick line to install nail*

Step 04: First layer 10 mm mortar work (rough plaster)



Figure A.2.9: *Cement grouting work*



Figure A.2.10: 10 mm mortar work without wire mesh (locally known as rough plaster)



Figure A.2.11: Checking the thickness of rough plaster

Step 05: Curing work- 7 days



Figure A.2.12: Spreading water for curing work

Step 06: Drill work for frame connection (both beam and column joint with brick surface and wire mesh)



Figure A.2.13: *Marking and drilling work for nailing*



Figure A.2.14: *Drilling work for dowel installation (downward)*



Figure A.2.15: *Drilling work for dowel installation (upward)*



Figure A.2.16: *Checking the distance of drill*

For frame connection, rebar anchoring is selected. Drill work is performed before installing wire mesh. 16 mm drill bit is used for installing 12 mm rebar.

Step 07: First layer wire mesh (vertical laying)



Figure A.2.17: *Wire mesh installation*



Figure A.2.18: *Checking the lap length of wire mesh-100 mm*

Step 08: Nail work to fix the wire mesh

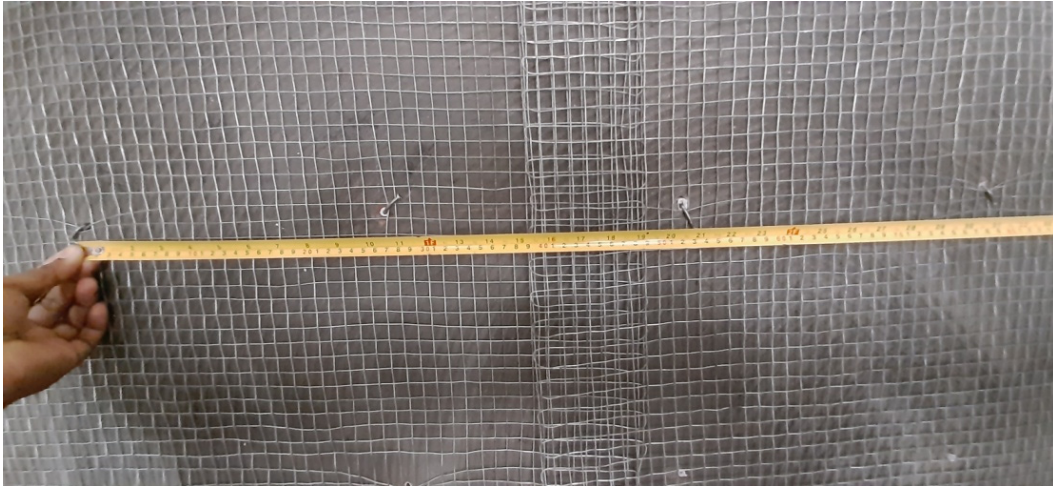


Figure A.2.19: *Checking the horizontal distance of nail*

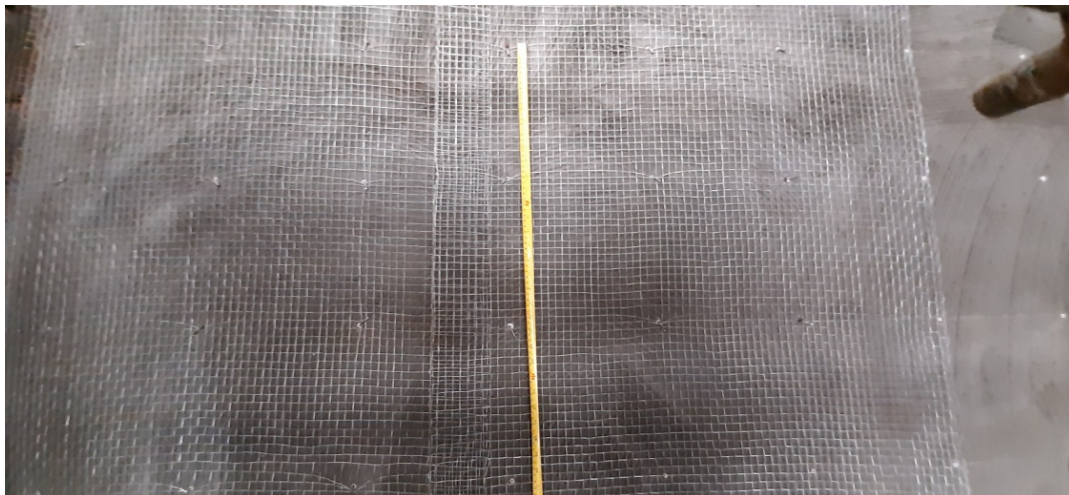


Figure A.2.20: *Checking the vertical distance of nail*

Step 09: Epoxy resin anchorage work



Figure A.2.21: *Injecting epoxy resin to install dowel*



Figure A.2.22: *Preparation of dowel before installation (bending as per design)*



Figure A.2.23: *Installation of dowel with epoxy resin/ Anchoring work*

- After installing wire mesh, epoxy resin anchorage was used to install 12 mm rebar. Rebar is needed to bend a minimum required amount before installation.
- Inside : 90 mm (epoxy length)
- Outside: 85 mm (open length to lock wire mesh)

Step 10: Final layer 15 mm mortar work



Figure A.2.24: *Checking the minimum length required for final mortar work to cover dowel.*



Figure A.2.25: *Checking the minimum length required for final mortar work to cover dowel.*



Figure A.2.26: *2nd Phase mortar work with wire mesh (20 mm)*



Figure A.2.27: 2nd Phase mortar work with wire mesh (20 mm)



Figure A.2.28: Finishing the final phase mortar work

Step 11: Curing work- 7 days



Figure A.2.29: Spreading the water for curing work



Figure A.2.30: minimum 7 days curing to avoid any form of crack

Step 12: Paint work

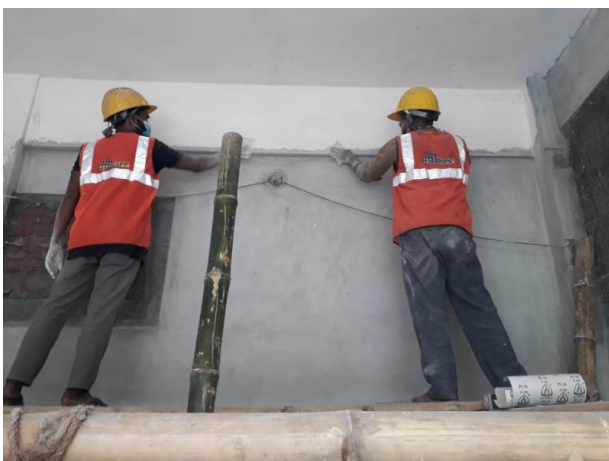


Figure A.2.31: First coat paint work



Figure A.2.32: Final coat paint work

Step 13: Display area



Figure A.2.33: Display of different layer of mortar work for SATREPS- TSUIB, Bangladesh portion, Wall-A



Figure A.2.34: Display of different layer of mortar work for SATREPS- TSUIB, Bangladesh portion, Wall-A

A.2.3.2 Steps of work for PWD-BSPP, WALL-B

Step 01: The first step of ferrocement plaster work is to remove existing plaster work.



Figure A.2.35: Removing existing plaster work of brick wall



Figure A.2.36: Removing brick joint plaster

Step 02: Cleaning brick surface



Figure A.2.37: Cleaning the brick surface



Figure A.2.38: Prepared surface for ferrocement mortar work

Step 03: Pointing/ marking the existing brick layer



Figure A.2.39: Marking and cleaning the existing brick line

Step 04: First layer 8 mm mortar work (rough plaster)



Figure A.2.40: 8 mm first layer mortar work (locally known as rough plaster)



Figure A.2.41: 8 mm first layer mortar work (without wire mesh)



Figure A.2.42: Checking the thickness of mortar work

Step 05: curing work- 1 day

Step 06: First layer wire mesh (horizontal laying)



Figure A.2.43: First layer wire mesh installation (horizontal laying)

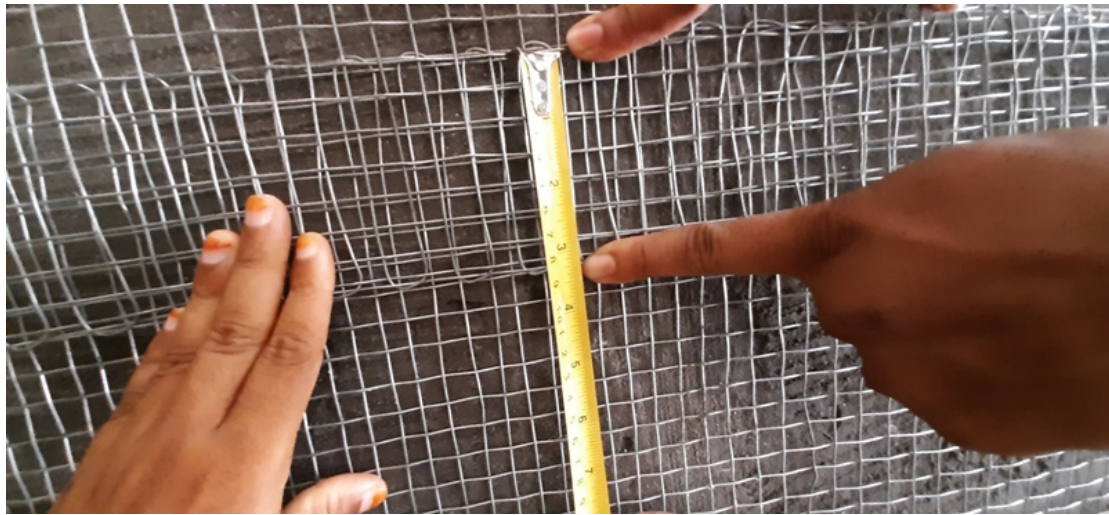


Figure A.2.44: Checking the lap length of wire mesh-75 mm

Step 07: Nail work to fix the wire mesh



Figure A.2.45: Marking the point for installation of nail



Figure A.2.46: Installation of nail

Step 08: Second layer 6 mm mortar work



Figure A.2.47: 8 mm second layer mortar work with wire mesh

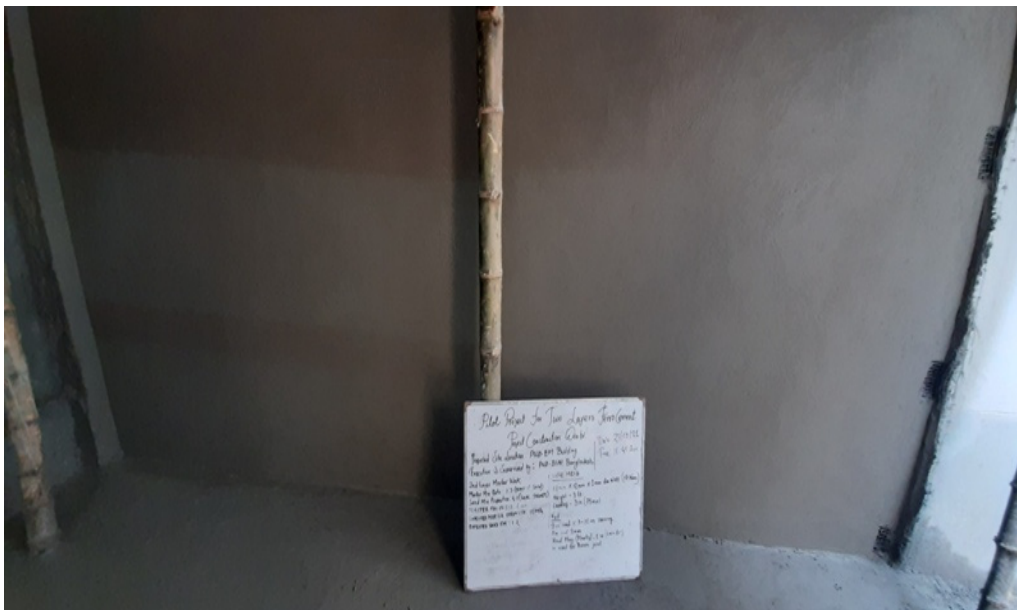


Figure A.2.48: second layer mortar work

Step 09: Curing work

Step 10: Drill work for frame connection (both beam and column joint with brick surface and wire mesh)



Figure A.2.49: Drill work to install angle, rawl plug and nut bolt if thickness of mortar work cannot cover the width of angle



Figure A.2.50: 75 mm wire mesh lapping before installation of angle (only where the thickness is inadequate)

For installing angle and bolt at frame connection, 12 mm rawl plug is used. Diameter and depth of drill work are 12 mm and 43 mm respectively.

Step 11: second layer wire mesh (vertical laying)



Figure A.2.51: Nail installation after wire mesh laying to avoid sag

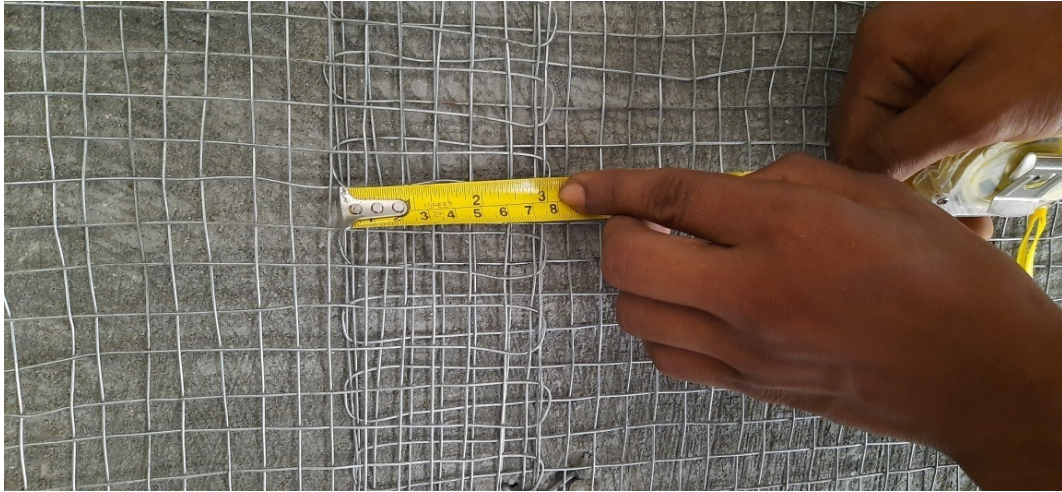


Figure A.2.52: Checking the lap length of wire mesh- 75 mm

Step 12: Nail work to fix the wire mesh

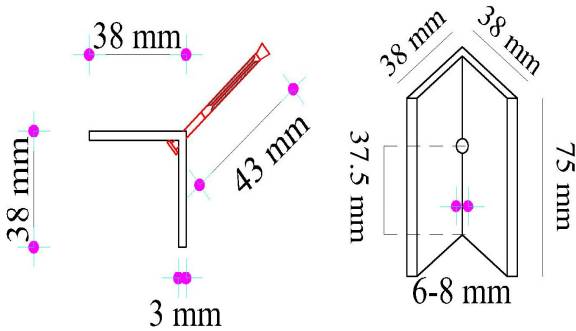


Figure A.2.53: Checking the distance of nail (vertical)



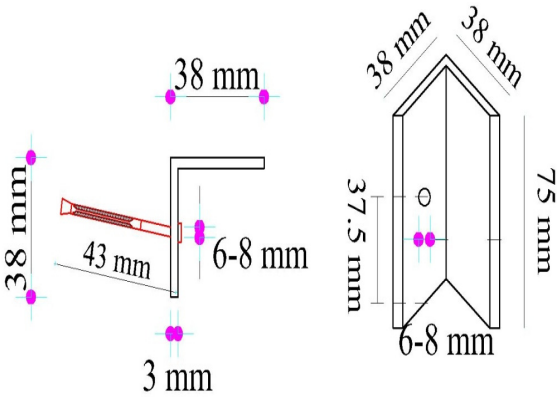
Figure A.2.54: Checking the distance of nail (horizontal)

Step 13: Frame connection



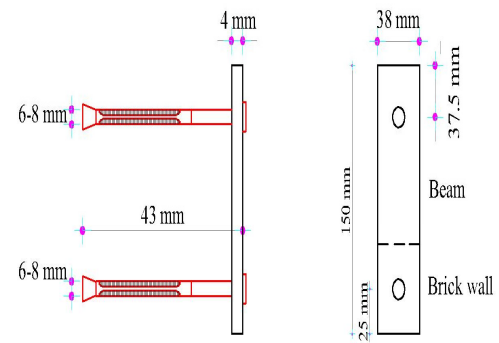
Angle Details

Figure A.2.55: Angle, rawl bolt and nut bolt details to connect existing brick and column with wire mesh (where the thickness is inadequate)



Angle Details

Figure A.2.56: Angle, rawl bolt and nut bolt details to connect existing brick and column with wire mesh (where the thickness is adequate)



Flat bar (38 mm X 150 mm X 4 mm) and 600 mm spacing.

Flat bar Details

Figure A.2.57: Flat bar, rawl bolt and nut bolt details to connect existing brick and beam with wire mesh



Figure A.2.58: Angle, rawl bolt and nut bolt installation to connect existing brick and column with wire mesh. Head of nut is removed after installation if required.



Figure A.2.59: Angle, rawl bolt and nut bolt installation to connect existing brick and column with wire mesh.

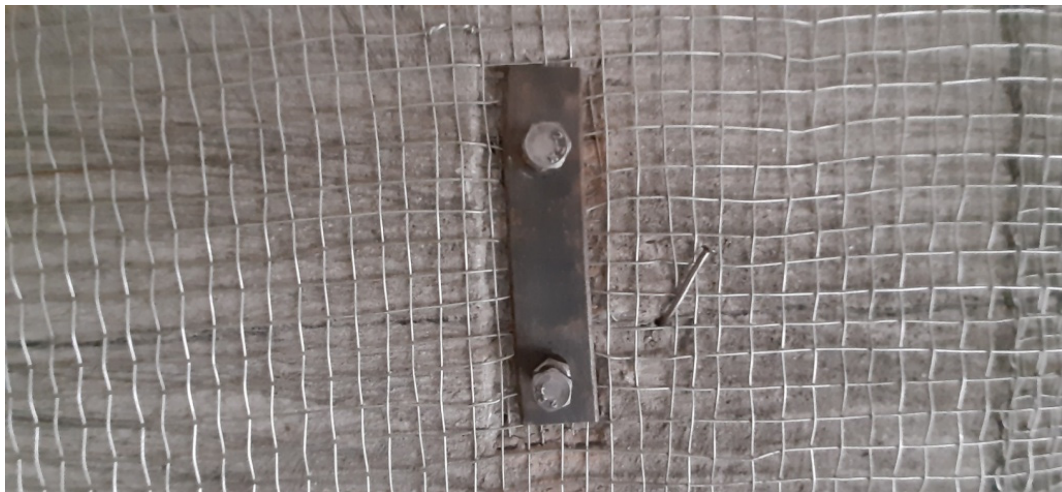


Figure A.2.60: Flat bar, rawl bolt and nut bolt installation to connect existing brick and beam with wire mesh. This head of nut can be removed if possible/required.

- Angle information: (38mm X 38 mm X 3 mm(thickness) X 75 mm (long) with nut-bolt.
- Flat bar information: 38 mm X 150 mm X 4 mm (thickness) flat bar was used instead of 50 mm X 150 mm X 3 mm (thickness)

Step 14: Final layer 10 mm mortar work



Figure A.2.61: Cement grouting spreading for final (3rd) layer mortar work



Figure A.2.62: Final (3rd) layer mortar work with second layer wire mesh



Figure A.2.63: Completion of 10 mm final layer mortar work



Figure A.2.64: Cube preparation for checking the strength of prepared mortar

Step 15: Curing work- 7 days



Figure A.2.65: Spreading water for curing work (7 days) to avoid crack



Figure A.2.66: Continuous 7 days water spreading for curing work

Step 16: Paint work



Figure A.2.67: First coat paint work for paint work



Figure A.2.68: Final coat paint work



Figure A.2.69: Final coat paint work

Step 17: Display work



Figure A.2.70: Display of different layer of mortar work for SATREPS-TSUIB, Wall-A



Figure A.2.71: Display of different layer of mortar work for PWD-BSPP, Wall-B



Figure A.2.72: Condition of the selected area (before work start)



Figure A.2.73: Condition of the selected area (after work completion)



Figure A.2.74: Condition of the selected area (after work completion)

A.2.4 Comparison between work plan and execution

A.2.4.1 Brief comparison on work plan of ferrocement test work between BSPP-PWD AND SATREPS-TSUIB

Sl.No	Subject	Items	BSPP- PWD	SATREPS- TSUIB
1	Wire mesh	Material specification	The ideal mesh is 20 BWG 13 mm x 13 mm x 1 mm (thickness) galvanized mesh.	1mm diameter square wire mesh having 13mm spacing
		Layer	Two-layer wire mesh	One-layer wire mesh
		Lapping	75 mm (3 in)	100 mm (4 in)
2	Nail work	Fixing Materials with infill brick	Nail	Nail/ Hook (with Rawl plug)
		Fixing process	Hammering	Drilling
		Position for Nailing	Brick joint	Brick surface
		Size	2mm (75 mm long)	3mm (38 mm long)
		Nail Spacing	610 mm	350 mm
3	Mortar work	Layer	Three-layer mortar	Two-layer mortar
		Thickness	<ul style="list-style-type: none"> 1st layer: 8 mm 2nd layer: 6 mm 3rd layer: 10 mm 	<ul style="list-style-type: none"> 1st layer: 10 mm 2nd layer: 15 mm
		Mortar strength	10 MPa	15 MPa
4	Connection work at edge with RC frame	Fixing Materials with RC frame	Angle/Flat bar and rawl bolt	Dowel bar with epoxy anchoring
		Fixing Materials Size	<ul style="list-style-type: none"> Angle (38+38 mm X 75 mm X 3 mm) with column Flat bar (50 mm X 150 mm X 3 mm) with beam Rawl bolt (6-8 mm X 75mm) 	12 mm diameter dowel with 175 mm length
		Fixing Materials Spacing	600 mm	300 mm
		Anchoring method	Drilling & rawl bolting	Drilling & epoxy anchoring
5	Curing work	Days of curing work	<ul style="list-style-type: none"> First and second layer: 1 day Final layer: 7 days 	<ul style="list-style-type: none"> Each layer: 7 days

A.2.4.2 Brief comparison between work plan and actual work of ferrocement test work of SATREPS-TSUIB, WALL-A

Sl. No	Subject	Items	Plan	Actual	Remarks
1	Wire mesh	Material specification	1mm diameter square wire mesh having 13mm spacing.	We used 19 no wire mesh having 13 mm x 13 mm x 1.02 mm (thickness) galvanized mesh.	Available thickness variation for <ul style="list-style-type: none"> • 18 number = 1.26 mm • 19 number = 1.02 mm • 20 number = 0.91 mm 18 and 20 numbers are locally available. 19 number is needed to order 2-3 days before installing.
2	Nail work	Size	Φ3mm (38 mm long)	Φ2.8 mm (38 mm long)	It is locally available.
		Nail Spacing	350 mm	250-275 mm	Trial and error method was used at BSPP-PWD to find the maximum spacing to avoid swelling/sag, the provided spacing was within 250-275 mm. Also, 9 nails were provided in 0.7 sq-m which satisfied the minimum nails requirement of SATREPS (9 nails in 1 sq-m).
3	Mortar work	Thickness	1 st layer : 10 mm 2 nd layer : 15 mm	1 st layer : 10 mm 2 nd layer : 20 mm	15 mm mortar work can not cover the anchored rebar. The diameter of rebar is 12 mm. during drilling work at horizontally, 2-3 mm (approx.) additional spacing is needed. In addition to that, the diameter of wire at wire mesh is 1 mm. As a result, the top surface of rebar is around 16-17 mm from previous mortar work. To cover it properly, 19-20 mm (approx.) thickness of mortar work is needed.
		Sand F.M	1.2	1.2-1.3	FM of Local sand was below 1. To reach the FM of 1.2, coarse sand (Sylhet-red sand) was mixed with local sand in ratio 4:1 (local: coarse).

A.2.4.3 Brief comparison between work plan and actual work of ferrocement test work of BSPP-PWD, WALL B

Sl.No	Subject	Items	Plan	Actual	Remarks
1	Wire mesh	Material specification	The ideal mesh is 20 BWG 13 mm x 13 mm x 1 mm (thickness) galvanized mesh.	The ideal mesh is 19 BWG 13 mm x 13 mm x 1.02 mm (thickness) galvanized mesh.	Available thickness variation for <ul style="list-style-type: none"> • 18 number = 1.26 mm • 19 number = 1.02 mm • 20 number = 0.91 mm 18 and 20 numbers are locally available. 19 number is needed to order 2-3 days before installing.
2	Nail work	Fixing process	Hammering (both layers)	<ul style="list-style-type: none"> • First layer: Hammering • Second layer: Drilling with rawl plug-plastic 	<ul style="list-style-type: none"> • 30-40% nails were wasted even following the marking of brick joint line during hammering work. • Insert of required length cannot be achieved accurately during hammering work. • On the contrary, noise was made during drilling work which was a hindrance during office time.
		Position for Nailing	Brick joint	<ul style="list-style-type: none"> • First layer: brick joint • Second layer: brick surface/ brick joint 	<ul style="list-style-type: none"> • Inserting nail via hammering was preferred at brick joint while inserting via drilling was at brick surface.
		Size	2mm (75 mm long)	2.9~3 mm (50 mm long)	<ul style="list-style-type: none"> • The thickness of 75 mm was higher than 3 mm. • 50 mm supported the requirement of attaching wire mesh properly with existing rough mortar surface.
		Nail Spacing	610 mm	250-275 mm	<ul style="list-style-type: none"> • Trial of nailing spacing was started from 610 mm and continuously minimized to avoid swelling. To completely avoid swelling /sag of wire mesh, it was found that the required spacing should be within 250-275 mm.
3	Mortar work	Thickness	1 st layer : 8 mm 2 nd layer : 6 mm 3 rd layer: 10 mm	1 st layer : 8 mm 2 nd layer : 6-6.5 mm 3 rd layer: 10 mm	<ul style="list-style-type: none"> • As accurate measurement of thickness of 6 mm mortar work is relatively difficult, the actual work (from 6 to 6.5 mm) was varied during execution.
		Sand F.M	1.2	1.3-1.4	<ul style="list-style-type: none"> • FM of Local sand was below 1. To reach the FM of 1.2, coarse sand (Sylhet-red sand) was mixed with local sand in ratio 4:1 (local: coarse).

4	Connection work at edge with RC frame	Fixing Materials with RC frame	Angle/Flat bar Rawl bolt	Angle/Flat bar Rawl plug Nut- bolt as a fastener.	<ul style="list-style-type: none"> Proper fastening and installing cannot be performed via Rawl bolt. Also, installing Rawl plug with nut- bolt is easy to install.
		Flat bar specification	50 mm X 150 mm X 3 mm (thickness)	38 mm X 150 mm X 4 mm(thickness)	<ul style="list-style-type: none"> As 3 mm thickness of 50 mm width flat bar was not locally available, 4 mm thickness of 38 mm width flat bar was approved to fix with Brick - beam joint area.
		Rawl bolt/ rawl plug specification	Thickness: 6-8 mm Length: 75 mm	Rawl plug: Thickness: 10 mm (inner surface) Length: 38 mm (before fastening) 43 mm (after fastening) Nut-bolt: Thickness: 10 mm Length: as per mortar thickness	

A.2.5 Report of compressive mortar strength of cube test

Sl.No	Test work	Location	Desired strength (MPa)	Location of mortar	Mortar thickness (mm)	Compressive strength (7 days in MPa)	Compressive strength (28 days in MPa)
1	BSPP-PWD	WALL-B	10 MPa	Rough plaster	8 mm	22.2	34.03
				First layer	6-6.5 mm	20.94	26.45
				2 nd /Final layer	10 mm	16.46	17.24
2	SATREPS-TSUIB	WALL-A	15 MPa	Rough plaster	10 mm	21.45	23.58
				1 st /single layer	20 mm	16.81	18.96

A.2.6 Wire mesh test

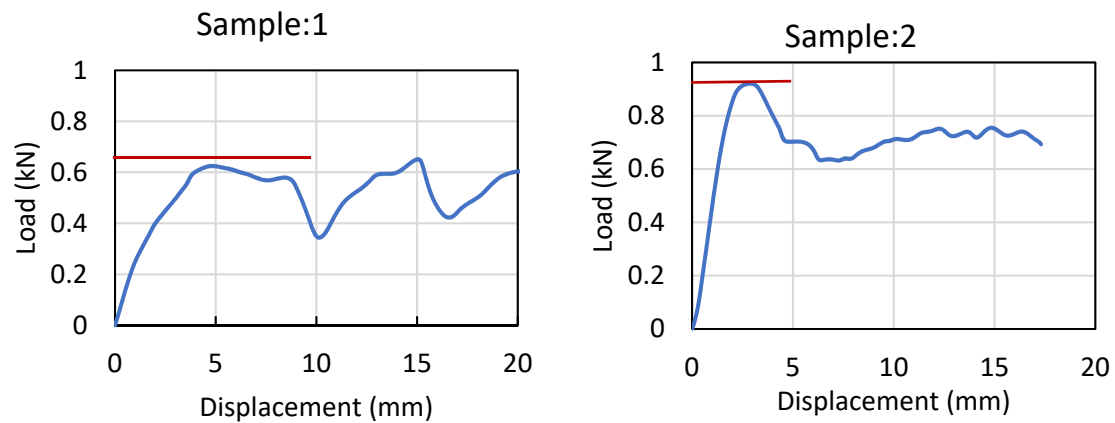
Summary of wire-mesh test at HBRI

1. Test setup



Figure A.2.75: Wire mesh test

2. Number of samples: 2



3. Test result:

Sample ID	Number and diameter	Max Load (kN)	Total cross-sectional area (mm ²)	Tensile stress (N/mm ²)	Average Tensile stress (N/mm ²)
Sample 1	5 number wires, 1mm	0.62	3.925	157.96	196.17
Sample 2	5 Number wires, 1 mm	0.92	3.925	234.39	

A.2.7 Comparison of costing and duration between SATREPS-TSUIB, WALL-A and BSPP-PWD, WALL-B

Cost comparison:

NAME OF WORK : FERROCEMENT TEST WORK (Ferrocement test work for Retrofitting at Annex Building of PWD-HQ Compound Under the Project of BSPP)								
Item	Items of Works	Unit	Unit rate (BDT)	BSPP-PWD	Total cost (BDT)	SATREPS	Total cost (BDT)	Remarks
1	Stripping of plaster including racking out joints, cleaning	sqm	290	16.81	4874.90	10.64	3,085.60	
2	15 mm thick cast-in-situ ferrocement wall with minimum cement content relates to mix ratio 1:2, cement conforming to BDS EN-197-1, 52.5 N(52.5 MPA)/ (ASTM-C 150 type-1, and best quality coarse sand (FM 2.2), 1 layer of 20 BWG galvanized wire mesh having minimum yield strength fy=450 MPa and 2 wire mesh per 25 mm, nailing/ anchoring at 600 cceach way casting and finishing the both surfacs with cement sand (FM 1.2) mortar (1:3) and curing at least for 21 days, including the cost of water, electricity and other charges in all complete as per drawing, design and accepted by the Engineer in charge	sqm	4200	0.00	0.00	10.64	44,688.00	Additional 1000 taka/sqm is considered as 30 mm mortar work is performed. (10 mm rough plaster/ mortar work+ 20mm (instead of 15mm) mortar work with wire mesh for covering 12mm dowel bar)
3	25 mm thick cast-in-situ ferrocement wall with minimum cement content relates to mix ratio 1:2, cement conforming to BDS EN-197-1, 52.5 N(52.5 MPA)/ (ASTM-C 150 type-1, and best quality coarse sand (FM 2.2), 2 layers of 20 BWG galvanized wire mesh having minimum yield strength fy=450 MPa and 2 wire mesh per 25 mm, nailing/ anchoring at 600 cceach way casting and finishing the both surfacs with cement sand (FM 1.2) mortar (1:3) and curing at least for 21 days, including the cost of water, electricity and other charges in all complete as per drawing, design and accepted by the Engineer in charge	sqm	5300	16.81	89093.00	-	-	
4	Anchoring galvanized wire mesh by 40 mm X 40 mm MS angle placing at edge of beams/ column boundary and brick wall, fixing by rawl bolt and screw @ 300mm	rm	700	11.98	8386.00	12.00	8,400.00	
5	for Display preparing 30% of the ferrocement and angle placing work with suitable transparent covering material as per Engineer in charge.	LS	18000	10800.00	10800.00	7,200.00	7,200.00	Display was prepared by using tempered glass and aluminium frame which cost 18000 bdt in total.
6	Plastic paint work	sqm	350	45.63	15970.50	30.42	10,647.00	Total paint area which includes all the wall and ceiling is 76.05 sqm is divided by 60% and 40% based on ferrocement work ratio.
7	Repair /renovation of the ground floor with paving tiles for the work area that have been damaged /dismanted for ferrocement work.	sqm	900	10.82	9741.60	7.22	6,494.40	Total parking tiles area is 18.04sqm is divided by 60% and 40% based on ferrocement work ratio.
8	Preparation of initial CAD drawing and as built drawing for ferrocement work	LS	60000	36000.00	36000.00	24,000.00	24,000.00	Total expenses of drawing preparation is divided by 60% and 40% based on work ratio.
9	Final Report of the Work	LS	100000	60000.00	60000.00	40,000.00	40,000.00	Total expenses of report preparation is divided by 60% and 40% based on work ratio.
10	Additional cost: Test Expenses (transportation and specimen preparation, curing, report collection, documentation)	LS	27500	16500.00	16500.00	11,000.00	11,000.00	Total expenses of report preparation is divided by 60% and 40% based on work ratio.
In Total :					251366.00		155,515.00	
Total area (sqm)					16.81		10.64	
Unit rate per Sqm					14953.36		14,616.07	

Duration comparison:

- SATREPS- TSUIB, Bangladesh portion, Wall-A (one-layer wire mesh): 31 days
- PWD-BSPP, Bangladesh portion, Wall-B (two-layer wire mesh): 38 days

It is clear that the number of layers affects both cost and duration. Also, it can be considered that cost and time vary according to the location of the site, such as number of stories, inside or outside of the room, and so on besides with the existing situation of the wall, such as deterioration, thickness, size.

A.2.8 Conclusion

It can be noted that, two different methods are used here. In one hand, one-layer wire mesh was laid and added with frame via dowel anchoring. On the other hand, two-layer wire mesh was laid and connected with frame with the help of angle and flat bar. Cost and duration comparison show the difference of both of these two methods. All of these can be helpful for the design and execution team to implement at site depending on the site condition and material availability.

This test work is completely new. Working side by side is helpful to know the complete comparison of the two steps and a proper guidance for the decision maker.

End Page